Cu(0)-mediated RDRP; Synthesis of multiblock copolymers and mechanistic studies

Fehaid Alsubaie

A thesis submitted in partial fulfilment of the requirements
of the degree of
Doctor of Philosophy in Chemistry

Department of Chemistry
University of Warwick
June 2016

Table of contents

List of figures

Chapter 1:

Chapter 2:

Chapter 5:

List of schemes

Chapter 1:

Chapter 2:

Chapter 3:

List of tables

Chapter 1:

Chapter 2:

Chapter 3:

Chapter 4:

Chapter 5:

Abbreviations

AIBN	Azobisisobutyronitrile
ARGET	Activators regenerated by electron transfer
ATRP	Atom Transfer Radical Polymerisation
Bipy	2,2'-Bipyridyl
BPO	Benzoyl peroxide
CRP	Controlled radical polymerisation
CTA	Chain transfer agent
DEAEMA	Diethyl aminoethyl methacrylate
DLS	Dynamic light scattering
DMF	Dimethylformamide
DMSO	Dimethylsulphoxide
DNA	Deoxyribonucleic acid
DRI	Differential refractive index
EBIB	Ethyl-2-bromoisobutyrate
EtOH	Ethanol
FRP	Free radical polymerisation
GPC	Gel permeation chromatography
ISET	Inner sphere electron transfer
k_i	Rate constant of initiation
k_p	Rate constant of propagation
k_t	Rate constant of termination
LCST	Low critical solution temperature
LRP	Living radical polymerisation
$[M]_0$	Concentration of monomer at t = 0
$[M]_t$	Concentration of monomer at t = t
MA	Methyl acrylate
MALDI	Matrix assisted laser desorption ionisation
Me_6TREN	N,N,N',N',N'',N''-Hexamethyl-[tris(aminoethyl)amine]
MeOH	Methanol
MMA	Methyl methacrylate
NMP	Nitroxide mediated polymerisation
NMR	Nuclear magnetic resonance
OSET	Outer sphere electron transfer
PDI	Polydispersity
PEG	Poly(ethylene glycol)
$PEGA_{454}$	Poly(ethylene glycol) methyl ether acrylate
$PEGMA_{475}$	Poly(ethylene glycol) methyl ether methacrylate
PI	Pyridine imine
PMDETA	N,N,N',N'',N''-pentamethyldiethylenetriamine
PRE	Persistent radical effect

Pn	Polymer chain with degree of polymerisation n
PS	Poly(styrene)
PVC	Poly(vinyl chloride)
RAFT	Reversible addition fragmentation chain transfer
SET-LRP	Single electron transfer living radical polymerisation
SFRP	Stable free radical polymerisation
TEA	Triethylamine
THF	Tetrahydrofuran
TMM-LRP	Transition metal mediated living radical polymerisation
TPMA	Tris(2-pyridylmethyl)amine
UV-Vis	Ultra violet-visible
VC	Vinyl chloride

Acknowledgements

Firstly, I would like to express my special appreciation and thanks to my supervisor, Professor David M Haddleton, for allowing me to grow as a research scientist and pushing me at every opportunity. I could not have imagined having a better supervisor for my PhD study and I really cannot thank him enough for what he is done for me.

My sincere thanks go to Dr. Paul Wilson, for his kind help and for the time that he has given it to me during this research.

At the beginning of my study, there were so many things (and still!) need to be known. Fortunately, Athina Anastasaki was year two PhD student in Haddleton group who has been the most patient person on my questions, whatever the level of question. She made my PhD time not only rich of scientific experience but also much more enjoyable. I cannot thank her enough.

Special thanks also go to Vasiliki, Alex and Gabit for the Kindness, help and friendship. I was lucky enough to have them in the same office during my PhD.

I would like also to thank all members of the Haddleton group the precedent and the current members: Zhang, Kristian, Nick, Glen, Richard, Ant, George, Chongyu, Sam (x2), Dan, Rachel, Jenny, Danielle, Patrick and Raj for being very kind.

I am also grateful to Professor Suzana Nunes at King Abdullah University of Science and Technology in Saudi Arabia for allowing me to work in her group a couple of months in 2014.

Last but not the least; I would like to thank my mother, brothers and sister for supporting me spiritually throughout these years. Finally, thanks to my family, wife and children, I cannot make this without your love.

Declaration

Experimental work contained in this thesis is original research carried out by the author, unless otherwise stated, in the Department of Chemistry at the University of Warwick, between August 2013 and July 2016. No material contained herein has been submitted for any other degree, or at any other institution.

Results from other authors are referenced in the usual manner throughout the text.

Date:

Fehaid Alsubaie

Abstract

The aim of this work is to investigate the versatility of Cu(0)-mediated reversible deactivation radical polymerisation (RDRP) in aqueous media in order to facilitate the synthesis of multiblock copolymers consisting of various acrylamides. Under carefully optimised conditions, a simple and highly efficient one-pot polymerisation procedure (full conversion for each block and no intermediate purification required) will be developed allowing access to iterative monomer additions, fast polymerisation rates and high level of control. As a result, complex microstructures (such as hexablocks) can be achieved in a quantitative manner in a matter of few hours, which consists the fastest synthesis of such material up to date.

However, the loss of the halide chain end will be shown to be the main limitation of the *in situ* chain extensions and block copolymerisations of acrylamides in water. In order to assess the effect of the nature of the monomer to the loss of the end group fidelity, a further investigation into the monomer nature and the lifetime of the ω-Br chain end will be conducted further highlighting the importance to monomer structure and sequence in poly(acrylamide)s multiblocks in order to maximise the retention of the bromine chain end.

At the second part of this thesis, a mechanistic investigation of Cu(0)-mediated polymerisation in organic and aqueous media will also be presented. The role of the Cu(0) on the polymerisation kinetics and will be extensively investigated differentiating Cu(0)-wire from the in situ generated Cu(0) particles. The extent of disproportionation and comproportionation reactions in aqueous, organic and aqueous/organic mixtures will be also evaluated and the effect of the monomer on

these reactions will also be shown demonstrating a completely different behaviour between organic and aqueous media. Finally, a direct comparison between Cu(0) and Cu(I) mediated polymerisation under exactly the same reaction conditions will be attempted indicating different active species depending on the conditions employed.

Nevertheless and regardless the mechanism, the ideal polymerisation protocol that allows access to the preparation of high ordered materials will be shown. Very fast polymerisation rates (achieving quantitative conversion within 10 min), high end group fidelity even at full monomer conversion and good control over the molecular weight distribution will highlight Cu(0)-mediated polymerisation as a versatile tool for the synthesis of a wide range of materials.

Chapter 1: Polymer synthesis: from free radical polymerisation (FRP) to single electron transfer living radical polymerisation (SET-LRP)

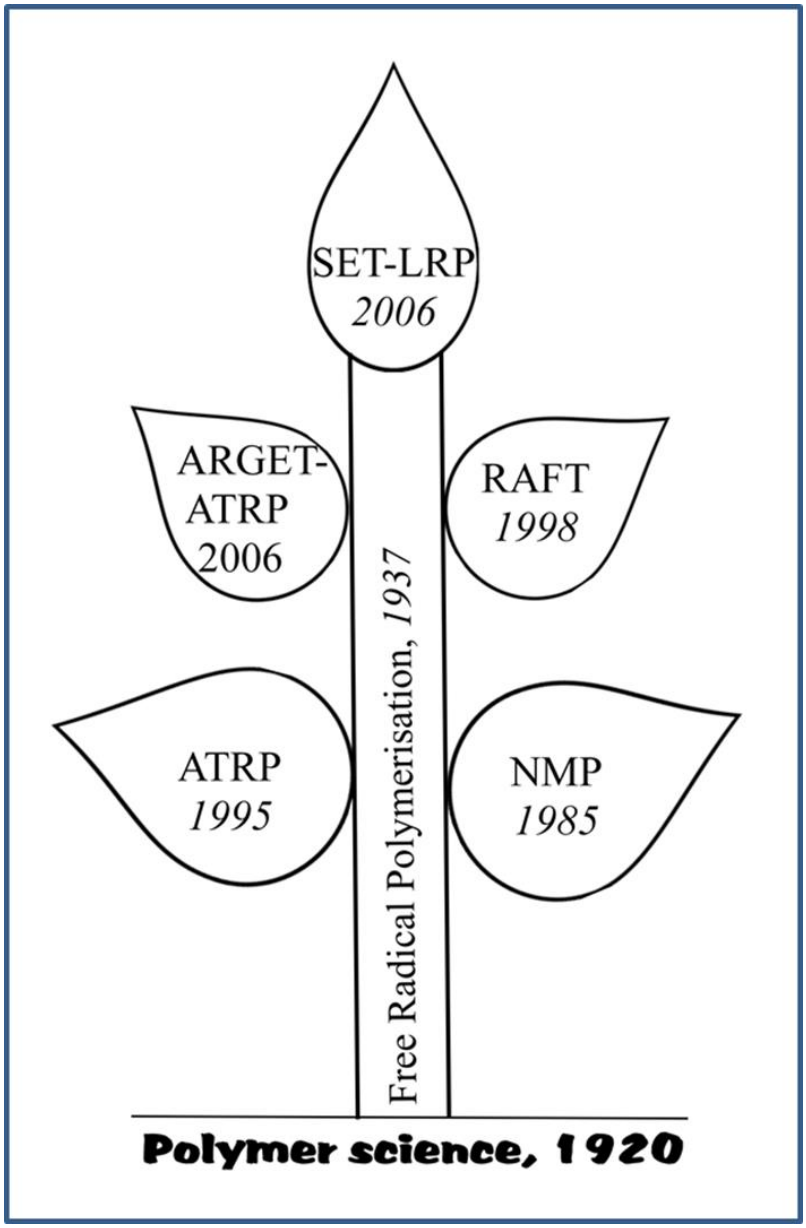

Reversible Deactivation Radical Polymerisation (RDRP) Tree

1.1 The concept of polymers

The simplest definition of a polymer is a macromolecule consisting of many small units (monomers/molecules) that can be linked together by a chemical reaction to form longer molecules. A polymer may consist of hundreds or thousands of monomers, for instance, polyethylene (CH_3-$(CH_2)_n$-CH_3) is a long chain polymer derived by the combination of ethylene monomers (CH_2 =CH_2) in which n is the number of repeating units.

Since the development of polymer chemistry, there have been several ways to classify polymers. One primary classification is based on the polymer source, and as such there are two types of polymers: natural and synthetic. Natural polymers are found in nature and can be extracted from plants or animals. Examples of naturally existing polymers are cellulose, starch, resins, rubber, silk, DNA, and proteins. Synthetic polymers are made by synthesis and derive from crude oil. Examples of artificial polymers include plastic, synthetic rubber, nylon, polyethylene, polyester and polystyrene.

The notion that synthetic polymers are high molecular weight molecules goes back to the early 19^{th} century. In 1920s the concept that high molecular weight molecules are repeating units linked together by covalent bonds forming macromolecules was coined by Staudinger, and he was awarded the Nobel Prize for chemistry in 1953. [1] This contribution paved the way for intense research and put the base for contemporary polymer chemistry.

1.2 The significance of polymers

The materials are used in real life and have shaped human history. In 2000 B.C, the "Stone Age" became the "Bronze Age" when humans used bronze instead of stone to develop some useful tools. A thousand years later, the prevalent use of iron shaped the Iron Age. In the present, we learn how to mimic and modify natural materials to improve the quality of life. This era began by utilising synthetic polymers in different aspects of our life so that it could be possible to name this era by ''The Polymer Age''.

There is a general misconception that polymers can be alternatively be defined as plastics and as such they could damage the environment. However, it is noted that plastics are polymers but all polymers are not plastic. In addition, nowadays there are biodegradable plastics which can be alternatively used.

Synthetic polymers have played a significant role in the world. They are found in agriculture, medicine, technology, sports and industry, to name just a few (Figure 1). The reason for polymers being found everywhere is that their chemical and physical properties can be adjusted to be feasible and meet the daily demand. Indeed, it is impossible to imagine our lives today without any polymers.

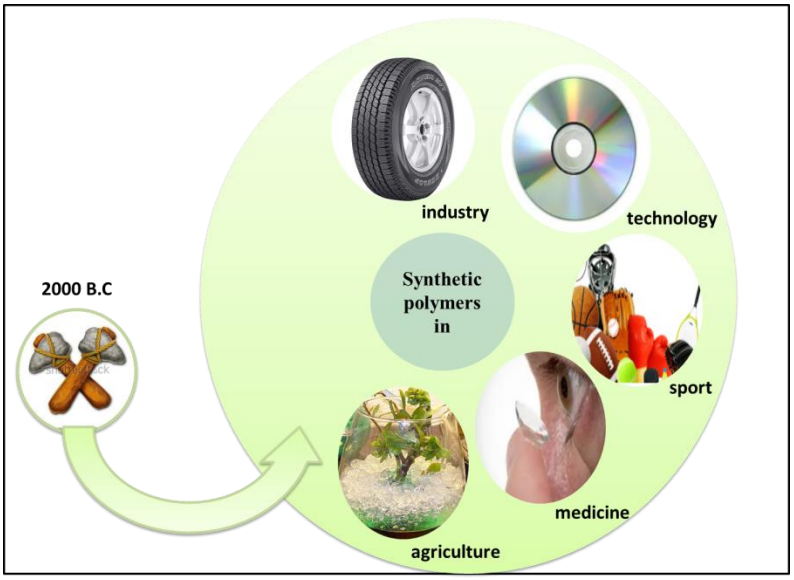

Figure 1. Examples of current synthetic polymers existing in different areas.

Academic research regarding polymeric materials has been of great interest. Although a revolution related to polymers has progressively continued over the last 100 years, a wide variety in the area of polymer science and engineering still promises a vast potential for exciting new applications. Industrial support has been the key factor behind the great progress in the field of polymeric materials. The global polymer industry shows the significance of the research investment by funding scientific projects.

1.3 Condensation and addition polymerisations

The study of polymers begins with categorising the techniques in which these macromolecules are produced. At the beginning of polymer science, two synthetic routes of polymerisation were introduced to classify different polymers namely, condensation polymerisation and addition polymerisation.

Firstly, condensation polymerisation is a reaction in which a small molecule, such as water is eliminated from polyfunctional monomers to form condensation polymers. The common example of this method is polyamides synthesised from diamines and dicarboxylic acid to give polyamide and water (Scheme 1)

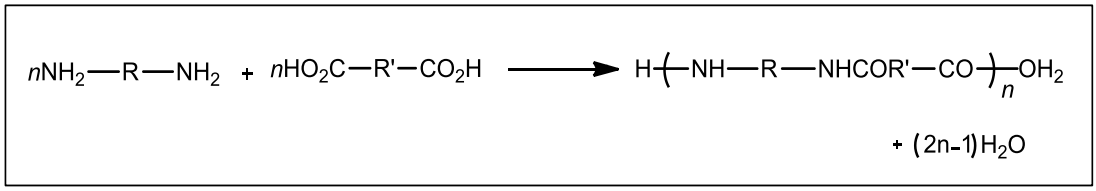

Scheme 1. Condensation polymerisation of a diamine and a diacid with the elimination of water yielding polyamide.

Secondly, unlike condensation polymers, addition polymers have the same composition in the repeat unit as in the monomer. In addition polymerisation, vinyl monomers (monomers containing the carbon-carbon double bond group attached to substituent) react with themselves to transform a double into a single bond between monomers to form polymer (Scheme 2).

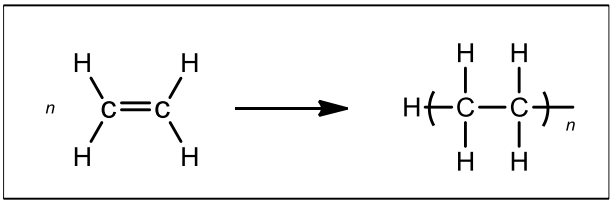

Scheme 2. Formation of the addition polymer poly(ethylene).

Although classifying polymers into two different types (condensation and addition polymer) was widely used, it became inadequate. The progress in polymer synthesis revealed inconsistencies in these naming methods so that the previous classification

could lead to ambiguous terminology. For example, ethylene oxide can be polymerised to produce polyethylene oxide not only from the condensation polymerisation of ethylene glycol but also *via* the ring opening polymerisation of ethylene oxide.

To avoid such ambiguity, the nature of polymer chains was alternatively considered to classify the type of polymer. Depending upon the structure of polymer (both alkyl and functional group), two categories of polymerisation; step growth and chain growth were coined.

Step growth polymerisations occur by the stepwise addition of bifunctional or multifunctional monomers. These monomers react to form first dimers which can subsequently react with each other or with free monomer and eventually long chain polymers will be produced. In this reaction system, the rate of polymer chains evolution remain steady and high molecular weight polymers can be obtained at the end of the reaction (>98% conversion) (Figure 2). Polymers that can be synthesised *via* these methods include polyamides, polyesters and polyurethanes.

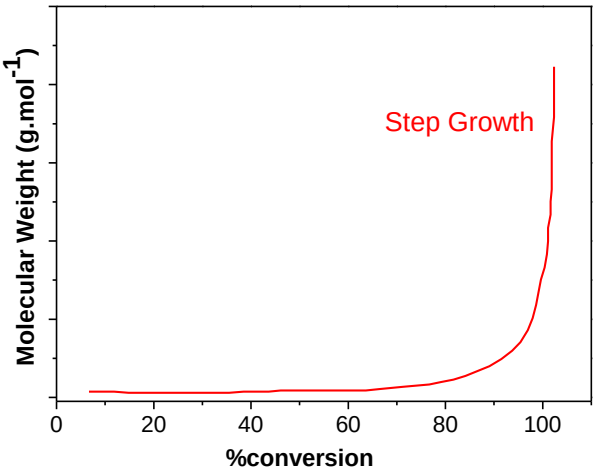

Figure 2. The evolution of molecular weight with increasing conversion for step growth polymers.

Chain growth polymerisation is quite different in which an initiator is utilised to start the reaction process. Conventional chain growth polymerisation consists of three mechanistic phases. An initiation step produces reactive centres, followed by propagation step in which all vinyl monomer (substituted ethene) is consumed and chain stopping by termination event. The addition of monomer is triggered by reactive centres which can be a free radical, cation or anion. In free radical polymerisation, rapid monomer consumption (propagation) results in the formation of a polymer (Figure 3). As shown in the figure, the evolution of molecular weight immediately occurs due to the active nature of free radicals. However, the evolution of polymer chains can be interrupted deactivated by one of the termination reactions. Controlled ‘’living’’ chain growth is similar to conventional; however, the evolution of molecular weight increases linearly with conversion suggesting that there is minimal termination reactions during polymerisation processes.

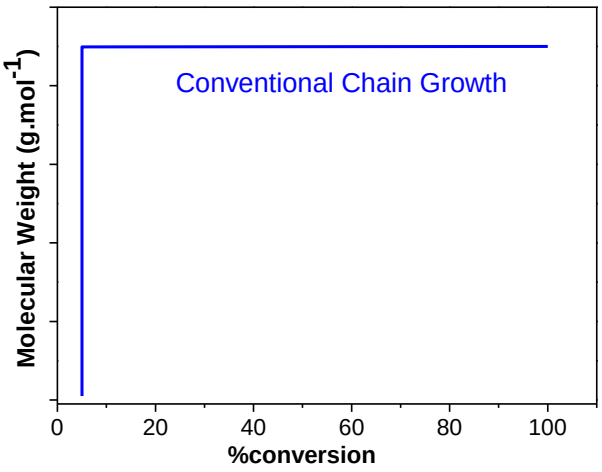

Figure 3. The evolution of molecular weight with increasing conversion for chain growth polymers.

The history of polymer synthesis is the subject of this chapter, from free radical polymerisation (FRP) to well controlled ‘’living’’ radical polymerisation (CRP). Brief descriptions of free radical polymerisation and living polymerisation will be given, whilst more details will be provided for CRP. Copper mediated ‘’living’’ radical polymerisation as a tool of controlled polymerisation will be mainly discussed. The discussion will be focused on Cu(0)-mediated polymerisation process; synthesis and mechanism, as it the key feature of this thesis.

1.3 Free radical polymerisation

Free radical polymerisation (FRP) is the most common method of chain growth polymerisations. It was not until 1930s, when Flory reported the most commercially used polymerisation technique. [2] In comparison to other chain growth polymerisation techniques, free radical polymerisation can be conducted under relatively undemanding conditions. This tolerance towards impurities resulted in its wide use and commercial success. Therefore, polymers with high molecular weights can be produced from commercially available monomers without removal of the monomer stabilisers/inhibitors. Moreover, exhausting solvent purification procedures and free oxygen atmosphere precautions are not required providing access to various important polymers, such as polyethylene (PE), polystyrene (PS) and polyvinylchloride (PVC).

From an industrial point of view, conventional radical polymerisation is the main synthetic route for the aforementioned features. These advantages facilitate the free radical polymerisation processes in bulk, solution or suspension. One of these three polymerisation processes can be preferentially utilised in order to circumvent any

production problems such as high viscosity. Three typical steps can be studied as a basic mechanism of FRP; initiation, propagation, and termination.

1.3.1 Free Radical Polymerisation Steps

The first stage towards conventional free radical polymerisation is the initiation step in which two reactions generate the free radicals. The decomposition of free radical initiators I produces a pairs of primary radicals 2 $I^{\bullet}$ **(**Eq. 1.1). Subsequently, the addition of these radicals to the monomer (vinyl bond) forms initiating radicals I-$M^{\bullet}$ (Eq. 1.2), where k_d and k_i are the rate constant for decomposition and initiation reaction respectively.

$$I_2 \xrightarrow{k_d} 2\,I^{\bullet} \qquad (1.1)$$

$$I^{\bullet} + M \xrightarrow{k_i} I\,M^{\bullet} \qquad (1.2)$$

$$P_n^{\bullet} + M \xrightarrow{k_p} P_{n+1}^{\bullet} \qquad (1.3)$$

Although there are several types of free radical initiators, the thermal initiators are mostly used for both commercial polymerisation and academic research. The thermal initiator dissociation can be simply triggered by heat to generate primary radicals. For example, 2,2'-azobis(2-methylproprionitrile) (AIBN) is a common azo compound that decompose to form carbon-centred radicals (cyanoisopropyl radicals) and N_2 (Scheme 3a) . Another example is dibenzoyl peroxide (BPO), one of the peroxides which dissociate by thermal homolysis to generate primary oxygen-centred radicals for thermal catalysed polymerisations (Scheme 3b).

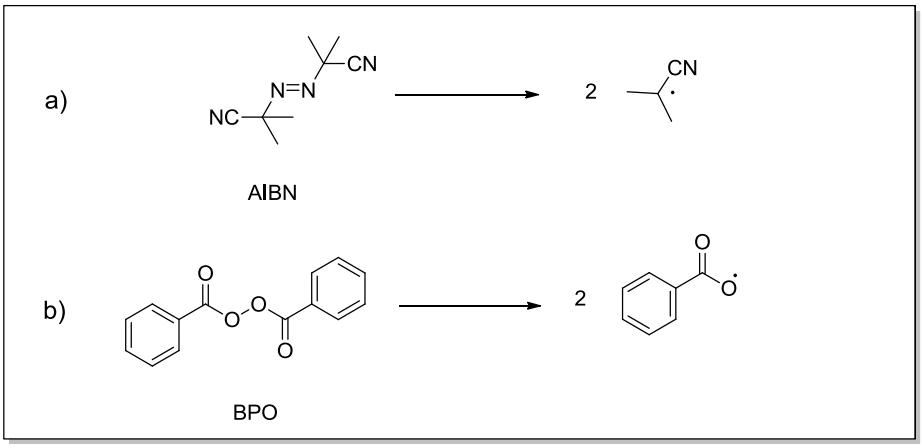

Scheme 3. Conventional free radical initiators decomposing to form primary radicals.

Propagation step is the growth of initiating radical I-M$^{\bullet}$ by the rapid and sequential addition of further monomer molecules (Eq. 1.3). The successive addition will continue and propagation of the polymer chain I-M_n-M$^{\bullet}$ to higher degree of polymerisation will take place. The rate constant of propagation is defined as k_p, and its value for typical monomer is in the range 10^2-10^4 L.mol^{-1} s^{-1}, bearing in mind the influence of the reaction conditions and the nature of the monomer. [3] It might be worth mentioning that such rate constants are clearly higher in comparison with step growth polymerisations. The FRP is ceased by either full monomer consumption [M] = 0 or termination reaction.

The last step during free radical polymerisation is chain termination. At some extent, the polymer chain will lose the radical centres by bimolecular termination between macro-radicals yielding ‘’dead’’ polymer chain *via* undesired side reaction events, combination and disproportionation. The first, termination by combination, in which two chains react with each other as represented in Eq. 1.4. This head to head coupling results in doubling of molecular weight. The second, termination by disproportionation, in which a hydrogen transfer from one macro-radical to the other

Eq. 1.5. The later termination route results in two dead macromolecules, saturated and unsaturated chains.

Both termination reactions could also happen during FRP, however, the dominant route of termination is combination except in the case of methacrylates. The rate constants for the two irreversible radical terminations (k_{tc} and k_{td}) could be relatively combined into a single rate constant k_{tr} as shown in Eq. 1.6. [4] Typical termination rate constant falls in the range 10^6-10^8 L mol^{-1} s^{-1} [3]. Although the value of k_t much greater than k_p, propagation proceeds, this due to the fact that the concentration of radicals is very low during polymerisation.

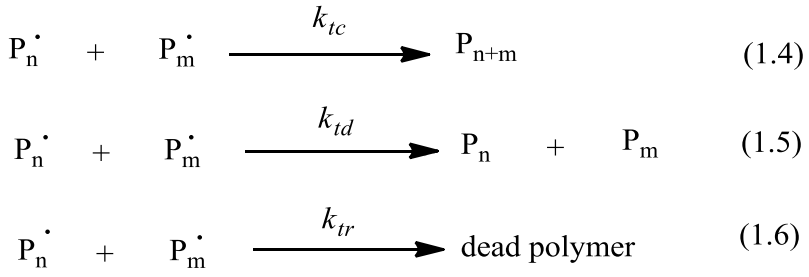

$$P_n^{\cdot} + P_m^{\cdot} \xrightarrow{k_{tc}} P_{n+m} \qquad (1.4)$$

$$P_n^{\cdot} + P_m^{\cdot} \xrightarrow{k_{td}} P_n + P_m \qquad (1.5)$$

$$P_n^{\cdot} + P_m^{\cdot} \xrightarrow{k_{tr}} \text{dead polymer} \qquad (1.6)$$

1.3.2 The kinetics of free radical polymerisation

The kinetics of free radical polymerisation have been a subject of fundamental importance as they need to be entirely understood for efficiently producing polymer. The polymerisation steps are now clearly elaborated; however, the determination of reaction rates and chain growth is far from simple. The difficulty of analysing the rate of free (conventional) radical polymerisation is attributed to the dual nature of the different reactions. The process will be expressed by a simplified series of fundamental reactions.

Primary radicals and small size of radicals are more reactive than propagating radicals, but the effect of this can be ignored because the effect of the size vanishes at the dimer or trimer size. [5] Therefore, it could be possible to assume that k_p and k_t are independent of the size of the radical.

Monomer throughout polymerisation (the initiation and propagation steps) is consumed, so that the rate of monomer consumption is giving by Eq. 1.7 where R_i and R_p are the rates of the initiation and propagation respectively. Actually, the number of monomer units reacting during initiation reaction is incomparable to the number consumed during the propagation step for a high molecular weight polymerisation. For that reason, the equation can be simplified and written as in Eq. 1.8.

$$-\frac{d[\mathrm{M}]}{dt} = R_i + R_p \qquad (1.7)$$

$$-\frac{d[\mathrm{M}]}{dt} = R_p \qquad (1.8)$$

Since the significant portion of the monomer is only consumed in the propagation step, it can be considered that the rate of propagation/polymerisation is the sum of many individual propagation reactions. Consequently, the overall propagation rate can be expressed by Eq. 1.9 where [M] is the monomer concentration and [M$^{\bullet}$] is the concentration of propagating radical species.

$$R_p = k_p [\mathrm{M}^{\bullet}][\mathrm{M}] \qquad (1.9)$$

In free (conventional) radical polymerisation, the concentration of propagating radical is difficult, in practice, to predict as it remains very low (~10^{-8}) during the

polymerisation, therefore the equation can be given by eliminating [M$^{\bullet}$]. A steady state theory can be applied if the radicals initially increases and reaches a constant value almost instantaneously. Thus, throughout the polymerisation the rate of change of the radical concentration can be considered to be zero.[6] This is equivalent to stating that the rates of initiation and termination are equal ($R_i = R_t$) (Eq 1.10).

$$R_i = R_t = 2k_t\,[\mathrm{M}^{\bullet}]^2 \qquad (1.10)$$

From the above equation, it can be seen that the rate of termination with no specification as termination mechanisms, combination or disproportionation follow the same kinetic expression. The factor of 2 in the termination rate equation follows generally accepted convention for radicals been destroyed in pairs.

Mathematically, if we rearrange Eq 1.10, the relationship will be:

$$[\mathrm{M}^{\bullet}] = \left(\frac{R_i}{2k_t}\right)^{1/2} \qquad (1.11)$$

The expression for the rate of propagation can be rewritten by substituting Eq. 1.11 into Eq. 1.10, which reveals the dependence of the rate of polymerisation on the square root of the initiation rate (Eq. 1.12).

$$R_p = k_p\,[\mathrm{M}]\left(\frac{R_i}{2k_t}\right)^{1/2} \qquad (1.12)$$

In the case of thermal initiation, the rate of generating both primary radicals and initiation radicals is giving by equation 1.13 where [I] is the concentration of the initiator and f is the initiator efficiency. The initiator efficiency is defined as a value used to predict the loss of primary radicals due to the early termination events. It has been mentioned earlier that there are two steps during the initiation reaction; decomposition (to generate primary radicals) and initiation (primary radicals react with monomer molecules). The second step is much faster than the first, thus the rate determining step is the homolysis of the initiator in the initiation reaction (Eq. 1.13) and the rate of initiation is expressed by Eq. 1.14.

$$R_d = 2f\ k_d\ [\mathrm{I}] \qquad (1.13)$$

$$R_i = R_d = 2f\ k_d\ [\mathrm{I}] \qquad (1.14)$$

Finally, the expression for the rate of propagation can be obtained by substituting Eq. 1.14 into Eq. 1.12 as presented in Eq. 1.15. [7-9]

$$R_p = k_p\,[M]\left(\frac{f k_d[\mathrm{I}]}{k_t}\right)^{1/2} \qquad (1.15)$$

The free (conventional) radical polymerisation has been successfully utilised, in the field of industry. This commercial success thanks to the possibility of conducting and adjusting the polymerisation processes with relative ease. The simplicity and feasibility (being tolerant to a variety of reaction conditions, temperatures and trace impurities) of this technique is also subject to some limitations. Perhaps, the main limitation of FRP is its inability to control the evolution of molecular weight

distributions. Therefore, relatively recent research in CRP has given great improvements in order to synthesise polymers with a desired and targeted composition, structure and topology.

1.4 Living anionic polymerisation

Living polymerisation was the alternative technique to overcome the challenge arising from a chain termination of radical polymerisation. The term 'living' was first introduced by Szwarc in 1956[10-12] who demonstrated the use of anions to regulate the controlled anionic polymerisation of styrene. A living system was initiated by using a combination of alkali metal with naphthalene to generate an anionic radical. During both initiation and propagation the anionic radicals are unable to react with each other due to the mutual repulsion of like charges. In parallel, all chains grow at similar rates that would then continue to consume all styrene monomer providing access to well-defined polymers (Scheme 4). Therefore, all of the propagating species are initiated simultaneously and chain termination reaction or/and chain transfer events are eliminated.

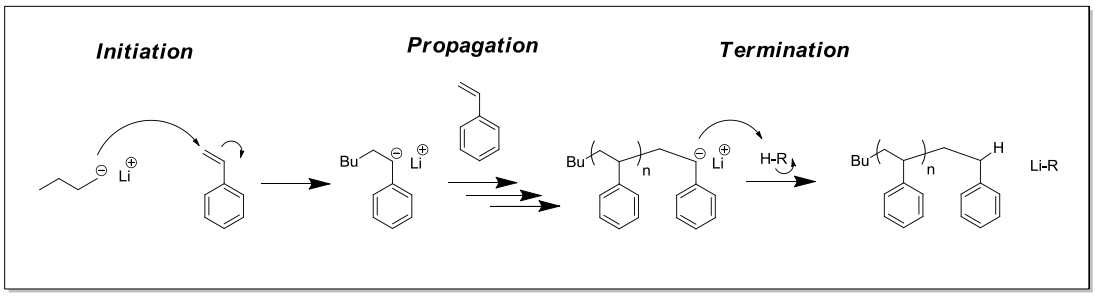

Scheme 4. Living anionic polymerisation of styrene with butyl lithium as initiator.

However, to maintain the propagating chains "living" and active until fully monomer consumption, rigorously purified reagents are required. Consequently, it is

true to say that such exhaustive process makes the technique commercially undesirable. This drawback encouraged polymer chemistry community to develop radical polymerisation, paving the way for further developments on the construction of well-known tailored polymers. Therefore, this breakthrough was followed by the introduction and evolution of controlled polymerisation techniques.

1.4.1 Proposed criteria for "living" polymerisations

Generally**,** living anionic polymerisation is one of the first living polymerisation methods that shows no termination events under carefully selected conditions and provides advanced polymers with precisely controlled molecular weight distributions (MWD). In order to define the livingness of a polymerisation process, various ways have been used.[13-17] The most common criteria were proposed by Quirk and Lee[13] to describe a living polymerisation system. First, the polymerisation proceeds until all of the additional monomer is consumed and the molecular weight linearly increases with conversion as shown in (Figure 4).

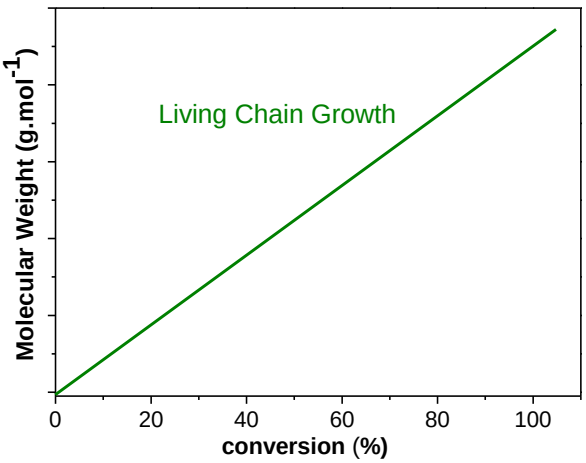

Figure 4. The evolution of molecular weight with increasing conversion for living chain polymers.

Second, the rate constant of initiation step should be higher enough than the rate constant of propagation step ($k_i > k_p$), then the concentration of active species remains constant during propagation stage. Thus, the system provides relatively narrow molecular weight distributions (dispersities $Đ < 1.2$) (scheme 5).

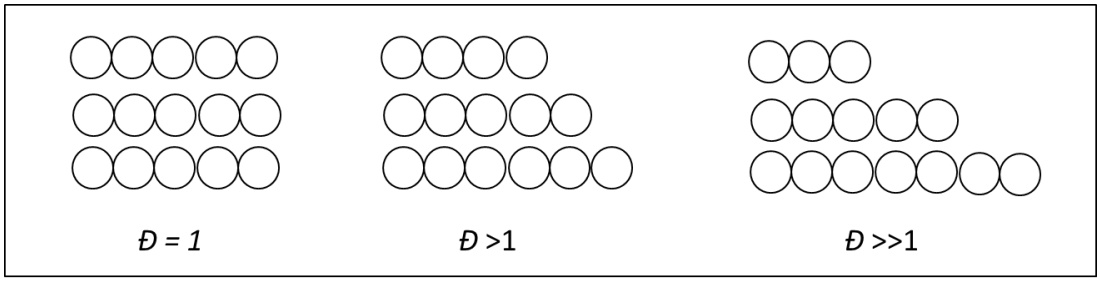

Scheme 5. Schematic arrangement of three different molecular weight distributions.

Finally, the polymer chain ends also should retain their functionality, allowing for the synthesis of block copolymers v*ia* sequential monomer addition as presented on (scheme 6).

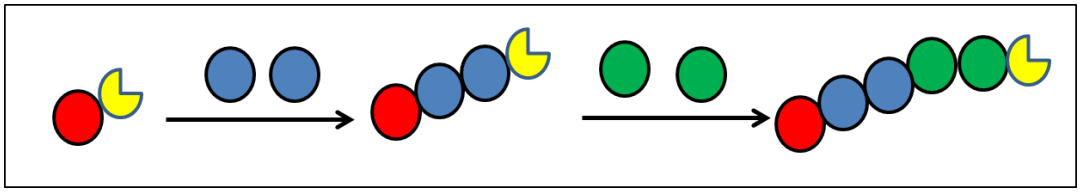

Scheme 6. Representation of controlled copolymerisation *via* sequential monomer addition.

In order to use the term ‘’living’’ for a polymerisation system, the above criteria must be taking into consideration. As mentioned previously, anionic polymerisation requires certain restrictive conditions and that, from industry point of view, make the process difficult to commercialise. This led to develop a new living system,

matching the criteria with tolerant towards the condition of reaction and reagents purification procedure.

1.5 Controlled ‘’living’’ radical polymerisation

1.5.1 Introduction to the controlled ‘’living’’ radical polymerisation

From radical polymerisation to anionic polymerisation, the term of ‘’living’’ attracts a lot of interest and accelerates the research development in modern polymer chemistry. Thus, living radical polymerisation (LRP) technique has emerged, and paved the way for the synthesis of advanced polymers with targeted composition and topology. It is one of the most important controlled polymerisations and probably the most studied for materials synthesis. This new approach showed the ability to replicate anionic polymerisation in which, narrow molecular weight distribution and end-functional polymer were obtained without any limitations in terms of purification requirements.

The main feature of living radical polymerisation methodology is a reversible termination process, so that the high activity of radicals towards each other is supressed. The livingness of LRP system is achieved by establishing an appropriate equilibrium between activation and deactivation step. A deactivation-activation equilibrium is a result of adding a controlling or mediating agent into the reaction that could reversibly associate with propagating radicals (active species) to form non-propagating species (dormant species). Therefore, the growth of all chains is regulated at similar rates resulting in comparable chain lengths, lower dispersity and precise control over the macromolecular structure. Also, the chain ends retain functionality, allowing for the iterative chain extension reaction or block copolymerisation by further addition of a new monomer.

The unavoidable chain termination events due to the reactive nature of radicals in living radical polymerisation, has led to the replacement of the term ‘’living’’ radical polymerisation (LRP) by reversible deactivation radical polymerisation (RDRP) as suggested by the International Union of Pure and Applied Chemistry (IUPAC). [17] However, some different names have been used and still in the literature, such as controlled radical polymerisation (CRP) and controlled/"living" radical polymerisation (CLRP). For this thesis the term LRP will be used as humans will also die one day but still there are considered ‘’living’’ before they die. Several examples of RDRP techniques including, nitroxide mediated polymerisation (NMP), atom transfer radical polymerisation (ATRP), reversible addition-fragmentation chain transfer (RAFT) and single electron transfer living radical polymerisation (SET-LRP) will be discussed in the following section.

1.5.2 Controlled ‘’living’’ radical polymerisation techniques

Living radical polymerisation was found to proceed in controlled manner with most termination reactions virtually absent. The balance between propagating radicals and non-propagating radicals can be obtained by introducing a mediating species to the system. The extensive investigation of living radical polymerisation provided the research community with relevant techniques that expanded the pool of monomers under appropriate conditions.

The probability of undesirable side reaction or chain termination to occur in LRP can be minimized by one of the two main different concepts. First, a reversible activation/deactivation process which is a basic mechanism that can be seen in the case of NMP, ATRP and SET-LRP. Second, a reversible chain transfer which can be obtained by utilising an efficient chain transfer agents (RAFT).

The middle 1980s, witnessed the beginning of LRP approach, when the idea of stable free radical polymerisation (SFRP) emerged, employing stable nitroxide radicals as the mediating species. A decade later, new synthetic strategies were introduced to both academic and industrial community, RAFT and ATRP.

1.5.3 Nitroxide mediated polymerisation

Stable free radical polymerisation (SFRP) was the first technique named in the field of LRP, employing several stable agents to mediate the polymerisation. Mainly, stabilised radical species such as (arylazo)oxy[13], substituted triphenyls[14], verdazyl[15] triazonilyn[16] and nitroxides[17] have been utilised to avoid fast radical-radical termination reactions. Nitroxide radicals are the most effective mediators or trapping agents and have been predominantly studied of SFRP. It is worth to note that the tendency of stable radicals to react with the propagating radical is much higher than with itself, reducing the radical concentration. Also, the obvious advantage of nitroxide mediators is that they are stable at ambient temperature and commercially available. Therefore, the method is alternatively called nitroxide mediated polymerisation (NMP).

The first example of LRP was patented by Solomon and Rizzardo in 1985[18]. In this radical trapping experiment, persistent free radicals, 2,2,6,6-tetramethylpiperidinyl-1-oxy (TEMPO) have been used to control polymerisations. The control over the polymerisation is described *via* a reversible deactivation process of a (macro)alkoxyamine (dormant), whereby a stable nitroxide will reversibly trap a propagating radical as represented in Scheme 7. In other words, the stable nitroxide radical mediates the reaction by associating with propagating centres to reduce their concentration. The equilibrium of system is now in favour of the deactivation step,

resulting in living radical polymerisation with narrow molecular weight distributions. Although NMP has proven to be a good method for controlled radical polymerisation, the reaction time was relatively long (> a day).

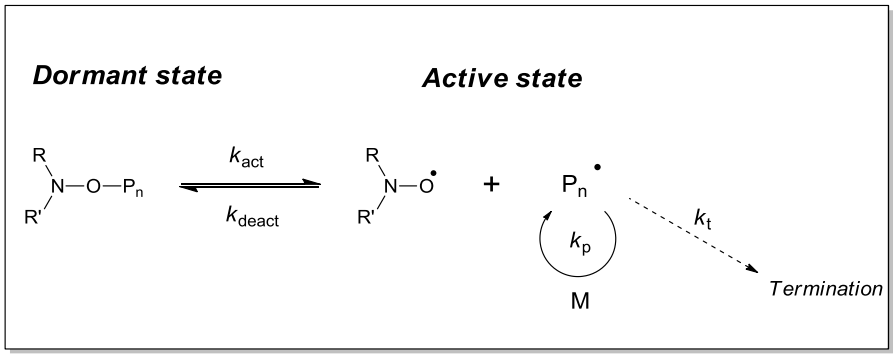

Scheme 7. Proposed mechanism of NMP.[18]

In 1993, Georges and co-worker published that the thermal decomposition of an alkoxyamine can be reversibly dissociated into a propagating radical (reactive radical) and a nitroxide (stable radical) at high temperatures to mediate polymerisation. However, at low temperature, nitroxide could trap chain radicals and the system efficiently supresses chain breaking reactions to proceed in a controlled fashion. [19] Perhaps, the main limitation of NMP is its inability to conduct controlled polymerisation of methacrylate monomers.[20]

1.5.4 Reversible addition-fragmentation chain transfer polymerisation

Reversible addition-fragmentation chain transfer (RAFT) polymerisation was first reported in 1998 by Moad and co-workers. [21] This method is a second successful LRP technique, in which a typical feature of radical polymerisation (chain termination) can be diminished by a reversible chain transfer process. An efficient

chain transfer agent (CTA) in the form of thiocarbonylthio compounds such as dithioesters plays a vital role in RAFT polymerisation. The CTA (also referred to as a RAFT agent) could be utilised to maintain control over chain growth in radical polymerisation *via* rapid equilibrium between the active propagating radicals and the dormant. [22, 23]

Typically, RAFT polymerisation process composes of a thermal radical initiator such as AIBN, appropriate RAFT transfer agent and monomer and it can be tolerant towards a wide range of solvents. In order to be able to conduct an ideal RAFT polymerisation, the CTA should behave as an ideal transfer agent based on the monomer employed. The mechanism of reversible chain transfer in RAFT polymerisation is described in scheme 8. In the early stages of the process, fast decomposition of thermal radical initiator occurs then primary radical reacts with monomer, generating the propagating radical ($P_n^{\bullet}$). The addition reaction of propagating radical can occur in the presence of thiocarbonylthio compound (RAFT transfer agent) producing, an intermediate radical. Then, the reaction of addition is followed by fragmentation of the intermediate radical resulted to a polymeric thiocarbonylthio compound (dormant macro-CTA) and a new radical ($R^{\bullet}$). This radical ($R^{\bullet}$) reinitiates a new polymer chain with, forming another propagating radical ($P_m^{\bullet}$). Repeatedly, reversible chain transfer process takes place and fast exchange among the active propagating chain ($P_n^{\bullet}$ and $P_m^{\bullet}$) and the dormant polymeric thiocarbonylthio compounds resulting in a controlled polymerisation with minimal termination and allowing for the production of well-defined polymers. [24]

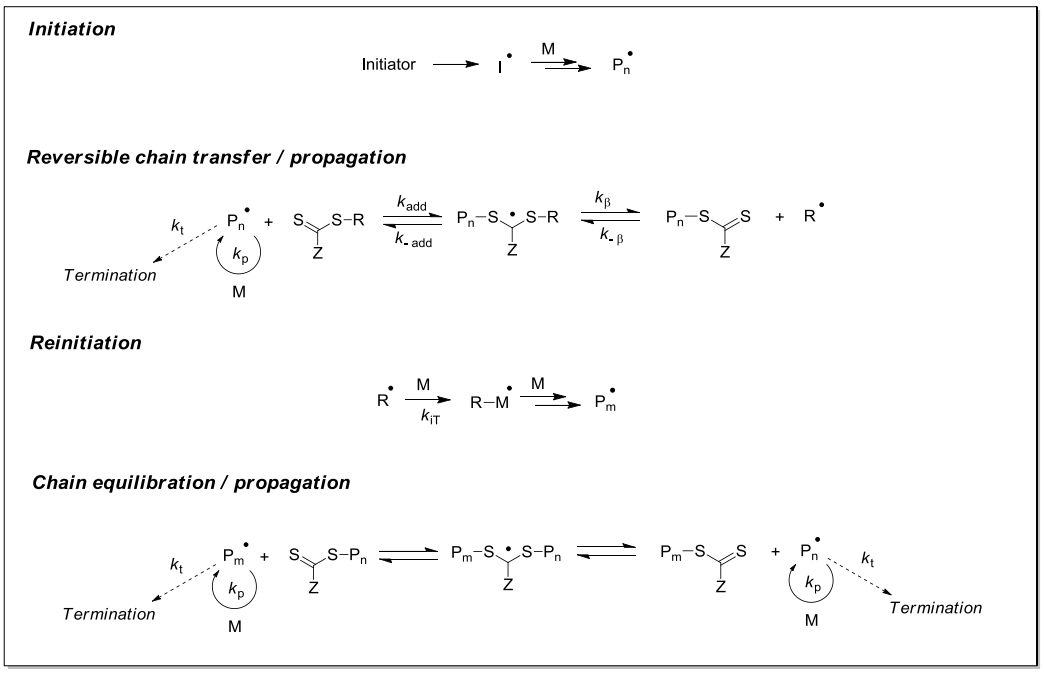

Scheme 8. Proposed mechanism of RAFT polymerisation[24].

It could be said that the main drawback of RAFT polymerisation is that RAFT transfer agents are commercially unavailable and unstable for long period of time. Therefore, widespread of RAFT polymerisation could be hampered by the extra synthetic reaction steps required for the synthesis of the chain transfer agent. In addition, it cannot be produced pure polymer without some associated sulfur and colours which might be undesirable for some applications. However, many advantages can be considered of this method. May be the most significant advantage is the compatibility of this technique with more activated monomers such as (meth)acrylic monomers and styrene or less activated monomers such as vinyl acetate (VAc), *N*-vinyl pyrrolidone (VP) or N-vinylcarbazole (NVC).[25, 26]

RAFT polymerisation as an efficient synthetic tool and has been proven to be versatile and robust enough for the synthesis of polymeric materials with design composition, structure and topology (multiblock copolymers,[27-29] and stars,[30]).

Moreover, exploiting this technique provided polymers with interesting properties that could be useful for some applications such as drug delivery system (DDS).

1.5.5 Copper mediated ‘’living’’ radical polymerisation

Copper mediated ‘’living’’ radical polymerisation (CM-LRP) belongs to transition metal-mediated ‘’living’’ radical polymerisation (TMM-LRP). TMM-LRP has been successfully catalysed by various transition metals, for instance, Ti[30], Mo[31], Re[32], Fe[33] and Cu[34]. Copper complexes have been determined to be the most efficient catalysts in the TMM-LRP of a wide range of monomers and solvents. Therefore, the Cu complex is mostly employed as the catalyst to govern the activation and deactivation of the growing chain yielding uniform polymer chain growth. In addition, copper is a preferred choice because of its low costs, large availability and ease handling compering with rest of transition metals.

TMM-LRP uses a catalytic system, whereby a halogen exchange occurs between an alkyl halide and the transition metal complex in which catalyst acts as a carrier of the halogen atom in the rapid redox reaction. The atom transfer redox process results in oxidation and reduction of the catalyst as it activates and deactivates a propagating radical.

To date, TMM-LRP is one of the most powerful polymer synthetic approaches that provides functional polymeric materials with precisely controlled molecular architecture. Moreover, TMM-LRP is the preferred procedure in the field, as evidenced by the extensive publications that have been annually published and commercial products made.

This thesis discusses copper mediated ‘’living’’ radical polymerisation, which is outlined in more details in the following sections, starting with the first protocol of this technique and the most popular, atom transfer radical polymerisation (ATRP).

1.5.5.1 Atom transfer radical polymerisation

The ‘’classical’’ atom transfer radical polymerisation (ATRP) was independently developed by Matyjaszewski[35] and Sawamoto[36] in 1995. ATRP is an extension of well-known reaction in organic synthesis, atom transfer radical addition (ATRA) in which carbon-carbon bond can be formed by the radical addition of halogens to alkenes. [37]

In general TMM-RDRP and ATRP involves an alkyl halide (R-X) as an initiator to generate radicals, which is not the case for both NMP and RAFT. In ATRP the control over the growing chain is gained by a reversible activation/deactivation process using a deactivating species, which is the case for NMP method. In NMP an alkoxyamine is used as a ‘trapping’ species; however, in ATRP a metal complex reversibly transfers a halogen atom (X) to trap the radical.

Initially, a transition metal compound such as cuprous halide, (Mt^n-X, where X is a halogen atom) is mixed with a nitrogen based ligand (L), to form the transition-metal complex catalyst ([Mt^m(L)X]). The catalyst (mediating species) abstracts the halogen atom X from the organic halide (R-X) yielding the oxidized catalyst (deactivating complex), Mt^{m+l}-X, and the radical ($R^{\bullet}$). This radical subsequently reacts with the first vinyl monomer (M) to initiate the intermediate radical species (R-$M^{\bullet}$), also known as propagating radical species ($P^{\bullet}_n$) (active species). Then, the deactivating species Mt^{m+l}-X caps the polymer propagating radical ($P^{\cdot}_n$) resulting in the target

product (P_n-X) (dormant species) and the reduced transition metal species Mt^m-X which further activates P_n-X and so on. Scheme 9 outlines the classic mechanism for ATRP, in which the process is dominated by the rapid equilibrium between the dormant (P_n-X) and active (P_n) chain species. It has also been suggested that the ATRP mechanism is described to proceed *via* an 'inner-sphere' electron transfer (ISET) mechanism, where the radical and the deactivating species Mt^{m+1}-X are formed through the homolytic atom transfer of the halogen (X) radical from the dormant species (P_n-X) to the activating species Mt^m-X. [38]

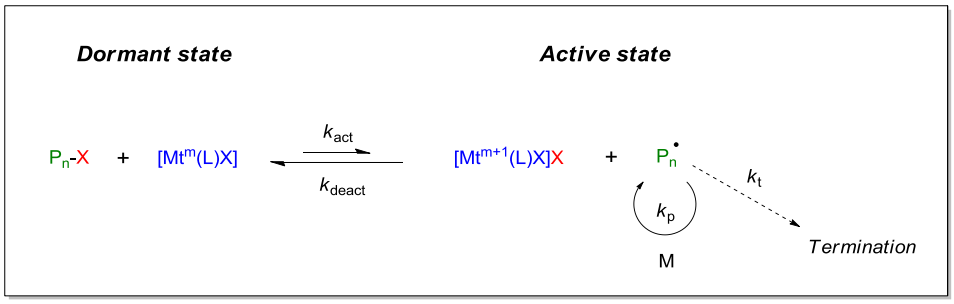

Scheme 9. ATRP mechanism as proposed by Matyjaszewski. [38]

Since the chain termination inevitably occurs, further control can be achieved by the small amount of bimolecular termination present during the initial stages of the reaction. Generally, radicals are terminating *via* any other method than the end-capping reaction with Mt^m-X, resulting in a slight excess of this deactivating species in the system, which is required to gain better control over the molecular weight distribution by shifting the equilibrium to the dormant species. This phenomenon is known as the persistent radical effect (PRE).[39]

The initial work by Sawamoto *et. al.* used $RuCl_2(PPh_3)_2$/$MeAl(ODBP)_2$ catalyst and CCl_4 initiator to mediate the controlled radical polymerisation of methyl

methacrylate.[36] A few months later, Matyjaszewski employed copper(I) catalysts and 1-phenylethyl chloride initiator for the controlled polymerisation of styrene.[40] Typically, α-halo esters-based compounds are commonly utilised as ATRP initiators, for example, ethyl 2-bromoisobutyrate (EBiB) and methyl 2-bromopropionate (MBP).[41] Nitrogen-based ligands are always employed as ATRP ligands, including derivatives of bidentate or multi-dentate such as 2-pyridylmethanimine, *N,N,N′,N′*-tetramethylethylenediamine (TMEDA), tris(2-aminoethyl)amine (TREN), *N,N,N',N',N'',N''*-hexamethyl-[tris(aminoethyl)amine] (Me_6TREN) and (tris(2-pyridylmethyl)amine (TPMA) (Figure 5).[42,43]

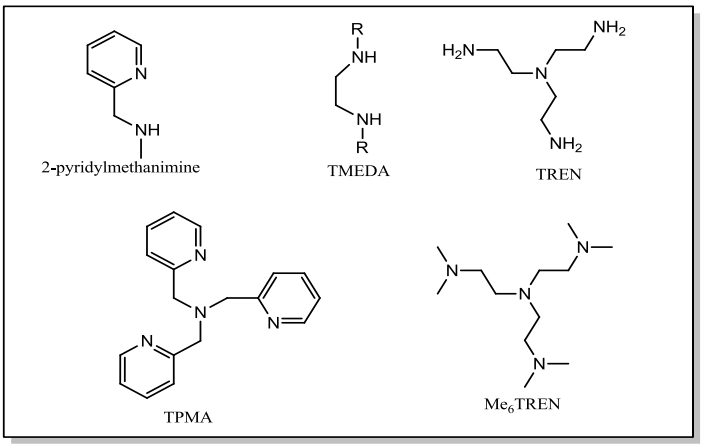

Figure 5. A selection of bidentate and multi-dentate nitrogen-based ligands developed for Cu(I)X mediated ATRP. [42, 43]

ATRP has been successfully utilised in the field of synthetic polymer chemistry however, suffers from two drawbacks. First, stoichiometric amount of copper catalyst is often needed meaning that the resulting polymer itself can also contain high trace of metal impurities. From an applications perspective, these contaminants could be undesirable, unless removed *via* some post-polymerisation process. Second,

ATRP system is sensitive to air. In other words, the oxygen sensitivity of the Cu(I) complexes typically employed for the polymerisation required careful deoxygenation of solvents and polymerisation vessels.

Efforts were directed toward reducing the catalyst loading and air-sensitivity of Cu(I) has led to the development of Activator Regenerated by Electron Transfer (ARGET-ATRP) and Initiators for Continuous Activator Regeneration (ICAR-ATRP).

1.5.5.2 Variation of ATRP

The living radical polymerisation by activators regenerated by electron transfer ATRP (ARGET-ATRP) was first reported in 2006 by Matyjaszewski and co-workers.[44, 45] The ARGET-ATRP possesses the advantages over standard ATRP as the amount of metal catalyst is significantly reduced and air-sensitivity is greatly eliminated in the system. This technique was found to be a good method for the synthesis of well-defined block copolymers or advanced polymeric structures. Having in mind, employing lower amount of required catalyst can be environmentally friendly and economically attractive.

ARGET-ATRP utilises a very small metal catalyst concentration (ppm) to improve the control over the polymerisation. In classic ATRP such small concentration would not be used due to inevitable bimolecular termination that accumulates the Cu (II) before being reduced back to the activating Cu(I) species. Therefore, ATRP process relatively requires high level of copper concentration in order to compensate a constant decrease in the Cu(I) caused by bimolecular termination which could eventually terminate the reaction. However, in ARGET-ATRP ppm quantities of catalyst continuously regenerated by a reducing agent in *situ* as shown in scheme 10.

The reduction of Cu (II) can be promoted in the presence of appropriate reducing agents such as glucose[46-48], ascorbic acid[49], phenol[50], hydrazine, phenylhydrazine[47], tin(II) 2-ethylhexanoate ($Sn(Oct)_2$)[45], excess of inexpensive ligands[51] and nitrogen containing monomers[52] or metallic Cu (see next section). Moreover, these reducing agents maintain the redox reaction cycle to proceed even in the presence of oxygen, allowing the normal ATRP to bring the polymerisation process back under control. It is noted that catalyst-induced side reactions can be also reduced to a significant degree, therefore the recently developed ATRP is able to drive the polymerisation/copolymerisation to higher conversion with high degrees of chain end functionality. [53-55]

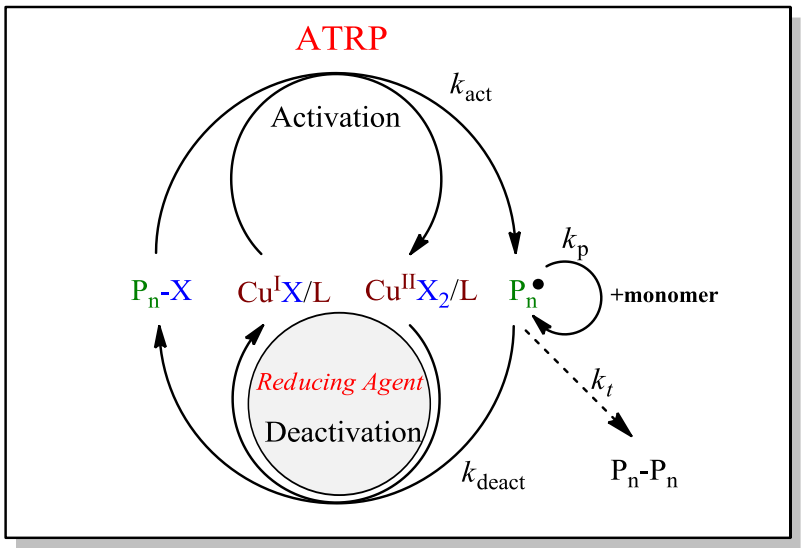

Scheme 10. Proposed mechanism for ARGET-ATRP. [55]

Another procedure to overcome the problems associated with the normal ATRP is the initiators for continuous activator regeneration (ICAR-ATRP) has been considered as a "reverse" ARGET-ATRP process or a reverse ATRP. In ICAR-ATRP the copper complex in its higher oxidation state Cu (II) and a source of

organic free radicals (*e.g.* AIBN) were employed as the starting components of process. Free radicals are slowly and continuously generated by conventional radical initiators throughout a polymerisation to reduce Cu (II) as a persistent radical and consequently generate Cu (I) activator (Scheme 11). A continuous addition of standard free radical promotes the copper complex in its lower oxidation state Cu (I) which would otherwise be consumed in chain terminations events, especially when the quantities of Cu (I) are used in very low concentrations. Therefore, ICAR-ATRP is governed by the slow release of radicals at lower temperatures so that overall radical concentration remains low and bimolecular termination is relatively diminished. For example, polystyrene and poly(meth)acrylates with low dispersity were produced by this technique employing low catalyst concentrations between 5 and 50 ppm.[57] The controlled addition of standard free radical initiators has driven the polymerisation to higher conversion while affording good control over molecular weights and molecular weight distributions.

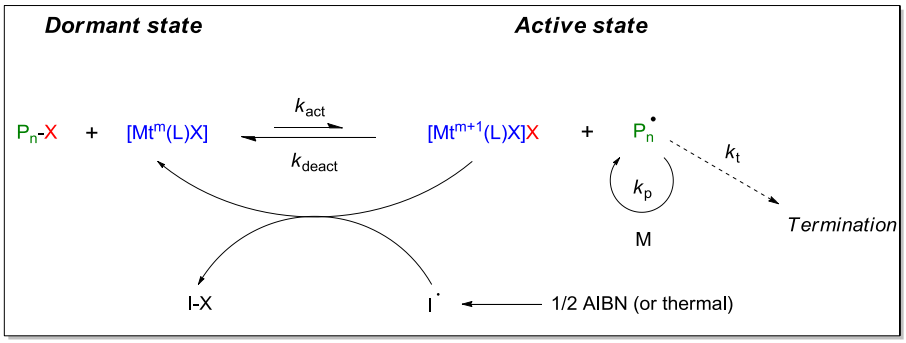

Scheme 11. Proposed mechanism for ICAR-ATRP. [57]

Although each method has great advantage and the amount of necessary copper catalyst is greatly reduced for the industrial viability, limitations also exist. Common limitations include a narrow pool of monomers from which to choose

from, the relatively long reaction times (> 24 h), the inability to reach higher monomer conversions (< 80 %) and the need to isolate macroinitiators from polymerisation mixtures requires sometimes, exhaustive purification steps prior to block copolymerisation.[58] Particularly, in reverse ATRP the external free radical initiator could initiate new chains which could then effect on the evolution of molecular weight.[48]

1.5.5.3 Single electron transfer living radical polymerisation (SET-LRP)

The term "Single electron transfer living radical polymerisation" (SET-LRP) was first introduced by Percec and co-workers in 2006.[59] The '*ultrafast*' synthesis of '*ultrahigh*' molecular weight polymers ($M_n > 1x10^6$) from activated monomers such as acrylates, methacrylates and vinyl chloride at 25°C was reported with excellent control over the molecular weight ($Đ = 1.1$). This developed technique facilitated by polar solvent such as DMSO, alcohols and water in the presence of nitrogen-based ligands and alkyl halide initiators previously used for ATRP and reverse ATRP. Moreover, a new polymerisation mechanism was discussed (Scheme 12).

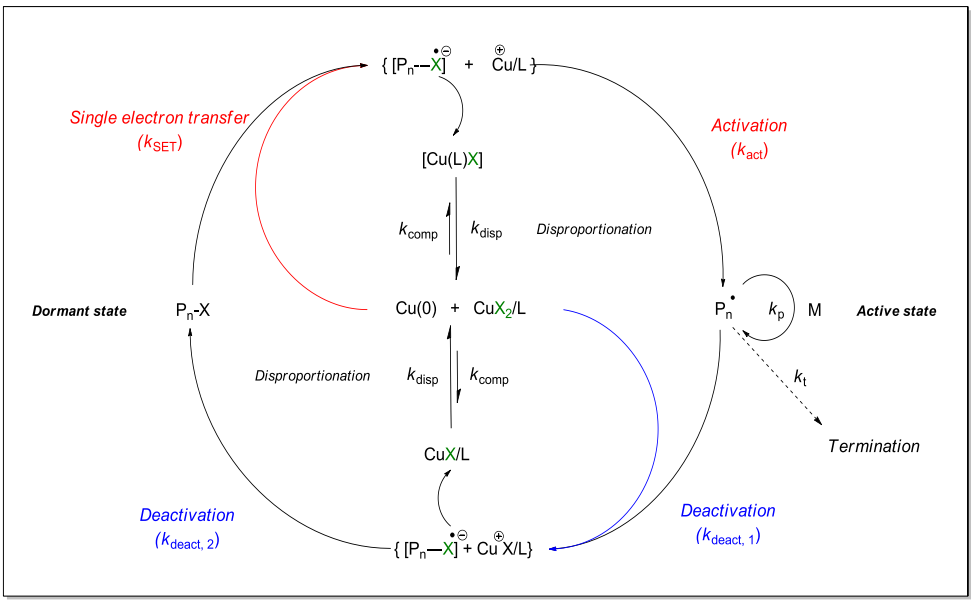

Scheme 12. Proposed mechanism for the SET-LRP. [59]

According to the mechanism proposed by Percec, SET-LRP (or Cu(0) mediated RDRP) is notionally similar to ATRP in which it involves an equilibrium between active (propagating chains) and dormant (halide terminated chains) species. However, the main difference is that the proposed activator is zero-valent copper rather than Cu(I). In SET-LRP Cu(0) activates alkyl halide by abstracting the halogen atom from the initiator *via* heterolytic outer-sphere electron transfer (OSET) process, whereas in ATRP the Cu(I) abstracts a halogen atom *via* a homolytic inner-sphere electron transfer from the dormant species to the copper to active the polymer chain.

The key step in the SET-LRP mechanism is the 'spontaneous' disproportionation of the Cu(I) halide species. According to Percec, the instantaneous and complete disproportionation of Cu(I)Br in the presence of nitrogen containing ligands generates both the activator Cu(0) and the deactivating Cu(II)Br_2 species that subsequently control the polymerisation. The Cu(I)Br is regenerated *in situ* when

'nascent' Cu(0) activates the dormant polymer chain which then rapidly undergoes disproportionation to again generate C(0) and the Cu(II) complex and the later can deactivate the new propagating polymer chain and so on. Based on this mechanism, polymer chains are not activated by Cu(I) as it instantaneously disproportionates into extremely reactive atomic Cu(0) and Cu(II).

Percec *et al.* used the UV-Vis technique to determine the extent of Cu(I)Br disproportionation with different *N*-containing ligand and solvent combinations. The typical disproportioning ligands are the aliphatic ligand such as Me_6TREN, TREN, and PMDETA and the most popular in the literature is Me_6TREN. These ligands stabilise Cu(II) which therefore push the position of k_{disp} towards the right. However, "non-disproportioning" ligands such as pyridine imine ligands and 2,2'-bipyridyl (Bipy) stabilise Cu(I). It is worthwhile to note that the equilibrium constants for the disproportionation rely primarily on the nature of the ligand and solvent which cooperatively and synergistically regulate the kinetics and control of SET-LRP.[59, 60]

1.5.5.4 Aspects of SET-LRP

The SET-LRP has proved to be highly effective methodology that allows for improving the synthesis of (co)polymers with predetermined structures, narrow MWDs, and high level retention of chain end functionalities. Recently, great interest has been devoted to SET-LRP, as it gives access to polymeric material libraries without the need of extensive purification of the reagents specifically in regard to monomer purification. This technique has showed excellent compatibility with catalyst, solvent and monomer.

SET-LRP is a catalytic system employing a metal complex, in which the facile interchange of the three different oxidation states of the transition metal is controlled by the appropriate ligands on the metal. The use of Cu(0) either in the form of powder or wire has been initially reported to be an efficient method due to the fact that the reaction rate can be tuned and the simplicity of the experimental setup.[61] Alternatively, several metallic catalytic sources have been studied, including iron (Fe)[62], nickel (Ni)[63], ytterbium (Yb)[64], lanthanum (La)[65], [66], gadolinium (Gd)[67], tin (Sn)[68], zinc (Zn)[69] and samarium (Sm)[70]. Among these catalytic sources, the most attractive catalysis may be Fe, since it is biocompatible, environmentally-friendly and its competitive cost. Utilising Fe as the catalyst, the controlled polymerisations of methyl methacrylate (MMA), styrene (St) and acrylonitrile (AN) were successfully conducted providing well-defined homo and block copolymers with narrow molecular weight distributions. Therefore, a larger diversity of transition metals was found to be compatible with SET-LRP.

Several organic solvents and water have also all demonstrated very good compatibility with SET-LRP and disproportionation providing excellent control over polymerisation. The most widely used solvent for SET-LRP is DMSO, as it enhances the polarity of the reaction mixture which therefore mediates electron transfer process. [71] In addition, it was recognized that DMSO could coordinate Cu(II)[72], enhancing the stability of deactivating species which then shift the position of k_{disp} towards the right, hence facilitating disproportionation. DMSO is the solvent of choice for Cu(0)-mediated polymerisation not only because of the aforementioned features, but also it dissolves a range of monomers and polymers. Other organic solvents that found to be compatible with SET-LRP are alcohols[73, 74] and DMF.[75] Also, many binary mixtures of disproportionating solvents have been used for

effective SET-LRP media (*e.g.* H_2O/MeOH mixtures[76], DMSO/H_2O[77] and DMF/H_2O[78]). Recently, the full disproportionation of [Cu(Me_6TREN)]Br was achieved in H_2O at ambient or below temperature providing a first order rate of polymerisation maintaining very high end-group functionality up to high monomer conversion.[79] This catalytic system provides a versatile and robust synthetic route for the synthesis of water-soluble polymers with unprecedented control over the acrylate and acrylamide polymerisation. Interestingly, SET-LRP has been proven to be tolerant even to a complex media such as commercial alcoholic beverages/solvents[80] (*e.g.*,beers, wines, spirits etc.) as well as biological media (specifically blood serum).[81]

A vast array of vinyl monomers is expected to be compatible with SET-LRP. Cu(0)-mediated polymerisation was initially employed for the polymerisation of methyl acrylate (MA) and vinyl chloride resulting in well-defined polymers.[59] The pool of monomers was subsequently expanded to include a wide range of monomers such as acrylates[82-98], methacrylates[59, 99-105], acrylamides[106-113], methacrylamides[114], and acrylonitrile[115]. Further, the functional monomers have been tested by this technique, for example, solketal acrylate[116] providing targeted polymers that could lead to various valuable applications. Last but not least, sugar monomers[117] were found to be compatible with SET-LRP system providing access to well-defined functional glycopolymers for applications in bioconjugation and biological targeting.

1.6 SET-LRP vs SARA-ATRP: The Mechanistic Debate

Since emergence of SET-LRP in 2006, there has been a growing interest in utilising and understanding the Cu(0)-mediated RDRP. Today, SET-LRP is one of the most

versatile polymer synthetic routes for providing high degrees of living/control characteristics to radical polymerisation, as evidenced by a large number of publications. Nevertheless, there has been a heated and continuous scientific debate in the polymer chemistry community over the true mechanistic process of Cu(0)-mediated RDRP.

The two proposed models are SET-LRP, proposed by Percec[59] and supplemental activator and reducing agent atom transfer radical polymerisation (SARA ATRP), proposed by Matyjaszewski.[118] Both systems are identical in which the same components are employed (*i.e.* metallic copper, acrylate monomers, alkyl halide initiators, polar solvents, amine ligands), but differ in terms of their proposed mechanisms. Both Pecec and Matyjaszewski claim to explain the role of the Cu(0) in the relatively fast polymerisation of monomers such as MA in polar solvents (*e.g.*, DMSO, water) in the presence of Cu(0) and ligands that form active Cu complexes. In order to confirm SET-LRP or SARA mechanisms, the effect of different components in the reaction mechanism have been investigated.

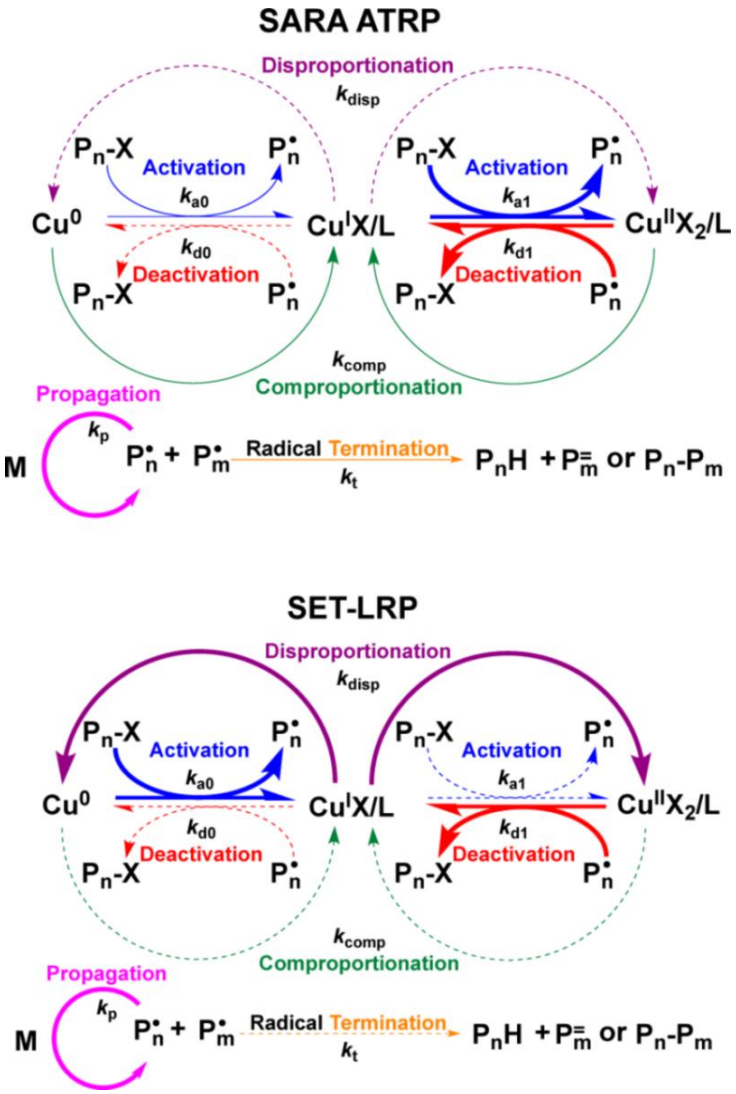

Scheme 13. Proposed mechanisms of SARA-ATRP and SET-LRP, according to Matyjaszewski et al.[119] Bold arrows indicate dominating reactions, thin solid arrows indicate contributing reactions and dashed arrows indicate reactions that have minimal contribution and can be neglected. k_{an} and k_{dn} are the rate constant of activation and deactivation respectively, involving a metal in the transitional state n (with n a integer). k_{disp} and k_{comp} are the rate constants of disproportionation and comproportionation respectively.

Percec and co-workers propose that Cu(0)[59] or ‘’nascent’’ Cu(0) particles[120, 121] is the predominant activating species of alkyl halides. According to this mechanism, Cu(I) mediated by the appropriate choice of *N*-ligand and solvent (polar solvent, Cu(II) stabilising ligands) in which it instead undergoes rapid/instantaneous and complete

disproportionation, thus no major activation occurs *via* Cu(I) complexes. In other words, the CuBr by itself or generated *in situ* by activation through Cu(0) wire or powder will instantaneously disproportionate into ‘’nascent’’ extremely reactive Cu(0) nanoparticles and $CuBr_2$ (Scheme 13). Moreover, this activation step is suggested to occur *via* an OSET mechanism through a radical anion intermediate.[59] This is supported by “lifting” and “decanting” experiments so that SET-LRP of MA in DMSO interrupted by removing Cu(0) wire, indicating that the Cu(0) generated by disproportionation plays a critical role for the activation of polymerisation.[121, 122] In these experiments the disproportionation reaction occurs quite rapidly relative to polymerisation time scales and a maximum amount of disproportionation occurs when [CuBr] : [Me_6TREN], [1] : [0.5] utilised.[122] Therefore, solvents that facilitate the disproportionation are required for excellent controlled living radical polymerisation as non-disproportionating solvents (such as toluene, acetonitrile) lead to the lack of first order kinetics, broad MWDs and significant loss of bromide chain-end functionality.

In contrast, Matyjaszewski argues that the Cu(0) is *merely* a supplemental activator and reducing agent (SARA), and much less active than Cu(I), therefore, the Cu(I) species formed *in situ* are the major activator of alkyl halides. [124, 125] Interestingly, he stated that to match the activity of 1 mM [Cu(Me_6TREN)]Br in DMSO, 2000 m of Cu(0) wire, with diameter 0.25 mm would be required.[126] Based on the Matyjaszewski’s perspective, the Cu(0) can also reduce Cu(II) to regenerate Cu(I) as a reducing agent, *via* comproportionation. Additional experiments showed that polymerisations in the presence of disproportionating ligand (Me_6TREN, which stabilises Cu(II)) or non-disproportionating ligand (TPMA, which stabilises Cu(I)) both proceeded in controlled manner resulting in well-defined polymer with narrow

MWDs[124, 127] , indicating that the polymerisations occur through the SARA ATRP mechanism even in the presence of Me_6TREN ligand. It is also shown that the fast polymerisation rate in DMSO in compare to MeCN is attributed to the higher k_{ATRP} in DMSO compared to less polar solvents.[127] Furthermore, under typical ATRP conditions (excess of [ligand]) comproportionation dominates over disproportionation and hence, Cu(I) actives alkyl halide rather than undergoing the disproportionation step. [124, 128, 129] Electrochemical studies were also reported to demonstrate that the activation event also occurs *via* an inner sphere electron transfer (ISET). [130]

However, in "lifting" and "decanting" experiments, Percec describes that the reaction mixture is carefully decanted into another vessel so that the whole flask content is separated from the Cu(0) catalyst. If the comproportionation dominates over disproportionation, the decanted mixture still contains soluble Cu(I) species. Since Cu(I) is an activator under these conditions then it would be expected that the reaction would still proceed to some extent. However, it was found that the reaction completely ceased, supporting the view that CuBr could not be the active catalyst as soluble Cu(I) and that Cu(0) is the major activator and disproportionation dominates comproporportion. [121-122]

Matyjaszewski and co-workers further dispute these findings by reporting that the ATRP is subject to the persistent radical effect (PRE), so that the very low concentrations of Cu(I) and Cu(II) exist in the reaction mixture cannot facilitate the reaction due to rapid termination resulting from the irreversible formation of Cu(II). Conversely, Percec argues that a continuous increase of [$CuBr_2$] throughout SET-LRP reactions suggested no comproportionation or reduction of $CuBr_2$ during the entire polymerisation process.[131] In addition, ^{1}H NMR of the polymerisation (from

10 - 95% conversion) were reported to have '100%' end group fidelity, indicating that bimolecular termination, which is required to provide the PRE in ATRP, was not responsible for the production of Cu(II). Thus, Cu(I) is not an activator in this process. This was also disputed by Matyjaszewski by reporting that SET-LRP violates the principle of halogen conservation.[132]

Table 1. Comparison of the various processes between SET-LRP and SARA-ATRP, reproduced from reference 133.

SET-LRP	SARA-ATRP
Differences	
Cu(0) is the main activator	Cu(I) is the main activator
similar monomers, SARA-ATRP except vinyl acetate	acrylates, methacrylates, acrylonitrile, acrylamide, methacrylamides
outer sphere single electron transfer (OSET)	inner sphere single electron transfer (ISET)
requires disproportionation solvents	disproportionation and non-disproportionation solvents
proceeds in the absence of termination, giving ultrafast polymerisation and ultrahigh molecular weight. (Complete preservation of chain end functionality at full conversion)	minimal extent of termination build-up of $CuBr_2$ species is directly correlated with loss of end-group functionality
Similarities	
Cu(II) is the deactivator	
similar initiators	
oxygen tolerant	

As such, the mechanism of copper-mediated living radical polymerisation has caused controversy, therefore, it is hard to draw definite conclusion. This system is rather complex and complicated due to the existing of both proposed catalysts in the reaction mixture. The following chapters discuss individually the pieces of the complicated system; however, the system must be entirely analysed in order to gain

a better understanding of the reaction. Regardless of the mechanistic differences, Cu(0)-mediated polymerisations has proven to be powerful technique providing the highest quality products for the desired polymeric materials as evidenced by the next experimental chapter.

1.7 Sequence control in mutiblock copolymer synthesis

1.7.1 Introduction

In the past, the discovery of steel (alloy) by heating iron in the presence of coal yielding a much stronger metal revolutionised the structural engineering. At present, macromolecular scientists seem to be heading towards a similar revolution at a much higher pace. Polymers of any combination of monomers display a range of properties due to the fact that the combination of monomers with different properties confined in that polymers.

Block copolymers are composed of two or more polymeric chains covalently linked together that can be found in different compositions and/or architectures ranging from simple AB-type linear structures to more complex structures such as multiblock copolymer stars.[134] The inherent immiscibility of different polymer blocks creates unique and useful properties so that the block copolymers undergo microphase separation in the solid state and in thin films.[135, 136] In solution, block copolymers enable to form micelles upon environmental changes (*i.e.* the solvent, temperature and pH are selective for one of the blocks).[135, 136] Evidently, the ability of block copolymers to form different micellar morphologies relies on changing the molecular weight, chemical structure, molecular architecture, and composition of

block copolymers. Due to these desirable properties, the possible applications for block copolymers have been tested in a range of very diverse areas including, chemistry, physics, materials science, as well as the biological and medical sciences.[137]

The discovery of the living character of anionic polymerisation has unveiled various approaches that have significantly enhanced the ability of designing targeted and tailored block copolymers and multiblock copolymers for a facile purification procedure. Block copolymers of predetermined block length and sequence can be synthesized by RDRP techniques including NMP, RAFT and ATRP.[138, 139] The sequential addition of a new aliquot of monomer following full consumption of the previous monomeric species is the widely used approach during controlled copolymerisation. However, when the polymerisations are allowed to proceed to higher conversions (> 90%), the loss of terminal functionality of polymer chains can be observed, compromising the integrity of the copolymer chain structures.[138, 139] Therefore, these polymeric chains must be isolated and purified from unreacted monomers/catalyst prior to a new monomer addition in order to form the next block. Consequently, the synthesis of multiblock copolymers requires multiple purification steps, minimising the number of blocks as well as the degree of control over multiblock copolymerisation. Hence, the development of sequence-controlled multiblock copolymerisation based on one-pot polymerisation protocol *via* iterative monomer addition is needed.

Recently, Cu(0)-mediated polymerisations has demonstrated an unprecedented maintenance of end group functionality even at very low concentrations of monomer in the polymerisation process.[140] Inevitably, in any radical polymerisation system, termination reactions always happen due to the reactive nature of the radicals;

however, Cu(0)-mediated polymerisation approach has an advantage over RDRP techniques in that the radical tendency is suppressed to the lower concentrations. Cu(0) polymerisation of acrylamides had not been reported and the sequence controlled multiblocks of acrylamide based monomers would be advantageous for many applications. Thus, the first experimental chapter of this thesis will aim to investigate the compatibility of this technique with new and useful monomers towards the synthesis of new mutiblock copolymers.

1.7.2 Multiblock copolymers in organic media

In 2011, Whittaker *et al* [141] for the first time employed Cu(0)-mediated polymerisation as a tool to prepare high-order multiblock copolymers at ambient temperature in DMSO (Scheme 14). The copolymers (consisting of four types of acrylates), were synthesised *via* sequential monomer addition in order to build multiblock copolymers model P(MA-*b*-MA...) homopolymer and P(MA-*b*-nBuA-*b*-EA-*b*-2EHA- *b*-EA-*b*-nBuA), so that each block comprises of very discreet blocks (ideally two monomer units). Interestingly, this communication illustrates that full monomer conversion can be achieved, reflecting the robustness of this technique. The molecular weight distributions remained relatively narrow (Đ ~ 1.2) after monomer additions (24 h per block), confirming the well-controlled nature of the polymerisation without the need for any purification steps. The successful and straightforward synthesis of sequence-controlled multiblock copolymers in a one-pot polymerisation reaction *via* iterative monomer addition paved the way for the design and synthesis of a new generation of synthetic polymers.

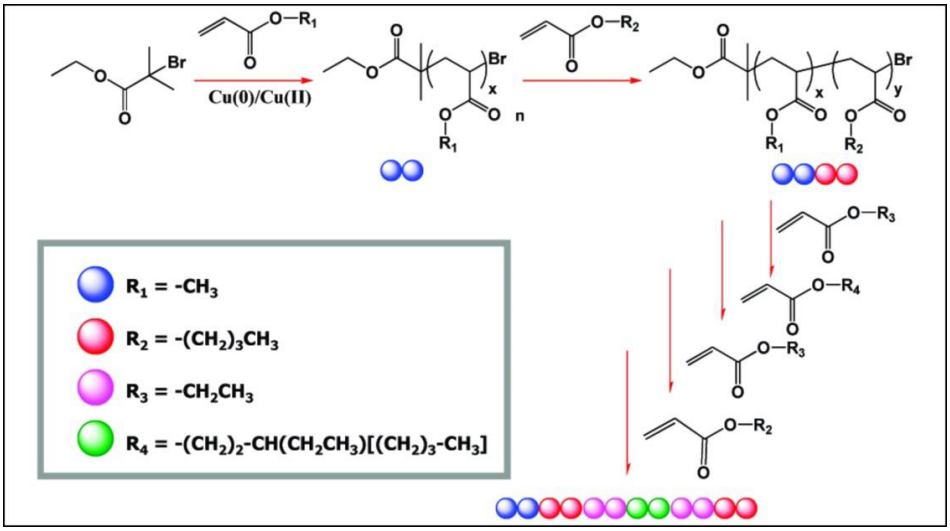

Scheme 14: Schematic representation of the synthesis of sequence-controlled multiblock copolymers in a one-pot polymerisation reaction as illustrated by Whittaker[141].

The retention of high end-group functionality associated with Cu(0)-mediated polymerisation was subsequently exploited by Whittaker and co-workers[134] to synthesize multiblock copolymer stars. A multifunctional core initiator was used which could lead to side reactions such as star-star coupling. In order to circumvent this undesirable side effect, an external amount of $CuBr_2$ initially added confirming the crucial role of deactivating species ratio and providing a pentablock star copolymer with unprecedented level of control over chain lengths.

Later, the same group utilized a similar approach for the synthesis of a decablock copolymer. However, the broad molecular weight distributions were obtained (Đ ~ 1.72) with non-quantitative conversion. Additionally, the effect of some parameters, such as the degree of polymerisation (DP) of each block and the number of cycles, on livingness has been estimated by GPC and ^{1}H NMR analysis of the synthesised decablock copolymers of these acrylates.[142] To overcome this limitation, another study was subsequently carried out by Whittaker group and Haddleton group

optimising the catalytic system (*i.e.* [$CuBr_2$] and [Me_6TREN],) to synthesise higher molecular weight block homopolymers and copolymers of different acrylates (each block $DP_n \approx 100$). Narrow dispersities were achieved (< 1.2) up to the sixth block, whereas the conversion of monomer (each block) was 92-100%.[143]

Moreover, multiblock glycopolymers (the degree of polymerisation (DP) = 2 for each single block, $(mannose)_2$-$(glucose)_2$-$(mannose)_2$-$(glucose)_2$-$(mannose)_2$-$(glucose)_2$) were prepared.[144] The copolymerisation was performed in DMSO at 25ºC and the total reaction time was 46 h resulted in good degree of control over the molecular weight distributions. Finally, Haddleton and Junkers have recently exploited Cu-mediated light induced system to report the successful synthesis of one-pot sequence-controlled multiblock copolymers *via* iterative addition at ambient temperature. [145, 146]

1.7.3 Multiblock copolymers in aqueous media

To be able to conduct aqueous RDRP, all reaction components including, initiator, radical mediator, monomer and polymer should be soluble in the reaction medium. A wide range of hydrophilic monomers such as 2- hydroxyethyl (meth)acrylate (HEMA, HEA), 2-hydroxyethyl (meth)acrylamide (HEMAA) and oligo(ethylene glycol) methacrylate (PEGA) have been tested to polymerise *via* RDRP in aqueous solutions (Figure 6).

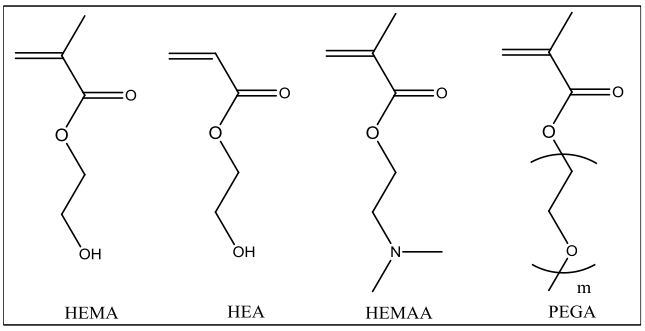

Figure 6. Monomers polymerisable by NMP and ATRP in aqueous solution.

In the last two decades, significant progress in the field of reversible-deactivation radical polymerisation has been achieved; however the RDRP of water-soluble monomers in pure aqueous media at or below ambient temperature remains a challenge.[147-152] Generally, in pure water, the RDRP process is fast and uncontrolled due to the high polarity of water causing high rates of activation and propagation steps and effecting on equilibrium between the dormant and active chain species. Therefore, uncontrollable radical concentrations can result in side reactions and termination events. Specifically, copper mediated ‘’living’’ radical polymerisation (CM-LRP) relies on careful manipulation of an equilibrium existing alkyl haileds (P_n–X) and macroradicals ($P_n^{\bullet}$) species, which is mainly mediated by Cu-ligand complexes. This limitation can be alleviated by performing the CM-LRP in the presence a cosolvent (usually an alcohol).[152] The polymerisation of acrylamide monomer and its derivatives are further complicated by undesirable termination reactions that lead to loss of ω-Br chain end functionality.[153-156]

The CM-LRP of acrylamide based monomers seems problematic with regard to the control of the polymerisation when water was employed as the only solvent at ambient temperature. [157, 158] Furthermore, in the literature few publications have reported controlled block copolymerisation and they are limited to just diblock.

Brittain *et al*. were reported the aqueous ATRP of dimethacrylamide employing a different copper salts[153]. Broad molecular weight distributions, poor agreement between theoretical and experimental M_n, and end group analysis were attributed to the fact that the Cu salts complex to the amide group of the chain ends and stabilise the radical which then the concentration of radical is increased causing ‘’spontaneous’’ termination reactions .

Broekhuis and coworkers, also employed ATRP method for acrylamide homopolymers and subsequent block copolymers with *N*-isopropylacrylamide in aqueous media at 25°C. However, broad molecular weight distribution was achieved (Đ < 1.48) and the final conversion was non-quantitative (~ 80%).[157] Another attempt by Kakuchi and coworkers, utilising similar method with different acrylamide monomers in mixed organic-aqueous solvent resulted in loss of control (*Đ* = 1.19-2.12) and the conversions were not quantitative. [158]

An alternative approach towards the one-pot synthesis of multiblock copolymers employs RAFT as a polymerisation tool. Perrier and co-workers[159-162] reported the synthesis of an icosablock (20 blocks), with each block comprising of three monomer units on average formed by three sorts of acrylamide monomers, namely *N*,*N*-dimethylacrylamide (DMA), 4-acryloylmorpholine (NAM) and *N*,*N*-diethylacrylamide (DEA). The highly efficient one-pot polymerisations were conducted in both organic (dioxane) and aqueous media at temperature (70ºC). Although this is a significant addition to the copolymerisation field, its utility potentially offset by the high reaction temperature. In addition, at this temperature polymerisation of other monomers (*e.g.* acrylates) would result in increased termination and side reactions that could limit the monomer pool to only acrylamides.[163]

The following chapter presents, for the first time, an unprecedented level of control for a variety of water-soluble block polymers and multiblock copolymers in a simple and efficient one-pot polymerisation. High and low molecular weight copolymers were synthesised, with each block reaching full conversion within less than 4 hours. Moreover, Cu(0)-mediated living radical polymerisation approach was performed at, or below, ambient temperature in water as a reaction medium, offering many applications that potentially take advantage of both the chemical and physical properties of water.

1.8 References

1. H. Staudinger, Ber. Dtsch. *Chem. Ges.*, 1920, **53**, 1073-1085.
2. P. J. Flory, *J. Am. Chem. Soc*., 1937**, 59**, 241-253.
3. G. Odian, Principles of Polymerisation, 4th Edition, Wiley, 2004.13. J. D. Druliner, *Macromolecules*, 1991, **24**, 6079-6082.
4. J. W. Nicholson, *The Chemistry of Polymers*, 2nd Edition, RSC Paperbacks, 1997.
5. A. A. Gridnev and S. D. Ittel, *Macromolecules*, 1996, **29**, 5864-5874.
6. V. N. Kondratiev, Chain Reactions, Comprehensive Chemical Kinetics, *Elsevier*, 1969.
7. M. Kamachi, J. Satoh and S. I. Nozakura, *J. Polym. Sci. Part A: Polym. Chem*., 1978, **16**, 1789-1800.
8. G. F. Santee, R. H. Marchessault, H. G. Clark, J. J. Kearny and V. Stannett, Macromol. *Chem. Phys*., 1964, **73**, 177-187.
9. G. V. Schulz and F. Blaschke, Z. *Phys. Chem*, 1942, **51**, 75.
10. M. Szwarc, M. Levy and R. Milkovich, *J. Am. Chem. Soc.*, 1956**, 78**, 2656-2657.
11. M. Szwarc, *J. Polym. Sci. Part A: Polym. Chem*., 1998, **36**, ix-xv.
12. M. Szwarc, *J. Polym. Sci. Part A: Polym. Chem*., 1998, **36**, v-xiii.
13. M. Szwarc, Nature, 1956, 178, 1168-1169
14. E. De León-Sáenz, G. Morales, R. Guerrero-Santos and Y. Gnanou, *Macromol. Chem.Phys.*, 2000, **201**, 74-83.
15. B. Yamada, Y. Nobukane and Y. Miura, *Polym. Bull*., 1998, **41**, 539-544.
16. M. Steenbock, M. Klapper and K. Müllen, Macromol. *Chem. Phys*., 1998, **199**, 763-769.
17. D. Jenkins Aubrey, G. Jones Richard and G. Moad, in *Pure Appl. Chem*.,2009, **82**, 483.
18. D. H. Solomon, E. Rizzardo, P. Cacioli, US **4581429**, 1986.
19. M. K. Georges, R. P. N. Veregin, P. M. Kazmaier and G. K. Hamer, *Macromolecules*, 1993, **26**, 2987-2988.

20. R. D. Puts and D. Y. Sogah, *Macromolecules*, 1996, **29**, 3323-3325.
21. J. Chiefari, Y. K. Chong, F. Ercole, J. Krstina, J. Jeffery, T. P. T. Le, R. T. A. Mayadunne, G. F. Meijs, C. L. Moad and G. Moad, *Macromolecules*, 1998, **31**, 5559-5562.
22. Chiefari, J.; Chong, Y. K., et al. *Macromolecules*, 1998, **31(16)**, 5559-5562.
23. Moad, G.; Chiefari, J., et al. *Polym. Int*., 2000, **49(9)**, 993-1001.
24. G. Moad, E. Rizzardo and S. H. Thang, *Aust. J. Chem*., 2005, **58**, 379-410.
25. G. Moad, E. Rizzardo and S. H. Thang, *Aust. J. Chem*., 2009, **62**, 1402-1472.
26. D. J. Keddie, *Chem. Soc. Rev.*, 2014, **43**, 496-505.
27. G. Gody, T. Maschmeyer, P. B. Zetterlund and S. Perrier, *Nat. Commun*., 2013, **4**. 2505-2513
28. G. Gody, T. Maschmeyer, P. B. Zetterlund and S. Perrier, *Macromolecules*, 2014, **47**, 3451-3460.
29. L. Martin, G. Gody and S. Perrier, *Polym. Chem*., 2015, **6**, 4875-4886.
30. C. Barner-Kowollik, T. P. Davis, J. P. A. Heuts, M. H. Stenzel, P. Vana and M. Whittaker, *J. Polym. Sci., Part A: Polym. Chem*., 2003, **41**, 365-375.
31. A. Kabachii, Y. Kochev, M. Bronstein, B. Blagodatskikh, M. Valetsky. *Polym. Bull* 2003, **50**, 271–8.
32. M. Brandts, P. van de Geijn, E. van Faassen, J. Boersma, G. Van Koten. *J Organomet. Chem*., 1999, **584**, 246–53.
33. T Ando, M. Kamigaito, M. Sawamoto. *Macromolecules*, 1997, **30**, 4507–10.
34. K. Matyjaszewski, J. Xia. *Chem. Rev.,* 2001, **101**, 2921–90.
35. J.-S. Wang and K. Matyjaszewski, *J. Am. Chem. Soc*., 1995, **117**, 5614-5615.
36. M. Kato, M. Kamigaito, M. Sawamoto and T. Higashimura, *Macromolecules*, 1995, **28**, 1721-1723
37. S. Kharasch,, H. Urry, V. Jensen, *J. Am. Chem. Soc.*, 1945, **67(9)**, 1626-1626.
38. C. Y. Lin, M. L. Coote, A. Gennaro and K. Matyjaszewski, *J. Am. Chem. Soc*., 2008, **130**, 12762-12774.
39. H. Fischer, *Macromolecules*, 1997, **30(19)**, 5666-5672.
40. K. Matyjaszewski. *J. Phys. Org. Chem.* 1995, **8(4)**, 197-207.
41**.** P. A. Gurr, M. F. Mills, G. G. Qiao and D. H. Solomon, *Polymer*, 2005, **46**, 2097-2104.
42. D. M. Haddleton, M. C. Crossman, B. H. Dana, D. J. Duncalf, A. M. Heming, D. Kukulj and A. J. Shooter, *Macromolecules*, 1999, **32**, 2110-2119.
43. D. M. Haddleton, C. B. Jasieczek, M. J. Hannon and A. J. Shooter, *Macromolecules*, 1997, **30**, 2190-2193.
44. K. Matyjaszewski, W. Jakubowski, K. Min, W. Tang, J. Huang, W. A. Braunecker and N.V. Tsarevsky, *Proc. Natl. Acad. Sci*., 2006, **103**, 15309-15314.
45. W. Jakubowski, K. Min, K. Matyjaszewski, *Macromolecules*, 2006, **39**, 39.
46. A. de Vries, B. Klumperman, D. de Wet-Roos and R. D. Sanderson, *Macromol. Chem. Phys*., 2001, **202**, 1645-1648.
47. K. Matyjaszewski, W. Jakubowski, K. Min, W. Tang, J. Huang, W. A. Braunecker and N. V. Tsarevsky, *P. Natl. Acad. Sci*. USA., 2006, **103**, 15309-15314.
48. W. Jakubowski and K. Matyjaszewski, *Angew. Chem. Int. Ed*., 2006, **45**, 4482-4486.
49. K. Min, H. Gao and K. Matyjaszewski, *Macromolecules*, 2007, **40**, 1789-1791.
50. Y. Gnanou and G. Hizal, *J. Polym. Sci., Part A: Polym. Chem*., 2004, **42**, 351-359.
51. Y. Kwak, A. J. D. Magenau and K. Matyjaszewski, *Macromolecules*, 2011, **44**, 811-819.

52. H. Dong and K. Matyjaszewski, *Macromolecules*, 2008, **41**, 6868-6870.
53. J. Pietrasik, H. Dong and K. Matyjaszewski, *Macromolecules*, 2006, **39**, 6384-6390.
54. H. Dong, W. Tang and K. Matyjaszewski, *Macromolecules*, 2007, **40**, 2974-2977.
55. L. Mueller, W. Jakubowski, W. Tang and K. Matyjaszewski, *Macromolecules*, 2007, **40**, 6464-6472.
56. W. Jakubowski and K. Matyjaszewski, *Angew. Chem., Int. Ed.*, 2006, **45**, 4482-4486.
57. K. Matyjaszewski, W. Jakubowski, K. Min, W. Tang, J. Huang, W. A. Braunecker and N.V. Tsarevsky, *Proc. Natl. Acad. Sci.*, 2006, **103**, 15309-15314.
58. A. Anastasaki, V. Nikolaou, G. Nurumbetov, P. Wilson, K. Kempe, J. F. Quinn, T. P. Davis, M. R. Whittaker and D. M. Haddleton, *Chem. Rev.*, 2016, **116**, 835−877
59. V. Percec, T. Guliashvili, J. S. Ladislaw, A. Wistrand, A. Stjerndahl, M. J. Sienkowska, M. J. Monteiro and S. Sahoo, *J. Am. Chem. Soc.*, 2006, **128**, 14156-14165.
60. M. Rosen; V.Percec, *J. Polym. Sci., Part A: Polym. Chem*. 2007, **45(21)**, 4950-4964.
61. N. H. Nguyen, B. M. Rosen, G. Lligadas and V. Percec, *Macromolecules*, 2009, **42**, 2379-2386.
62. L. Zhou, Z. Zhang, W. Wang, Z. Cheng, N. Zhou, J. Zhu, W. Zhang and X. Zhu, J. *Polym. Sci., Part A: Polym. Chem*., 2012, **50**, 936-943.
63. X.-H. Liu, Y.-H. Yu, D. Jia, B.-W. Cheng, F.-J. Zhang, H.-N. Li, P. Chen and S. Xie, J.
Polym. Sci., Part A: Polym. Chem., 2013, **51**, 1559-1564.
64. D. Liu, J. Ma, H. Chen, P. Yin, N. Ji and G. Zong, *J. Polym. Sci., Part A: Polym. Chem.*, 2011, **49**, 5109-5115.
65. J. Zhang, Z. Hao and H. Chen, *J. Polym. Sci., Part A: Polym. Chem.*, 2013, **51**, 3323-3327.
66. Z. Hao, J. Zhang, H. Chen, D. Liu, D. Wang, H. Qu and J. Lang, *J. Polym. Sci., Part A: Polym. Chem.*, 2013, **51**, 4088-4094.
67. D. Liu, H. Chen, P. Yin, Z. Hao and L. Fan, *J. Polym. Sci., Part A: Polym. Chem.*, 2012, **50,** 4809-4813.
68. Z. Hao, H. Chen, D. Liu and L. Fan, *J. Polym. Sci., Part A: Polym. Chem.*, 2012, **50**, 4995-4999.
69. Y.-H. Yu, X.-H. Liu, D. Jia, B.-W. Cheng, F.-J. Zhang, H.-N. Li, P. Chen and S. Xie, J. *Polym. Sci., Part A: Polym. Chem.*, 2013, **51**, 1468-1474.
70. H. Chen, G. Zong, L. Chen, M. Zhang, C. Wang and R. Qu, *J. Polym. Sci., Part A: Polym. Chem.*, 2011, **49**, 2924-2930.
71. C. A. Bell, M. R. Whittaker, L. R. Gahan and M. J. Monteiro, *J. Polym. Sci., Part A: Polym. Chem.,* 2008, **46**, 146-154.
72. S. Monge, V. Darcos and D. M. Haddleton, *J. Polym. Sci., Part A: Polym. Chem.*, 2004, **42,** 6299-6308.
73. G. Lligadas, V.Percec, *J. Polym. Sci., Part A: Polym. Chem*. 2008, **46**, 2745−2754.
74. N. Nguyen, V. Percec, *J. Polym. Sci., Part A: Polym. Chem.* 2011, **49**, 4756−4765.
75. L. Voorhaar, S. Wallyn, F. E. Du Prez, R. Hoogenboom, *Polym. Chem.* 2014, **5**, 4268−4276.

76. X. Leng, N. H. Nguyen, B. van Beusekom, D. A.Wilson, V. Percec, *Polym. Chem.* 2013, **4**, 2995−3004.
77. N. H Nguyen, X. Leng, H.-J. Sun, V. Percec, *J. Polym. Sci., Part A: Polym. Chem.* 2013, **51**, 3110−3122.
78. W. Ding, C.Lv, Y. Sun, X. Liu, T. Yu, G. Qu, H. Luan, *J. Polym. Sci., Part A: Polym. Chem.* 2011, **49**, 432−440.
79. Q. Zhang, P. Wilson, Z. Li, R. McHale, J. Godfrey, A. Anastasaki, C. Waldron and D. M. Haddleton, *J. Am. Chem. Soc.*, 2013, **135**, 7355-7363.
80. C. Waldron, Q. Zhang, Z. Li, V. Nikolaou, G. Nurumbetov, J. Godfrey, R. McHale, G. Yilmaz, R. K. Randev, M. Girault, K. McEwan, D. M. Haddleton, M. Droesbeke, A. J. Haddleton, P. Wilson, A. Simula, J. Collins, D. J. Lloyd, J. A. Burns, C. Summers, C. Houben, A. Anastasaki, M. Li, C. R. Becer, J. K. Kiviaho and N. Risangud, *Polym. Chem.*,2014, **5**, 57-61.
81. Q. Zhang, Z. Li, P. Wilson and D. M. Haddleton, *Chem. Commun.*, 2013, **49**, 6608-6610.
82. B. M. Rosen and V. Percec, *Chem. Rev*., 2009, **109**, 5069-5119.
83. V. Percec, T. Guliashvili, J. S. Ladislaw, A. Wistrand, A. Stjerndahl, M. J. Sienkowska, M. J. Monteiro and S. Sahoo, *J. Am. Chem. Soc.*, 2006, **128**, 14156-14165.
84. N. H. Nguyen, B. M. Rosen, G. Lligadas and V. Percec, *Macromolecules*, 2009, **42**, 2379-2386.
85. X. Jiang, B. M. Rosen and V. Percec, *J. Polym. Sci., Part A: Polym. Chem*., 2010, **48**, 403-409.
86. G. Lligadas and V. Percec, *J. Polym. Sci., Part A: Polym. Chem*., 2007, **45**, 4684-4695.
87. N. H. Nguyen, M. E. Levere and V. Percec, *J. Polym. Sci., Part A: Polym. Chem*., 2012, **50**, 860-873.
88. S. Zhai, B. Wang, C. Feng, Y. Li, D. Yang, J. Hu, G. Lu and X. Huang, *J. Polym. Sci., Part A: Polym. Chem.*, 2010, **48,** 647-655.
89. X. Leng, N. H. Nguyen, B. van Beusekom, D. A. Wilson and V. Percec, *Polym. Chem.*, 2013, **4**, 2995-3004.
90. S. Zhai, J. Shang, D. Yang, S. Wang, J. Hu, G. Lu and X. Huang, *J. Polym. Sci., Part A: Polym. Chem.*, 2012, **50**, 811-820.
91. S. Zhai, X. Song, D. Yang, W. Chen, J. Hu, G. Lu and X. Huang, *J. Polym. Sci., Part A: Polym. Chem.*, 2011, **49**, 4055-4064.
92. A. Anastasaki, C. Waldron, V. Nikolaou, P. Wilson, R. McHale, T. Smith and D. M. Haddleton, *Polym. Chem.*, 2013, **4**, 4113-4119.
93. C. Boyer, A. Atme, C. Waldron, A. Anastasaki, P. Wilson, P. B. Zetterlund, D. Haddleton and M. R. Whittaker, *Polym. Chem.*, 2013, **4**, 106-112.
94. M. J. Monteiro, T. Guliashvili and V. Percec, *J. Polym. Sci., Part A: Polym. Chem.*, 2007, **45**, 1835-1847.
95. G. Lu, Y. Li, H. Gao, H. Guo, X. Zheng and X. Huang, *J. Polym. Sci., Part A: Polym. Chem.*, 2013, **51**, 1099-1106.
96. G. Lu, Y. Li, H. Guo, W. Du and X. Huang, *Polym. Chem*., 2013, **4**, 3132-3139.
97. G. Lu, Y. Li, B. Dai, C. Xu and X. Huang, *J. Polym. Sci., Part A: Polym. Chem.*, 2013, **51**,1880-1886.
98. C. Boyer, A. Derveaux, P. B. Zetterlund and M. R. Whittaker, *Polym. Chem.*, 2012, **3**, 117-123.
99. G. Chen, P. M. Wright, J. Geng, G. Mantovani and D. M. Haddleton, *Chem. Commun*., 2008, **9**, 1097-1099.

100. M. W. Jones, M. I. Gibson, G. Mantovani and D. M. Haddleton, *Polym. Chem.*, 2011, **2**, 572-574.
101. S. Fleischmann and V. Percec, *J. Polym. Sci., Part A: Polym. Chem.*, 2010, **48**, 4884-4888.
102. S. Fleischmann and V. Percec, *J. Polym. Sci., Part A: Polym. Chem.*, 2010, **48**, 2236-2242.
103. N. H. Nguyen, X. Leng and V. Percec, *Polym. Chem.*, 2013, **4**, 2760-2766.
104. X. Song, Y. Zhang, D. Yang, L. Yuan, J. Hu, G. Lu and X. Huang, *J. Polym. Sci., Part A: Polym. Chem.*, 2011, **49**, 3328-3337.
105. Y. Deng, Y. Li, J. Dai, M. Lang and X. Huang, *J. Polym. Sci., Part A: Polym. Chem.*, 2011, **49**, 4747-4755.
106. N. H. Nguyen, B. M. Rosen and V. Percec, J. Polym. Sci., Part A: Polym. Chem., 2010, 48, 1752-1763.
107. X. Tang, X. Liang, Q. Yang, X. Fan, Z. Shen and Q. Zhou, *J. Polym. Sci., Part A: Polym. Chem.*, 2009, **47**, 4420-4427.
108. Y. Deng, J. Z. Zhang, Y. Li, J. Hu, D. Yang and X. Huang, *J. Polym. Sci., Part A: Polym. Chem.*, 2012, **50**, 4451-4458.
109. C. Feng, Y. Li, D. Yang, Y. Li, J. Hu, S. Zhai, G. Lu and X. Huang, *J. Polym. Sci., Part A: Polym. Chem.*, 2010, **48**, 15-23.
110. C. Feng, Z. Shen, Y. Li, L. Gu, Y. Zhang, G. Lu and X. Huang, *J. Polym. Sci., Part A: Polym. Chem.*, 2009, **47**, 1811-1824.
111. C. Feng, Z. Shen, D. Yang, Y. Li, J. Hu, G. Lu and X. Huang, J. Polym. Sci., Part A: Polym. Chem., 2009, 47, 4346-4357.
112. A. Ding, G. Lu, H. Guo, X. Zheng and X. Huang, *J. Polym. Sci., Part A: Polym. Chem.*, 2013, **51**, 1091-1098.
113. A. Anastasaki, A. J. Haddleton, Q. Zhang, A. Simula, M. Droesbeke, P. Wilson and D. M. Haddleton, *Macromol. Rapid Commun.*, 2014, **35**, 965-970.
114. N. H. Nguyen, C. Rodriguez-Emmenegger, E. Brynda, Z. Sedlakova and V. Percec, *Polym. Chem.*, 2013, **4**, 2424-2427.
115. X.-H. Liu, G.-B. Zhang, B.-X. Li, Y.-G. Bai and Y.-S. Li, *J. Polym. Sci., Part A: Polym. Chem.*, 2010, **48**, 5439-5445.
116. M. R. Whittaker, C. N. Urbani and M. J. Monteiro, *J. Polym. Sci., Part A: Polym. Chem.*, 2008, **46**, 6346-6357.
117. Q. Zhang, J. Collins, A. Anastasaki, R. Wallis, D. A. Mitchell, C. R. Becer and D. M. Haddleton, *Angew. Chem., Int. Ed.*, 2013, **52**, 4435-4439.
118. D. Konkolewicz, Y. Wang, P. Krys, M. Zhong, A. A. Isse, A. Gennaro and K. Matyjaszewski, *Polym. Chem.*, 2014, **5**, 4396-4417.
119. D. Konkolewicz, P. Krys, J. R. Góis, P. V. Mendonça, M. Zhong, Y. Wang, A. Gennaro, A. A. Isse, M. Fantin and K. Matyjaszewski, *Macromolecules*, 2014, **47**, 560-570.
120. G. Lligadas, B. M. Rosen, C. A. Bell, M. J. Monteiro and V. Percec, *Macromolecules*, 2008, **41**, 8365-8371.
121. N. H. Nguyen, H.-J. Sun, M. E. Levere, S. Fleischmann and V. Percec, *Polym. Chem.*, 2013, **4**, 1328-1332.
122. M. E. Levere, N. H. Nguyen, H.-J. Sun and V. Percec, *Polym. Chem.*, 2013, **4**, 686-694.
123. B. M. Rosen, X. Jiang, C. J. Wilson, N. H. Nguyen, M. J. Monteiro and V. Percec, *J. Polym. Sci., Part A: Polym. Chem.*, 2009, **47**, 5606-5628.

124. K. Matyjaszewski, N. V. Tsarevsky, W. A. Braunecker, H. Dong, J. Huang, W. Jakubowski, Y. Kwak, R. Nicolay, W. Tang and J. A. Yoon, *Macromolecules*, 2007, **40**, 7795-7806.
125. Y. Zhang, Y. Wang, C.-h. Peng, M. Zhong, W. Zhu, D. Konkolewicz and K. Matyjaszewski, *Macromolecules*, 2011, **45**, 78-86.
126. C.-H. Peng, M. Zhong, Y. Wang, Y. Kwak, Y. Zhang, W. Zhu, M. Tonge, J. Buback, S. Park, P. Krys, D. Konkolewicz, A. Gennaro and K. Matyjaszewski, *Macromolecules*, 2013, **46**, 3803-3815.
127. Y. Wang, Y. Kwak, J. Buback, M. Buback and K. Matyjaszewski, *ACS Macro Lett.*, 2012, **1**, 1367-1370.
128. Y. Wang, M. Zhong, W. Zhu, C.-H. Peng, Y. Zhang, D. Konkolewicz, N. Bortolamei, A.A. Isse, A. Gennaro and K. Matyjaszewski, Macromolecules, 2013, 46, 3793-3802.
129. M. Zhong, Y. Wang, P. Krys, D. Konkolewicz and K. Matyjaszewski, *Macromolecules*, 2013, **46**, 3816-3827.
130. C. Y. Lin, M. L. Coote, A. Gennaro and K. Matyjaszewski, *J. Am. Chem. Soc*., 2008, **130**, 12762-12774.
131. M. E.Levere, N. H. Nguyen, V.Percec, *Macromolecules*, 2012, **45**, (20), 826 8274.
132. Y. Wang, M. Zhong, Y. Zhang, A. J. D. Magenau and K. Matyjaszewski, *Macromolecules*, 2012, **45**, 8929-8932.
133. C. Boyer, N. Corrigan, K. Jung, D. Nguyen, T. Nguyen, N Adnan, S. Oliver, S. Shanmugam, J. Yeow, *Chem. Rev.* 2016, **116**, 835−877.
134. C. Boyer, A. Derveaux, P. Zetterlund, M. Whittaker, Polym. Chem., 2012, 3, 117–123
135. C. Tang, W. Wu, D. Smilgie, K.Matyjaszewski, Kowalewski, T. *J. Am. Chem. Soc*. 2011, **133 (30)**, 11802–11809.
136. K. R. Shull, K. I. Winey, E. L. Thomas, E. J. Kramer, *Macromolecules* 1991, **24**, 2748–51.
137. H. Felix Schacher, A. Paul Rupar, M. Ian, *Angew. Chem. Int. Ed*. 2012, **51**, 7898 – 7921.
138. W. A. Braunecker,; K. Matyjaszewski, *Prog. Polym. Sci*. 2007, **32**, 93–146.
139. C. Boyer,; M. H. Stenzel,; T. P. Davis, *J. Polym. Sci., Part A: Polym. Chem*. 2011, **49**, 551–595.
140. M. E. Levere,; I. Willoughby, S. O'Donohue,; A. de Cuendias,; A. J. Grice,; Fidge,; C. R Becer,; Haddleton, D. M. *Polym. Chem*. 2010, **1**, 1086–94.
141. Soeriyadi Alexander H., Boyer Cyrille, Nystrom Fredrik, Zetterlund Per B., and Whittaker Michael R. *J. Am. Chem. Soc.* 2011, **133**, 11128–11131
142. C. Boyer, A. Soeriyadi., B. Zetterlund, and M. Whittaker. Macromolecules, *Polym. Chem.*, 2011, **44**, 8028–8033.
143. A. Anastasaki, C. Waldron, P. Wilson, C. Boyer, B. Zetterlund.,M. Whittaker R., and D. Haddleton, *ACS Macro Lett.* 2013, **2**, 896−900.
144. Q. Zhang, J. Collins, A. Anastasaki, R. Wallis, D. A. Mitchell, C. R. Becer and D. M. Haddleton, *Angew. Chem., Int. Ed.*, 2013, **52**, 4435-4439.
145. A. Anastasaki, V. Nikolaou, G. S. Pappas, Q. Zhang, C. Wan, P. Wilson, T. P. Davis, M. R. Whittaker and D. M. Haddleton, *Chem. Sci.*, 2014, **5,** 3536–3542.
146. Y.-M. Chuang, A. Ethirajan and T. Junkers, *ACS Macro Lett*., 2014, **3**, 732–737.
147. C. J. Hawker, A. W. Bosman and E. Harth, *Chem. Rev*., 2001, **101**, 3661–3688.

148. J. Nicolas, Y. Guillaneuf, C. Lefay, D. Bertin, D. Gigmes and B. Charleux, *Prog. Polym. Sci.*, 2013, **38**, 63–235.
149. J. Chiefari, Y. K. Chong, F. Ercole, J. Krstina, J. Jeffery, T. P. T. Le, R. T. A. Mayadunne, G. F. Meijs, C. L. Moad, G. Moad, E. Rizzardo and S. H. Thang, *Macromolecules*, 1998, **31**, 5559–5562.
150. G. Moad, E. Rizzardo and S. H. Thang, *Aust. J. Chem*., 2009,**62**, 1402–1472.
151. J.-S. Wang and K. Matyjaszewski, *J. Am. Chem. Soc.*, 1995, **117**, 5614–5615.
152. P. D. Iddon, K. L. Robinson and S. P. Armes, *Polymer*, 2004, **45**, 759–768.
153. J. T. Rademacher, M. Baum, M. E. Pallack, W. J. Brittain and W. J. Simonsick, *Macromolecules*, 2000, **33**, 284–288.
154. M. Teodorescu and K. Matyjaszewski, *Macromolecules*, 1999, **32**, 4826–4831.
155. M. Teodorescu and K. Matyjaszewski, *Macromol. Rapid Commun*., 2000, **21**, 190–194.
156. J. Ye and R. Narain, *J. Phys. Chem. B*, 2008, **113**, 676–681.
157. D. A. Z. Wever, P. Raffa, F. Picchioni and A. A. Broekhuis, *Macromolecules*, 2012, **45**, 4040–4045
158. Narumi, A.; Chen, Y.; Sone, M.; Fuchise, K.; Sakai, R.; Satoh, T.; Duan, Q.; Kawaguchi, S.; Kakuchi, T. *Macromol. Chem. Phys*. 2009, **5**, 349.
159. G. Gody, T. Maschmeyer, P. B. Zetterlund and S. Perrier, *Nat. Commun*., 2013, **4**, 2505.
160. G. Gody, T. Maschmeyer, P. B. Zetterlund and S. b. Perrier, *Macromolecules*, 2014, 639–649.
161. P. B. Zetterlund, G. Gody and S. Perrier, *Macromol. Theory Simul*., 2014, 331–339.
162. G. Gody, T. Maschmeyer, P. B. Zetterlund and S. Perrier, *Macromolecules*, 2014, **47**, 3451–3460.
163. J. Chiefari, J. Jeffery, R. T. A. Mayadunne, G. Moad, E. Rizzardo and S. H. Thang, *Macromolecules*, 1999, **32**, 7700–7702.

Chapter 2: Sequence-controlled multiblock copolymerisation of acrylamides *via* aqueous SET-LRP at 0°C

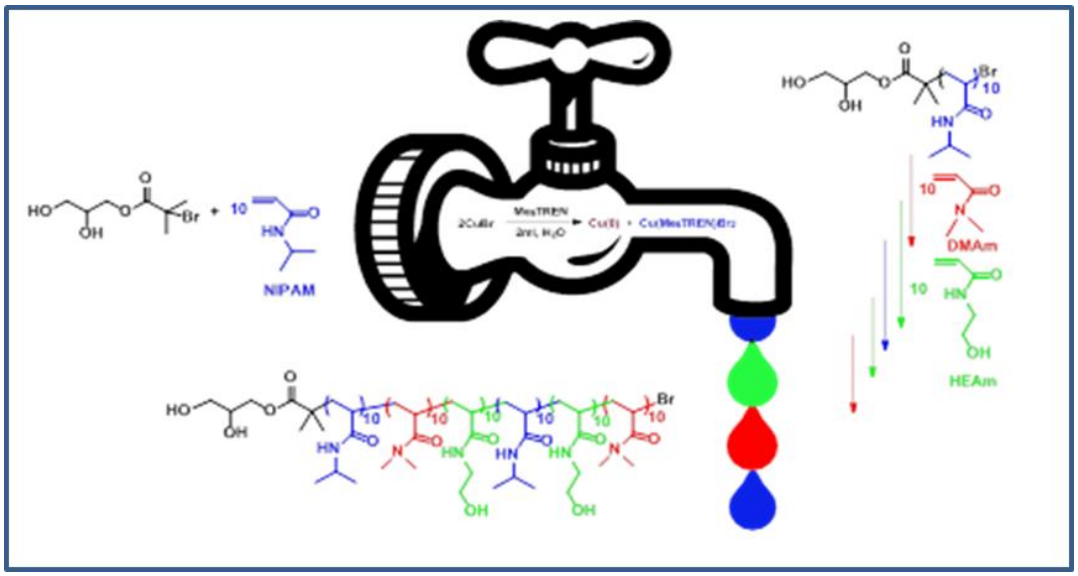

Aqueous single electron transfer living radical polymerisation (SET-LRP) has been employed to synthesise multiblock homopolymers and copolymers of a range of acrylamide monomers including N-isopropylacrylamide (NIPAM), 2-hydroxyethyl acrylamide (HEAA) and N,N-dimethyl acrylamide (DMA). Disproportionation of Cu(I)Br in the presence of Me_6TREN in water was exploited to generate reactive Cu(0) particles and $[Cu^{II}(Me_6TREN)]Br_2$ in situ resulting in unprecedented rates of reaction whilst maintaining control over chain lengths and molecular weight distributions (Đ < 1.10). Kinetic studies enabled optimisation of iterative chain extensions or block copolymerisations furnishing complex compositions in a matter of minutes/hours. In the multiblock copolymer system, the monomer sequence was successfully varied and limiting effects on the polymerisation have been examined.

2.1 Introduction

Control over monomer sequence, polymer composition and thus ensuing material properties is a key challenge facing polymer scientists. Natural polymers such as peptides, proteins, nucleic acids and carbohydrates are precisely constructed, at the cellular level, according to their intended application and function. Synthetically, this level of precision is some way off, though progress over the last 30-40 years has significantly improved the limits of control now possible over the polymer primary sequence.[1-6] Various approaches to precision polymers and materials, including single monomer addition,[7] tandem monomer addition and modification,[8, 9] kinetic control,[10-13] solution[14-20] and segregated[21] templating have been explored.

Single monomer addition *via* radical chain-growth polymerisation techniques is challenging given the reactive nature of the radical intermediates involved. This has given rise to a new field in synthetic polymer science, focusing on controlling the sequence of multiple discrete regions within the polymer. The retention of chain-end functionality is often critical in the design of materials and to this end, Whittaker and co-workers exploited Cu(0)-mediated living radical polymerisation in a one-pot synthesis of multiblock copolymers via iterative monomer addition.[22-24] Multiblock (up to decablock) copolymers containing discrete block lengths (2-10) were attained and the versatility of the protocol was emphasized by preparation of copolymers in both linear and star architectures as well higher molecular weight block lengths.[25] However, a limitation of this exemplary work was recognized during the synthesis of linear decablock copolymers, whereby molecular weight distributions were found to gradually increase, indicative of the accumulation of terminated chains. The same

technique was employed to synthesise a number of multiblock glycopolymers with a good degree of monomer sequence control in various compositions containing mannose, glucose, and fucose moieties in the presence and absence of spacer comonomers.[26, 27] Higher molecular weight multiblocks with lower dispersities have also been attained but the yield of the intermediate blocks was often < 95%, compromising the integrity of the multiblock structures.[25]

Despite the progress made in the field of reversible deactivation radical polymerisation (RDRP) over the last 20 years, controlled polymerisation in pure aqueous media has remained a challenge. Control in radical polymerisation protocols such as nitroxide-mediated polymerisation (NMP),[28, 29] reversible addition fragmentation chain transfer (RAFT)[30, 31] and transition metal mediated controlled radical polymerisation (TMM-CRP)[32-35] relies on careful manipulation of an equilibrium existing dormant (P_n-X) and active (P_n-$^{\cdot}$) species. In Cu-mediated polymerisation this equilibrium is largely controlled by Cu-ligand complexes. Higher rates of activation and propagation compared to less polar organic media can result in uncontrollable radical concentrations resulting in enhanced termination. The polymerisation of acrylamide based monomers is further complicated by deleterious side reactions and chain transfer that lead to loss of ω-Br chain end functionality and branching.[36-38]

The TMM-CRP of acrylamide (and its derivatives) has proved to be problematic with respect to the control of the polymerisation when water was employed as the only solvent at, or below, ambient temperature.[39, 40] Furthermore, according to the literature, only a few publications have reported controlled diblock copolymerisation of acrylamides via TMM-CRP. Brittain *et al* reported attempts to polymerise

dimethacrylamide using a range of copper salts with different ligands and solvents.[36] They concluded that the Cu salts complex to the amide group of the chain ends stabilizing the radical leading to an unacceptably high concentration of radicals which leads to 'spontaneous' termination reactions. This was in agreement with previous work by Matyjaszewski.[37, 38] Even the use of amide initiators in place of esters has been problematic.[41] Homopolymerisation of acrylamide (AA) and subsequent block copolymerisation with *N*-isopropylacrylamide (NIPAM) in aqueous media at 25°C resulted in polymers with broad molecular weight distribution ($Đ$ > 1.40).[42] Narrower distributions have been reported in mixed organic-aqueous solvent systems[43, 44] but again overall control was found to be variable. Thus it is apparent that polymerisation of acrylamides mediated via copper(I) has been unsuccessful and where good control has indeed been reported it is apparent that these reactions were carried out under conditions where copper(I) is unstable relative to disproportionation.[45]

Perrier and co-workers reported the synthesis of multiblock copolymers comprised of acrylamide monomers using RAFT. Under optimised conditions they achieved up to an icosablock (20 block) copolymer in both organic (dioxane) and aqueous media.[46-49] However, the high temperature (~ 70°C) that was utilised potentially limits the possibility of simultaneous biological applications while at the same time shortens the monomer pool only to acrylamides as polymerisation of other monomers (*e.g.* acrylates) at these temperature would result in unavoidable termination and side reactions (backbiting, chain transfer).[50] This has been somewhat addressed by the use of a *fac*-[Ir(ppy)$_3$] photoredox catalyst, previously employed by Hawker *et al.* to induce photomediated ATRP of methacrylates.[51] Boyer *et al.* have reported RAFT polymerisation of activated and unactivated vinyl

monomers at ambient temperature, highlighting the utility of the photoredox catalysis *via* recycling in iterative chain extension experiments.[52] Haddleton and Junkers have also reported the successful synthesis of sequence-controlled multiblock copolymers in a one-pot polymerisation at ambient temperature *via* a Cu-mediated light induced system. [53, 54]

In this chapter, water has been utilised as the solvent for the preparation of multiblock copolymers of various acrylamides at or below ambient temperature implying compatibility with biological systems. An unprecedented level of control is achieved by the catalyst system which is prepared *in situ via* disproportionation of Cu(Me_6TREN)Br *prior* to introduction of monomer and initiator. Enhanced rates of homo and copolymerisation are reported relative to preceding TMM-CRP protocols, without detrimental effects on the polymerisation control. Following homopolymerisation , up to eight chain extensions are possible furnishing multiblock compositions within 3.5 hours. In addition, the undesirable side reaction is investigated which sequesters the ω-Br chain end of poly(acrylamides) in water offering an insight into the importance of the precise knowledge of the polymerisation rate and subsequent management of the reaction.

2.2 Results and discussion

Recently, Haddleton and co-workers introduced a Cu-mediated polymerisation protocol enabling preparation of poly(acrylamide)s and poly(acrylate)s in aqueous,[55, 56] biological[57] and complex alcoholic[58] media. Within this study the successful *in situ* chain extension and block copolymerisation of P(NIPAM) prepared by aqueous SET-LRP was reported. However, in this original work the reaction was not

optimised and termination was evident following each chain extension either through increasingly broad dispersities or low molecular weight shoulders detected in SEC chromatograms. The termination was attributed to a deleterious side reaction leading to loss of the ω-Br chain end of the poly(acrylamides) in water.[36-38] Cu-mediated polymerisation in aqueous media had previously been difficult to control owing to enhanced rates of activation and propagation and potential dissociation of deactivating CuX_2 species. Additional complexity is introduced by the rate of the competing side reaction, namely the nucleophilic substitution of the ω-Br by H_2O. Experimentally, at high monomer concentration the rate of propagation dominates, thus substitution of the chain end is negligible. However, as the polymerisation proceeds the monomer concentration, and therefore the rate of propagation decreases, and thus the substitution of the bromine becomes more prevalent relative to propagation and the affected chains are unable to undergo further activation and propagate. Moreover, in previous work, the rate of the competing side reaction was effectively suppressed by performing the homo and block (co)polymerisations at 0°C but no further optimisation was sought.[55]

2.2.1 Investigating the potential for multiblock homopolymer synthesis *via* homo chain extension of PNIPAM

In accordance with the previously reported procedure, CuBr was allowed to fully disproportionate in an aqueous solution of the tetradentate tertiary amine ligand Me_6TREN. An aqueous mixture of initiator and monomer was subsequently added and polymerisation was allowed to proceed under a nitrogen atmosphere (Scheme 1).

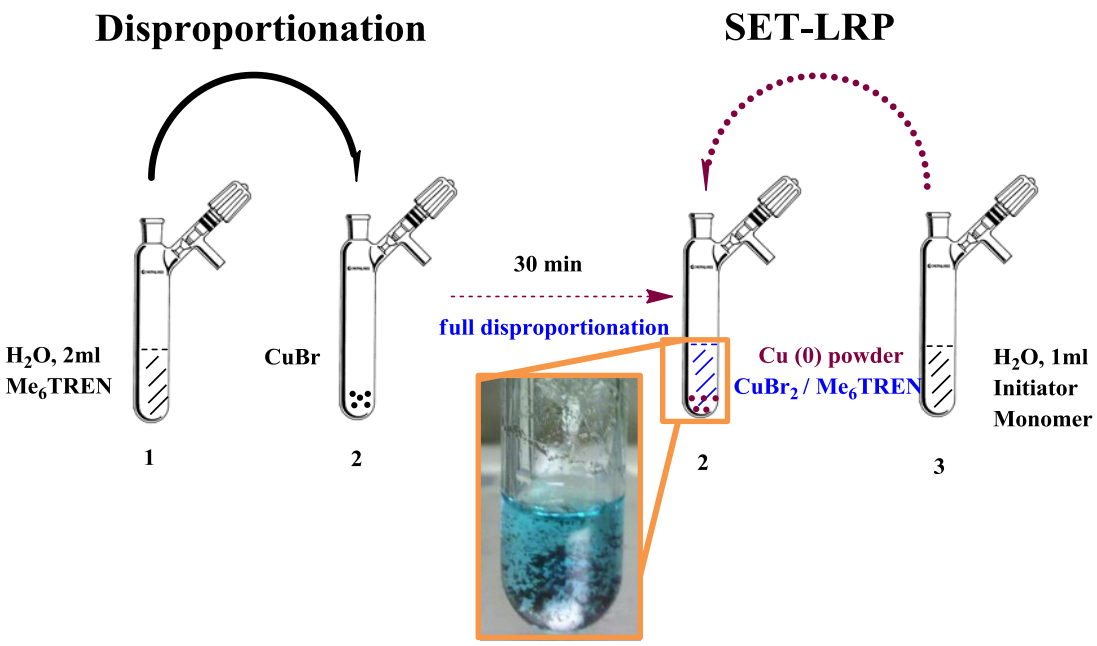

Scheme 1. Schematic of a typical aqueous SET-LRP proceeding with disproportionation of CuBr/Me_6TREN *prior* to monomer/initiator addition in pure water at 0°C as described by reference 55.

Upon sampling, conversions were determined by ^{1}H NMR analysis by monitoring the disappearance of the vinylic signals against appearance of the isopropyl methine signal from the NIPAM present in the side chain of the polymer (Figure 1). After one hour full conversion was attained (Table 1, entry 1) and a deoxygenated solution of NIPAM was injected into the reaction mixture. Chain extension was allowed to proceed for 4 hours at which time all of the NIPAM had been consumed (Table 1, entry 2) affording PNIPAM with narrow dispersity ($Đ$ = 1.07). Likewise, control over the polymerisation was retained upon addition of a third aliquot of NIPAM which was incorporated into the polymer within an additional 5.5 hours (Table 1, entry 3). However, attempts to chain extend further after this cumulative reaction time were unsuccessful (Figure 1 and 2).

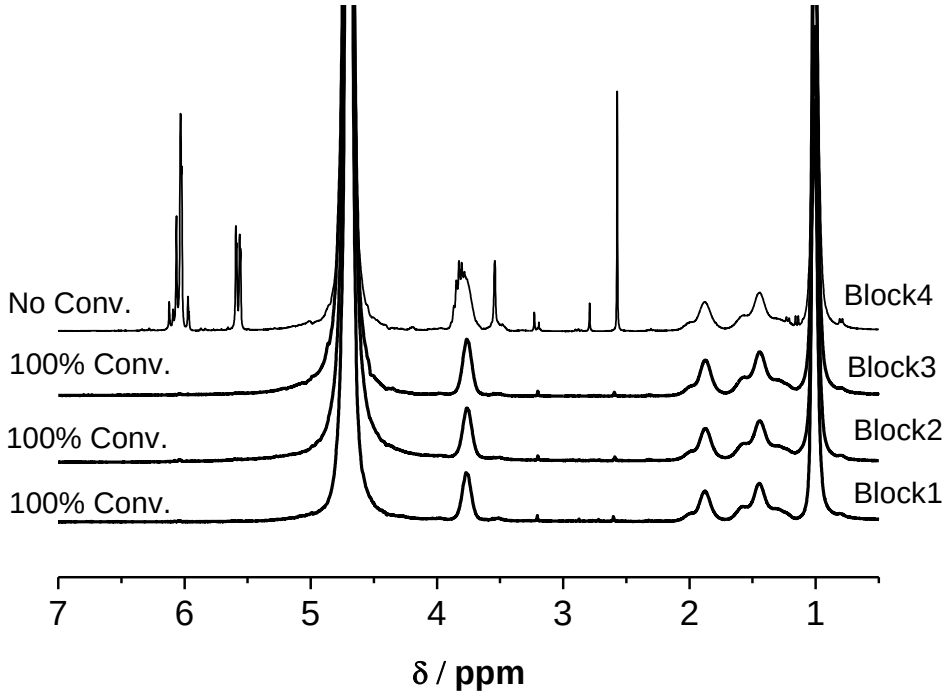

Figure 1. ^{1}H NMR (D_2O) show the conversion during multiblock homopolymerisation (unoptimised) of NIPAM. $[M]_0 : [I]_0 : [CuBr] : [Me_6TREN]$ = [10] : [1] : [0.04] : [0.04].

Table 1. Preparation of multiblock homopolymers prepared by sequential addition of deoxygenated aliquots of aqueous NIPAM (10 eq) to PNIPAM during SET-LRP at 0ºC in H_2O. $[M]_0 : [I]_0 : [CuBr] : [Me_6TREN]$ = [10] : [1] : [0.04] : [0.04].

Entry	Block number	Conv. (%)	Time per block (min)[a]	$M_{n,th}$ g.mol^{-1}	$M_{n,SEC}$[b] g.mol^{-1}	$Đ$
1	Block 1	100	60 (60)	1400	2900	1.06
2	Block 2	100	240 (300)	2500	4800	1.07
3	Block 3	100	320 (620)	3600	6700	1.08
4	Block 4	0	1200 (1820)	4700	6900	1.08

[a] Cumulative time in parentheses. [b] DMF SEC, calibrating with PMMA standard.

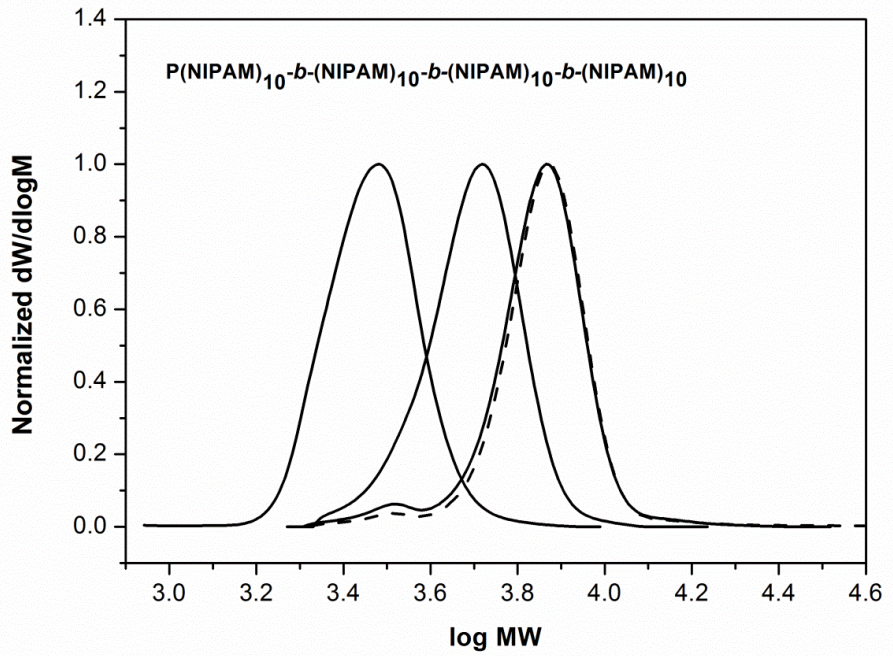

Figure 2. DMF SEC for evolution of block molecular weight of multiblock homopolymers (unoptimised) prepared by sequential addition of deoxygenated aliquots of aqueous NIPAM (10 eq) to PNIPAM via SET-LRP at 0ºC. $[M]_0$: $[I]_0$: [CuBr] : [Me_6TREN] = [10] : [1] : [0.04] : [0.04].

The integrity of multiblock compositions is contingent on the maximal retention of the end group, thus considering the deleterious effect of the H_2O mediated side reaction, a more accurate understanding of the polymerisation kinetics is required. Therefore a kinetic study on the homopolymerisation of NIPAM was performed. During homopolymerisation , regular sampling and analysis by ^{1}H NMR and SEC revealed that full monomer conversion was reproducibly attained within 11 min with retention of the narrow, symmetrical, monomodal molecular weight distributions (*Đ* = 1.06, Table 2, entry 1, Figure 3).

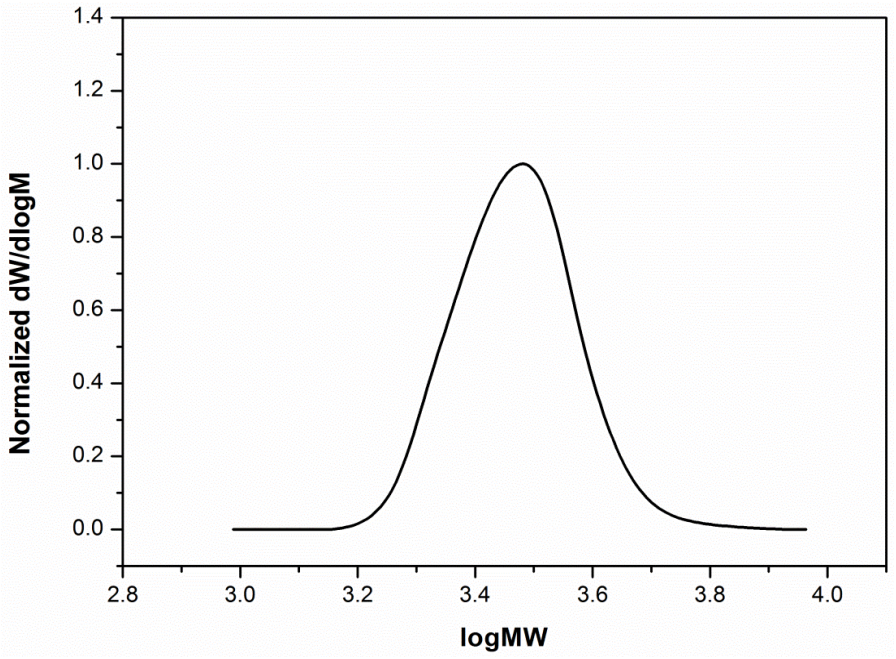

Figure 3. DMF SEC for the homopolymerisation of NIPAM by aqueous SET-LRP [NIPAM] : [I] : [CuBr] : [Me_6TREN] = [10] : [1] : [0.04] : [0.04].

It can be hypothesised that in order to maximize the integrity of targeted multiblock systems, monomer additions should occur at, or as close to full conversion as possible, and certainly higher than 95%, with minimal exposure to [M] ≈ 0. The homopolymerisation of NIPAM was therefore repeated and after 11 min a second aliquot of NIPAM, deoxygenated in water, was injected into the system. Pleasingly, ^{1}H NMR analysis confirmed quantitative conversion of the second NIPAM feed within an additional 8 min (19 min total, Table 2, entry 2, Figure 4) at which point the polymerisation was stopped, and SEC analysis revealed successful chain extension with a narrow dispersity ($Đ$ = 1.06, Figure 5). This process was repeated for each chain extension until a nonablock PNIPAM was obtained via iterative chain extension in a total reaction time of ~ 3.5 h (Scheme 2, Table 2).

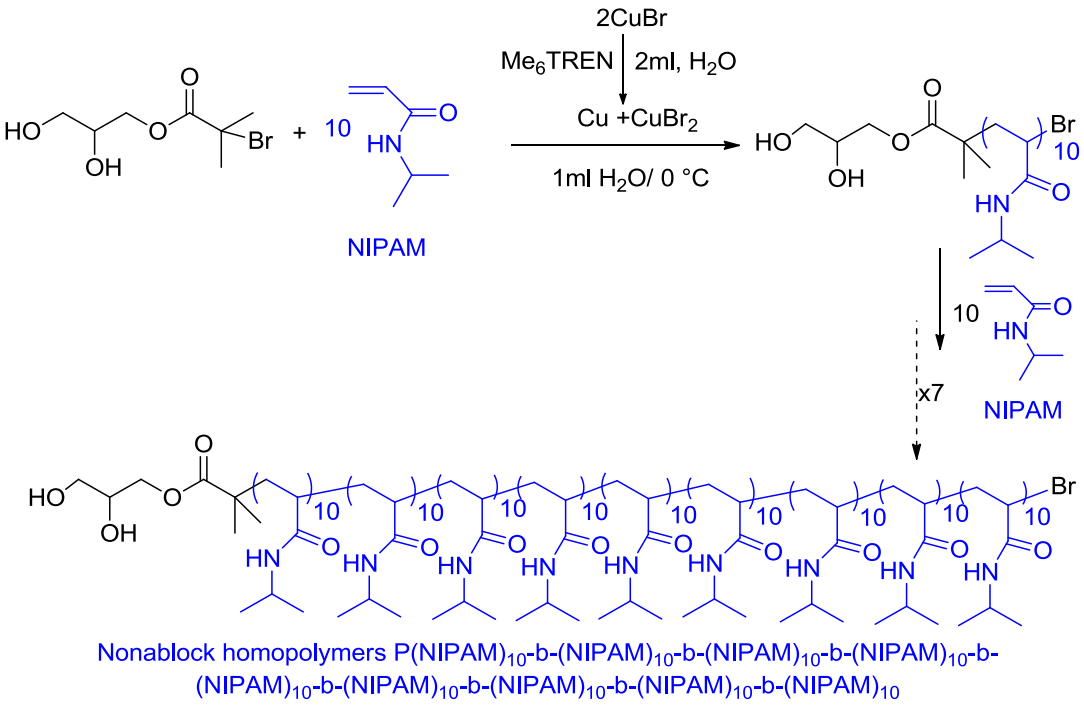

Scheme 2. Synthesis of multiblock homopolymers of NIPAM by iterative SET-LRP in pure H_2O.

Table 2. Optimisation of multiblock homopolymers prepared by sequential addition of deoxygenated aliquots of aqueous NIPAM (10 eq) to PNIPAM during SET-LRP at 0°C in H_2O. $[M]_0 : [I]_0 : [CuBr] : [Me_6TREN] = [10] : [1] : [0.04] : [0.04]$.

Entry	Block number	Conv. (%)	Time per block (min)[a]	$M_{n,th}$ g.mol^{-1}	$M_{n,SEC}$[b] g.mol^{-1}	$Đ^b$
1	Block 1	100	11 (11)	1400	2500	1.06
2	Block 2	99	8 (19)	2500	4300	1.06
3	Block 3	100	15 (34)	3600	6500	1.05
4	Block 4	98	16 (50)	4700	8900	1.05
5	Block 5	100	16 (66)	5900	11000	1.07
6	Block 6	99	20 (86)	7000	13300	1.06
7	Block 7	99	30 (116)	8200	15700	1.06
8	Block 8	99	40 (156)	9300	18700	1.06
9	Block 9	99	50 (206)	10400	22800	1.08

[a] Cumulative time in parentheses. [b] DMF SEC, calibrating with PMMA standard.

Successive extensions were confirmed by ^{1}H NMR (Figure 4) and low dispersities were retained throughout ($Đ$ < 1.08, Figure 5), implying the potential for precise control over discrete monomer sequences within the final polymer composition. However, it is noted that attempts to prepare a decablock or beyond were unsuccessful, rendering the nonablock PNIPAM as the current limit in this system.

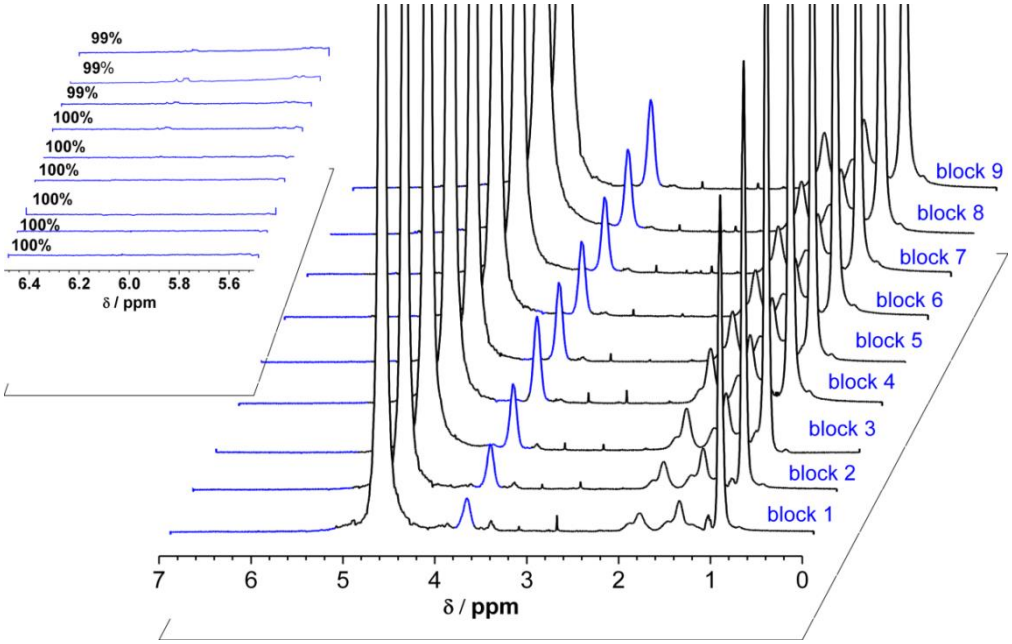

Figure 4. ^{1}H NMR spectra for multiblock homopolymers prepared by sequential addition of deoxygenated aliquots of aqueous NIPAM (10 eq) to PNIPAM via SET-LRP at 0°C in D_2O. $[M]_0 : [I]_0 : [CuBr] : [Me_6TREN] = [10] : [1] : [0.04] : [0.04]$.

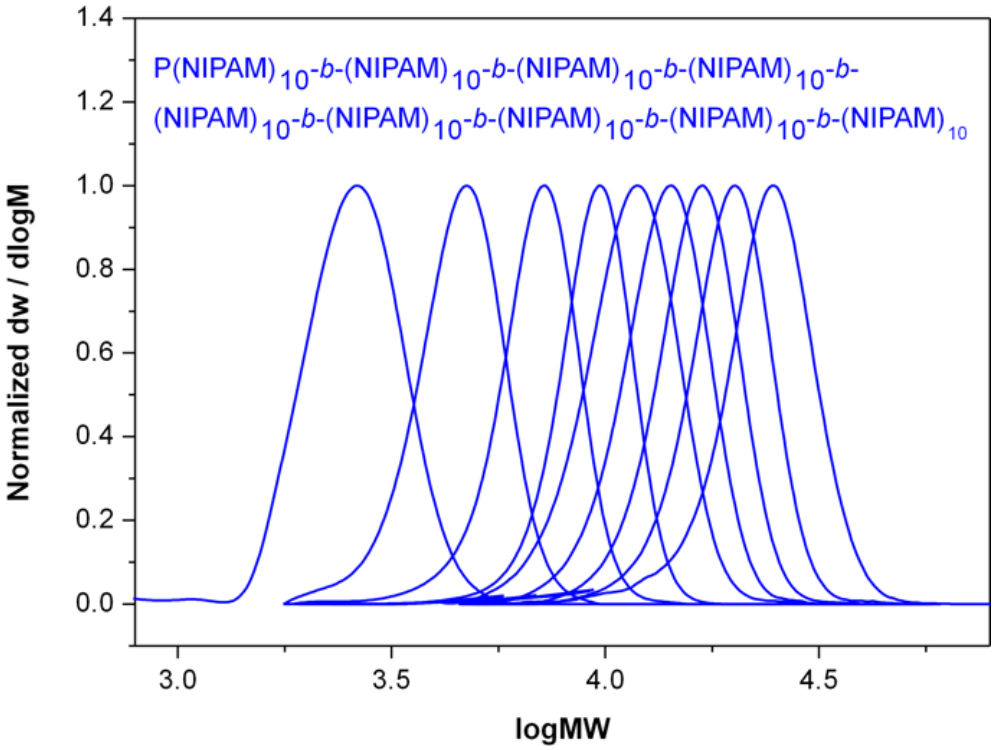

Figure 5. Evolution of block molecular weight by DMF SEC for multiblock homopolymers prepared by sequential addition of deoxygenated aliquots of aqueous NIPAM (10 eq) to PNIPAM via SET-LRP at 0°C $[M]_0$: $[I]_0$: [CuBr] : $[Me_6TREN]$ = [10] : [1] : [0.04] : [0.04].

The current data points to an apparent sudden cessation of polymerisation during chain extension from a nona to decablock polymer when NIPAM is employed as monomer. It is unlikely that such an abrupt transition occurs and this observation could be attributed to a number of factors. Competing termination reactions can result in a gradual accumulation of 'dead' chains. Though this is not obvious by NMR and SEC analyses, it is illustrated in plot of $M_{n,exp}$ and $M_{w,exp}$ versus block number which initially shows an increase in molecular weight cumulatively deviating from $M_{n,th}$ (Figure 6). Likewise the number of manipulations heightens the chance of termination through introduction of unwanted reagents such as oxygen.

This combination of termination events also confers a global increase in the concentration of deactivating species which causes the equilibrium to shift towards dormant chains, an observation which has been noted in a number of related systems.

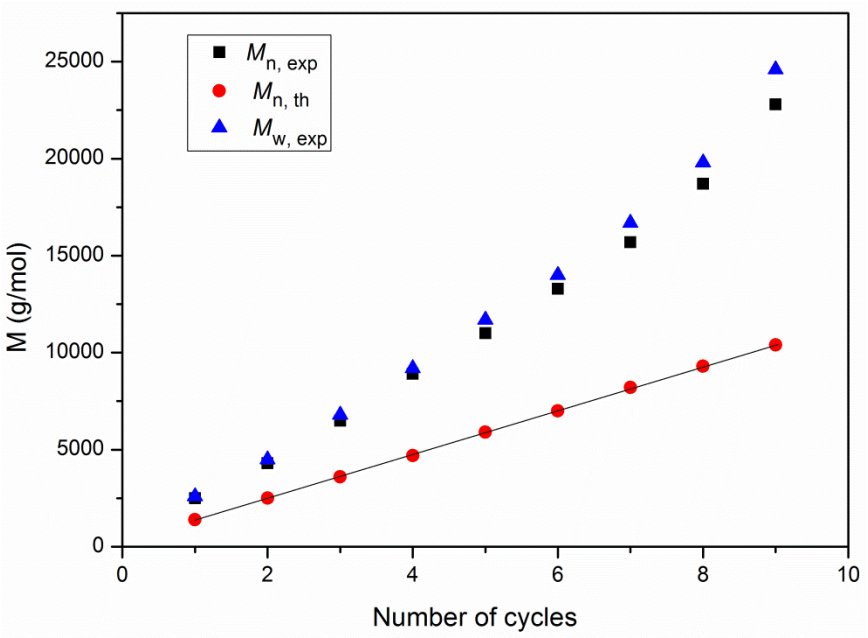

Figure 6. Relative increase in molecular weight as a function of block number (cycles).

2.2.2 Sequence controlled multiblock copolymerisation *via* aqueous SET-LRP

The precise sequence of monomer units present in the biomolecules such as proteins, polysaccharides and nucleic acids determines the natural properties and function of these biomacromolecules. Therefore, the control over monomer sequences in polymerisation is an interesting target in order to synthesise sequence-controlled macromolecules with different ordered monomer sequences and potentially tuneable properties. Preceding examples of Cu-mediated multiblock copolymerisation of acrylates have been relatively slow with the rate of polymerisation increasing with

each iterative addition culminating in reaction times of up to 48 hours per block in DMSO.[22-26, 53] Using three commercially available, hydrophilic, acrylamide monomers, the conditions described for the PNIPAM polymerisation to synthesise a true hexablock copolymer P(NIPAM)$_{10}$-*b*-(DMA)$_{10}$-*b*-(HEAA)$_{10}$-*b*-(NIPAM)$_{10}$-*b*-(HEAA)$_{10}$-*b*-(DMA)$_{10}$ in a pure aqueous system at 0°C was applied (Scheme 3).

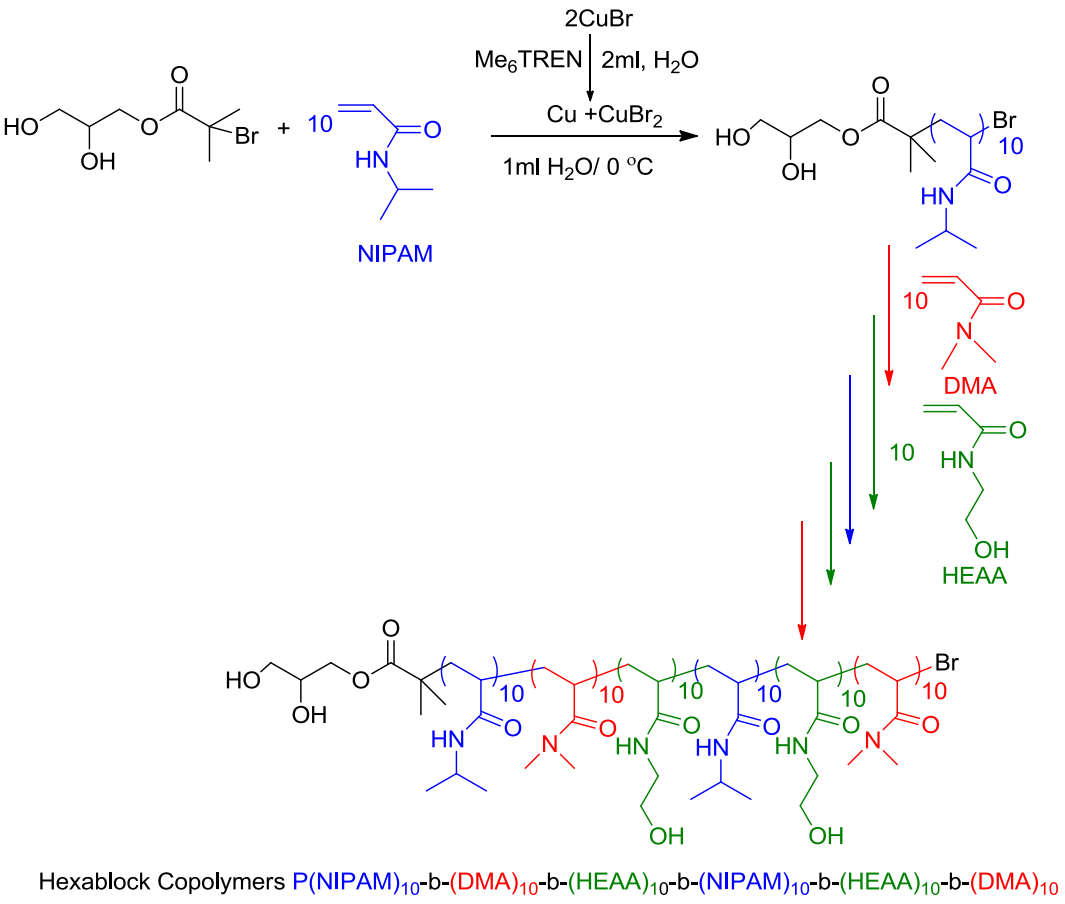

Scheme 3. Synthesis of multiblock copolymers composed of NIPAM, DMA and HEAA by iterative SET-LRP in H_2O at 0ºC.

These conditions address some of the challenges facing synthetic chemists particularly those working close to the interface of biology/medicine. The conditions are conducive to biological applications, in particular grafting-from strategies of protein/peptide/nucleic acid conjugation.[59, 60] Previously, this has been difficult in

pure aqueous solution, requiring binary mixtures with, or, pure polar organic solvents, which can have a detrimental effect on the biomolecules employed and complicate the polymerisation process.

In line with the PNIPAM investigation, each polymerisation and chain extension was screened to identify the optimum reaction time per block (Table 3). The conversion of each block extension was quantitative according to integration of the vinyl protons (~ 6.50–5.70 ppm) of the monomer with the isopropyl methine proton of NIPAM (-C<u>H</u> (CH_3)$_2$) (~ 3.50–3.90 ppm), the methyl signal of DMA (N(C<u>H</u>$_3$)$_2$ (~ 3.0 ppm)) and the *N*-methylene signal of HEAA (NH(-C<u>H</u>$_2$-) (~ 3.3 ppm)) (Figure 7).

Table 3. Preparation of multiblock copolymers composed of NIPAM DMA and HEAA by iterative aqueous SET-LRP at 0°C in H_2O. $[M]_0$: $[I]_0$: [CuBr] : [Me_6TREN] = [10] : [1] : [0.04] : [0.04].

Entry	Block number	Monomer	Conv. (%)	Time per block (min)[a]	$M_{n,th}$ g.mol^{-1}	$M_{n,SEC}$[b] g.mol^{-1}	$Đ$[b]
1	Block 1	NIPAM	99	11 (11)	1400	2700	1.09
2	Block 2	DMA	99	6 (17)	2400	4800	1.11
3	Block 3	HEAA	99	25 (42)	3500	8300	1.09
4	Block 4	NIPAM	99	40 (82)	4600	10200	1.07
5	Block 5	HEAA	100	45(127)	5800	14500	1.09
6	Block 6	DMA	97	70(197)	6800	17400	1.11
7	Block 7	NIPAM	0	24(221)	-	-	-

[a] Cumulative time in parentheses. [b] DMF SEC, calibrating with PMMA standard.

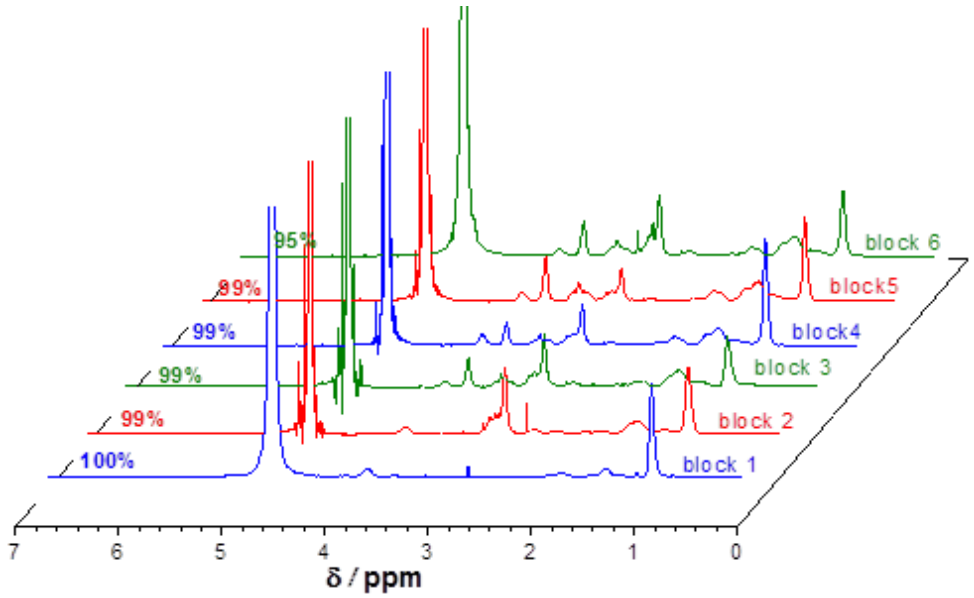

Figure 7. ^{1}H NMR spectra for multiblock copolymers composed of NIPAM, DMA and HEAA by iterative aqueous SET-LRP at 0°C in D_2O. $[M]_0$: $[I]_0$: [CuBr] : [Me_6TREN] = [10] : [1] : [0.04] : [0.04].

SEC analysis showed that the molecular weight evolution and distributions were controlled as confirmed by the narrow final dispersity (*Đ* = 1.11) (Figure 8). The total reaction time for synthesis of this hexablock was 3 h, which is considerably faster than any previously reported Cu-mediated multiblock systems in organic media.

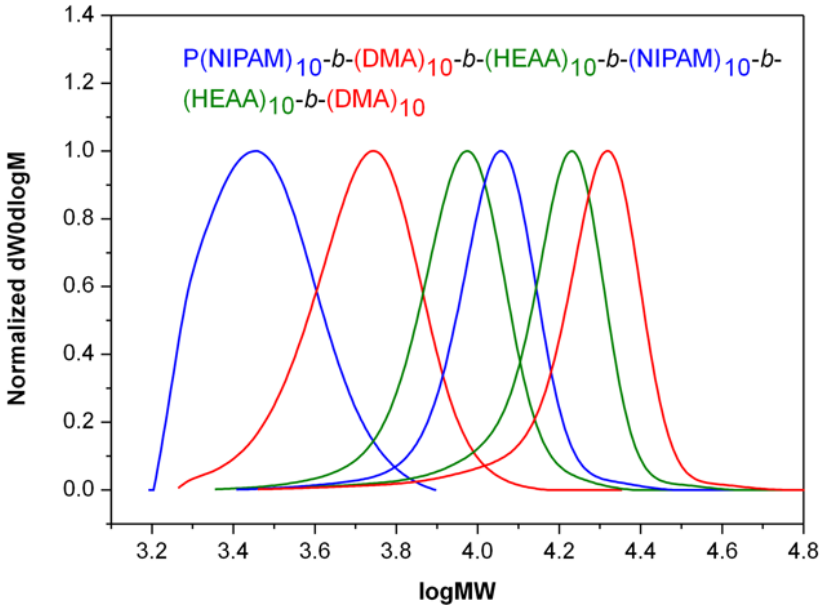

Figure 8. Evolution of block molecular weight by DMF SEC for multiblock copolymers composed of NIPAM, DMA and HEAA by iterative aqueous SET-LRP at 0°C $[M]_0 : [I]_0 : [CuBr] : [Me_6TREN] = [10] : [1] : [0.04] : [0.04]$.

Unfortunately, attempts to form a heptablock copolymer were unsuccessful in this case, presenting a significant deviation from the results obtained when just NIPAM was employed as monomer. It was thought that this may have been due to consumption of the activating species as the Cu(0) formed during disproportionation are visibly consumed as the reaction proceeds.[61, 62] In an attempt to circumvent this, a new aliquot of Cu(0) and $Cu(Me_6TREN)Br_2$ was fed into the reaction mixture *prior to* the fifth addition of monomer (Section 2.4.4, Scheme 6). Upon addition of NIPAM as the 7th monomer the reaction mixture was allowed to stir overnight, affording 70% conversion (Section 2.4.4, Table 5, entry 7, Figure 14). However, although an expected shift in molecular weight distribution was observed by SEC, the bimodality of the resulting peak indicated that significant loss of chain-end,

rather than consumption of activating species, was responsible for limiting the number of possible chain extensions (Section 2.4.4, Figure 15).

Considering that it was possible to prepare a nonablock homopolymer when NIPAM alone was employed as monomer, the effect of monomer structure was investigated as a possible cause for these observations. Comparing these monomers, it was recognized that a notably difference arose from the nature of substitution at the amide bond. Both secondary (NIPAM, HEAA) and tertiary (DMA) amide based acrylamides have been employed throughout this and previous studies with little insight into differences in chain-end fidelity and relative rates of deleterious side reactions. Therefore, two copolymerisations were conducted in which NIPAM was block copolymerised, in an alternating sequence, with HEAA and DMA respectively.

A heptablock copolymer of NIPAM and HEAA was prepared by sequential, alternating additions of NIPAM and HEAA to the aqueous polymerisation mixture at 0°C in a total reaction time of 3.5 hours (Scheme 4).

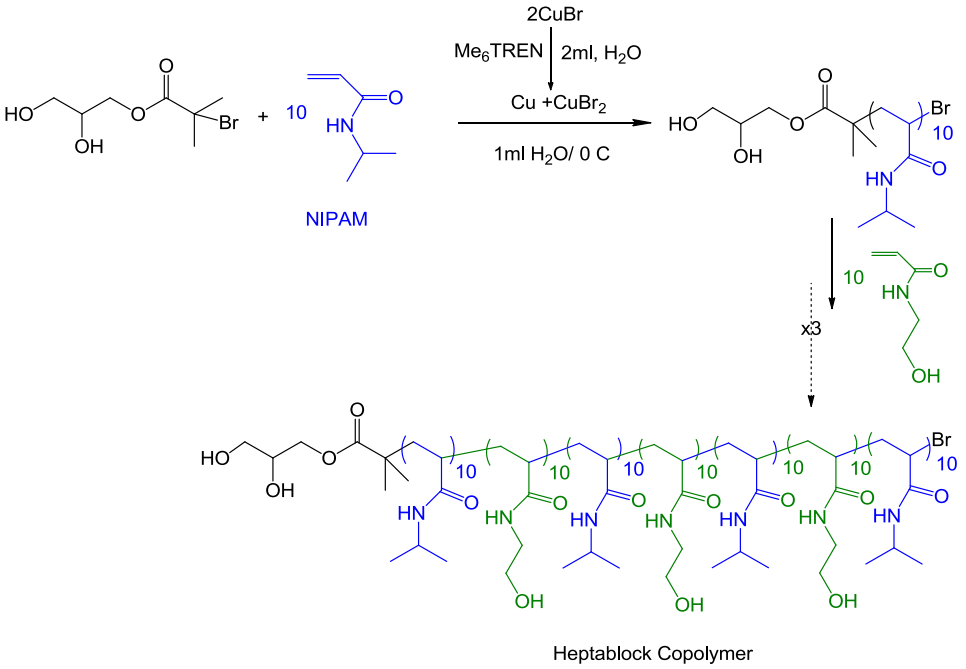

Scheme 4. Synthesis of alternating block copolymers composed of NIPAM and HEAA by iterative SET-LRP in H_2O. $[M]_0 : [I]_0 : [CuBr] : [Me_6TREN] = [10] : [1] : [0.04] : [0.04]$.

The conversion after each iteration was quantitative (Table 4, Figure 9) and narrow molecular weight distributions were retained throughout ($Đ$ = 1.07, Table 4, Figure 10).

Table 4. Preparation of alternating block copolymers composed of NIPAM and HEAA by iterative SET-LRP in H_2O. $[M]_0 : [I]_0 : [CuBr] : [Me_6TREN] = [10] : [1] : [0.04] : [0.04]$.

Entry	Block number	Monomer	Conv. (%)	Time per block (min)[a]	$M_{n,th}$ g.mol^{-1}	$M_{n,SEC}$[b] g.mol^{-1}	$Đ$[b]
1	Block 1	NIPAM	100	11 (11)	1400	2600	1.05
2	Block 2	HEAA	99	25 (36)	2600	5100	1.10
3	Block 3	NIPAM	100	20 (56)	3800	7100	1.09

4	Block 4	HEAA	98	24 (80)	5000	9900	1.10
5	Block 5	NIPAM	100	30 (110)	6200	12200	1.08
6	Block 6	HEAA	98	50 (160)	7400	15600	1.10
7	Block 7	NIPAM	100	60 (240)	8600	18800	1.07

[a] Cumulative time in parentheses. [b] DMF SEC, , calibrating with PMMA standard

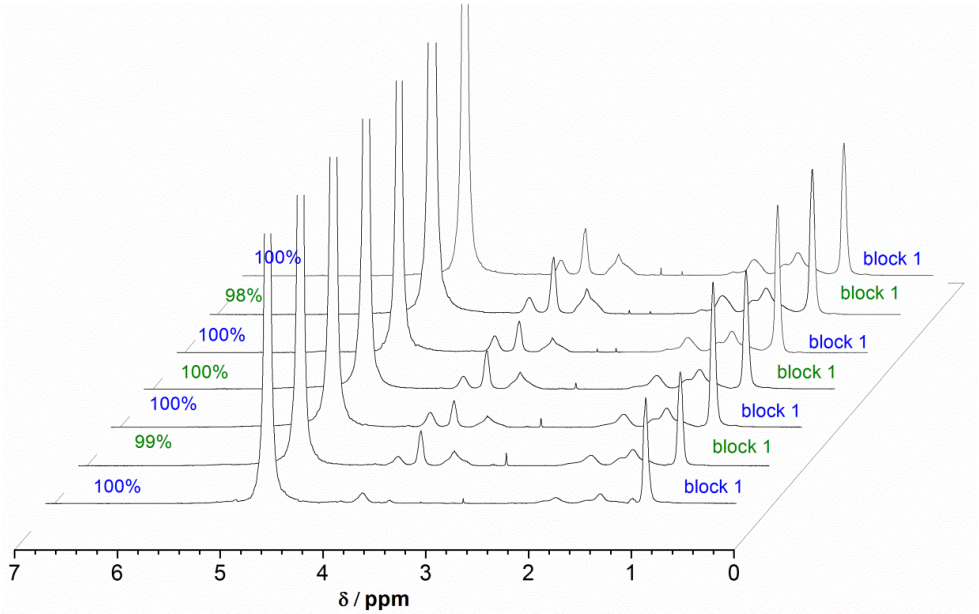

Figure 9: ^{1}H NMR (D_2O) showing the conversions for alternating block copolymers composed of NIPAM and HEAA by iterative SET-LRP in H_2O. $[M]_0 : [I]_0 : [CuBr] : [Me_6TREN] = [10] : [1] : [0.04] : [0.04]$.

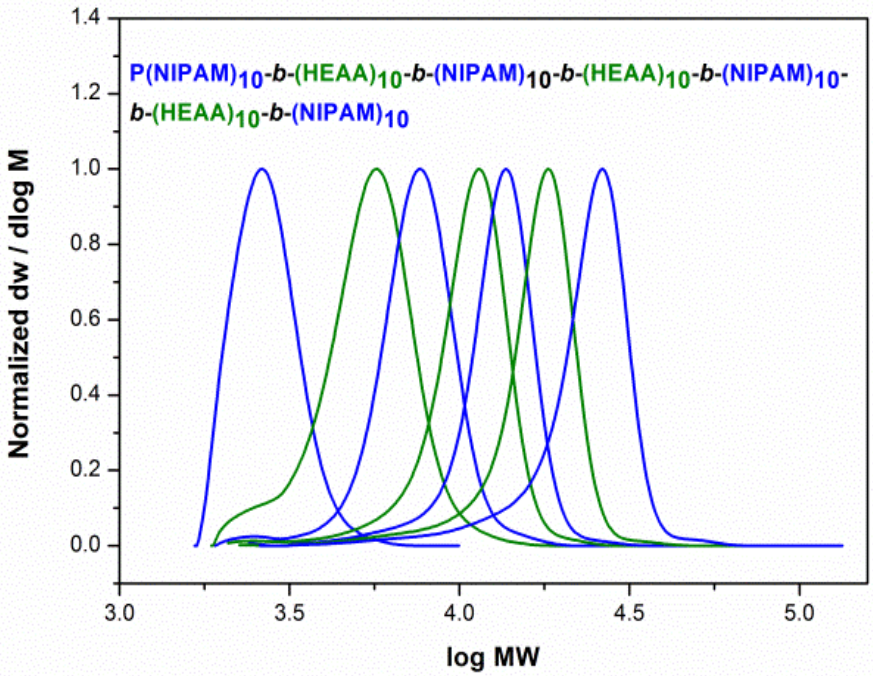

Figure 10. DMF SEC for alternating multiblock copolymers of NIPAM and HEAA in H_2O at 0°C. $[M]_0 : [I]_0 : [CuBr] : [Me_6TREN] = [10] : [1] : [0.04] : [0.04]$.

Surprisingly, when the tertiary acrylamide DMA was employed as comonomer, the copolymerisation was compromised following addition of the second aliquot of DMA (Section 2.4.4, Table 6). Conversion, according to ^1H NMR (Section 2.4.4, Figure 16), ceased upon addition of the 7th monomer feed (Section 2.4.4, Table 6, entry 7) and evidence for premature termination was manifest as low molecular weight shoulder peak which was found to increase during subsequent monomer additions (Figure 11).

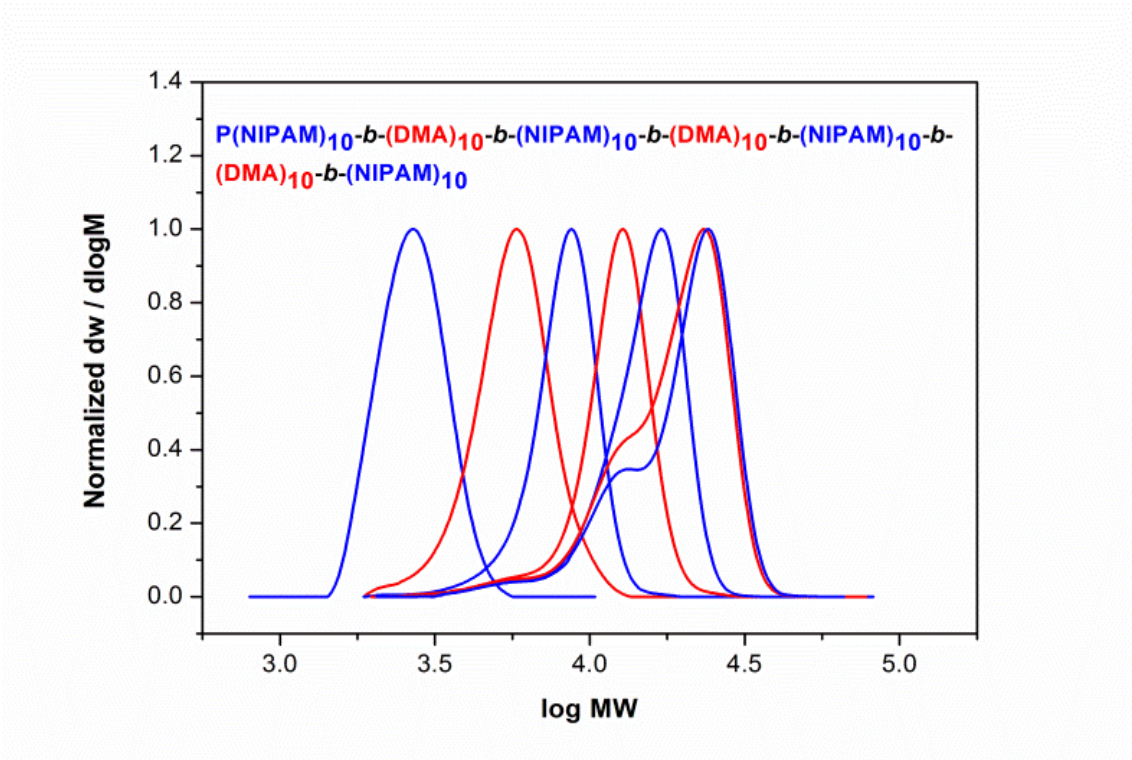

Figure 11. DMF SEC for alternating multiblock copolymers of NIPAM and DMA in H_2O at 0°C. $[M]_0 : [I]_0 : [CuBr] : [Me_6TREN] = [10] : [1] : [0.04] : [0.04]$.

This suggests that the limiting factor for chain extension is the lifetime of the ω-Br chain end, and that the rate of loss of this end group is faster in the presence of tertiary acrylamides such as DMA.

In order to probe this assumption block homopolymerisations of both HEAA and DMA were carried out. Secondary acrylamide HEAA was polymerised under the conditions described previously with chain extension afforded by sequential addition of degassed aliquots of HEAA at full conversion (Scheme 5). Comparable conversions to NIPAM were obtained (98-100%, Section 2.4.4, Figure 17) and low dispersities were retained throughout ($Đ$ = 1.07, Section 2.4.4, Table 7 and Figure 12a).

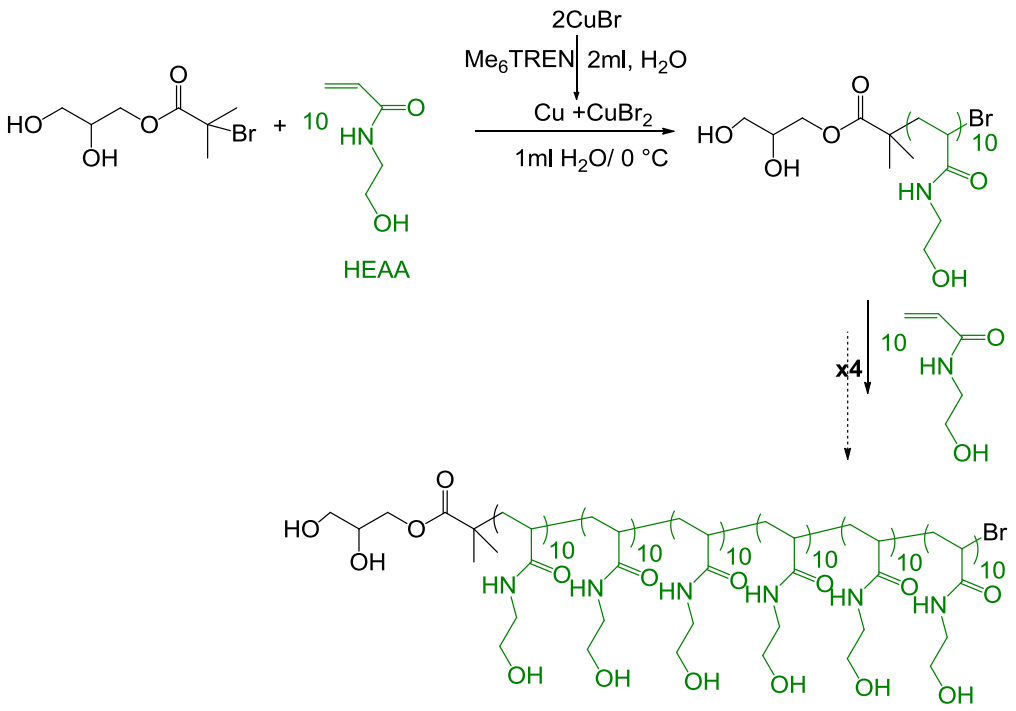

Hexablock homopolymers P(HEAA)$_{10}$-*b*-(HEAA)$_{10}$-*b*-(HEAA)$_{10}$-*b*-(HEAA)$_{10}$-*b*-(HEAA)$_{10}$-*b*-(HEAA)$_{10}$

Scheme 5. Synthesis of multiblock homopolymers of HEAA by iterative SET-LRP in pure H_2O at 0ºC.

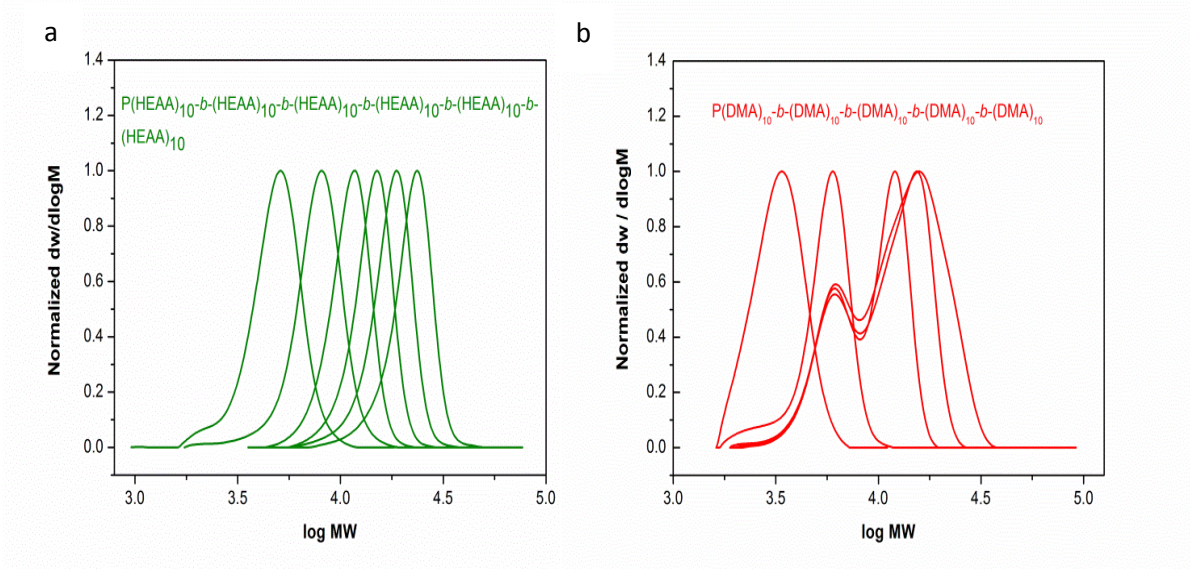

Figure 12. DMF SEC analyses for aqueous SET-LRP of multiblock homopolymers of HEAA and DMA (a, b). $[M]_0$: $[I]_0$: [CuBr] : [Me_6TREN] = [10] : [1] : [0.04] : [0.04].

However, the limit to chain extension was found to be the hexablock polymer which was synthesised in 3.5 hours (Section 2.4.4, Table 7, entry 6). The rate of reaction was slower than that observed for NIPAM, which could furnish a nonablock polymer in 3.5 hours, explaining, at least in part, the limited number of blocks possible for HEAA. Interestingly, homopolymerisation and a single chain extension of DMA were found to proceed in comparable rate and with comparable control to that observed for NIPAM (Section 2.4.4, Table 8, entry 1-2). However, following injection of a second aliquot of DMA, towards yielding a triblock homopolymer, significant low molecular weight termination was observed, indicative of ω-Br chain end loss (Figure 12b, 13). It should be noted that this is apparent after only 30 minutes in the presence of the tertiary acrylamide, as opposed to 3.5 hours in the presence of secondary acrylamides.

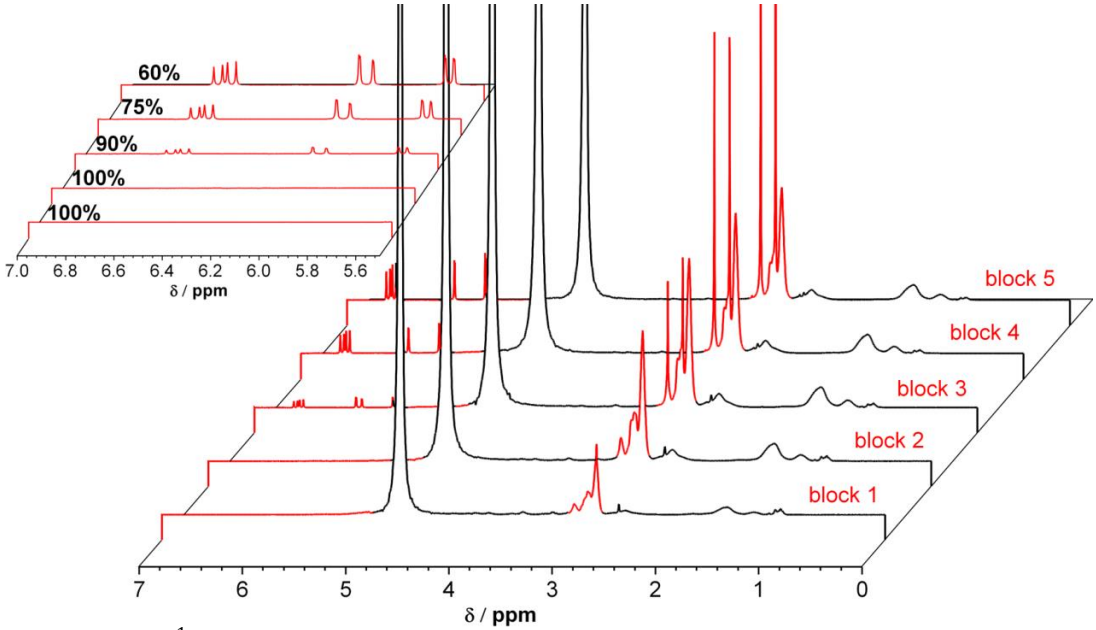

Figure 13. ^{1}H NMR analyses for aqueous SET-LRP of block homopolymers of DMA. $[M]_0 : [I]_0 : [CuBr] : [Me_6TREN] = [10] : [1] : [0.04] : [0.04]$.

2.3 Conclusion

The synthesis of multiblock acrylamide copolymers *via* Cu-mediated radical polymerisation of acrylamide monomers is reported. Disproportionation of unstable Cu(Me_6TREN)Br in water results in formation of highly active Cu(0) and deactivating Cu(Me_6TREN)Br_2 *prior* to addition of initiator and monomer. Good knowledge of the rate of polymerisation is required and subsequent management of the reaction can minimise the amount of termination by both conventional radical processes and adventitious side reactions. Thus, a 'nonablock' PNIPAM and a true multiblock comprised of three alternating acrylamides can be obtained within 3.5 hrs reaction time. The successive chain extensions and the compositions of the multiblock copolymers were confirmed *via* ^{1}H NMR and SEC analyses.

2.4 Experimental

2.4.1 Materials and methods

N-Isopropylacrylamide (NIPAM, 97%) was purchased from commercial supplier (Sigma-Aldrich) and was purified by recrystallization from hexane to remove the inhibitor. 2-Hydroxyethyl acrylamide (HEAA, 97%, Sigma-Aldrich), and *N*,*N*-Dimethyl acrylamide (DMA, 99%, Sigma-Aldrich) were passed over a column filled with basic alumina to remove the inhibitor prior to use.

HPLC grade water (H_2O, VWR international, LLC) was used as the solvent for disproportionation and polymerisations.

The water soluble initiator 2, 3-dihydroxypropyl 2-bromo-2-methylpropanoate was prepared as reported in the literature. [63]

Tris(2-(dimethylamino)ethyl)amine (Me_6TREN) was synthesised according to literature procedures and stored under nitrogen prior to use. [64]

Copper(I) bromide (CuBr, 98%, Sigma-Aldrich) was sequentially washed with acetic acid and ethanol and dried under vacuum.

2.4.2 Instrumentation

Proton Nuclear Magnetic Resonance (^{1}H NMR) spectra were recorded on Bruker DPX-300 and DPX-400 spectrometers using deuterated solvents obtained from Aldrich. Monomer conversion for NIPAM, HEAA, DMA, DEA and NAM homopolymerisation was determined, comparing the integral of vinyl protons with isopropyl, ethyl, dimethyl, diethyl, morphline protons, respectively.

Size-exclusion chromatography (SEC) was conducted on Varian 390-LC system using DMF as the mobile phase (5 mM NH_4BF_4) at 50^oC, equipped with refractive index, UV and viscometry detectors, 2 × PLgel 5 mm mixed-D columns (300 × 7.5 mm), 1 × PLgel 5 mm guard column (50 × 7.5 mm) and autosampler. Commercial narrow linear poly (methyl methacrylate) standards in range of 200 to 1.0 × 10^6 g · mol^{-1} were used to calibrate the system. All samples were passed through 0.45 μm PTFE filter before analysis.

All reactions were carried out under an inert atmosphere of oxygen-free nitrogen, using standard Schlenk techniques.

2.4.3 General procedures

General procedure for homopolymerisation by aqueous SET-LRP (DPn = 10).

To a Schlenk tube fitted with a magnetic stir bar and a rubber septum, H_2O (2 mL) and Me_6TREN (0.1 mmol) were charged and the mixture was bubbled with nitrogen for 15 min. CuBr (0.1 mmol) was then carefully added under slight positive pressure of nitrogen. The mixture immediately became blue Cu(II) and a purple/red precipitate Cu(0) was observed. In a separate vial fitted with a magnetic stir bar and a rubber septum monomer (2.5 mmol) was dissolved in H_2O (1.0 mL) prior to addition of initiator (2,3-dihydroxypropyl 2-bromo-2-methylpropanoate, 0.25 mmol) and the resulting mixture was bubbled with nitrogen for 15 min. The degassed monomer / initiator aqueous solution was then transferred via cannula to the Schlenk tube containing Cu(0) / $CuBr_2$ / Me_6TERN catalyst. The Schlenk tube was sealed and the mixed solution was allowed to polymerise at 0°C. Sample of the reaction

mixture were then removed for analysis. The sample for ^{1}H NMR was directly diluted with D_2O. Catalyst residues were removed by filtering through a column of neutral alumina prior to DMF SEC analysis.

General procedure for kinetic investigation of aqueous SET-LRP polymerisation

Reactions were performed in triplicate. The general procedure for homopolymerisation by aqueous SET-LRP was followed. Homopolymer conversions were monitored by regular sampling to accurately determine the time at which full monomer conversion was reached according to ^{1}H NMR (D_2O). In subsequent experiments (also performed in triplicate) hompolymerisation was allowed to proceed to this time and a sample was taken, in order to confirm the anticipated full conversion, *prior* to addition of freshly deoxygenated aqueous solutions of monomer (DP_n eq). Regular sampling was again employed to identify the time required to reach full monomer conversion. This was repeated until conversion and/or molecular weight distributions were compromised by termination. Samples taken for ^{1}H NMR were directly diluted with D_2O. Catalyst residues were removed by filtering through a column of neutral alumina prior to DMF SEC analysis.

General procedure for chain extension/multiblock copolymerisation by aqueous SET-LRP

The general procedure for homopolymerisation by aqueous SET-LRP was followed. At specific times determined by control experiments a sample was taken for conversion analysis before addition of freshly deoxygenated aqueous solutions of monomer (DP_n eq). This process was repeated until conversion and/or molecular

weight distributions were compromised by termination. Samples taken for ^{1}H NMR were directly diluted with D_2O. Catalyst residues were removed by filtering through a column of neutral alumina prior to DMF SEC analysis.

2.4.4 Additional characterisation

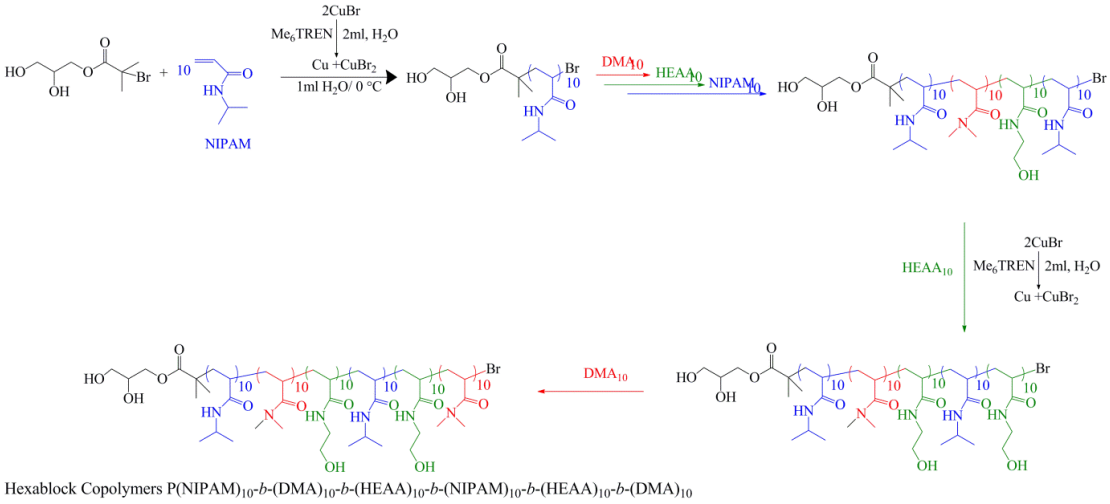

Hexablock Copolymers P(NIPAM)$_{10}$-*b*-(DMA)$_{10}$-*b*-(HEAA)$_{10}$-*b*-(NIPAM)$_{10}$-*b*-(HEAA)$_{10}$-*b*-(DMA)$_{10}$

Scheme 6: Synthesis of multiblock copolymers composed of NIPAM, DMA and HEAA by iterative SET-LRP in H_2O with an additional feed of catalyst with the 5th monomer addition. $[M]_0 : [I]_0 : [CuBr] : [Me_6TREN] = [10] : [1] : [0.04] : [0.04]$.

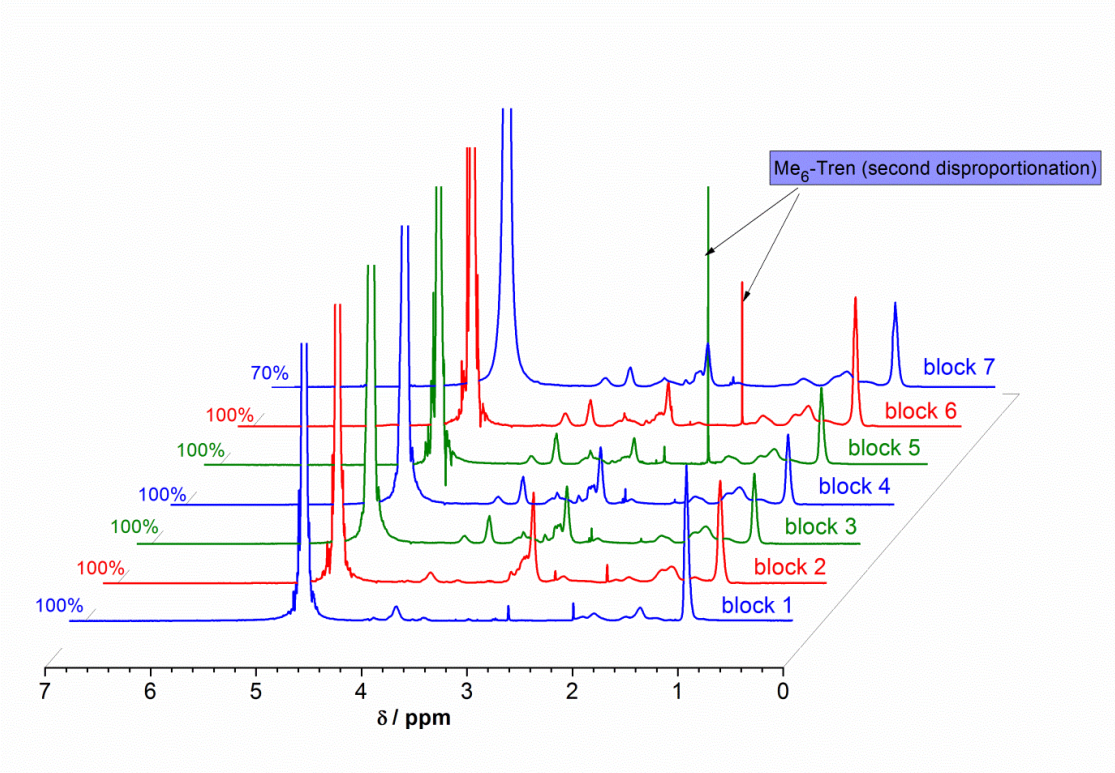

Figure 14: ^{1}NMR (D_2O) of multiblock copolymers composed of NIPAM, DMA and HEAA by iterative SET-LRP in H_2O with an additional feed of Cu(0) and Cu(Me_6TREM)Br_2 with the 5th monomer addition. $[M]_0$: $[I]_0$: [CuBr] : [Me_6Tren] = [10] : [1] : [0.04] : [0.04].

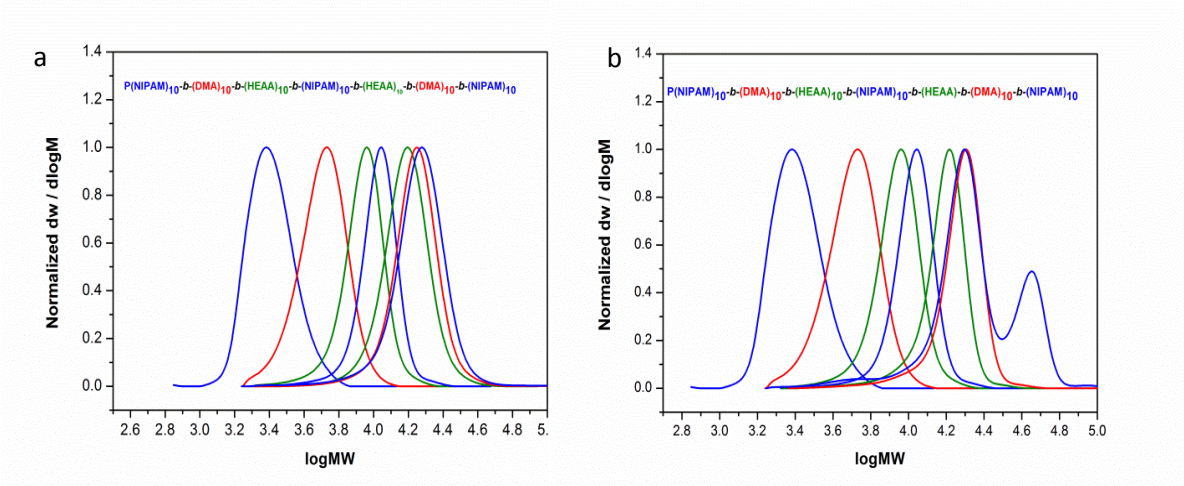

Figure 15. DMF SEC for mulitblock copolymers composed of NIPAM, HEAA and DMA (a) and NIPAM, HEAA and DMA with an addition feed of catalyst (b) Cu(0) and Cu(Me_6TREM)Br_2

Table 5. Preparation of multiblock copolymers composed of NIPAM, DMA and HEAA by iterative SET-LRP in H_2O with an additional feed of Cu(0) and $Cu(Me_6TREM)Br_2$ with the 5th monomer addition. $[M]_0 : [I]_0 : [CuBr] : [Me_6TREN] = [10] : [1] : [0.04] : [0.04]$.

Entry	Block number	Conv. (%)	Monomer	Time per block (min)[a]	$M_{n,th}$ g.mol^{-1}	$M_{n,SEC}$[b] g.mol^{-1}	$Đ$[b]
1	Block 1	100	NIPAM	11 (11)	1400	2700	1.09
2	Block 2	100	DMA	6 (17)	2400	4800	1.11
3	Block 3	100	HEAA	25 (42)	3500	8300	1.09
4	Block 4	100	NIPAM	40 (82)	4600	10200	1.07
5	Block 5	100	HEAA	45 (127)	5800	14500	1.09
6	Block 6	100	DMA	70 (197)	6800	17400	1.11
7	Block 7	70	NIPAM	overnight	7900	18700	1.37

[a] Cumulative time in parentheses. [b] DMF SEC, , calibrating with PMMA standard

Table 6. Preparation of alternating block copolymers composed of NIPAM and DMA by iterative SET-LRP in H_2O. $[M]_0 : [I]_0 : [CuBr] : [Me_6TREN] = [10] : [1] : [0.04] : [0.04]$.

Entry	Block number	Monomer	Conv. (%)	Time per block (min)[a]	$M_{n,th}$ g.mol^{-1}	$M_{n,SEC}$[b] g.mol^{-1}	$Đ$[b]
1	Block 1	NIPAM	100	11 (11)	1400	2600	1.06
2	Block 2	DMA	100	6 (17)	2400	5200	1.09
3	Block 3	NIPAM	99	20 (37)	3500	7600	1.07
4	Block 4	DMA	99	15 (52)	4500	10900	1.10
5	Block 5	NIPAM	99	40 (92)	5600	13400	1.12
6	Block 6	DMA	90	180 (272)	6600	15400	1.22
7	Block 7	NIPAM	0	180 (452)	7700	16300	1.21

[a] Cumulative time in parentheses. [b] DMF SEC, , calibrating with PMMA standard

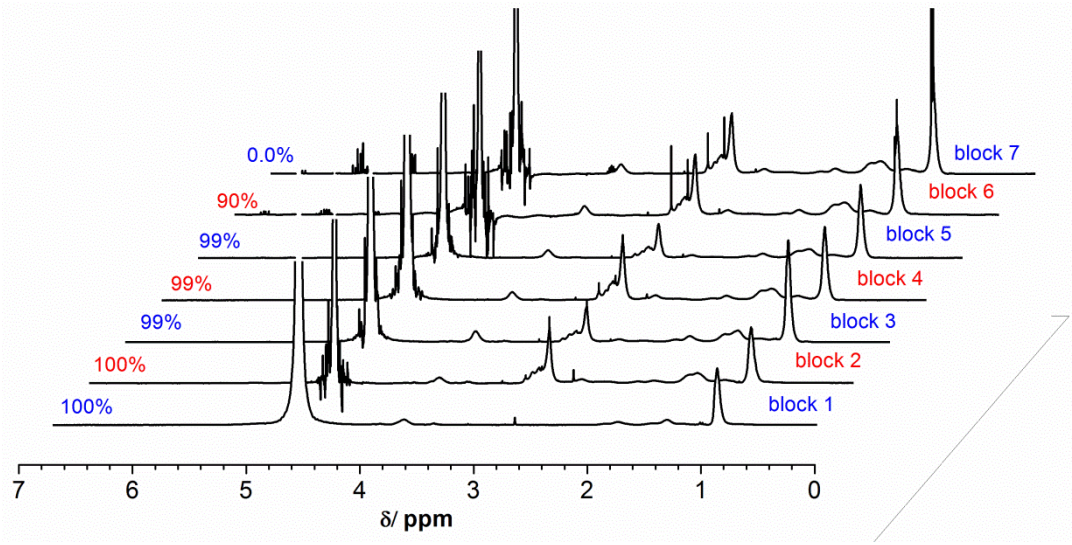

Figure 16: ^{1}H NMR (D_2O) showing the conversions for alternating block copolymers composed of NIPAM and DMA by iterative SET-LRP in H_2O. $[M]_0$: $[I]_0$: [CuBr] : [Me_6TREN] = [10] : [1] : [0.04] : [0.04].

Table 7. Preparation of multiblock homopolymers prepared by sequential additon of deoxygenated aliquots of aqueous HEAA (10 eq) to PHEAA during SET-LRP in H_2O. $[M]_0$: $[I]_0$: [CuBr] : [Me_6TREN] = [10] : [1] : [0.04] : [0.04].

Entry	Monomer	Conv. (%)	Time per block (min)[a]	$M_{n,th}$ g.mol^{-1}	$M_{n,SEC}$[b] g.mol^{-1}	$Đ$[b]
1	HEAA	100	25 (25)	1400	4500	1.08
2	HEAA	100	20 (45)	2500	7200	1.09
3	HEAA	99	20 (65)	3700	10700	1.06
4	HEAA	99	20 (85)	4800	13700	1.05
5	HEAA	98	70 (155)	6000	16900	1.06
6	HEAA	100	70 (225)	7100	20900	1.07

[a] Cumulative time in parentheses. [b] DMF SEC, calibrating with PMMA standard.

Table 8. Preparation of multiblock homopolymers prepared by sequential addition of deoxygenated aliquots of aqueous DMA (10 eq) to PDMA during SET-LRP at in H_2O. $[M]_0 : [I]_0 : [CuBr] : [Me_6TREN] = [10] : [1] : [0.04] : [0.04]$.

Entry	Monomer	Conv. (%)	Time per block (min)[a]	$M_{n,th}$ g.mol^{-1}	$M_{n,SEC}$[b] g.mol^{-1}	$Đ$[b]
1	DMA	98	6 (6)	1200	3100	1.08
2	DMA	100	20 (26)	2200	5100	1.10
3	DMA	90	20 (46)	3200	8000	1.17
4	DMA	74	20 (66)	4200	90010	1.25
5	DMA	60	120 (186)	5200	10200	1.30

[a] Cumulative time in parentheses. [b] DMF SEC, calibrating with PMMA standard.

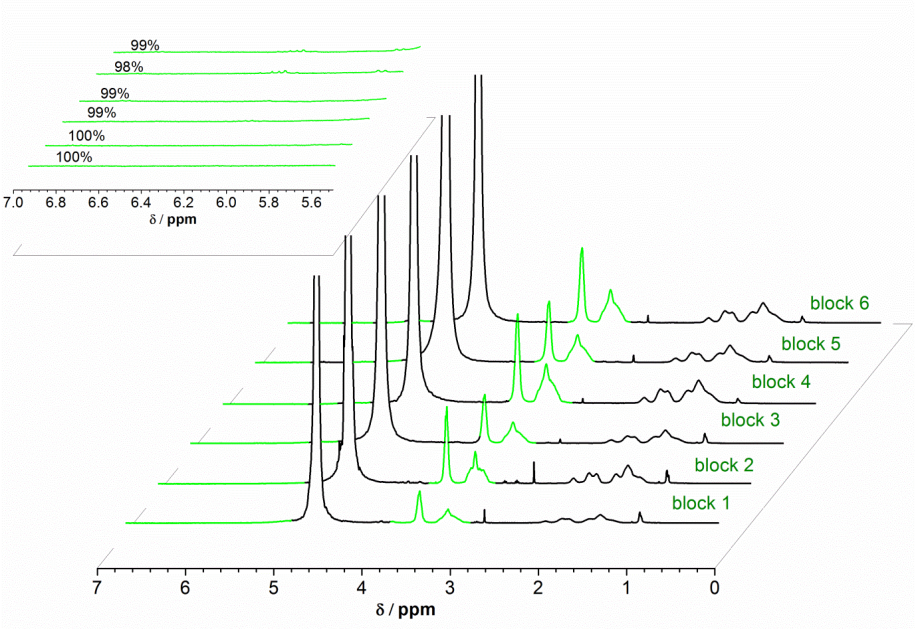

Figure 17. ^{1}H NMR analyses for aqueous SET-LRP of multiblock homopolymers of HEAA. $[M]_0 : [I]_0 : [CuBr] : [Me_6TREN] = [10] : [1] : [0.04] : [0.04]$.

2.5 References

1. N. Badi and J.-F. Lutz, *Chem. Soc. Rev.*, 2009, **38**, 3383-3390.
2. M. Ouchi, N. Badi, J. F. Lutz and M. Sawamoto, *Nature Chem.*, 2011, **3**, 917-924.
3. J. F. Lutz, M. Ouchi, D. R. Liu and M. Sawamoto, *Science*, 2013, **341**, 1238149.
4. M. Ouchi, T. Terashima and M. Sawamoto, *Chem. Rev.*, 2009, **109**, 4963-5050.
5. M. Minoda, M. Sawamoto and T. Higashimura, *Macromolecules*, 1990, **23**, 4889-4895.
6. J.-F. Lutz, *Polym. Chem.*, 2010, **1**, 55-62.
7. J. Vandenbergh, G. Reekmans, P. Adriaensens and T. Junkers, *Chem Commun*, 2013, **49**, 10358-10360.
8. K. Nakatani, T. Terashima and M. Sawamoto, *J. Am. Chem. Soc.*, 2009, **131**, 13600-13601.
9. K. Nakatani, Y. Ogura, Y. Koda, T. Terashima and M. Sawamoto, *J. Am. Chem. Soc.*, 2012, **134**, 4373-4383.
10. S. Pfeifer and J.-F. Lutz, *J. Am. Chem. Soc.*, 2007, **129**, 9542-9543.
11. M. Zamfir and J.-F. Lutz, *Nat Commun*, 2012, 1138.
12. D. Moatsou, C. F. Hansell and R. K. O'Reilly, *Chem. Sci.*, 2014, **5**, 2246.
13. J.-F. Lutz, *Acc. Chem. Res.*, 2013, **46**, 2696-2705.
14. A. Khan, D. M. Haddleton, M. J. Hannon, D. Kukulj and A. Marsh, *Macromolecules*, 1999, **32**, 6560-6564.
15. A. Marsh, A. Khan, D. M. Haddleton and M. J. Hannon, *Macromolecules*, 1999, **32**, 8725-8731.
16. P. J. Milnes, M. L. McKee, J. Bath, L. Song, E. Stulz, A. J. Turberfield and R. K. O'Reilly, *Chem. Commun.*, 2012, **48**, 5614-5616.
17. S. Ida, T. Terashima, M. Ouchi and M. Sawamoto, *J. Am. Chem. Soc.*, 2009, **131**, 10808-10809.
18. S. Ida, M. Ouchi and M. Sawamoto, *J. Am. Chem. Soc.*, 2010, **132**, 14748-14750.
19. Y. Hibi, M. Ouchi and M. Sawamoto, *Angew. Chem., Int. Ed.*, 2011, **50**, 7434-7437.
20. Y. Hibi, S. Tokuoka, T. Terashima, M. Ouchi and M. Sawamoto, *Polym. Chem.*, 2011, **2**, 341-347.
21. R. McHale, J. P. Patterson, P. B. Zetterlund and R. K. O'Reilly, *Nat Chem*, 2012, **4**, 491-497.
22. C. Boyer, A. Derveaux, P. B. Zetterlund and M. R. Whittaker, *Polym. Chem.*, 2012, **3**, 117-123.
23. C. Boyer, A. H. Soeriyadi, P. B. Zetterlund and M. R. Whittaker, *Macromolecules*, 2011, **44**, 8028-8033.
24. A. H. Soeriyadi, C. Boyer, F. Nystrom, P. B. Zetterlund and M. R. Whittaker, *J. Am. Chem. Soc.*, 2011, **133**, 11128-11131.
25. A. Anastasaki, C. Waldron, P. Wilson, C. Boyer, P. B. Zetterlund, M. R. Whittaker and D. Haddleton, *ACS Macro Lett.*, 2013, **2**, 896-900.
26. Q. Zhang, A. Anastasaki, G.-Z. Li, A. J. Haddleton, P. Wilson and D. M. Haddleton, *Polym. Chem.*, 2014, **5**, 3876.
27. Q. Zhang, J. Collins, A. Anastasaki, R. Wallis, D. A. Mitchell, C. R. Becer and D. M. Haddleton, *Angew. Chem. Int. Ed. Engl.*, 2013, **52**, 4435-4439.

28. C. J. Hawker, A. W. Bosman and E. Harth, *Chem. Rev.*, 2001, **101**, 3661-3688.
29. J. Nicolas, Y. Guillaneuf, C. Lefay, D. Bertin, D. Gigmes and B. Charleux, *Prog. Polym. Sci.*, 2013, **38**, 63-235.
30. J. Chiefari, Y. K. Chong, F. Ercole, J. Krstina, J. Jeffery, T. P. T. Le, R. T. A. Mayadunne, G. F. Meijs, C. L. Moad, G. Moad, E. Rizzardo and S. H. Thang, *Macromolecules*, 1998, **31**, 5559-5562.
31. G. Moad, E. Rizzardo and S. H. Thang, *Aust. J. Chem.*, 2009, **62**, 1402-1472.
32. M. Kato, M. Kamigaito, M. Sawamoto and T. Higashimura, *Macromolecules*, 1995, **28**, 1721-1723.
33. J.-S. Wang and K. Matyjaszewski, *J. Am. Chem. Soc.*, 1995, **117**, 5614-5615.
34. D. M. Haddleton, C. B. Jasieczek, M. J. Hannon and A. J. Shooter, *Macromolecules*, 1997, **30**, 2190-2193.
35. V. Percec, T. Guliashvili, J. S. Ladislaw, A. Wistrand, A. Stjerndahl, M. J. Sienkowska, M. J. Monteiro and S. Sahoo, *J. Am. Chem. Soc.*, 2006, **128**, 14156-14165.
36. J. T. Rademacher, M. Baum, M. E. Pallack, W. J. Brittain and W. J. Simonsick, *Macromolecules*, 2000, **33**, 284-288.
37. M. Teodorescu and K. Matyjaszewski, *Macromolecules*, 1999, **32**, 4826-4831.
38. M. Teodorescu and K. Matyjaszewski, *Macromol Rapid Commun*, 2000, **21**, 190-194.
39. P. D. Iddon, K. L. Robinson and S. P. Armes, *Polymer*, 2004, **45**, 759-768.
40. J. Ye and R. Narain, *J. Phys. Chem. B*, 2008, **113**, 676-681.
41. A. Limer and D. M. Haddleton, *Macromolecules*, 2006, **39**, 1353-1358.
42. D. A. Z. Wever, P. Raffa, F. Picchioni and A. A. Broekhuis, *Macromolecules*, 2012, **45**, 4040-4045.
43. N. H. Nguyen, B. M. Rosen and V. Percec, *J. Polym. Sci., Part A: Polym. Chem.*, 2010, **48**, 1752-1763.
44. E. A. Appel, J. del Barrio, X. J. Loh, J. Dyson and O. A. Scherman, *J. Polym. Sci., Part A: Polym. Chem.*, 2012, **50**, 181-186.
45. H. D. Maynard, K. L. Heredia, R. C. Li, D. P. Parra and V. Vazquez-Dorbatt, *J. Mater. Chem.*, 2007, **17**, 4015-4017.
46. G. Gody, T. Maschmeyer, P. B Zetterlund and S. Perrier, *Nat Commun*, 2013, **4**.
47. G. Gody, T. Maschmeyer, P. B. Zetterlund and S. b. Perrier, *Macromolecules*, 2014.
48. P. B. Zetterlund, G. Gody and S. Perrier, *Macromol. Theory Simul.*, 2014.
49. G. Gody, T. Maschmeyer, P. B. Zetterlund and S. Perrier, *Macromolecules*, 2014, **47**, 3451-3460.
50. J. Chiefari, J. Jeffery, R. T. A. Mayadunne, G. Moad, E. Rizzardo and S. H. Thang, *Macromolecules*, 1999, **32**, 7700-7702.
51. B. P. Fors and C. J. Hawker, *Angew. Chem., Int. Ed.*, 2012, **51**, 8850-8853.
52. J. Xu, K. Jung, A. Atme, S. Shanmugam and C. Boyer, *J. Am. Chem. Soc.*, 2014, **136**, 5508-5519.
53. A. Anastasaki, V. Nikolaou, G. S. Pappas, Q. Zhang, C. Wan, P. Wilson, T. P. Davis, M. R. Whittaker and D. M. Haddleton, *Chem. Sci.*, 2014.
54. Y.-M. Chuang, A. Ethirajan and T. Junkers, *ACS Macro Lett.*, 2014, **3**, 732-737.
55. Q. Zhang, P. Wilson, Z. Li, R. McHale, J. Godfrey, A. Anastasaki, C. Waldron and D. M. Haddleton, *J. Am. Chem. Soc.*, 2013, **135**, 7355-7363.

56. Q. Zhang, P. Wilson, A. Anastasaki, R. McHale and D. M. Haddleton, *ACS Macro Letters*, 2014, 491-495.
57. Q. Zhang, Z. Li, P. Wilson and D. M. Haddleton, *Chem. Commun.*, 2013, **49**, 6608-6610.
58. C. Waldron, Q. Zhang, Z. Li, V. Nikolaou, G. Nurumbetov, J. Godfrey, R. McHale, G. Yilmaz, R. K. Randev, M. Girault, K. McEwan, D. M. Haddleton, M. Droesbeke, A. J. Haddleton, P. Wilson, A. Simula, J. Collins, D. J. Lloyd, J. A. Burns, C. Summers, C. Houben, A. Anastasaki, M. Li, C. R. Becer, J. K. Kiviaho and N. Risangud, *Polym. Chem.*, 2014, **5**, 57.
59. B. Le Droumaguet and J. Nicolas, *Polym. Chem.*, 2010, **1**, 563-598.
60. Y. Qi and A. Chilkoti, *Polym. Chem.*, 2014, **5**, 266-276.
61. D. Konkolewicz, Y. Wang, M. Zhong, P. Krys, A. A. Isse, A. Gennaro and K. Matyjaszewski, *Macromolecules*, 2013, **46**, 8749-8772.
62. S. Harrisson and J. Nicolas, *ACS Macro Lett.*, 2014, **3**, 643-647.
63. S. Perrier, S. P. Armes, X. S. Wang, F. Malet and D. M. Haddleton, *J. Polym. Sci., Part A: Polym. Chem.*, 2001, **39**, 1696-1707.
64. M. Ciampolini and N. Nardi, *Inorg. Chem.*, 1966, **5**, 41-44.

Chapter 3: An investigation into the effect of several *N*-substituted acrylamide monomers on chain-end fidelity under aqueous SET-LRP conditions

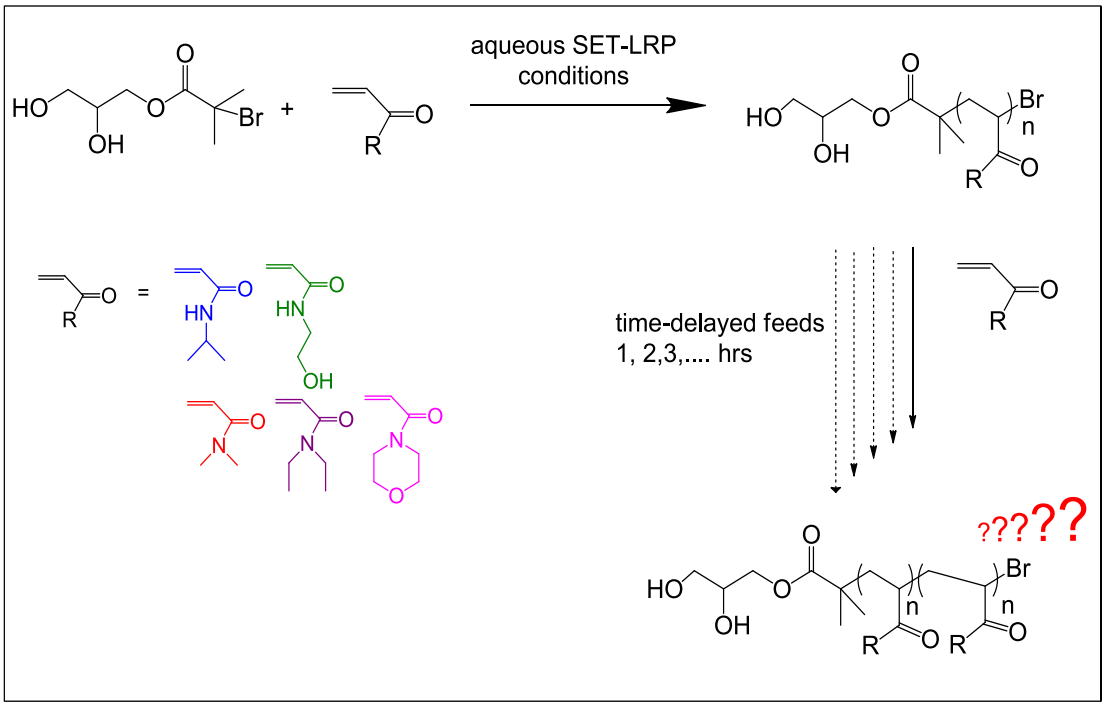

An investigation into the relative rates of ω-Br chain end loss for secondary (NIPAM, HEAA) and tertiary (DMA, N,N-diethylacrylamide (DEA), N-acryloylmorpholine (NAM)) acrylamides under aqueous SET-LRP conditions is reported. In the diblock copolymer system, the monomer sequence was successfully varied and limiting effects on the copolymerisation have been comprehensively examined through a series of control experiments which suggest that the rate of ω-Br chain end loss is enhanced in tertiary acrylamides relative to secondary acrylamides. In addition, by utilising aqueous SET-LRP, high molecular weights of homopolyacrylamides were targeted. Well-defined polymeric materials including PNIPAM, PHEAA and PDMA were obtained with full conversions and narrow MWDs. Remarkably, successive in situ chain extension and block copolymerisation were achieved via iterative monomer addition in one-pot.

3.1 Introduction

Hydrophilic polyacrylamides (PAMs) have been widely used in wastewater treatment, oil recovery, cosmetics, and biomedical applications.[1, 2] The synthesis of PAMs has been extensively studied, however, in order to expand their potential applications and enhance the quality of polymeric materials, controlled polymerisation processes have also been employed. In the last two decades, significant progress in the field of reversible deactivation radical polymerisation (RDRP) has been achieved; however, the RDRP of hydrophilic monomers in aqueous media still remains a challenge. Generally, in pure water, the RDRP process is fast and uncontrolled resulting in side reactions and affecting on equilibrium between the dormant and active chain species. Several methods have been exploited in order to suppress these side reactions including, nitroxide mediated polymerisation (NMP),[3-5] reversible addition-fragmentation chain transfer (RAFT),[6-8] atom transfer radical polymerisation (ATRP)[9, 10] and single electron transfer living radical polymerisation (SET-LRP).[11-14]

Transition metal mediated controlled radical polymerisation (TMM-CRP) relies on careful manipulation of the equilibrium between alkyl halides (Pn–X) and macroradicals (Pn•) species, which is mediated by Cu-ligand complexes. The increased side reactions in water have been alleviated by performing the TMM-CRP in the presence a cosolvent (usually an alcohol). [15-24] In addition, the polymerisation of acrylamide monomer and its derivatives is further complicated by undesirable termination reactions that lead to loss of ω-Br chain end functionality.[25-27]

The TMM-CRP of acrylamide based monomers seems problematic with regard to the control of the polymerisation when water was employed as the only solvent at

ambient temperature.[10, 28] Furthermore, in the literature few publications have reported controlled block copolymerisation and they are limited to the synthesis of just diblock copolymers. Matyjaszewski and co-workers first reported the challenges of conducting successful aqueous ATRP.[25, 27] Brittain *et al.* subsequently reported of polydimethacrylamide employing a different copper salts.[26] Broad molecular weight distributions, and poor end group fidelity were attributed to the fact that the Cu salts complex to the amide group of the chain ends stabilising the radical which then the concentration of radical is increased causing ‘’spontaneous’’ termination reactions.

In order to explain this further, they proposed a cyclization reaction involving nucleophilic bromide displacement to undergo hydrolysis to form a hydroxy-terminated polymer (Scheme 1). Thus it is apparent that the aqueous ATRP of acrylamides mediated via CuX remains a challenge.

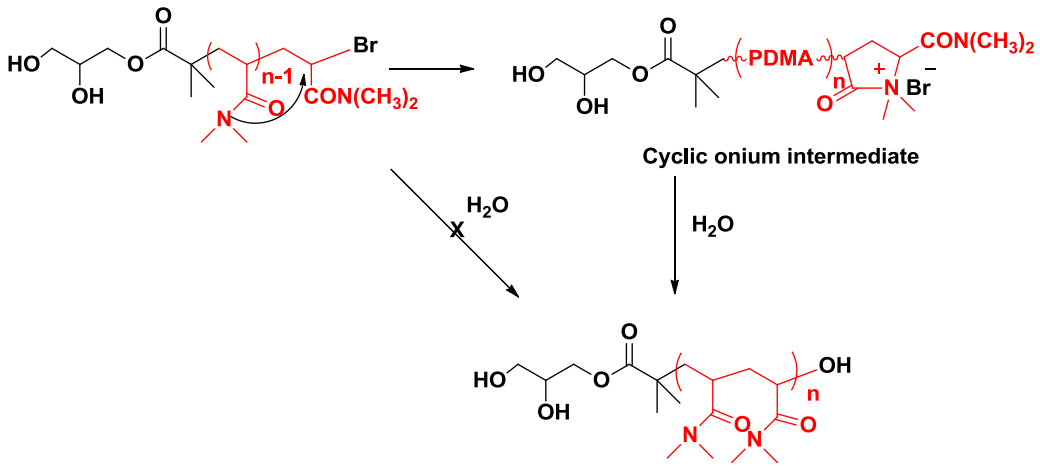

Scheme 1. Termination *via* formation of a cyclic onium species as described by Brittain.[26]

SET-LRP is one of the RDRP techniques which allows for the synthesis of polymers with high end-group functionality. The disproportionation of Cu(I)Br in

the presence of nitrogen containing ligands is the key step in the SET-LRP mechanism as it generates both the activator Cu(0) and the deactivating $Cu(II)Br_2$ species.[13, 29-33] It is worthwhile to note that the equilibrium constants for the disproportionation rely primarily on the nature of the ligand[13] and solvent.[34, 35] This constant is significantly high in the presence of Me_6TREN in aqueous media as opposed to organic solvents.[35, 36]

In 2013 Haddleton *et al*. introduced a simple approach for conducting TMM-LRP (SET-LRP) of poly(acrylamide)s and poly(acrylate)s in water.[37, 38] The key step in this method is the full disproportionation of the CuBr in water prior to the addition of monomer and initiator.

In previous chapter the advantage of full disproportionation of $Cu(I)Br/Me_6$TREN in water *prior to* monomer and initiator addition to synthesise both homo and multiblock copolymer has been exploited. Perhaps, the most obvious advantage of this work is that quantitative conversion was achieved in very short time scale (within minutes) with final dispersity as low as 1.15. Interestingly, high end group fidelity could be achieved not only by employing lower reaction temperatures (i.e., ice/water bath) but also by regulating the time of monomer additions, which allowed for the copolymerisation to proceed without appreciable loss of the polymerisation control.[29] In addition, the limiting factor for the chain extension of hexablock copolymer was attributed to the fast loss of ω-Br chain end in the presence of DMA.

Therefore, in this chapter, aqueous SET-LRP process is employed to study the effect of various acrylamide based monomers on chain extension at or below ambient temperature. Kinetic chain extension experiments are conducted to investigate the relative rates of ω-Br chain end loss for secondary (NIPAM, HEAA) and tertiary

(DMA, DEA and NAM) acrylamides. The capability of different acrylamides to retain the chain-end group was examined by delaying the chain extension reaction for certain period of times. The structure of *N*-substituted acrylamide monomers showed different influences on the chain end functionality, offering an insight into the importance of monomer selection and sequence in poly(acrylamide)s. This provides *prior* knowledge of the best combination of monomers that allowed for optimising the synthesis of higher MW acrylamide block copolymers. The ability of Cu(0)-mediated polymerisation to synthesise high MW of (co)polyacrylamides in water is investigated towards industrial applications. Well-defined homo and block copolymers are obtained, yielding polymers with high conversions and narrow MWDs as evidenced by NMR and SEC analyses.

3.2 Results and discussion

In previous work, the Haddleton group described the successful synthesis of poly(acrylamides) *via* SET-LRP technique in aqueous media. [37, 38] Although narrow molecular weight distributions were obtained, the loss of the end group fidelity was also highlighted. [25-27] In the first chapter it was shown that the loss of the bromine chain end can be minimized by optimising the reaction conditions and therefore nona/hexablock (co)polyacrylamides were successfully synthesised. However, different results were observed when DMA was used as a building block to facilitate the synthesis of multiblock copolymers. DMA structurally differs from NIPAM and HEAA in containing *N,N*-dialkyl-substituted amide. It has been reported that aqueous copper-mediated polymerisation is difficult to control due to the nucleophilic substitution of the ω-Br by H_2O.[25-27] Therefore, the effect of monomer

structure on the substitution of the bromine will be further investigated utilising three different tertiary acrylamides.

3.2.1 The effect of monomer on chain-end fidelity

The increased low MW shoulder present during polymerisation of DMA (see previous chapter) led to an investigation into the relative rates of ω-Br chain end loss for secondary (NIPAM, HEAA) and tertiary (DMA, NAM and DEA) acrylamides. Each monomer was homopolymerised *via* aqueous SET-LRP and then in all experiments NIPAM was employed as the model monomer and added at different time-delayed feeds. The extent of chain extension was subsequently evaluated by ^{1}H NMR and SEC analyses.

In chapter 2 it was reported that the homopolymerisation of NIPAM was completed within 11 minutes (DP=10). In order to assess the retention of end group fidelity as a function of time, the homopolymerisation was allowed to proceed for 2-8 hours before addition of the second aliquot of NIPAM (Scheme 2). It is noted that in all cases, full monomer conversion was achieved prior to the addition of NIPAM.

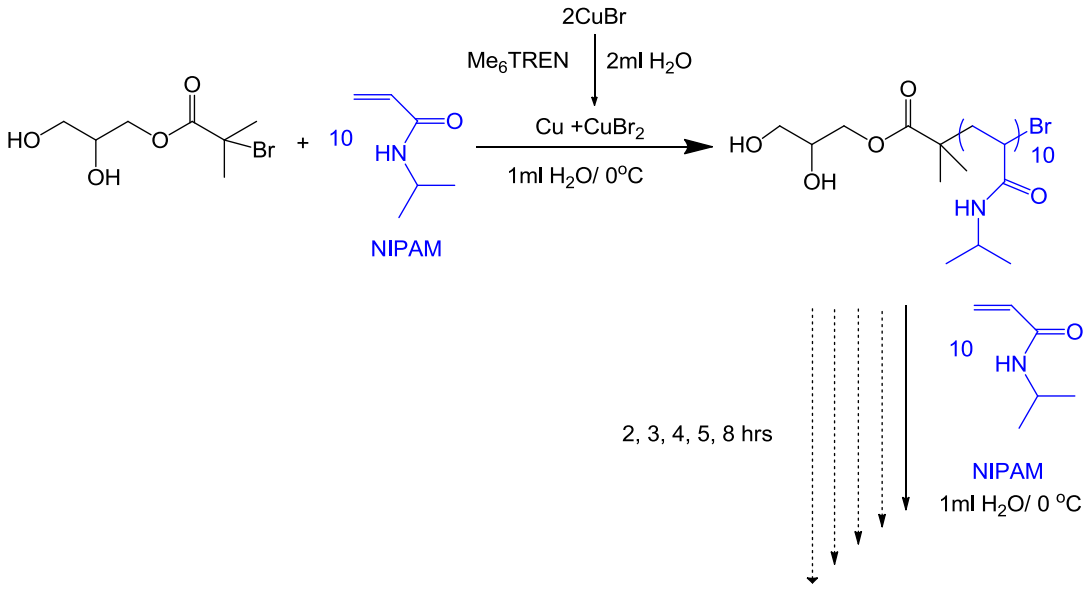

Scheme 2. Assessment of the chain end fidelity of PNIPAM by *in situ* chain extension using deoxygenated NIPAM (10 eq) following chain extension at delayed feed times. $[M]_0 : [I]_0 : [CuBr] : [Me_6TREN] = [10] : [1] : [0.04] : [0.04]$.

Despite the fast rate of the initial homopolymerisation, successful chain extension was achieved upon addition of the second portion of NIPAM after 2, 3, 4 and 5 hours respectively (each time point consists a different experiment when the homopolymerisation of NIPAM is repeated and left in the aqueous solutions for different time scales), ^{1}H NMR analysis confirmed 100% conversion (Table 1, Figure 1) for the chain extension and SEC analysis supported the retention of the *ω*-Br chain end as demonstrated by a complete shift in the molecular weight distribution (Figure 2, 2 hrs) and (Section 3.4.4, Figure 17). When the addition of NIPAM was delayed for 8 hours, ^{1}H NMR revealed that the conversion was limited to 55%, even when the reaction was left to proceed overnight. SEC also revealed minimal shift in the molecular weight distribution suggesting loss of the *ω*-Br chain end (Figure 2, 8 hrs).

Table 1. Investigating the effect of delayed feed time on the chain end fidelity of PNIPAM under aqueous SET-LRP conditions. $[M]_0$: $[I]_0$: [CuBr] : $[Me_6TREN]$ = [10] : [1] : [0.04] : [0.04].

Reaction No.	Monomer	Conv. (%)	Time per block (hr)	$M_{n,th}$ g.mol^{-1}	$M_{n,SEC}{}^{a}$ g.mol^{-1}	$Đ^{a}$
1	NIPAM	100	2	1400	2600	1.05
	NIPAM	100	overnight	2500	4500	1.09
2	NIPAM	100	3	1400	2600	1.05
	NIPAM	100	overnight	2500	4300	1.07
3	NIPAM	100	4	1400	2600	1.05
	NIPAM	100	overnight	2500	4200	1.11
4	NIPAM	100	5	1400	2600	1.05
	NIPAM	100	overnight	2500	4600	1.08
5	NIPAM	100	8	1400	2600	1.05
	NIPAM	50	overnight	2500	3500	1.16

[a] DMF SEC, calibrating with PMMA standard.

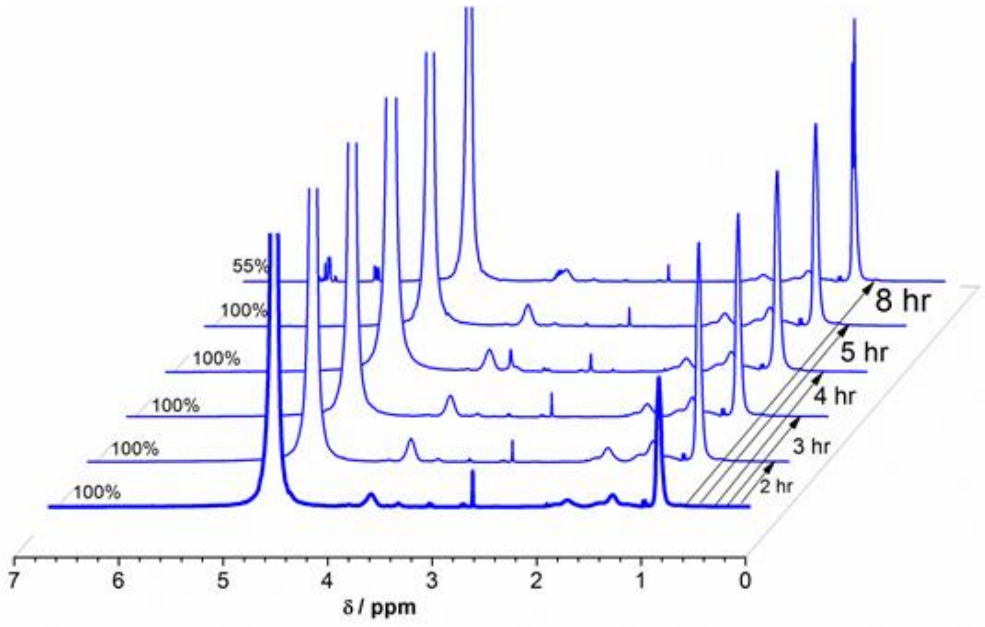

Figure 1. Assessment of the chain end fidelity of PNIPAM by *in situ* chain extension using deoxygenated NIPAM (10 eq). ^{1}H NMR for following chain extension at delayed feed times. $[M]_0$: $[I]_0$: [CuBr] : $[Me_6TREN]$ = [10] : [1] : [0.04] : [0.04].

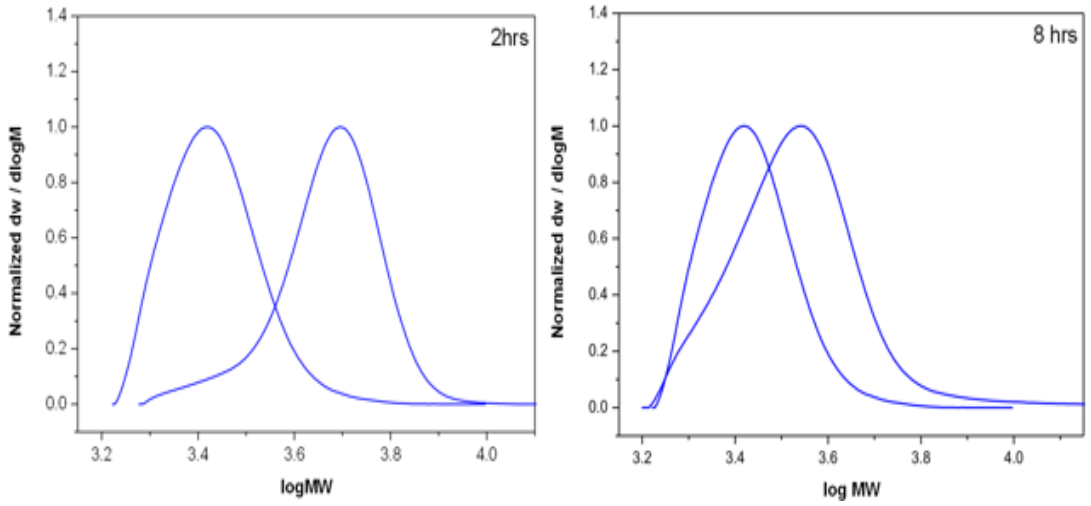

Figure 2. Assessment of the chain end fidelity of PNIPAM by in situ chain extension using deoxygenated NIPAM (10 eq). DMF SEC for following chain extension at delayed feed times. $[M]_0$: $[I]_0$: [CuBr] : [Me_6TREN] = [10] : [1] : [0.04] : [0.04].

In previous work[37] describing aqueous SET-LRP, compositional and end group analysis was conducted on poly(acrylamides) using low molecular weight PNIPAM (DP_n = 8). It was found that even at 0°C, two modes of termination were operational. Hydrolysis of the ω-Br end group *via* a cyclic onium species (Scheme 1) and elimination of HBr to furnish either an OH or internal vinylic ω-end group. The present data suggests that, qualitatively, the extent of termination increases as a function time.

Similar results were obtained when a secondary acrylamide (HEAA) was initially homopolymerised achieving full monomer conversion followed by the chain extension with NIPAM. Retention of the *ω*-Br chain end was evident when chain extension was delayed for up to 4 hrs (Table 2, Figure 3, 4) (Section 3.4.4, Figure 18).

Table 2. Investigating the effect of delayed feed time on the chain end fidelity of PHEAA under aqueous SET-LRP conditions. $[M]_0 : [I]_0 : [CuBr] : [Me_6TREN] = [10] : [1] : [0.04] : [0.04]$.

Reaction No.	Monomer	Conv. (%)	Time per block (hr)	$M_{n,th}$ g.mol^{-1}	$M_{n,SEC}$[a] g.mol^{-1}	$Đ$[a]
1	HEAA	100	2	1400	3600	1.07
	NIPAM	100	Overnight	2500	5500	1.07
2	HEAA	100	3	1400	3600	1.09
	NIPAM	100	overnight	2500	4900	1.08
3	HEAA	100	4	1400	3600	1.07
	NIPAM	95	overnight	2500	5000	1.07
4	HEAA	100	5	1400	3600	1.07
	NIPAM	75	overnight	2500	4400	1.09

[a] DMF SEC, calibrating with PMMA standard.

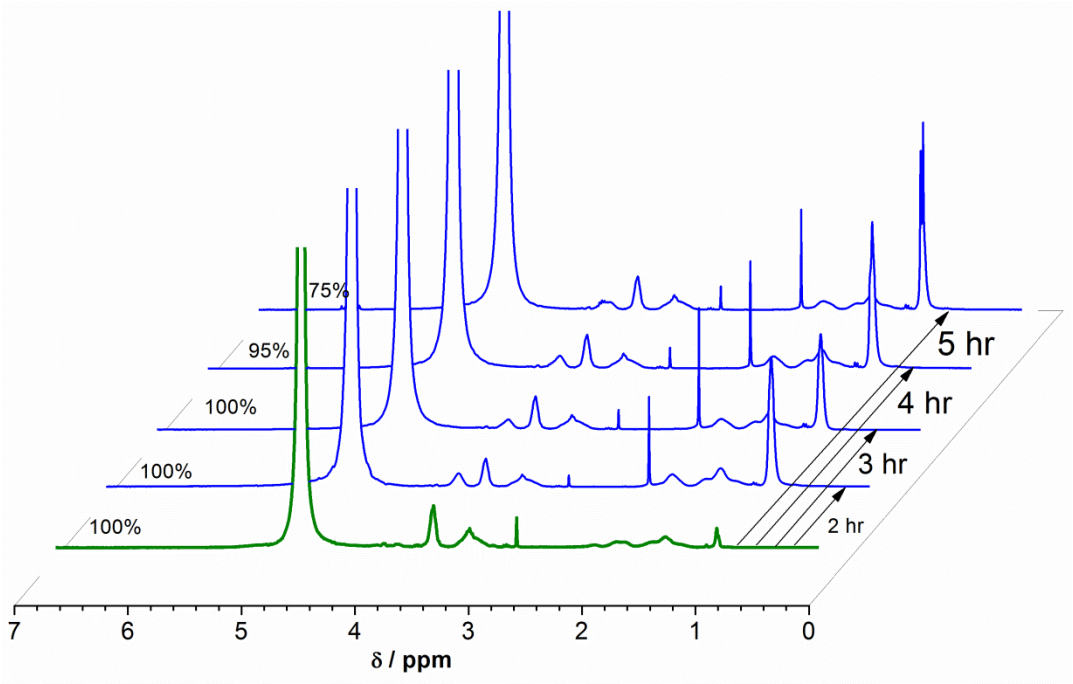

Figure 3. Assessment of the chain end fidelity of PHEAA by in situ chain extension using deoxygenated NIPAM (10 eq). ^{1}H NMR for following chain extension at delayed feed times. $[M]_0 : [I]_0 : [CuBr] : [Me_6TREN] = [10] : [1] : [0.04] : [0.04]$.

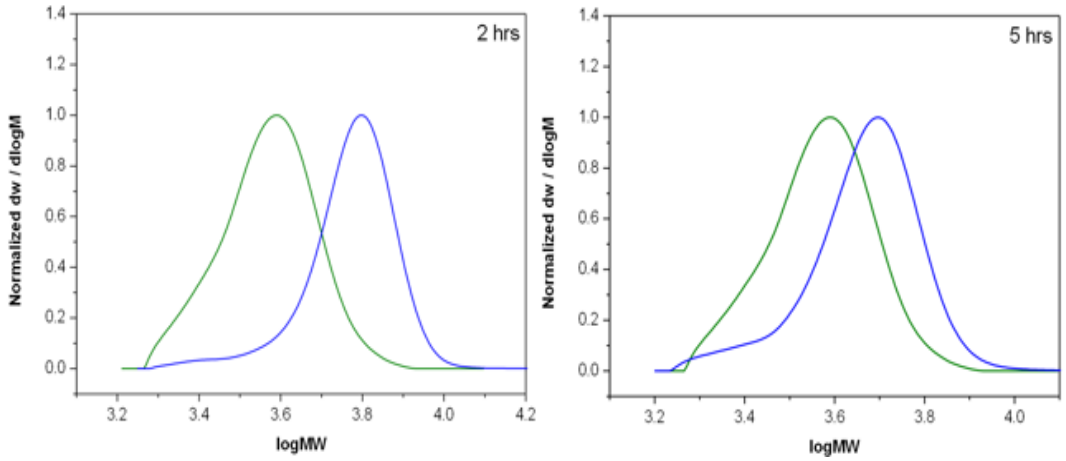

Figure 4. Assessment of the chain end fidelity of PHEAA by in situ chain extension using deoxygenated NIPAM (10 eq). DMF SEC for following chain extension at delayed feed times. $[M]_0 : [I]_0 : [CuBr] : [Me_6TREN] = [10] : [1] : [0.04] : [0.04]$.

However, after a 5 hour delay, conversion appeared to be limited by H NMR (75 %, Table 2, Figure 3) and SEC revealed a low MW shoulder and an incomplete shift of the MWDs (the reaction was left to proceed overnight) suggesting that the end group fidelity had been compromised (Figure 4), (Section 3.4.4, Figure 18).

Attempts to chain extend the tertiary acrylamide DMA (Table 3, Figure 5, 6) were successful when the aliquot of NIPAM was injected into the reaction mixture after a delay of up to 30 minutes. With delay times of an hour, or more, conversions and molecular weight shifts were significantly compromised, implying an enhancement in the loss of end group, in line with results obtained in previous chapter.

Table 3. Investigating the effect of delayed feed time on the chain end fidelity of PDMA under aqueous SET-LRP conditions. $[M]_0$: $[I]_0$: [CuBr] : $[Me_6TREN]$ = [10] : [1] : [0.04] : [0.04].

Reaction No.	Monomer	Conv. (%)	Time per block (hr)	$M_{n,th}$ g.mol^{-1}	$M_{n,SEC}{}^{a}$ g.mol^{-1}	$Đ^{a}$
1	DMA	100	0.5	1200	2400	1.04
	NIPAM	100	overnight	2300	4400	1.10
2	DMA	100	1	1200	2500	1.07
	NIPAM	20	overnight	2300	3100	1.11
3	DMA	100	2	1200	2600	1.07
	NIPAM	15	overnight	2300	2700	1.08

[a] DMF SEC, calibrating with PMMA standard.

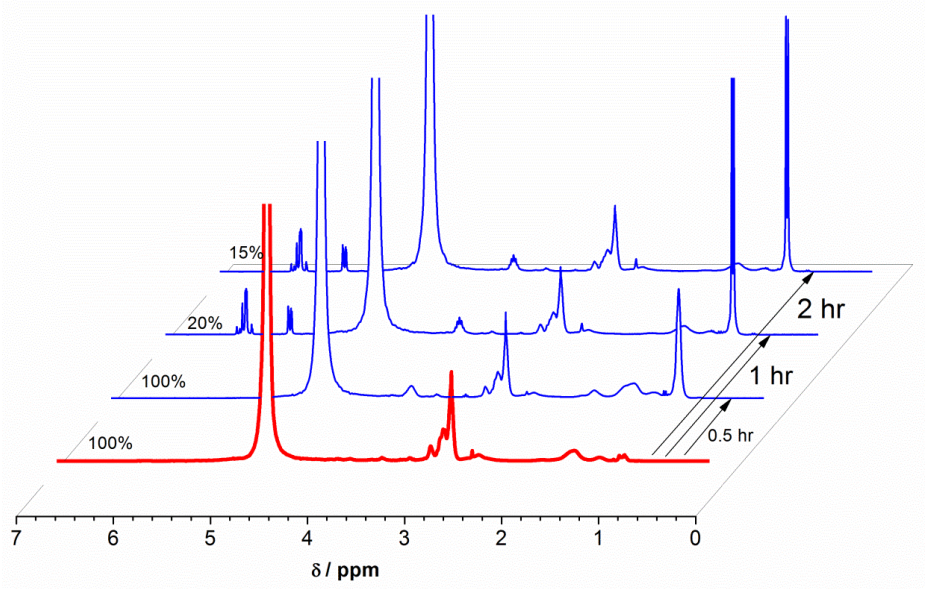

Figure 5. Assessment of the chain end fidelity of PDMA by *in situ* chain extension using deoxygenated NIPAM (10 eq).^{1}H NMR (c) following chain extension at delayed feed times. $[M]_0$: $[I]_0$: [CuBr] : $[Me_6TREN]$ = [10] : [1] : [0.04] : [0.04].

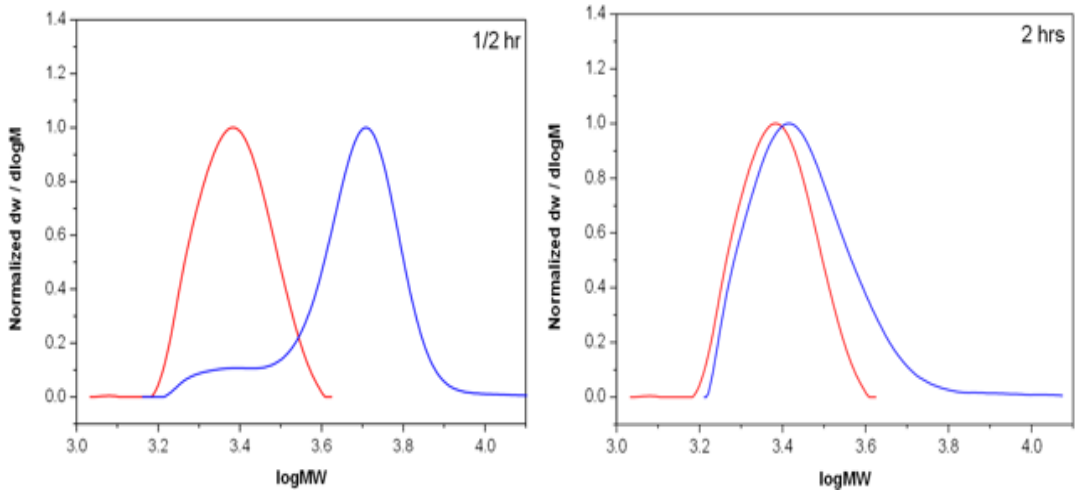

Figure 6. Assessment of the chain end fidelity of PDMA by in situ chain extension using deoxygenated NIPAM (10 eq). DMF SEC for following chain extension at delayed feed times. $[M]_0 : [I]_0 : [CuBr] : [Me_6TREN] = [10] : [1] : [0.04] : [0.04]$.

In order to further explore the inability of tertiary acrylamides to retain high end group fidelity at prolonged period of times, a second tertiary acrylamide, *N*-acryloylmorpholine, NAM, was also investigated. Homopolymerisation of NAM *via* aqueous SET-LRP was recently reported highlighting the inability to successfully chain extend from a NAM macroinitiator *via* sequential monomer addition.[39] Therefore, to complete this investigation, NAM was also screened to establish if this was due to an enhanced rate of chain end loss (Table 4). Following homopolymerisation of NAM, addition of NIPAM after 30 minutes resulted in 100 % conversion according to ^{1}H NMR (Figure 7). However, even after just 30 minutes, SEC revealed a bimodal mass distribution (Figure 8), whereby a big part of the homopolymer was unable to chain extend following addition of NIPAM. Increasing the delay time resulted in an increase in chain end loss (Section 3.4.4, Figure 20) until after a 2 hour delay; no chain extension was detected by SEC (Figure 8).

Table 4. Investigating the effect of delayed feed time on chain end fidelity of PNAM under aqueous SET-LRP conditions. $[M]_0 : [I]_0 : [CuBr] : [Me_6TREN] = [10] : [1] : [0.04] : [0.04]$.

Reaction No.	Monomer	Conv. (%)	Time per block (hr)	$M_{n,th}$ g.mol^{-1}	$M_{n,SEC}{}^{a}$ g.mol^{-1}	$Đ^{a}$
1	NAM	100	0.5	1400	3400	1.09
	NIPAM	100	overnight	2500	6300	1.32
2	NAM	100	1	1400	3400	1.09
	NIPAM	45	overnight	2500	4500	1.30
3	NAM	100	2	1400	3500	1.06
	NIPAM	20	overnight	2500	3500	1.08

[a] DMF SEC, calibrating with PMMA standard.

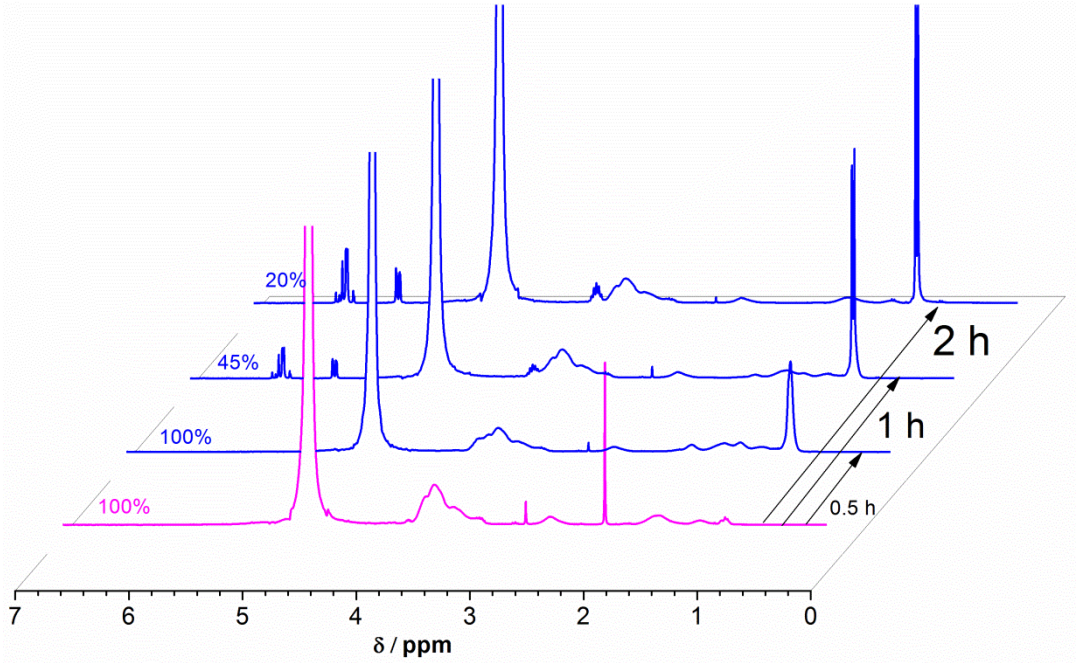

Figure 7. Assessment of the chain end fidelity of PNAM by in situ chain extension using deoxygenated NIPAM (10 eq).^{1}H NMR (c) following chain extension at delayed feed times. $[M]_0 : [I]_0 : [CuBr] : [Me_6TREN] = [10] : [1] : [0.04] : [0.04]$.

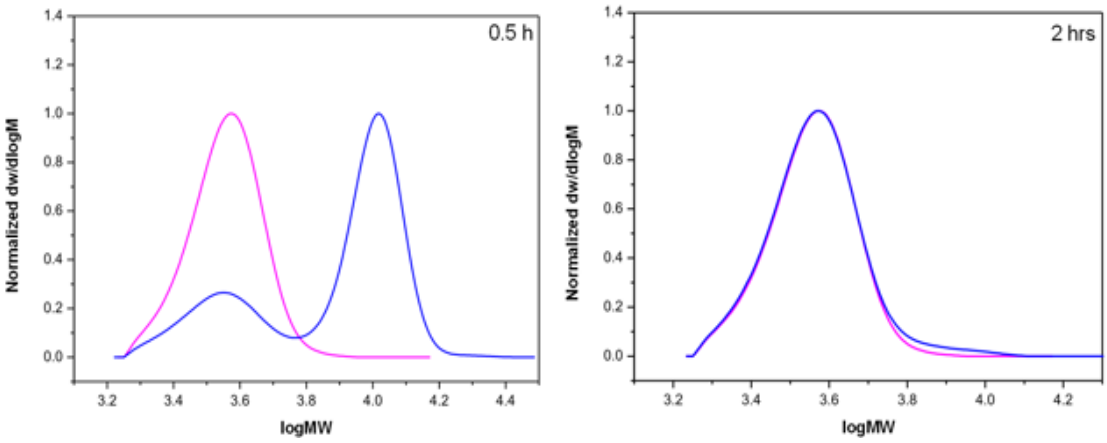

Figure 8. Assessment of the chain end fidelity of PNAM by in situ chain extension using deoxygenated NIPAM (10 eq). DMF SEC for following chain extension at delayed feed times. $[M]_0 : [I]_0 : [CuBr] : [Me_6TREN] = [10] : [1] : [0.04] : [0.04]$.

Similarly, *N*,*N*-diethylacrylamide, DEA, showed the same behaviour when identical conditions and procedures were applied (Section 3.4.4, Table 7, Figure 21). Though consistent with the results obtained for DMA, NAM and DEA, this represents the fastest rate of ω-Br chain end loss for the tertiary acrylamides screened and offers an explanation for the results in the earlier publication.

Finally, in order to further confirm the effect of the tertiary acrylamide on the loss of end group fidelity, homopolymers of PNIPAM and PDMA were synthesised and chain extension was attempted using a feed of DMA at the timed intervals reported in the first chapter. According to ^{1}H NMR (Figure 9) and SEC (Figure 10a), PNIPAM was successfully chain extended upon addition of DMA following a delay of up to 3 hours ((Section 3.4.4, Table 8). However, upon monomer injection after 4 hours limited conversion was observed (28 %), and after a delay time of 24 hours, no conversion or chain extension was detected by ^{1}H NMR of SEC analysis (Figure 9, 10b).

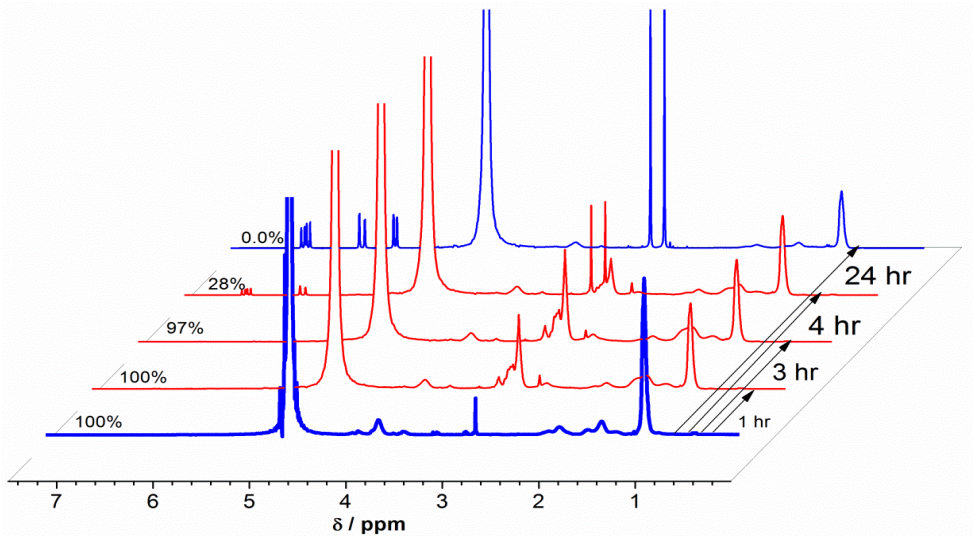

Figure 9: ^{1}NMR (D_2O) for the chain extension of PNIPAM with deoxygenated aqueous DMA (10 eq) after various time delays.

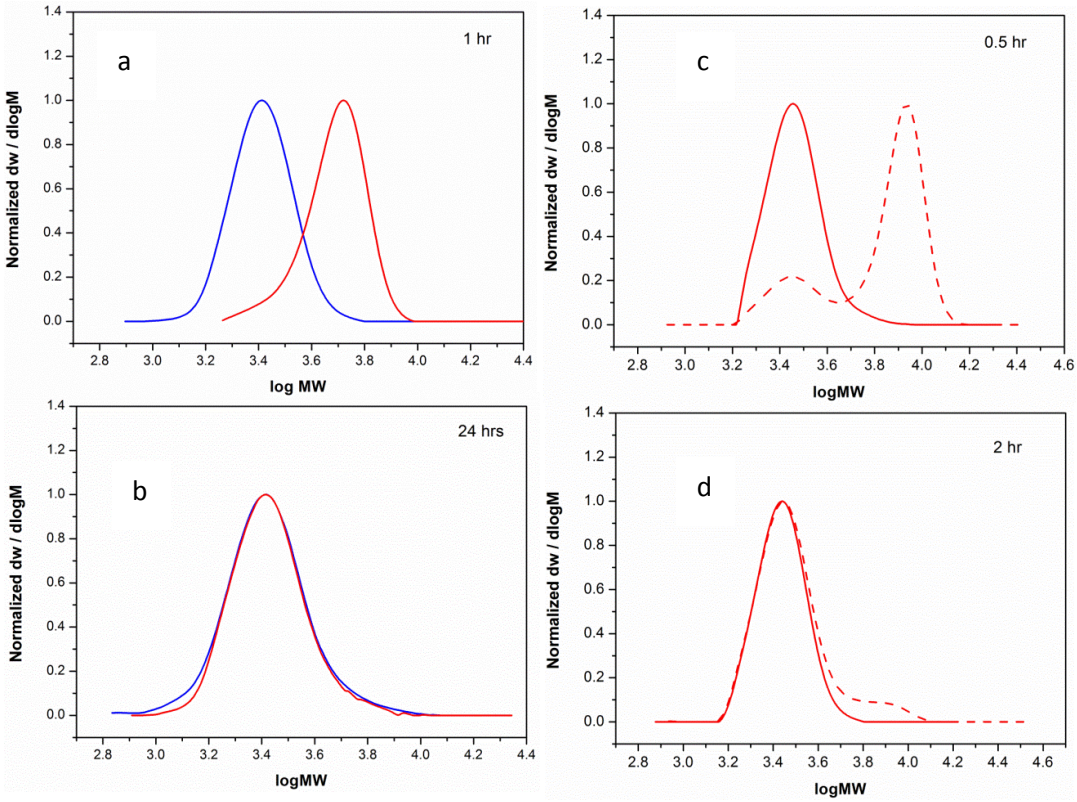

Figure 10: DMF SEC illustrating the effect of delayed feed time on chain end retention during homopolymerisation of NIPAM (a, b) and DMA (c, d). Chain

extension attempted using deoxygenated DMA (10 eq). $[M]_0$: $[I]_0$: [CuBr] : [Me_6TREN] = [10] : [1] : [0.04] : [0.04].

Switching to PDMA macroinitiator an increase in the rate of loss of ω-Br was noticed with a bimodal mass distribution apparent after a 30 minute delay *prior to* chain extension (Section 3.4.4, Table 9), (Figure 11, 10c-d,). These findings also suggest that, the extent of termination increases as a function time and monomer structure.

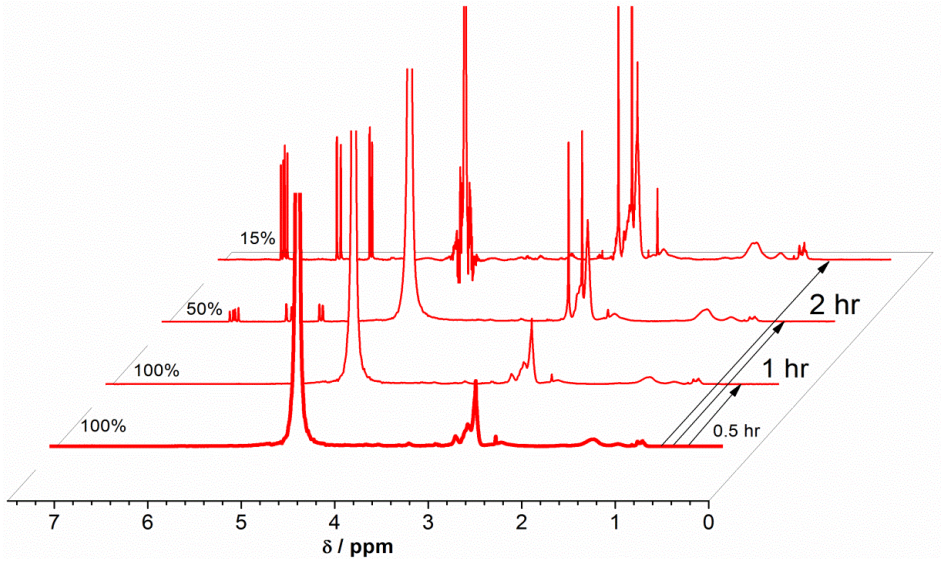

Figure 11. ^{1}NMR (D_2O) for the chain extension of PDMA with deoxygenated aqueous DMA (10 eq) after various time delays.

It has been proposed that one of the reasons for loss of control during the aqueous Cu-mediated polymerisation of (meth)acrylamides is substitution of the terminal bromine to form a cylic onium species.[25, 40] Teodorescu and Matyjaszewski have used small molecule models to show that substitution can occur through both the nitrogen and oxygen of the penultimate acrylamide monomer unit. This current study, qualitatively suggests that increasing the alkyl substitution and therefore the electron density of the amide group through inductive effects, increases the rate of

this cyclisation reaction resulting in an enhanced rate of termination and loss of active bromine chains.

3.2.2 Higher molecular weight block copolymers by aqueous SET-LRP

In order to investigate the dependence of block molecular weight upon the aqueous system, the average chain length per block was increased tenfold. Secondary acrylamides NIPAM and HEAA were polymerised with target DP_n = 100. The optimum amount of CuBr and Me_6TREN has been shown to vary with chain length.[41] Thus, the initial feed ratio was changed from $[M]_0$: $[I]_0$: [CuBr] : [Me_6TREN] = [10] : [1] : [0.04] : [0.04] to [100] : [1] : [0.008] : [0.004]. Although reactions were slower, full conversion was attained within 60 and 90 minutes respectively, and narrow molecular weight distributions were retained ($Đ \approx 1.10$, Figure 12, 13).

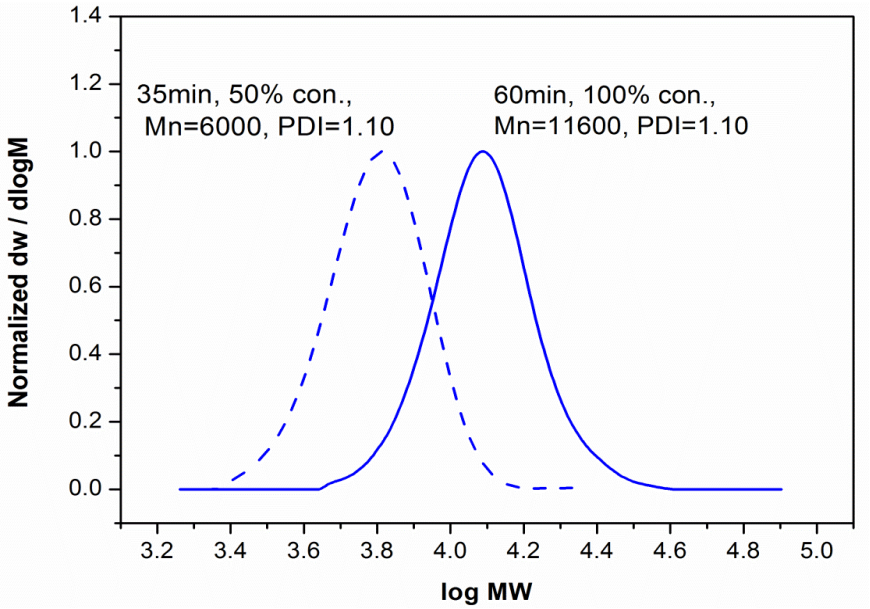

Figure 12. DMF SEC of higher molecular weight PNIPAM prepared by aqueous SET-LRP. [M] : [I] : [CuBr] : [Me_6TREN] = [100] : [1] : [0.008] : [0.004]

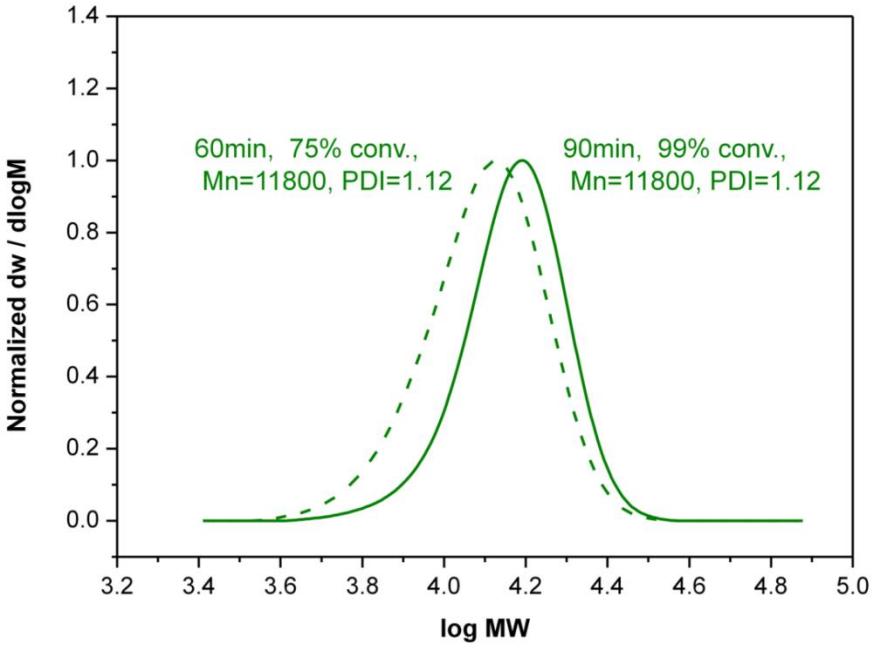

Figure 13. DMF SEC of higher molecular weight PHEAA prepared by aqueous SET-LRP. [M] : [I] : [CuBr] : [Me_6TREN] = [100] : [1] : [0.008] : [0.004]

The PNIPAM homopolymer was successfully chain extended upon two additional, sequential feeds of 100 molar equivalents (with respect to $[I]_0$) of deoxygenated aqueous NIPAM (Table 5). Diblock PNIPAM was obtained within a total reaction time of 2.5 hours ($Đ$ = 1.09), whilst the triblock was attained when the reaction was allowed to proceed overnight ($Đ$ = 1.08, Table 5, Figure 14).

Table 5. Preparation of higher molecular weight triblock homopolymer prepared by sequential addition of deoxygenated aliquots of aqueous NIPAM (100 eq) to PNIPAM during SET-LRP at 0ºC in H_2O. $[M]_0$: $[I]_0$: [CuBr] : [Me_6TREN] = [100] : [1] : [0.008] : [0.004].

Entry	Block number	Monomer	Conv. (%)	Time per block (min)[a]	$M_{n,th}$ g.mol^{-1}	$M_{n,SEC}$[b] g.mol^{-1}	$Đ$[b]
1	Block 1	NIPAM	100	60 (60)	11600	11600	1.11

2	Block 2	NIPAM	100	90 (150)	22900	19800	1.09
3	Block 3	NIPAM	100	Overnight	34200	38800	1.08

[a] Cumulative time in parentheses. [b] DMF SEC, calibrating with PMMA standard.

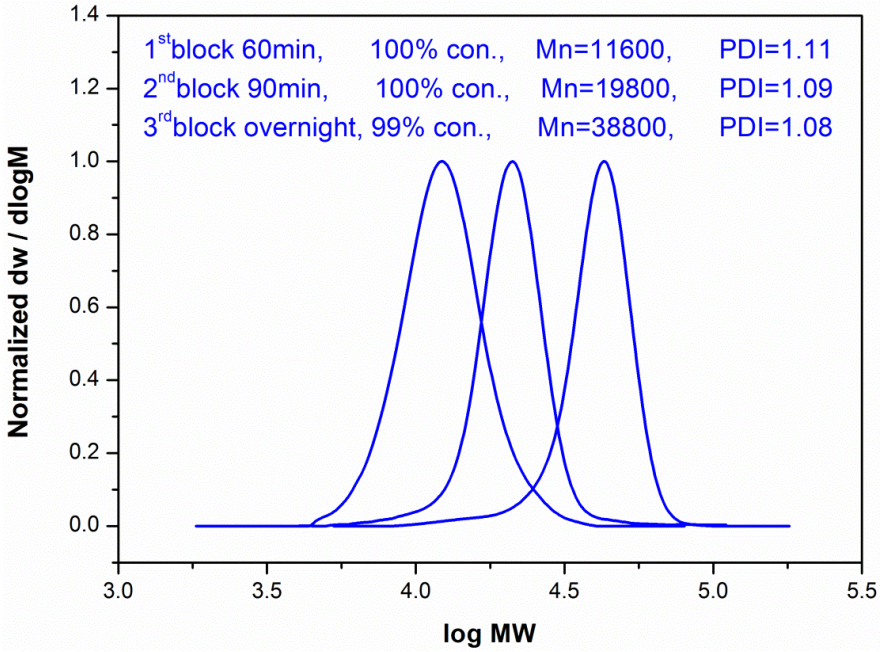

Figure 14. Evolution of block molecular weight by DMF SEC for high molecular weight triblock of PNIPAM. $[M]_0 : [I]_0 : [CuBr] : [Me_6TREN] = [100] : [1] : [0.008] : [0.004]$.

Furthermore, by switching the second aliquot of NIPAM with HEAA, a AB diblock copolymer P($NIPAM_{100}$-*b*-$HEAA_{100}$) was obtained with 4.5 hours ($Đ$ = 1.08, Table 6, entry 2). Addition of an aliquot of deoxygenated aqueous NIPAM to the diblock macroinitiator yielded an ABA triblock copolymer P($NIPAM_{100}$-*b*-$HEAA_{100}$- *b*-$NIPAM_{100}$) in a one pot process with retention of low dispersity ($Đ$ = 1.14 Table 6, Figure 15).

Table 6. Preparation of higher molecular triblock copolymer prepared by sequential monomer additon during SET-LRP at 0°C in H_2O. $[M]_0 : [I]_0 : [CuBr] : [Me_6TREN] = [100] : [1] : [0.008] : [0.004]$.

Entry	Block number	Monomer	Conv. (%)	Time per block (min)[a]	$M_{n,th}$ g.mol^{-1}	$M_{n,SEC}$[b] g.mol^{-1}	$Đ$[b]
1	Block 1	NIPAM	98	15 (15)	11600	13000	1.06
2	Block 2	HEAAm	99	250 (265)	23100	29000	1.08
3	Block 3	NIPAM	90	overnight	34200	42200	1.14

[a] Cumulative time in parentheses. [b] DMF SEC, calibrating with PMMA standard.

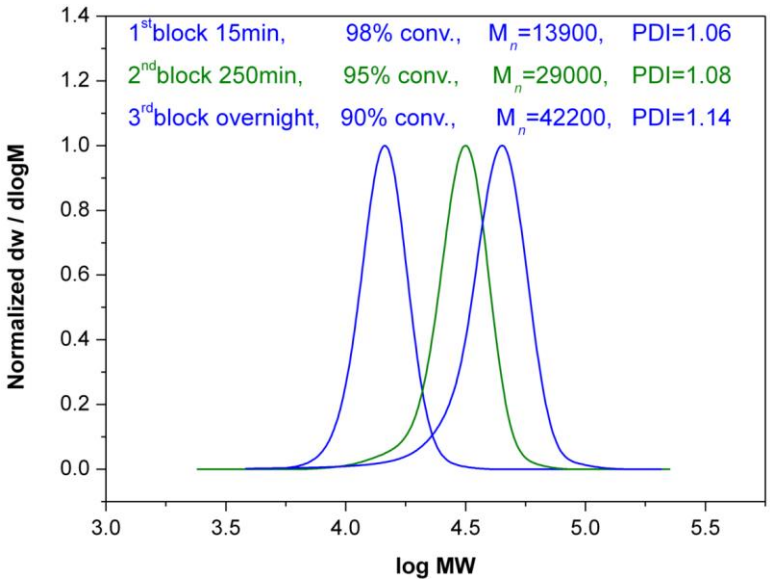

Figure 15. DMF SEC of ABA triblock copolymer P($NIPAM_{100}$-*b*-$HEAA_{100}$-*b*-$NIPAM_{100}$) prepared by aqueous SET-LRP with sequential monomer addition.

However, by employing DMA as the second building block, a multimodal molecular weight distribution of ABC triblock copolymer P($NIPAM_{100}$-*b*-$HEAA_{100}$-*b*-DMA_{100}) was observed ($Đ$ = 1.76, Figure 16) (Section 3.4.4, Table 10, entry 3). This

confirmed the effect of tertiary acrylamide on the end group functionality even when high molecular weights were targeted.

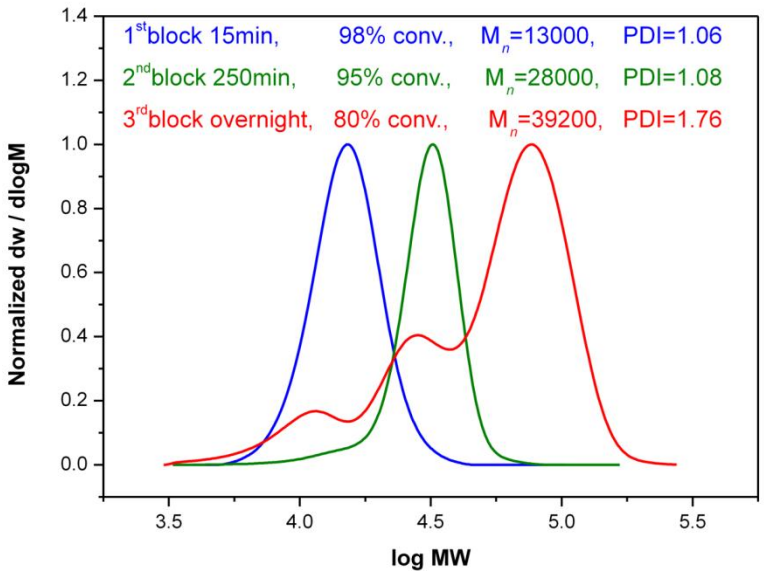

Figure 16. DMF SEC of ABC triblock copolymer P(NIPAM$_{100}$-*b*-HEAA$_{100}$-*b*-DMA$_{100}$) prepared by aqueous SET-LRP with sequential monomer addition.

3.3 Conclusion

The loss of the ω-Br chain end is a common limitation in Cu-mediated multiblock copolymerisation. During aqueous polymerisation it was recognised that tertiary acrylamides (DMA, DEA, NAM) invoke an enhanced rate of chain end loss relative to secondary acrylamides (NIPAM, HEAA), as exemplified by a variety of kinetic chain extension experiments. This highlights the need for careful consideration of monomer choice and sequence when designing a multiblock copolymer composition. In addition, the chain length per block can be successfully increased from DP$_n$ = 10 to DP$_n$ = 100 to facilitate the synthesis of higher molecular weight block copolymers. The synthesis of well-defined homopolymers including PNIPAM, PHEAA and PDMA has been obtained utilising aqueous Cu(0)-mediated RDRP.

Moreover, under carefully optimised conditions, the successive *in situ* chain extension and block copolymerisation of PNIPAM and PHEAA can be achieved.

3.4 Experimental

3.4.1 Materials and methods

N-Isopropylacrylamide (NIPAM, 97%) was purchased from commercial supplier (Sigma-Aldrich) and was purified by recrystallization from hexane to remove the inhibitor. 2-Hydroxyethyl acrylamide (HEAA, 97%, Sigma-Aldrich), *N*,*N*-dimethyl acrylamide (DMA, 99%, Sigma-Aldrich), *N*,*N*-diethyl acrylamide (DEA, 99%, Sigma-Aldrich) and 4-acryloylmorpholine (NAM, 97%, Sigma-Aldrich) were passed over a column filled with basic alumina to remove the inhibitor prior to use.

HPLC grade water (H_2O, VWR international, LLC) was used as the solvent for disproportionation and polymerisations.

The water soluble initiator 2, 3-dihydroxypropyl 2-bromo-2-methylpropanoate was prepared as reported in the literature.[42]

Tris(2-(dimethylamino)ethyl)amine (Me_6TREN) was synthesized according to literature procedures and stored under nitrogen prior to use.[43]

Copper(I) bromide (CuBr, 98%, Sigma-Aldrich) was sequentially washed with acetic acid and ethanol and dried under vacuum.

3.4.2 Instrumentation

Proton Nuclear Magnetic Resonance (^{1}H NMR) spectra were recorded on Bruker DPX-300 and DPX-400 spectrometers using deuterated solvents obtained from

Aldrich. Monomer conversion for NIPAM, HEAA, DMA, DEA and NAM homopolymerisation was determined, comparing the integral of vinyl protons with isopropyl, ethyl, dimethyl, diethyl, morphiline protons, respectively.

Size-exclusion chromatography (SEC) was conducted on Varian 390-LC system using DMF as the mobile phase (5 mM NH_4BF_4) at 50^oC, equipped with refractive index, UV and viscometry detectors, 2 × PLgel 5 mm mixed-D columns (300 × 7.5 mm), 1 × PLgel 5 mm guard column (50 × 7.5 mm) and autosampler. Commercial narrow linear poly (methyl methacrylate) standards in range of 200 to 1.0 × 10^6 g · mol^{-1} were used to calibrate the system. All samples were passed through 0.45 μm PTFE filter before analysis.

All reactions were carried out under an inert atmosphere of oxygen-free nitrogen, using standard Schlenk techniques.

3.4.3 General procedures

General procedure for homopolymerisation by aqueous SET-LRP (DPn = 10).

To a Schlenk tube fitted with a magnetic stir bar and a rubber septum, H_2O (2 mL) and Me_6TREN (0.1 mmol) were charged and the mixture was bubbled with nitrogen for 15 min. CuBr (0.1 mmol) was then carefully added under slight positive pressure of nitrogen. The mixture immediately became blue Cu(II) and a purple/red precipitate Cu(0) was observed. In a separate vial fitted with a magnetic stir bar and a rubber septum monomer (2.5 mmol) was dissolved in H_2O (1.0 mL) *prior to* addition of initiator (2,3-dihydroxypropyl 2-bromo-2-methylpropanoate, 0.25 mmol) and the resulting mixture was bubbled with nitrogen for 15 min. The degassed

monomer / initiator aqueous solution was then transferred via cannula to the Schlenk tube containing Cu(0) / $CuBr_2$ / Me_6TREN catalyst. The Schlenk tube was sealed and the mixed solution was allowed to polymerise at 0°C. Sample of the reaction mixture were then removed for analysis. The sample for ^{1}H NMR was directly diluted with D_2O. Catalyst residues were removed by filtering through a column of neutral alumina prior to DMF SEC analysis.

General procedure for homopolymerisation by aqueous SET-LRP (DP_n = 100)

To a Schlenk tube fitted with a magnetic stir bar and a rubber septum, H_2O (2 mL) and Me_6TREN (28 μmol) were charged and the mixture was bubbled with nitrogen for 15 min. CuBr (56 μmol) was then carefully added under slight positive pressure of nitrogen. The mixture immediately became blue Cu(II) and a purple/red precipitate Cu(0) was observed. In a separate vial fitted with a magnetic stir bar and a rubber septum monomer (7.0 mmol) was dissolved in H_2O (4.0 mL) prior to addition of initiator (2,3-dihydroxypropyl 2-bromo-2-methylpropanoate, 0.07 mmol) and the resulting mixture was bubbled with nitrogen for 15 min. The degassed monomer / initiator aqueous solution was then transferred *via* cannula to the Schlenk tube containing Cu (0) / $CuBr_2$ / Me_6TREN catalyst. The Schlenk tube was sealed and the mixed solution was allowed to polymerise at 0°C. Samples of the reaction mixture were then removed for analysis. The sample for ^{1}H NMR was directly diluted with D_2O. Catalyst residues were removed by filtering through a column of neutral alumina prior to DMF SEC analysis.

General procedure for kinetic investigation of aqueous SET-LRP polymerisation

Reactions were performed in triplicate. The general procedure for homopolymerisation by aqueous SET-LRP was followed. Homopolymer conversions were monitored by regular sampling to accurately determine the time at which full monomer conversion was reached according to ^{1}H NMR (D_2O). In subsequent experiments (also performed in triplicate) hompolymerisation was allowed to proceed to this time and a sample was taken, in order to confirm the anitcipated full conversion, *prior* to addition of freshly deoxygenated aqueous solutions of monomer (DP_n eq). Regular sampling was again employed to identify the time required to reach full monomer conversion. This was repeated until conversion and/or molecular weight distributions were compromised by termination. Samples taken for ^{1}H NMR were directly diluted with D_2O. Catalyst residues were removed by filtering through a column of neutral alumina prior to DMF SEC analysis.

General procedure for chain extension/multiblock copolymerisation by aqueous SET-LRP

The general procedure for homopolymerisation by aqueous SET-LRP was followed. At specific times determined by control experiments a sample was taken for conversion analysis before addition of freshly deoxygenated aqueous solutions of monomer (DP_n eq). This process was repeated until conversion and/or molecular weight distributions were compromised by termination. Samples taken for ^{1}H NMR

were directly diluted with D_2O. Catalyst residues were removed by filtering through a column of neutral alumina prior to DMF SEC analysis.

3.4.4 Additional characterisation

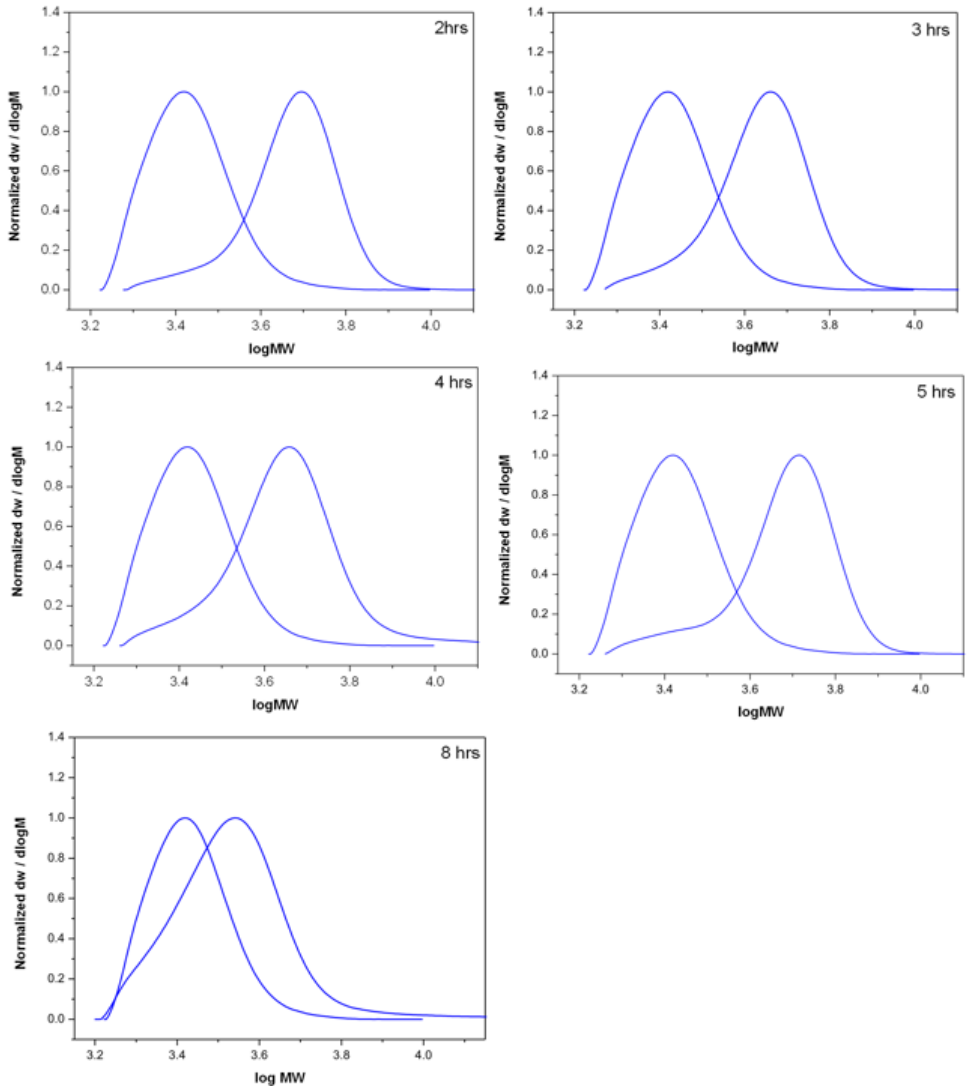

Figure 17. Assessment of the chain end fidelity of PNIPAM by in situ chain extension using deoxygenated NIPAM (10 eq). DMF SEC for following chain extension at delayed feed times. $[M]_0$: $[I]_0$: [CuBr] : [Me_6TREN] = [10] : [1] : [0.04] : [0.04].

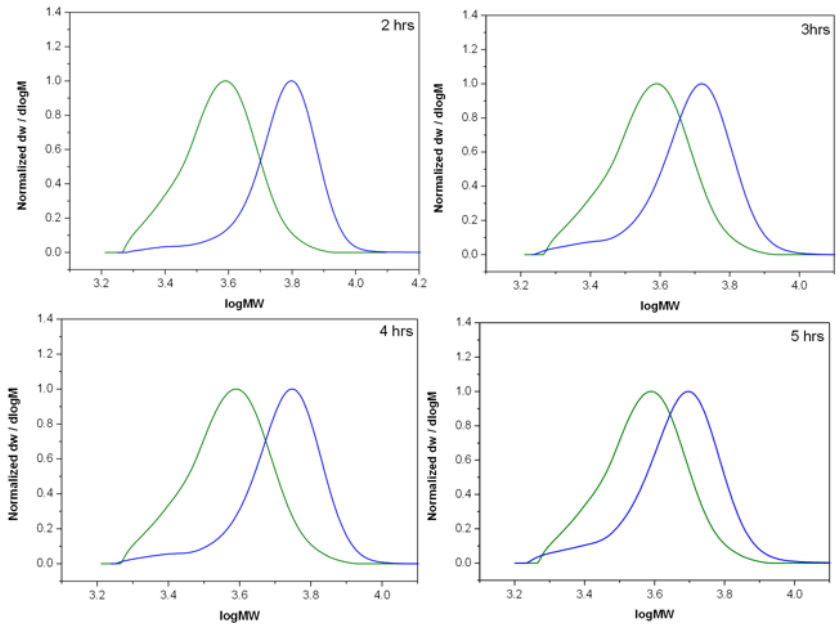

Figure 18. Assessment of the chain end fidelity of PHEAA by in situ chain extension using deoxygenated NIPAM (10 eq). DMF SEC for following chain extension at delayed feed times. $[M]_0$: $[I]_0$: [CuBr] : [Me_6TREN] = [10] : [1] : [0.04] : [0.04].

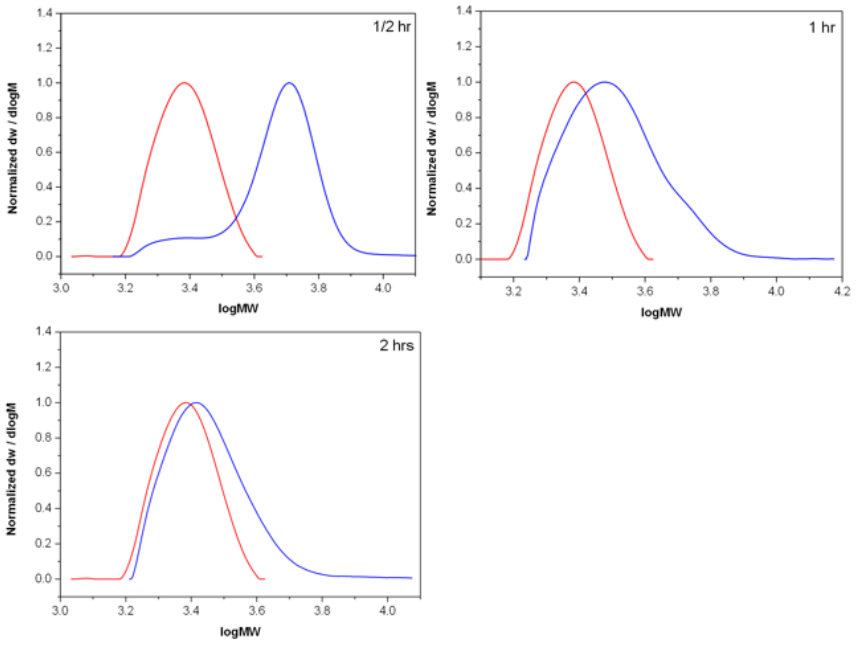

Figure 19. Assessment of the chain end fidelity of PDMA by in situ chain extension using deoxygenated NIPAM (10 eq). DMF SEC for following chain extension at delayed feed times. $[M]_0$: $[I]_0$: [CuBr] : [Me_6TREN] = [10] : [1] : [0.04] : [0.04].

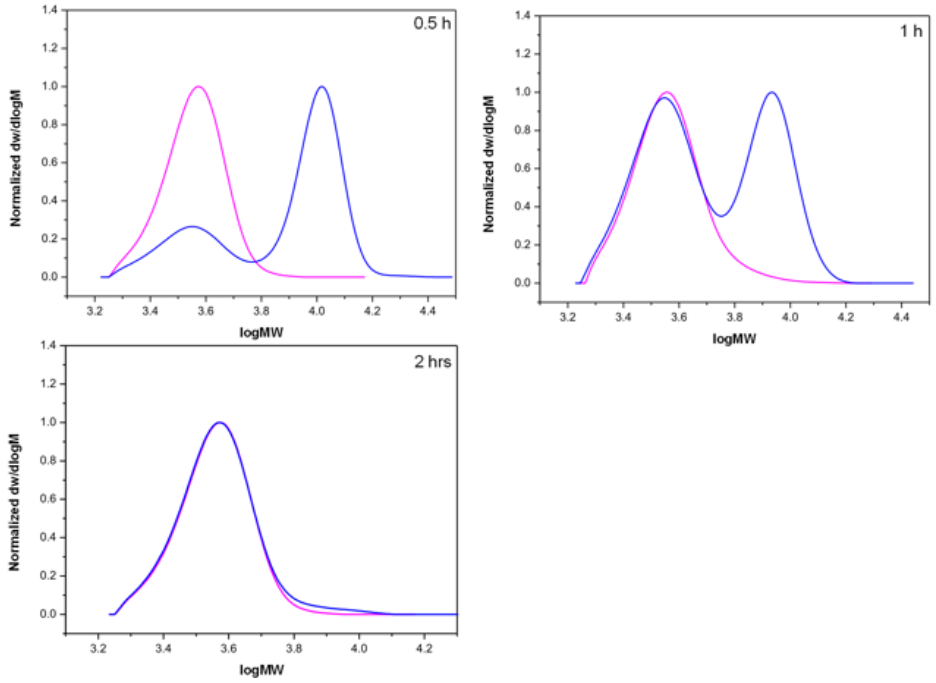

Figure 20. Assessment of the chain end fidelity of PNAM by *in situ* chain extension using deoxygenated NIPAM (10 eq). DMF SEC for following chain extension at delayed feed times. $[M]_0 : [I]_0 : [CuBr] : [Me_6TREN] = [10] : [1] : [0.04] : [0.04]$.

Table 7. Investigating the effect of delayed feed time of chain end fidelity of PDEA under aqueous SET-LRP.$[M]_0 : [I]_0 : [CuBr] : [Me_6TREN] = [10] : [1] : [0.04] : [0.04]$.

Reaction No.	Monomer	Conv. (%)	Time per block (hr)	$M_{n,th}$ g.mol^{-1}	$M_{n,SEC}$[a] g.mol^{-1}	$Đ$[a]
1	DEA	100	0.5	1500	2600	1.53
	NIPAM	98	overnight	2600	3200	1.15
2	DEA	100	1	1500	2600	1.51
	NIPAM	65	overnight	2600	3300	1.40
3	DEA	100	2	1500	2600	1.53
	NIPAM	30	overnight	2600	2600	1.54

[a] DMF SEC, calibrating with PMMA standard.

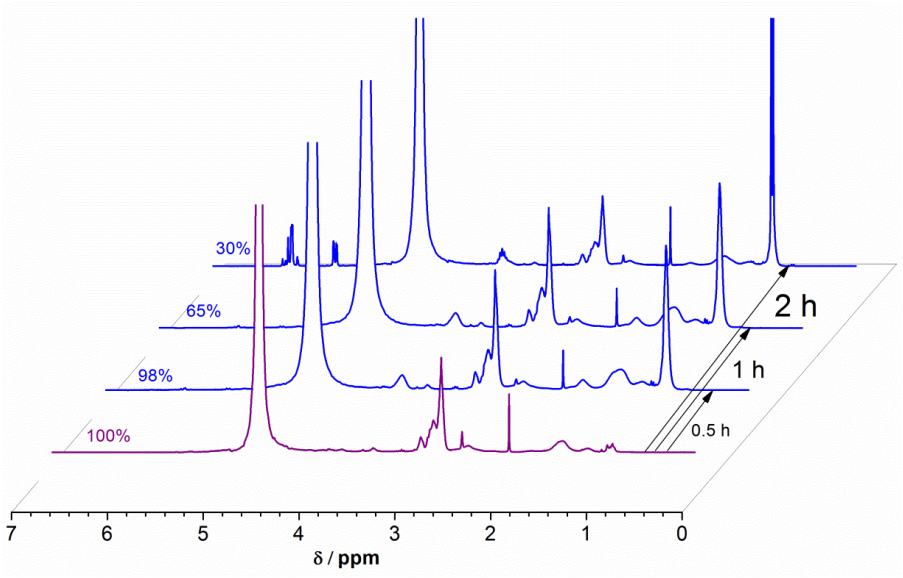

Figure 21. ^{1}NMR (D_2O) for the chain extension of PDEA with deoxygenated aqueous NIPAM (10 eq) after various time delays.

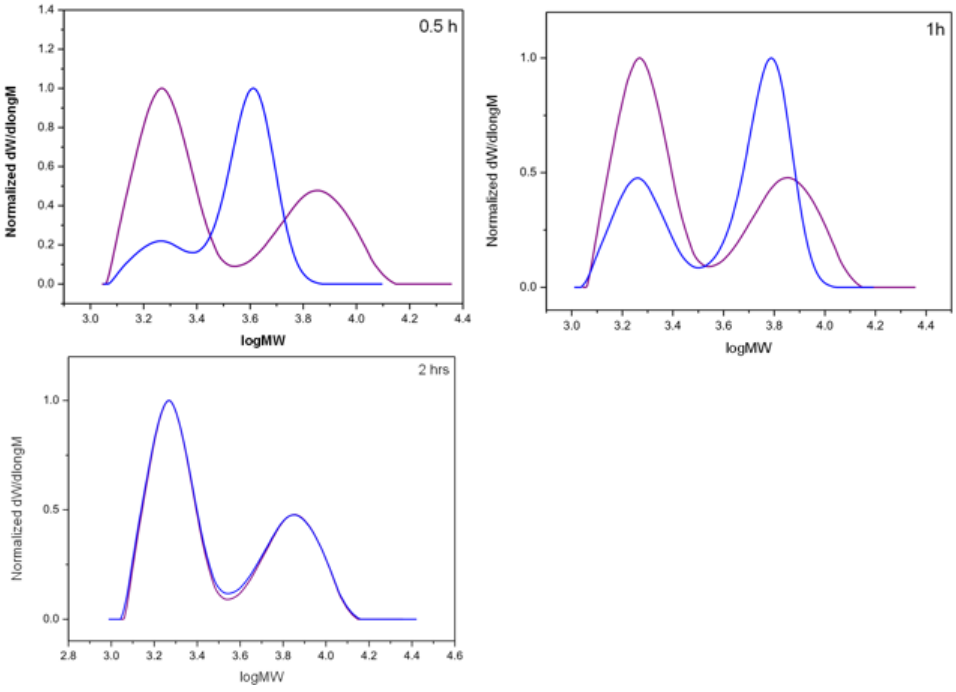

Figure 22. Assessment of the chain end fidelity of PDEA by in situ chain extension using deoxygenated NIPAM (10 eq). DMF SEC for following chain extension at delayed feed times. $[M]_0 : [I]_0 : [CuBr] : [Me_6TREN] = [10] : [1] : [0.04] : [0.04]$.

Table 8. Investigating the effect of delayed feed time on chain end fidelity of PNIPAM under aqueous SET-LRP conditions. $[M]_0 : [I]_0 : [CuBr] : [Me_6TREN] = [10] : [1] : [0.04] : [0.04]$.

Reaction No.	Monomer	Conv. (%)	Time per block (hr)	$M_{n,th}$ g.mol^{-1}	$M_{n,SEC}{}^{a}$ g.mol^{-1}	$Đ^{a}$
1	NIPAM	100	2	1400	2400	1.07
	DMA	100	overnight	2400	4600	1.07
2	NIPAM	100	3	1400	2400	1.09
	DMA	97	overnight	2400	5200	1.11
3	NIPAM	100	4	1400	2400	1.07
	DMA	28	overnight	2400	3800	1.12
4	NIPAM	100	10	1400	2400	1.07
	DMA	00	overnight	2400	2500	1.09

[a] DMF SEC, calibrating with PMMA standard.

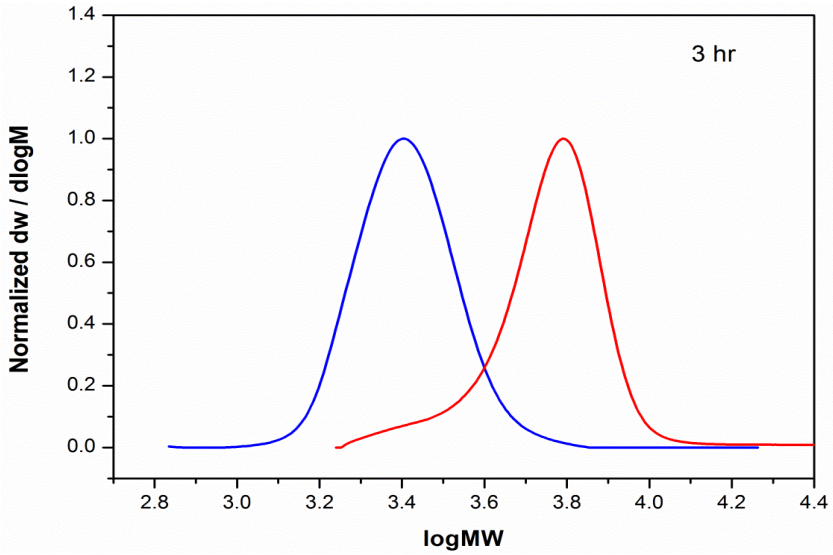

Figure 23. DMF SEC for the chain extension of PNIPAM with deoxygenated aqueous DMA (10 eq) after a 3 hour delay. $[M]_0 : [I]_0 : [CuBr] : [Me_6TREN] = [10] : [1] : [0.04] : [0.04]$.

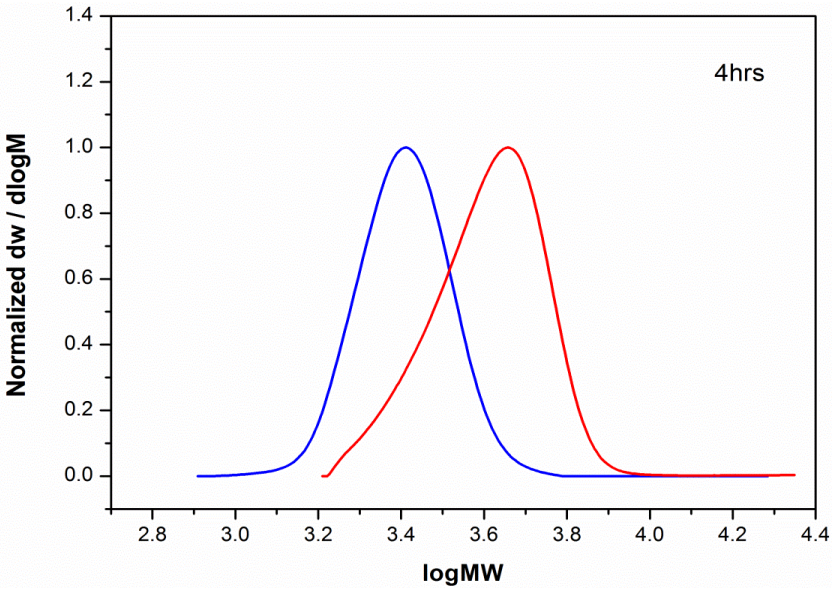

Figure 24. DMF SEC for the chain extension of PNIPAM with deoxygenated aqueous DMA (10 eq) after a 4 hour delay. $[M]_0$: $[I]_0$: [CuBr] : [Me_6TREN] = [10] : [1] : [0.04] : [0.04].

Table 9. Investigating the effect of delayed feed time of chain end fidelity of PNIPAM under aqueous SET-LRP conditions. $[M]_0$: $[I]_0$: [CuBr] : [Me_6TREN] = [10] : [1] : [0.04] : [0.04].

Reaction No.	Monomer	Conv. (%)	Time per block (hr)	$M_{n,th}$ g.mol^{-1}	$M_{n,SEC}{}^{a}$ g.mol^{-1}	$Đ^{a}$
1	DMA	100	0.5	1200	2800	1.08
	DMA	100	overnight	2200	5600	1.27
2	DMA	100	1	1200	2700	1.06
	DMA	50	overnight	2200	40000	1.34
3	DMA	100	2	1200	2700	1.06
	DMA	15	overnight	2200	2800	1.15

[a] DMF SEC, calibrating with PMMA standard.

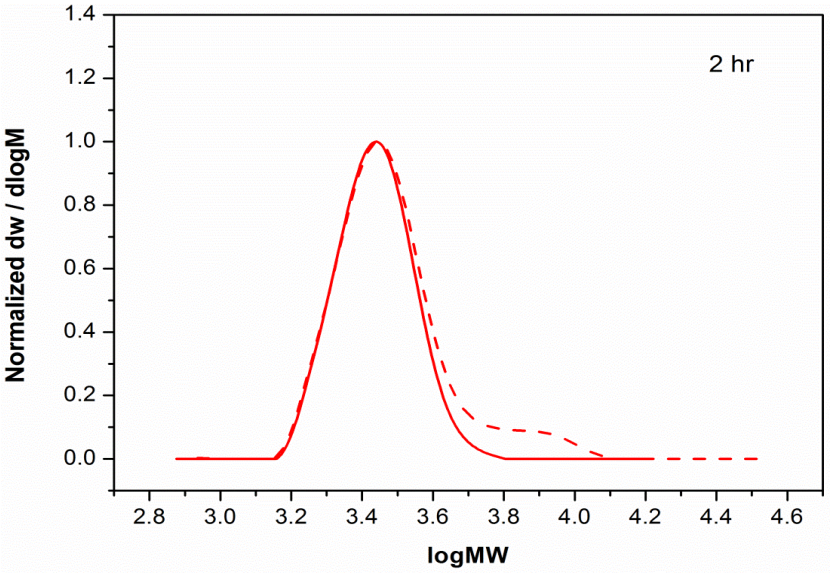

Figure 25. DMF SEC for the chain extension of PDMA with deoxygenated aqueous DMA (10 eq) after a 2 hour delay. $[M]_0$: $[I]_0$: [CuBr] : [Me_6TREN] = [10] : [1] : [0.04] : [0.04].

Higher molecular weight block copolymers by aqueous SET-LRP

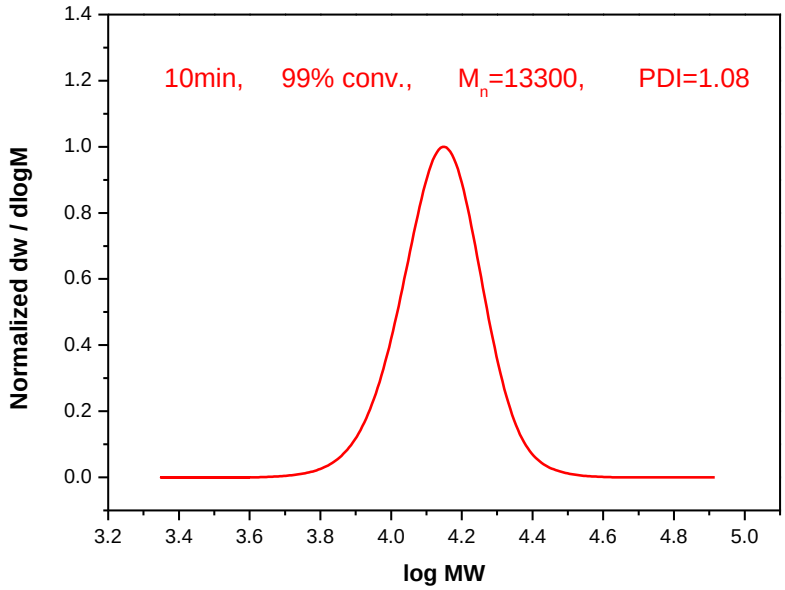

Figure 26. DMF SEC for PDMA DP= 100. $[M]_0$: $[I]_0$: [CuBr] : [Me_6TREN] = [10] : [1] : [0.08] : [0.04].

Table 10. Preparation of higher molecular triblock copolymer prepared by sequential monomer addition during SET-LRP at 0°C in H_2O. $[M]_0 : [I]_0 : [CuBr] : [Me_6TREN] = [100] : [1] : [0.008] : [0.004]$.

Entry	Block number	Monomer	Conv. (%)	Time per block (min)[a]	$M_{n,th}$ g.mol^{-1}	$M_{n,SEC}$[b] g.mol^{-1}	$Đ^b$
1	Block 1	NIPAM	98	15 (15)	11600	12500	1.15
2	Block 2	HEAAm	99	250 (265)	23100	28800	1.10
3	Block 3	DMA	70	overnight	34200	35000	1.76

[a] Cumulative time in parentheses. [b] DMF SEC, calibrating with PMMA standard.

3.5 References

1. D. A. Z. Wever, F. Picchioni and A. A. Broekhuis, *Prog. Polym. Sci.*, 2011, **36**, 1558-1628.
2. W. Gu, Z. Jia, N. P. Truong, I. Prasadam, Y. Xiao and M. J. Monteiro, *Biomacromolecules*, 2013, **14**, 3386-3389.
3. C. J. Hawker, A. W. Bosman and E. Harth, *Chem. Rev.*, 2001, **101**, 3661-3688.
4. J. Nicolas, Y. Guillaneuf, C. Lefay, D. Bertin, D. Gigmes and B. Charleux, *Prog. Polym. Sci.*, 2013, **38**, 63-235.
5. A. W. Bosman, R. Vestberg, A. Heumann, J. M. J. Fréchet and C. J. Hawker, *J. Am. Chem. Soc.*, 2002, **125**, 715-728.
6. J. Chiefari, Y. K. Chong, F. Ercole, J. Krstina, J. Jeffery, T. P. T. Le, R. T. A. Mayadunne, G. F. Meijs, C. L. Moad and G. Moad, *Macromolecules*, 1998, **31**, 5559-5562.
7. G. Moad, E. Rizzardo and S. H. Thang, *Aust. J. Chem.*, 2012, **65**, 985-1076.
8. G. Gody, T. Maschmeyer, P. B. Zetterlund and S. Perrier, *Nat Commun*, 2013, **4**.
9. M. Kato, M. Kamigaito, M. Sawamoto and T. Higashimura, *Macromolecules*, 1995, **28**, 1721-1723.
10. J. Ye and R. Narain, *J. Phys. Chem. B*, 2009, **113**, 676-681.
11. J.-S. Wang and K. Matyjaszewski, *J. Am. Chem. Soc.*, 1995, **117**, 5614-5615.
12. D. M. Haddleton, C. B. Jasieczek, M. J. Hannon and A. J. Shooter, *Macromolecules*, 1997, **30**, 2190-2193.
13. V. Percec, T. Guliashvili, J. S. Ladislaw, A. Wistrand, A. Stjerndahl, M. J. Sienkowska, M. J. Monteiro and S. Sahoo, *J. Am. Chem. Soc.*, 2006, **128**, 14156-14165.
14. B. M. Rosen and V. Percec, *Chem. Rev.*, 2009, **109**, 5069-5119.
15. P. D. Iddon, K. L. Robinson and S. P. Armes, *Polymer*, 2004, **45**, 759-768.
16. G. Masci, L. Giacomelli and V. Crescenzi, *Macromol. Rapid Commun.*, 2004, **25**, 559-564.
17. Y. Xia, X. Yin, N. A. D. Burke and H. D. H. Stöver, *Macromolecules*, 2005, **38**, 5937-5943.
18. Y. Xia, N. A. D. Burke and H. D. H. Stöver, *Macromolecules*, 2006, **39**, 2275-2283.
19. Q. Duan, Y. Miura, A. Narumi, X. Shen, S.-I. Sato, T. Satoh and T. Kakuchi, *J. Polym. Sci., Part A: Polym. Chem.*, 2006, **44**, 1117-1124.
20. H. Akiyama and N. Tamaoki, *Macromolecules*, 2007, **40**, 5129-5132.
21. E. A. Appel, J. del Barrio, X. J. Loh, J. Dyson and O. A. Scherman, *J. Polym. Sci., Part A: Polym. Chem.*, 2012, **50**, 181-186.
22. D. Bontempo, R. C. Li, T. Ly, C. E. Brubaker and H. D. Maynard, *Chem comm*, 2005, 4702-4704.
23. C. Feng, Z. Shen, Y. Li, L. Gu, Y. Zhang, G. Lu and X. Huang, *J. Polym. Sci., Part A: Polym. Chem.*, 2009, **47**, 1811-1824.
24. X. Tang, X. Liang, Q. Yang, X. Fan, Z. Shen and Q. Zhou, *J. Polym. Sci., Part A: Polym. Chem.*, 2009, **47**, 4420-4427.
25. M. Teodorescu and K. Matyjaszewski, *Macromolecules*, 1999, **32**, 4826-4831.
26. J. T. Rademacher, M. Baum, M. E. Pallack, W. J. Brittain and W. J. Simonsick, *Macromolecules*, 1999, **33**, 284-288.

27. M. Teodorescu and K. Matyjaszewski, *Macromol. Rapid Commun.*, **21**, 190-194.
28. D. A. Z. Wever, P. Raffa, F. Picchioni and A. A. Broekhuis, *Macromolecules*, 2012, **45**, 4040-4045.
29. F. Alsubaie, A. Anastasaki, P. Wilson and D. M. Haddleton, *Polym. Chem.*, 2015, 6, 406-417.
30. C. Boyer, A. H. Soeriyadi, P. B. Zetterlund and M. R. Whittaker, *Macromolecules*, 2011, **44**, 8028-8033.
31. C. Boyer, A. Derveaux, P. B. Zetterlund and M. R. Whittaker, *Polym. Chem.*, 2012, **3**, 117-123.
32. A. H. Soeriyadi, C. Boyer, F. Nyström, P. B. Zetterlund and M. R. Whittaker, *J. Am. Chem. Soc.*, 2011, **133**, 11128-11131.
33. A. Anastasaki, C. Waldron, P. Wilson, C. Boyer, P. B. Zetterlund, M. R. Whittaker and D. Haddleton, *ACS Macro Lett.*, 2013, **2**, 896-900.
34. N. H. Nguyen and V. Percec, *J. Polym. Sci., Part A: Polym. Chem.*, 2011, **49**, 4227-4240.
35. X. Jiang, S. Fleischmann, N. H. Nguyen, B. M. Rosen and V. Percec, *J. Polym. Sci., Part A: Polym. Chem.*, 2009, **47**, 5591-5605.
36. N. H. Nguyen, B. M. Rosen, X. Jiang, S. Fleischmann and V. Percec, *J. Polym. Sci., Part A: Polym. Chem.*, 2009, **47**, 5577-5590.
37. Q. Zhang, P. Wilson, Z. Li, R. McHale, J. Godfrey, A. Anastasaki, C. Waldron and D. M. Haddleton, *J. Am. Chem. Soc.*, 2013, **135**, 7355-7363.
38. Q. Zhang, P. Wilson, A. Anastasaki, R. McHale and D. M. Haddleton, *ACS Macro Lett.*, 2014, **3**, 491-495.
39. A. Anastasaki, A. J. Haddleton, Q. Zhang, A. Simula, M. Droesbeke, P. Wilson and D. M. Haddleton, *Macromol Rapid Commun*, 2014, **35**, 965-970.
40. J. T. Rademacher, M. Baum, M. E. Pallack, W. J. Brittain and W. J. Simonsick, *Macromolecules*, 2000, **33**, 284-288.
41. Q. Zhang, P. Wilson, Z. Li, R. McHale, J. Godfrey, A. Anastasaki, C. Waldron and D. M. Haddleton, *J. Am. Chem. Soc.*, 2013, **135**, 7355-7363.
42. S. Perrier, S. P. Armes, X. S. Wang, F. Malet and D. M. Haddleton, *J. Polym. Sci., Part A: Polym. Chem.*, 2001, **39**, 1696-1707.
43. M. Ciampolini and N. Nardi, *Inorg. Chem.*, 1966, **5**, 41-44.

Chapter 4: Investigating the mechanism of copper(0)-mediated living radical polymerisation in organic media

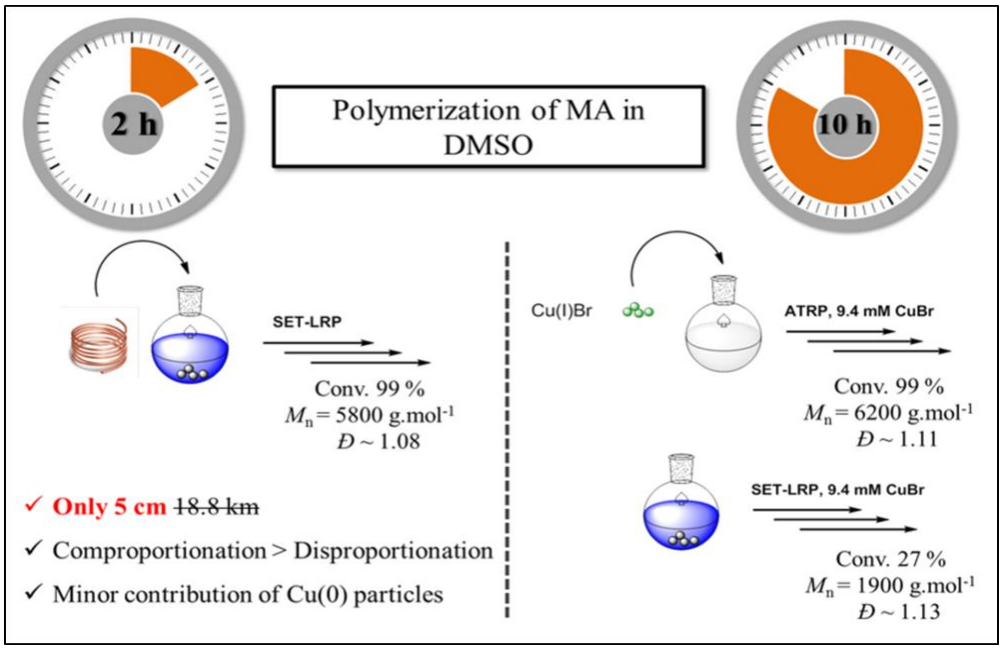

As shown in previous chapters, single electron transfer living radical polymerisation (SET-LRP) is a versatile polymerisation tool that allows for the synthesis of functional materials for a range of potential applications. An interesting scientific debate has dominated the literature during the last few years regarding the mechanism of Cu(0)-mediated polymerisations in both aqueous and organic media. This chapter is the first part of a mechanistic study regarding the role of Cu(0) and CuBr in these systems with the aim of offering some increased level of understanding of the mechanism to aid application. In this chapter, disproportionation and comproportionation studies reveal significant variations in the thermodynamic and kinetic equilibria depending on the solvent composition, the nature of the monomer and the ligand concentration. Interestingly, the sequence of reagent addition significantly affects the disproportionation equilibrium, which is attributed to competitive complexation reactions between monomer, solvent, ligand and copper species. The Cu(0) particles generated via the in situ disproportionation of [Cu(Me_6TREN)]Br in DMSO prior to addition of monomer and initiator were demonstrated to contribute in different extents over the rate and control of the polymerisation, depending on the equivalents of ligand employed. It was found that an increase in the concentration of the Cu(0) particles result in slower polymerisation rates while when conditions that stabilise CuBr were employed, faster polymerisation rates were observed. On the contrary, 5 cm of copper wire showed faster polymerisation rates when compared with 9.4 mM of CuBr, highlighting that copper wire is essential for the efficient polymerisation of acrylates in organic solvents.

4.1 Introduction

The rapid development of reversible deactivation radical polymerisation (RDRP) methods has revolutionized polymer synthesis allowing relatively easy access to well-defined polymers with dispersities comparable to living anionic polymerisations. Among them, copper mediated living polymerisation presents one of the most popular methods of controlling molecular weight, dispersity, polymer architecture and end-group functionality. The discovery of ATRP[1-3] and SET-LRP[4, 5] has significantly contributed towards this field *via* exploiting the activation-deactivation equilibrium between active and dormant species enabling excellent control over the molecular weight distributions.

Despite the versatile nature of these techniques,[6] the literature currently provides two very different mechanisms[7-9] to explain polymerisations in the presence of Cu(0). The two models are SET-LRP[4] as proposed by Percec and co-workers and the supplemental activator and reducing agent mechanism (SARA-ATRP),[7] as suggested by Matyjaszewski and co-workers. Although both polymerisations utilise the same components (Cu(0), monomer, donor ligand, solvent, initiator), the contribution of every reagent/reaction is reported to be different, thus pointing out different major and minor catalytic species.

According to SET-LRP, Cu(0)[4] or extremely reactive "nascent" Cu(0) nanoparticles[10, 11] act as the major activator of alkyl halides and no major activation occurs from CuBr, which is generated *in situ*, from disproportionation into Cu(0) and $CuBr_2$ in the presence of *N*-containing ligands (*e.g.* tris[2-(dimethylamino)ethyl]amine) Me_6TREN[12, 13] *etc*.) in polar solvents (*e.g.* dimethyl sulfoxide (DMSO), H_2O). The activation step (a surface activation process)[10, 14, 15] is

proposed to occur *via* an outer sphere electron transfer (OSET) mechanism[4] through a radical anion intermediate, which is reported to have lower dissociation energies.[16] Several papers have been published reporting that CuBr is inactive during the Cu(0)-mediated living radical polymerisations. In one report, the Cu(0) wire was lifted out of the reaction solution, leaving behind colloidal Cu(0) particles, CuBr and $CuBr_2$. Upon their removal the polymerisation still proceeded (although at a much slower rate) indicating the existence of active species. However, when the polymerisation mixture was decanted from one Schlenk tube containing Cu(0) wire to a second without the Cu(0) catalyst, the polymerisation ceased, supporting the view that CuBr could not be the active catalyst as soluble CuBr, if present, would have been transferred to the second Schlenk tube while Cu(0) nanoparticles (due to higher density) would remain in the original vessel.[11] One of the key features of SET-LRP is the rapid (on the polymerisation timescale) disproportionation of CuBr to Cu(0) and $CuBr_2$ which has been visualized in protic, dipolar aprotic and non-polar solvents as well as protic, polar and non-polar monomers.[20-22] Particularly in the case of DMSO, disproportionation occurs rapidly reaching a maximum value (~69%) when 0.5 eq. of Me_6TREN relative to CuBr is employed.[23] Thus, DMSO is often the solvent of choice for SET-LRP. On the contrary, when non-disproportionating solvents (*e.g.* acetonitrile (MeCN), toluene *etc*.) are employed, two linear first-order kinetic regions were reported, while the end group functionality was poor, indicating a significant loss of polymerisation control.[24-28]

The SARA-ATRP model states that CuBr is the major activator of alkyl halides and that Cu(0) is a supplemental activator and reducing agent that regenerates CuBr through comproportionation while disproportionation is negligible.[29-33] The rate coefficients for activation of two alkyl halide initiators by Cu(0) have been

determined, showing that the rate of activation is increased upon the employment of longer copper wire and it was calculated that 2 km of copper wire gives the activity of just 1 mM of [Cu(Me_6TREN)]Br.[32] These findings were supported by kinetic simulations and evaluation of the rates and contributions of all species which revealed that the control over the polymerisation is attributed mainly to CuBr as the main activator and $CuBr_2$ as the main deactivator, thus proceeding *via* an ATRP dynamic equilibrium.[33] In further work, it was shown that comproportionation dominates over disproportionation when there is an adequate [ligand] present to stabilize all soluble copper species with disproportionation being negligible under typical polymerisation conditions.[34] Nevertheless, both comproportionation and disproportionation rates are reported to be slow and thus, not contributing significantly to the polymerisation kinetics. Harrisson and co-workers further supported these results by concluding that the extent of comproportionation is low relative to activation by the Cu(0) wire.[35, 36]

Moreover, although Percec and co-workers attribute the rate acceleration during polymerisation to the rapid disproportionation of CuBr or the stabilization of Cu(0) particles in specific solvents[23] (*e.g.* DMSO), Matyjaszewski attributes this change in kinetics to the polarity of the media and the extremely high activity of CuBr.[37, 38] In order to verify this, the polymerisation of MA in a disproportionating (DMSO) and a non-disproportionating solvent (MeCN) was conducted, both giving a similar level of control and thus leading the authors to conclude that the effect of disproportionation must be negligible.[30] Furthermore, when tris (2-pyridylmethyl)amine (TPMA), which essentially promotes zero disproportionation, and Me_6TREN, which allows a high extent of disproportionation were utilised for the polymerisation of acrylates in the presence of metallic copper, both were found

to control the polymerisation efficiently.[39] Moreover, Matyjaszewski and co-workers further dispute the SET-LRP mechanism by reporting that it violates the principle of halogen conservation (PHC)[40] and the principle of microscopic reversibility (PMR).[30] Finally, high-level *ab initio* molecular orbital calculations were used to study the thermodynamics and electrochemistry relevant to ATRP, showing that for monomers bearing electron-withdrawing groups, such as acrylates, catalysts favouring inner sphere electron transfer (ISET) over OSET are required in order to avoid chain-breaking side reactions.[41]

In this present chapter, a series of polymerisations and mechanistic studies will be presented in order to gain further understanding of the copper mediated living radical polymerisation in the presence of Cu(0) when polar organic solvents are employed. The effect of the solvent composition, the monomer structure and the ligand concentration on the disproportionation and comproportionation reactions will be investigated and the contributions of every component to the overall mechanism will be determined. Competitive complexation of the reagents (monomer, solvent, ligand, and copper species) will be shown to influence the disproportionation and comproportionation equilibria, dictating that a correct sequence of reagent addition is required for optimum polymerisations and control over the molecular weight distributions. *In situ* disproportionation of [Cu(Me_6TREN)]Br in DMSO will be shown to reveal slower polymerisation rates upon increasing the Cu(0) particles concentration and faster rates when CuBr is stabilized by an increased concentration of ligand. A comparison between experiments mediated by Cu(0) and CuBr will also be conducted, assessing the role of the copper wire during the polymerisation of acrylates in DMSO.

4.2 Results and discussion

Cu(0)-mediated living radical polymerisation is a multicomponent system, composed of monomer, initiator, ligand, catalyst, and solvent. As such, it can be considered as either a complicated or a complex system. Ottino underlines[42, 43] that complex is different than complicated, as the pieces of a complicated system can be fully understood in isolation and the whole can be reassembled from its parts. On the contrary, complex systems cannot be understood by studying parts in isolation and the system must be analysed as a whole. Nevertheless, in order to gain a better understanding of the reaction it is important to consider a given system in both ways, as a whole and as individual components.

4.2.1 The extent of disproportionation of [Cu(Me_6TREN)]Br in DMSO and other organic solvents

It has been reported that a crucial step in SET-LRP is the *in situ* disproportionation of CuBr generated by activation of either Cu(0) wire[14, 44] or powder[10, 45] into reactive, "nascent" Cu(0) nanoparticles and the deactivating species, $CuBr_2$.[11, 15, 20] Thus, it is important to quantify the extent to which disproportionation occurs. For this purpose, UV-Vis spectroscopy has been employed. In order to avoid, previously reported, scattering by particlulates [23] by Cu(0) in the UV cuvettes, Cu(0) was removed by filtration prior to each UV measurement. Filtration was carried out under a nitrogen blanket designed to avoid potential oxidation of remaining CuBr to $CuBr_2$, which would result in an overestimation of the amount of disproportionation. Under these conditions, the disproportionation of CuBr in the presence of Me_6TREN ([CuBr]:[Me_6TREN]=1:1) was investigated in a range of organic solvents, including

DMSO, methanol (MeOH), *N*-methyl-2-pyrrolidone (NMP), *N*,*N*-dimethylformamide (DMF) and *N*,*N*-dimethylactamide (DML). (Section 4.4.3, Scheme 5).

In DMSO (the most popular solvent for organic SET-LRP), the disproportionation of [Cu(Me_6TREN)]Br was visualized ([CuBr] : [Me_6TREN = [1] : [1]) by the observation of insoluble Cu(0) particles and the evolution of a green colouration, corresponding to the *in situ* generated [Cu(Me_6TREN)]Br_2 complex. Disproportionation was subsequently monitored by UV-Vis absorbance (λ_{max} ~ 950 nm) corresponding to the *in situ* generated [Cu(Me_6TREN)]Br_2 complex and was found to be 31% (Table 1, entry 1, Figure 1).

Table 1. Degree of [Cu(Me_6TREN)]Br disproportionation (the percentage of [Cu(Me_6TREN)]Br that converts into Cu(0) and [Cu(Me_6TREN)]Br_2) in DMSO, MeOH, NMP, DMF and DML. Conditions: [CuBr]:[Me_6TREN] = 1:1, 2 mL solvent at 22˚C.

entry	solvent	degree of disp. %
1	DMSO	31
2	MeOH	66
3	DML	44
4	NMP	37
5	DMF	29

A time period of 15 min was chosen for all of the measurements for a direct comparison with the aqueous system, as the majority of the aqueous and aqueous/organic polymerisations using this process reach full conversion within this time.[5, 46-49]

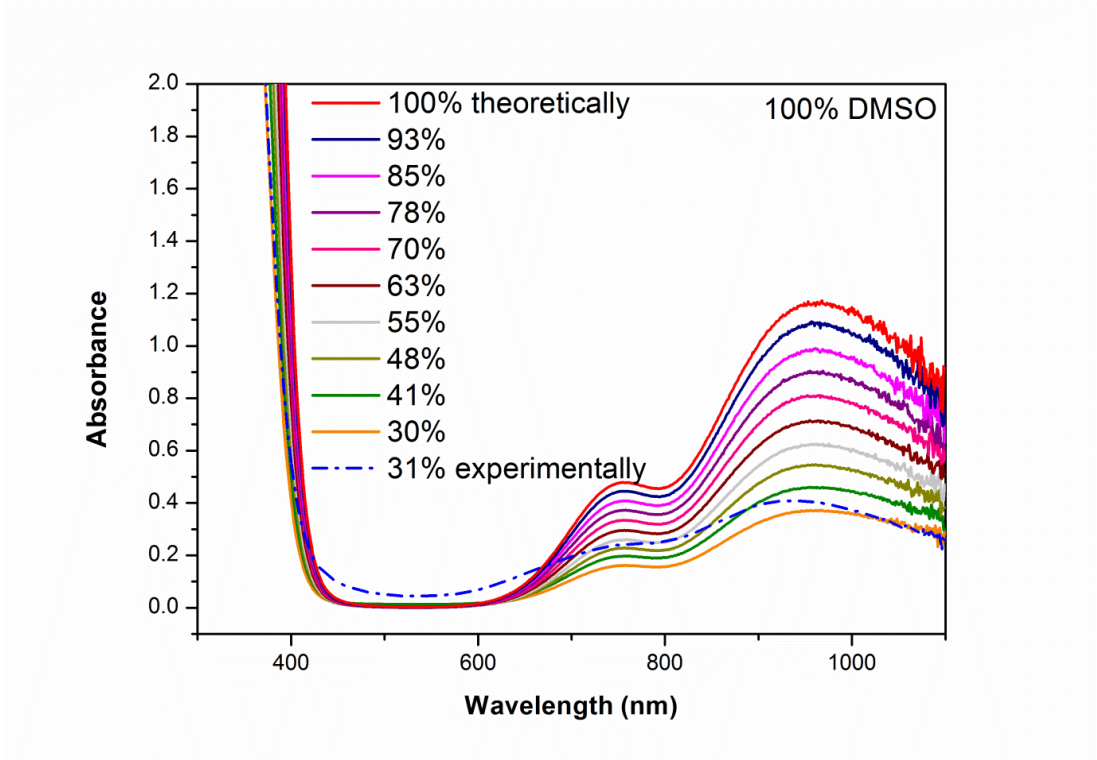

Figure 1. UV-Vis spectra of ten solutions of varying amounts of $CuBr_2$ in the presence of fixed amount of Me_6TREN in 2 mL DMSO at 22 ˚C. The dashed line represents the UV-Vis spectrum of the disproportionation of CuBr (Conditions [CuBr] : [Me_6TREN] = 1:1 in 2 mL DMSO at 22 ˚C). All the samples were diluted before analysis into degassed DMSO.

For the case of DMSO, typically full conversion is achieved between 1-2 h. However, even when the disproportionation was allowed to occur for prolonged periods of times similar values were obtained (Section 4.4.4, Figure 12), thus 15 min was chosen as the time to study the extent of disproportionation. A similar trend was observed for other polar organic solvents. When MeOH, DML, NMP, and DMF were employed, values of 66, 44, 37 and 29% disproportionation respectively were obtained within 15 min (Table 1, entries 2, 3 , 4, 5) (Section 4.4.4, Figure 13). It is noted that although MeOH gives the second largest amount of disproportionation,

DMSO gives the second highest polymerisation rate (after H_2O) as it has been reported to stabilise the Cu(0) particles, as opposed to MeOH.[20] Nevertheless, when purely organic solvents are employed, the disproportionation was neither quantitative nor instantaneous.

4.2.2 The effect of ligand concentration on the disproportionation of Cu(I) in DMSO

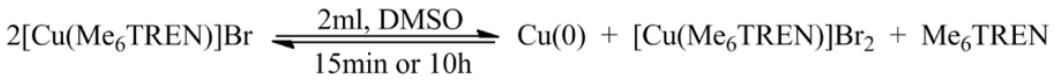

Scheme 1. Disproportionation of [Cu(Me_6TREN)]Br utilising different concentrations of Me_6TREN (0.25, 0.5, 1, 2, 3 and 6 with respect to CuBr) in DMSO at 22 ˚C.

Since ligands play a significant role in Cu-mediated polymerisation, an investigation on the ability of Me_6TREN to enhance or prohibit the disproportionation of CuBr *via* preferential stabilisation of $CuBr_2$ is required. In order to address this, UV-Vis studies were conducted utilising various amounts of Me_6TREN relative to CuBr (Scheme 1). The maximum value for the disproportionation in DMSO (~ 50%) was detected when 0.25 or 0.5 eq. of ligand were employed (Figure 2) as in these cases there would be either no or less uncomplexed ligand to move the equilibrium towards CuBr.

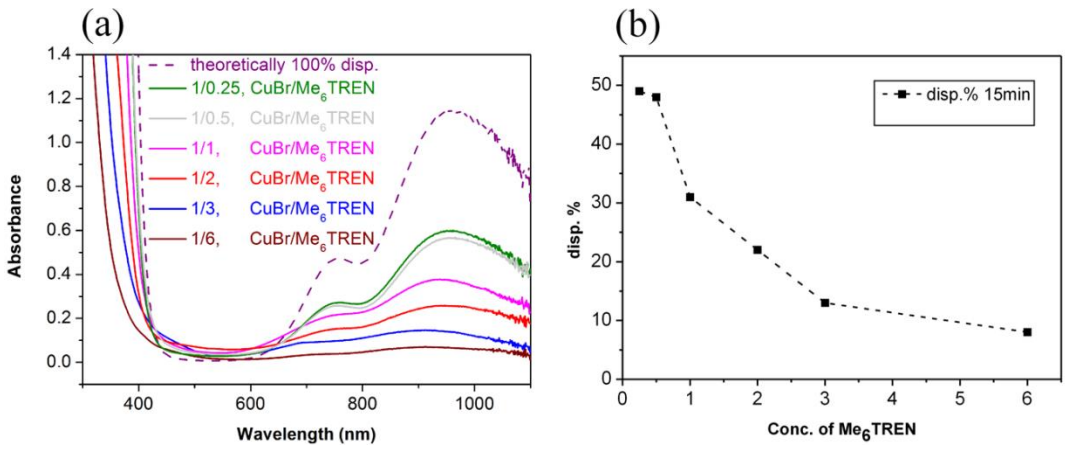

Figure 2. UV-Vis spectra of a) solutions of [Cu(Me_6TREN)]Br utilising different equivalents of Me_6TREN with respect to [CuBr] in 2 mL DMSO at 22 ˚C, b) the degree of disproportionation in 15 min.

It is noted that the maximum amount of disproportionation is twice that of the ligand as for every mole of $CuBr_2$ produced one mole of Cu(0) is precipitated which does not ligate with the Me_6TREN. On the contrary, when 1 eq. of Me_6TREN relative to CuBr was added, the extent of disproportionation decreased to 31%. A further increase to 2, 3 and 6 eq. of Me_6TREN resulted in even less disproportionation (23, 13 and 7% respectively). It is evident that the extent of disproportionation is dramatically decreased in DMSO upon an increase of the ligand concentration. Thus, an increase in [ligand] in DMSO solution stabilises CuBr which results in less Cu(0) produced and a lower [$CuBr_2$] obtained *via* disproportionation. A similar decreasing trend upon increasing the ligand concentration was also observed when the disproportionation reaction was left to occur for longer period of time (Section 4.4.4, Figure 14). These results are in agreement with that previously reported by both Percec[23] and Matyjaszewski.[34]

4.2.3 Disproportionation of [Cu(Me$_6$TREN)]Br in DMSO in the presence of monomer

As the polymerisation occurs in the presence of initiator and a high concentration of monomer this is an important factor which may affect the extent of disproportionation. Unfortunately, it is difficult to measure disproportionation in the presence of the initiator *via* UV-Vis analysis, given that $CuBr_2$ would be generated simultaneously by a number of events including disproportionation, activation by CuBr and/or bimolecular termination.

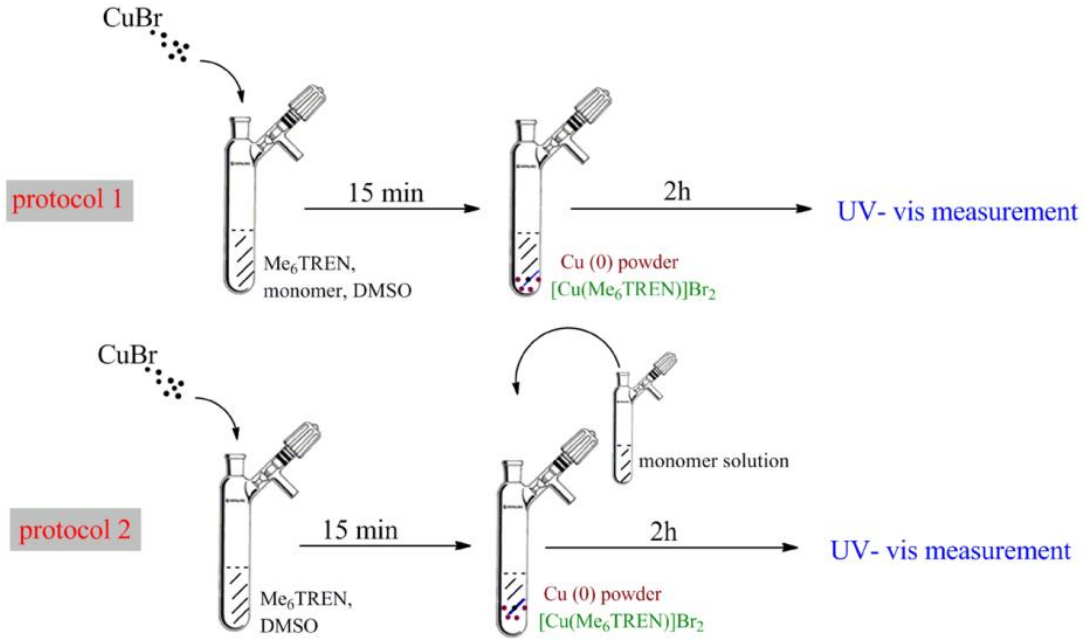

Scheme 2. Schematic representation of a typical disproportionation of [Cu(Me$_6$TREN)]Br *via* protocol 1 (top), and protocol 2 (bottom) under typical polymerisation conditions ([CuBr]:[Me$_6$TREN] = 1:1, 50% *v*/*v* monomer in DMSO at 22 ˚C.

For the reaction in DMSO, when methyl acrylate (MA) is present (Scheme 2, protocol 1) the extent of disproportionation decreases from 31% (in the absence of monomer) to ~10% within 2 h which equates to the time required for a typical

polymerisation in DMSO in order to reach full monomer conversion (Table 2, Figure 3a). When MA is replaced with a more hydrophilic monomer, such as hydroxyethyl acrylate (HEA), disproportionation is reduced less significantly (~17%) (Table 2, Figure 3b), suggesting that HEA facilitates the disproportionation relative to MA. However, in both cases the extent of disproportionation is relatively low and thus disproportionation does not appear to be significant with DMSO as solvent.

Table 2. Percentage of [Cu(Me_6TREN)]Br disproportionation (after 2h) in the presence of MA and HEA in DMSO at 22 ˚C.

entry	conditions	protocol	degree of disp. %
1	[CuBr]:[Me_6TREN] = 1:1, 50% *v/v* MA	1	10
		2	21
2	[CuBr]:[Me_6TREN] = 1:1, 50% *v/v* HEA	1	17
		2	25

Interestingly, if the disproportionation of [Cu(Me_6TREN)]Br in DMSO is allowed to occur (~ 31%) prior to addition of MA (Scheme 2, protocol 2) the amount decreases to 21% (as opposed to a decrease to 10% when all reagents are premixed). Similarly, when HEA is added to the same pre-disproportionated mixture, disproportionation drops from 31 to 25% (Table 2, Figure 3a, b). It should be noted that in these disproportionation studies a ratio of 1:1 ([CuBr]:[Me_6TREN]) was utilised. It is therefore expected that higher concentrations of ligand should result in less disproportionation in the presence of these and other related monomers. Indeed, when a ratio of [CuBr]:[Me_6TREN] = 1:2.2 was employed for the pre-disproportionating protocol (protocol 2) (resembling the typical ratio of [copper]:[ligand] in polymerisation),[50] a reduced value of 7 and 15% was observed,

for MA and HEA respectively (Section 4.4.4, Figure 15a). Similarly, the mixing protocol (protocol 1) gave rise to 5 and 10% of disproportionation within 2 h for MA and HEA respectively (Section 4.4.4, Figure 15b). Thus, it is evident that in the presence of both hydrophilic and hydrophobic monomers the extent of disproportionation in DMSO is somewhat limited.

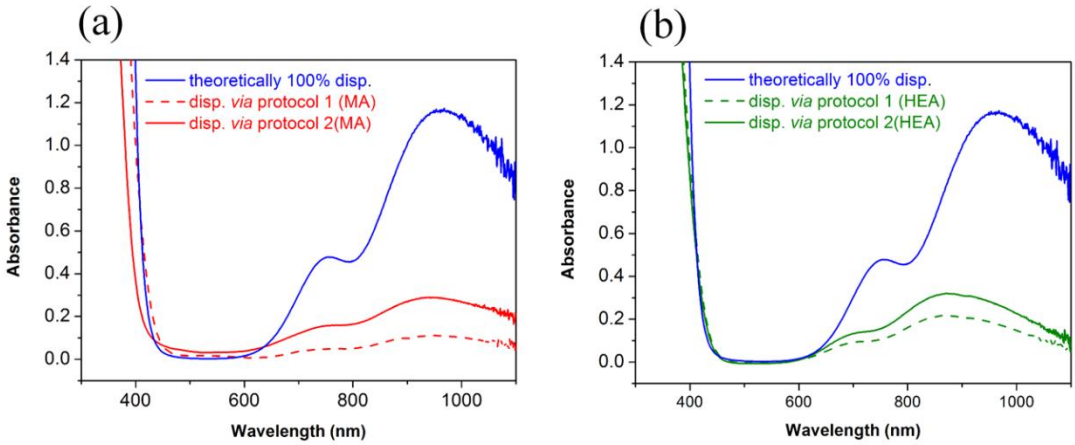

Figure 3. UV-Vis spectra of [Cu(Me_6TREN)]Br in the presence of a) MA and b) HEA. Conditions: [CuBr]:[Me_6TREN] = 1:1, 50% *v*/*v* monomer in DMSO at 22 ˚C.

4.2.4 The extent of comproportionation of Cu(0) wire and $CuBr_2$ in DMSO in the presence/absence of monomers

In order to investigate the degree of comproportionation (the percentage of [Cu(Me_6TREN)]Br that formed by Cu(0) and [Cu(Me_6TREN)]Br_2), Cu(0) wire and $CuBr_2$ were employed (Scheme 3). Activation of copper wire in the literature has been reported using two different methods; by washing with concentrated HCl or treatment with hydrazine.[27, 28, 51, 52] For completion, both methods were investigated during this study. When the HCl activation method was employed, 53% comproportionation was detected within 2 h (Table 3, Figure 4a) with 58% when hydrazine was used as the activation method (Section 4.4.4, Figure 16). Thus, an

appreciable amount of comproportionation is evident under the relevant polymerisation conditions ([$CuBr_2$]:[Me_6TREN] = 1:2.2). It is noted that under similar conditions, disproportionation was only ~ 20% (Figure 2), suggesting that in pure DMSO comproportionation is favoured over disproportionation.

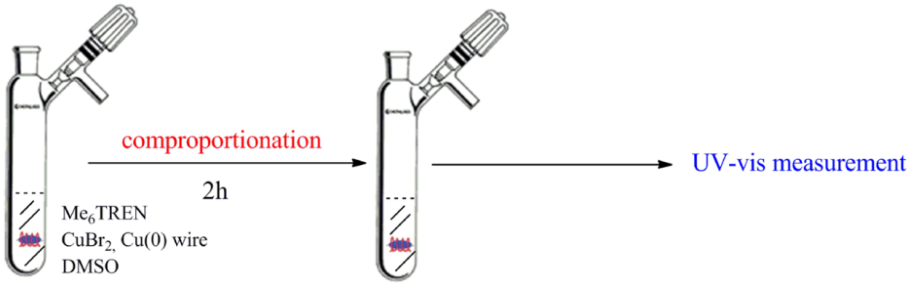

Scheme 3. Schematic representation of a typical comproportionation of Cu(0) wire and [Cu(Me_6TREN)]Br_2 in 2mL DMSO at 22 ˚C, under typical polymerisation conditions: [$CuBr_2$]:[Me_6TREN] = 1:2.2, Cu(0) wire (5cm, diameter (Ø) 0.25mm) activated by HCl.

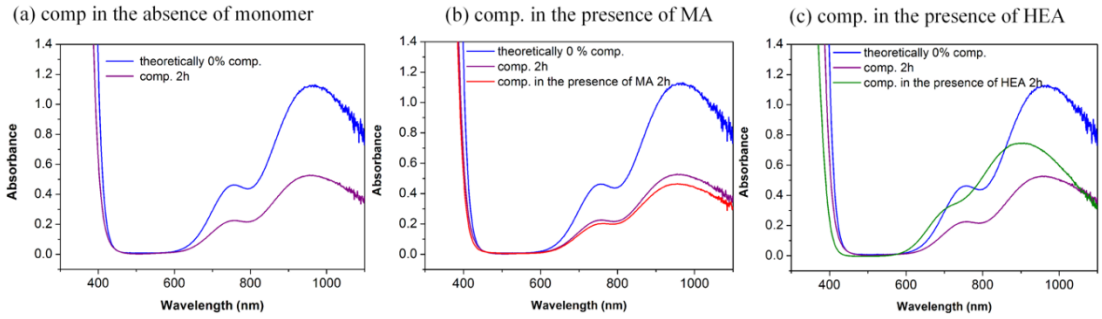

Figure 4. UV-Vis spectra of Cu(0) wire and [Cu(Me_6TREN)]Br_2 comproportionation (a) in the absence of monomer under typical conditions: [$CuBr_2$]:[Me_6TREN] = 1:2.2, (b) and (c) comproportionation in the presence of MA and HEA respectively under typical conditions [$CuBr_2$]:[Me_6TREN] = 1:2.2, 50% *v/v* monomer in DMSO at 22 ˚C. Cu wire (5cm, Ø 0.25mm) activated by HCl.

Table 3. Percentage of comproportionation (after 2h) of Cu(0) and [Cu(Me_6TREN)]Br_2 in DMSO in the presence/absence of monomers at 22 ˚C. Cu(0) wire (5 cm, Ø 0.25 mm) activated by HCl or hydrazine.

entry	conditions	Cu(0) wire activated by	degree of comp. %
1	[$CuBr_2$]:[Me_6TREN] = 1:2.2	HCl	53
	0% *v/v* monomer	hydrazine	58
2	[$CuBr_2$]:[Me_6TREN] = 1:2.2	HCl	56
	50% *v/v* MA	hydrazine	64
3	[$CuBr_2$]:[Me_6TREN] = 1:2.2	HCl	25
	50% *v/v* HEA	hydrazine	32

The effect of the monomer on the disproportionation equilibrium was also considered. The presence of MA increased the extent of comproportionation to 56 and 64%, when HCl and hydrazine was selected as the activation methods respectively (Table 3, Figure 4b) and (Section 4.4.4, Figure 17). Conversely, the presence of HEA decreased the extent of comproportionation to 25 and 32% for HCl and hydrazine respectively (Table 3, Figure 4c) and (Section 4.4.4, Figure 17). Thus, the nature of the monomer in DMSO can both facilitate and reduce comproportionation, suggesting monomer complexation.

4.2.5 Exploiting the pre-disproportionation protocol for polymerisation in DMSO

The pre-disproportionation of [Cu(Me_6TREN)]Br in water has proved a very efficient protocol to prepare well-controlled polymers in water within a short time period (minutes) at ambient or sub-ambient temperatures. Thus, it would be useful to investigate the potential of a pre-disproportionation step in DMSO for a range of reaction conditions. Initially, the optimum conditions for the disproportionation was selected, utilising a ratio [CuBr]:[Me_6TREN] = [1]:[0.5] (Scheme 4).

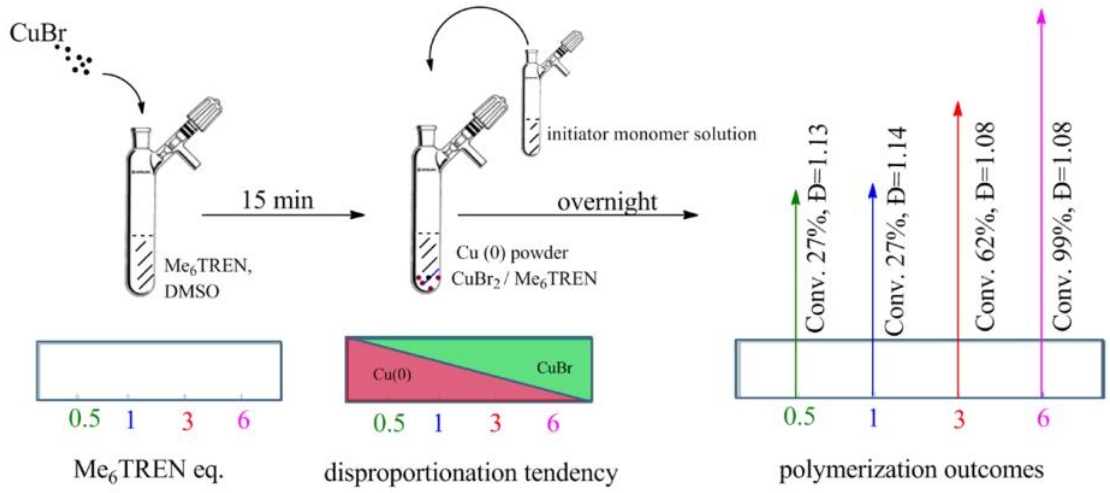

Scheme 4. Schematic of polymerisation of MA using different Me_6TREN equivalents, [CuBr]:[Me_6TREN] = 1:0.5, 1, 3 and 6, 50% *v*/*v* MA in DMSO at 22 ˚C.

Following the protocol developed in water,[5, 49] disproportionation was allowed to occur for 15 min *prior to* monomer and initiator addition. However, only 26% conversion (^{1}H NMR, Table 4, entry 1) was detected within 2 h and although the

reaction was left to proceed overnight, no further monomer consumption was observed.

Table 4. Summary of polymerisation of MA using different Me_6TREN equivalents, [CuBr]:[Me_6TREN] = 1:0.5,1,3 and 6, 50% *v*/*v* MA in DMSO at 22 ˚C.

entry	[I]:[CuBr]:[Me_6TREN]	T (h)	conv. %	M*n* g.mol^{-1}	*Đ*	t (h)	conv. %	M$_n$ g.mol^{-1}	*Đ*
1	[1]:[0.1]:[0.05]	2	26	1600	1.16	overnight	27	1900	1.13
2	[1]:[0.1]:[0.1]		15	1800	1.19		27	1800	1.14
3	[1]:[0.1]:[0.3]		27	1000	1.16		62	3600	1.08
4	[1]:[0.1]:[0.6]		60	3600	1.08		99	6900	1.08

Nevertheless, a well-defined polymer was obtained with good correlation between the theoretical and the experimental molecular weight at this conversion with a narrow molecular weight distribution (*Đ* ~ 1.13, Figure 5).

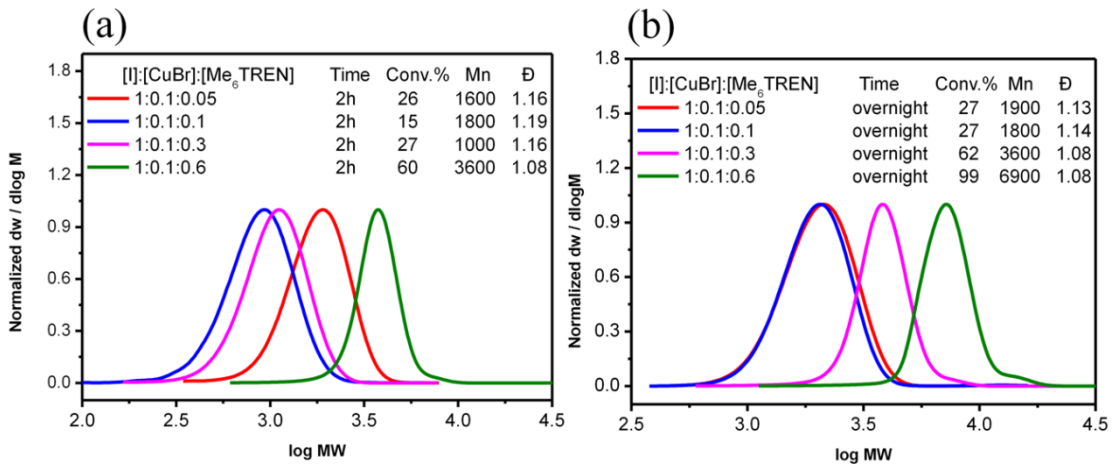

Figure 5. Molecular weight distributions of PMA by SET-LRP protocol, (a) polymerisation time is 2 h, (b) overnight. Conditions: MA in 50% *v*/*v* DMSO at 22 ˚C *via* $CHCl_3$ SEC.

Thus, under conditions where disproportionation of [Cu(Me_6TREN)]Br is favoured and the maximum amount of Cu(0) is generated the polymerisation is slow and eventually stops. This could be interpreted in two different ways. Either "nascent" Cu(0) particles that are generated *in situ* are extremely fast activating species resulting in fast initiation leading to high radical concentration and subsequently termination *via* radical-radical events or the existence of high concentration of Cu(0) is compromising the polymerisation rate as the activation (by Cu(0)) is slower than the activation by CuBr. Very high end-group fidelity was observed by ^{1}H NMR, even when the reaction was left overnight (Section 4.4.4, Figure 19). In addition, MALDI-ToF-MS revealed two polymer peak distributions corresponding to bromine and chlorine terminal groups, (Figure 6). It is noted that samples were taken directly from the SEC eluent, ($CHCl_3$) which facilitates halogen exchange[53]. The high end-group fidelity in conjunction with the good agreement between the theoretical and the experimental molecular weight suggest that no termination occurs under these conditions and thus Cu(0) particles generated by the *in situ* disproportionation of CuBr in DMSO are not extremely reactive species. In addition, after the cessation of the polymerisation (10h, 26% conversion) a second aliquot of active species (either CuBr/Me_6TREN or 5 cm of copper wire) were added in the reaction mixture. In both experiments the molecular weight distribution shifted further to higher MW which suggests that the end group fidelity is maintained and the reaction was lacking of activating species (Cu(0) wire or CuBr) (Section 4.4.4, Figure 20). Similar results were obtained when a ratio of [CuBr]:[Me_6TREN] = [1]:[1] was employed, as disproportionation is still relatively high under these conditions (~31%), suggesting that pre-disproportionation of [Cu(Me_6TREN)]Br in DMSO is undesired for effective polymerisation.

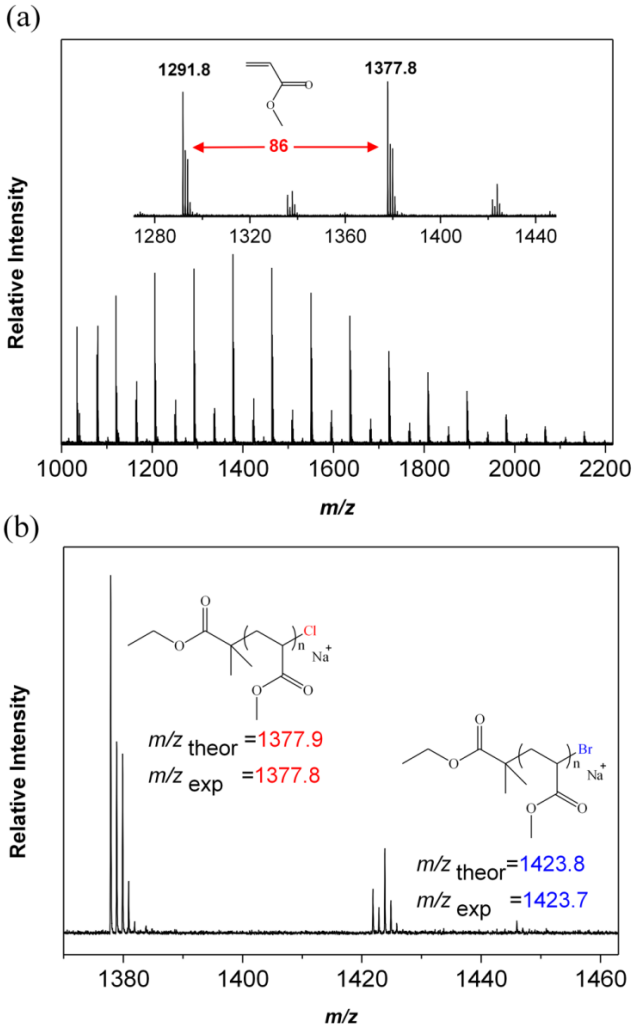

Figure 6. MALDI-ToF-MS of PMA (n = 14) employing [CuBr]:[Me_6TREN] = [0.1]:[0.05], relative to initiator (ethyl 2-bromoisobutyrate, Ebib), polymerisation time = overnight, 50% *v*/*v* MA in DMSO at 22 ˚C.

Increasing the [ligand] has been shown to reduce the degree of disproportionation resulting in 13 and 7% of disproportionation when the ratios of [CuBr]:[Me_6TREN] = [1]:[3] and [CuBr]:[Me_6TREN] = [1]:[6] were used respectively. Less disproportionation results in the generation of less Cu(0) with a corresponding increase in [CuBr] in the reaction. Interestingly, utilising a ratio = [1]:[3], the final

conversion (overnight) increased to 62% (Table 4, entry 3) while the narrow molecular weight distributions were maintained (*Đ* ~ 1.08). When an even higher concentration of ligand was employed ([1]:[6]), the conversion increased further, resulting in 60% within 2 h and 99% overnight (Table 4, entry 4) (*Đ* ~ 1.08). Further increasing the amount of Cu(0) or the [CuBr] activator had no major influence on the overall polymerisation kinetics (Figure 7), (Section 4.4.4, Table 5).

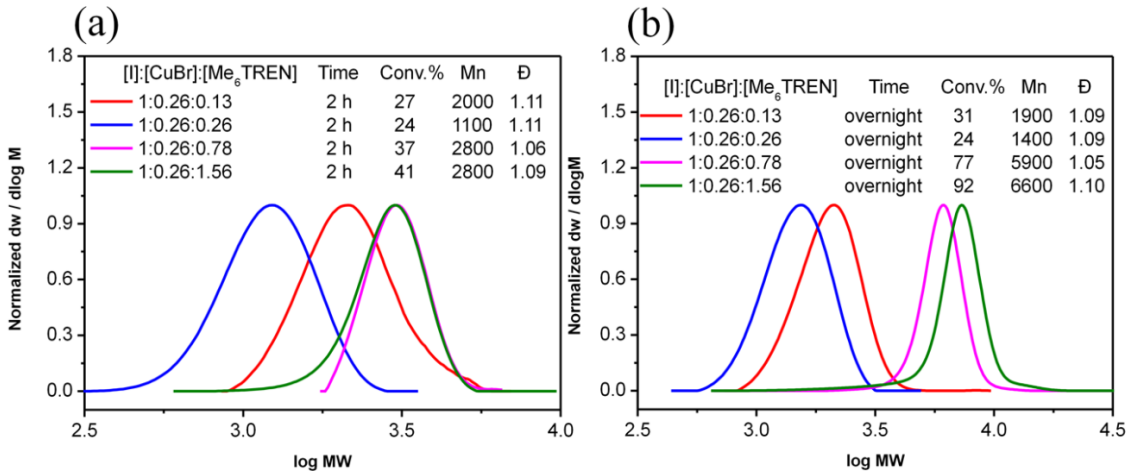

Figure 7. Molecular weight distributions of PMA by SET-LRP protocol, MA in 50% *v/v* DMSO at 22 ˚C *via* $CHCl_3$ SEC.

Additionally, since the optimum conditions for the pre-disproportionation experiments were when a higher [ligand] was utilised, ([CuBr]:[Me_6TREN] = [1]:[6]) the same conditions as used for a classical ATRP polymerisation was subsequently employed, without allowing CuBr to disproportionate *prior to* monomer and initiator addition. Since disproportionation under these conditions is low (~ 7%) it was anticipated that the ATRP should resemble the pre-disproportionation experiment. Indeed, identical results were obtained with 60% conversion achieved in 2 h and 99% overnight with a narrow molecular weight

distribution (*Đ* ~ 1.11) (Section 4.4.4, Figure 21). However, when the [ligand] was further increased to [CuBr]:[Me_6TREN] = [1]:[12], premature termination events were evident after 2 h (Figure 8), suggesting that higher concentrations of ligand are not ideal for this polymerisation as consistent with previous reports.[50] Nevertheless, these experiments highlight further that Cu(0) particles obtained by the *in situ* disproportionation of CuBr are slow activating species and when [CuBr] is maximized (at high ligand concentrations), the rate of the polymerisation is accelerated.

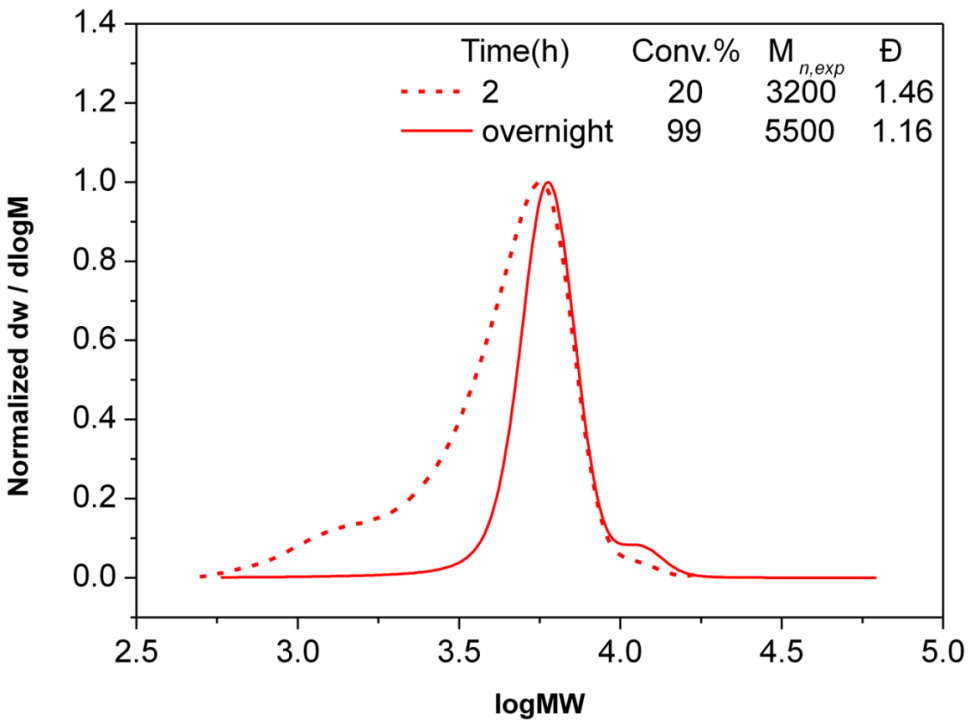

Figure 8. Molecular weight distributions of PMA by ATRP polymerisation, conditions: [CuBr] : [Me_6TREN] = [1] : [12], MA in 50% *v/v* DMSO at 22 ˚C.*via* $CHCl_3$ SEC.

4.2.6 The role of copper wire as an activator and/or reducing agent

Recently, it was reported that alkyl halides are predominantly activated by CuBr.[32-34] Specifically, it was reported that the activation rate of 2-methylbromopropionoate (MBrP) towards initiation by a 1 mM CuBr/Me_6TREN solution is similar to the activation rate by 2 km of Cu(0) wire with a diameter of 0.25 mm. In previous experiments (above section), 0.1 eq of CuBr (with respect to initiator) was utilised giving 60% conversion within 2 h (M_n = 3600, $Đ$ = 1.08). This corresponds to a concentration of ~ 9.4 mM of CuBr. According to the previous report,[32] in order to match the activity of CuBr with Cu(0) approximately 19 km of copper wire would be required. When 5 cm of copper wire (diameter = 0.25 mm) was utilised, as the only copper source (no additional $CuBr_2$ was added externally), in the polymerisation of MA, 99% conversion was achieved within 2 h (M_n = 5800, $Đ$ = 1.08, Scheme 5, Figure 9).

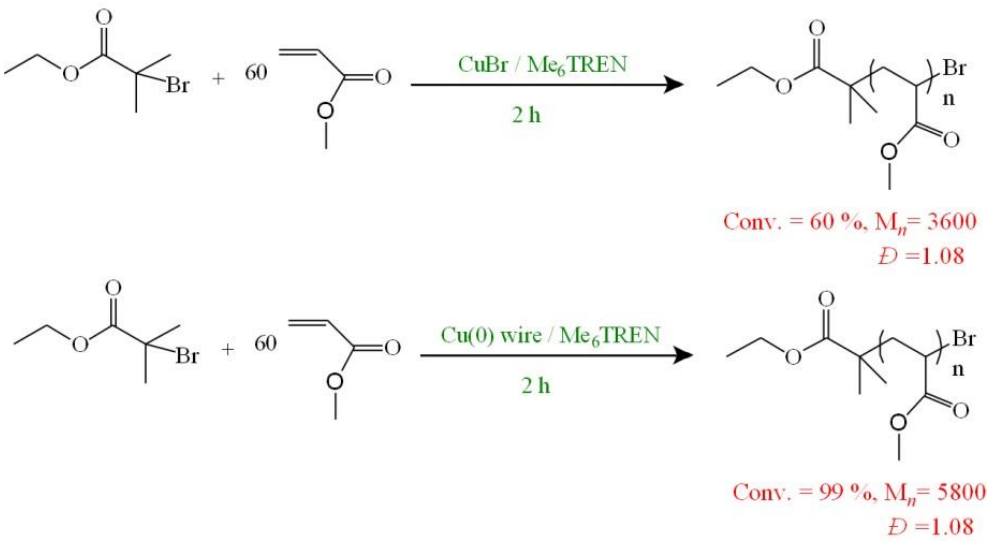

Scheme 5. The polymerisation of MA by classic ATRP (top), condition: [CuBr]:[Me6TREN] = [1]:[6], 50% v/v MA in DMSO at 22 ˚C. PMA by Cu(0) wire (bottom), conditions: [Me_6TREN] = 0.12 with respect to initiator, 50% v/v monomer in DMSO at 22 ˚C, (5 cm, Ø 0.25 mm) activated by HCl.

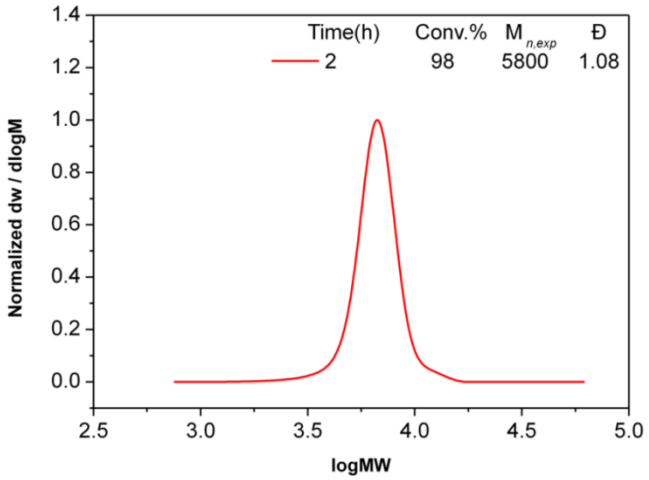

Figure 9. Molecular weight distributions of PMA by Cu(0) wire polymerisation, conditions: [Me_6TREN] = 0.12 with respect to initiator, 50% *v/v* monomer in DMSO at 22 ˚C. Cu wire (5 cm, Ø 0.25 mm) activated by HCl.

Thus, only 5 cm of copper wire resulted in a faster polymerisation rate when compared with 9.4 mM of CuBr. Similar results were obtained in the presence of an initial amount of $CuBr_2$ (Figure 10).

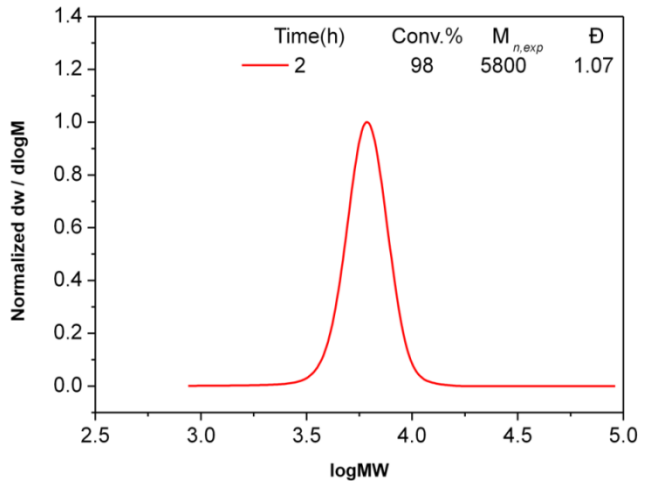

Figure 10. Molecular weight distributions of PMA by Cu(0) wire polymerisation, conditions: [$CuBr_2$]:[Me_6TREN] = 1(4mg): 2.2, 50% *v/v* monomer in DMSO at 22 ˚C. Cu wire (5cm, Ø 0.25mm) activated by HCl. at 22 ˚C.*via* $CHCl_3$ SEC.

As shown earlier, disproportionation of CuBr in DMSO is negligible under these conditions. Thus, in this case, Cu(0) wire could potentially have the role of the alkyl bromide activator (major, supplemental *etc.*) or a reducing agent. The role of Cu(0) wire has previously been attributed to an initial activation by Cu(0), resulting in formation of CuBr/L *in situ* which subsequently acts as the primary activator, as disproportionation is negligible. Thus, Cu(0) would only act as a supplemental activator and reducing agent. Many groups have shown that an initial amount of $CuBr_2$ can enhance the end group fidelity.[54, 55] However, with high amounts of $CuBr_2$ at the beginning of the polymerisation, comproportionation can also occur in the presence of Cu(0). In comproportionation studies section, it was observed that within 2 h, 54% comproportionation is detected (starting with 0.05 eq of $CuBr_2$ and 5 cm of copper wire), resulting in the generation of 0.054 eq of CuBr with respect to initiator (Section 4.4.3, Scheme 6). However, this amount of CuBr gave rise to almost no polymerisation within 2 h (~ 5%, [CuBr]:[Me_6TREN] = [0.05]:[0.12]). Thus, the amount of CuBr generated *in situ via* comproportionation had a negligible effect on the polymerisation rate and CuBr can be mainly generated by the oxidation of Cu(0). One could argue say that under these conditions ([CuBr]:[Me_6TREN] = [1]:[2.2]), CuBr is not efficiently stabilised (insufficient ligand available) and that under polymerisation conditions, a small amount of CuBr will always be generated *in situ* and thus the ratio between copper and ligand will always be << 1 and thus stabilization of CuBr would be favoured. However, it is noted that for higher ligand concentrations (*e.g.* [CuBr]:[Me_6TREN] = [1]:[12]), a large extent of premature termination occurs, by unknown processes, which is not the case for the experiments using copper wire (Figure 11).

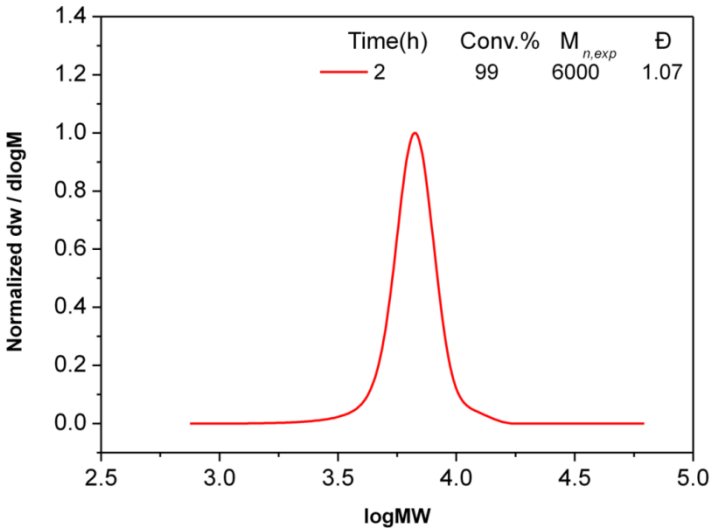

Figure 11. Molecular weight distributions of PMA by Cu(0) wire polymerisation, conditions: [$CuBr_2$]: [Me_6TREN] = [1] : [12], M in 50% *v/v* DMSO at 22 ˚C *via* $CHCl_3$ SEC.

At the same time, it has been reported that a slow dosing of CuBr should essentially mimic a system in which Cu(0) slowly generates CuBr *via* comproportionation. Under these conditions, well-defined polymers were reported reaching 71% conversion in 5 h.[30] A second paper reported > 80% conversion within 2 h when copper wire was utilised for the same degree of polymerisation (without feeding).[4] However, it must be noted that different initiators were employed in the two studies and thus the comparison is not strictly valid. Nevertheless, the existing data suggests that the role of Cu(0) wire as an alkyl halide activator is more important that the role of Cu(0) wire as a reducing agent. Thus, Cu(0) wire significantly contributes to the efficient polymerisation of acrylates, as opposed to Cu(0) particles generated *in situ* that play only a minor role in the polymerisation kinetics. Therefore, additional factors should be taken into consideration when modelling such complex systems in order to match the experimental data with the theoretical predictions.

4.3 Conclusions

The mechanism of copper(0) mediated living radical polymerisation of acrylates in the presence of Cu(0) wire and/or Cu(0) particles has been investigated in organic media. Disproportionation and comproportionation equilibria were determined and found to be strongly affected by the nature of the solvent and the monomer, and the concentration of the ligand employed. UV-Vis experiments demonstrated that in pure DMSO disproportionation (31%) is unfavored over comproportionation while increasing the [ligand] decreases the extent of disproportionation. Importantly, in the presence of monomer the disproportionation of CuBr/Me_6TREN is further suppressed (10%) when the hydrophobic MA is present in the disproportionating mixture. The sequence of the reagent addition was also studied and proved to be crucial for the outcome of the polymerisation, potentially due to competitive complexation of the reagents (monomer, solvent, ligand and copper species). The role of the Cu(0) particles obtained *via* the *in situ* disproportionation of [Cu(Me_6TREN)]Br in DMSO was also assessed. It was concluded, that for the case of DMSO, the Cu(0) particles obtained by the *in situ* disproportionation of CuBr are slow activating species and when [CuBr] is maximized (at high ligand concentrations), the rate of the polymerisation is accelerated without compromising the control over the molecular weight distribution. Interestingly, only 5 cm of copper wire resulted in faster polymerisation rate when compared with 9.4 mM of CuBr, which is contrary to a suggestion in a previous report, further highlighting that although the role of Cu(0) is still not fully understood, it undoubtedly leads to fast rates of polymerisation and low levels of termination while it is apparent that both homogeneous and heterogeneous processes take place. Hence, for the case of DMSO, the slow disproportionation and the relatively inactive Cu(0) particles are in

contrast with the initially proposed SET-LRP mechanism, where instantaneous disproportionation and extremely reactive "nascent" Cu(0) particles is reported. At the same time, copper wire leads to extremely fast polymerisation rates although the mechanism for the latter case has not been yet fully clarified.

4.4 Experimental

4.4.1 Materials and methods

All chemicals were purchased from Sigma-Aldrich or Fischer Scientific unless otherwise stated. All monomers were passed through a basic alumina column prior to remove the inhibitor. Ethyl 2-bromoisobutrate (Ebib, Aldrich, 98 %) was used as received. *Tris*(2-(dimethylamino)ethyl)amine (Me_6TREN) was synthesized according to literature procedures and stored under nitrogen prior to use[56, 57]. Copper(I) bromide (CuBr), was sequentially washed with acetic acid and ethanol and dried under vacuum[58]. Copper wire (diameter = 0.25 mm) was pre-treated by washing in hydrochloric acid or hydrazine for 30 min and rinsed thoroughly with MiliQ water, dried under nitrogen and used immediately.

4.4.2 Instrumentation

Proton Nuclear Magnetic Resonance (^{1}H NMR) spectra were recorded on Bruker DPX-300 and DPX-400 spectrometers using deuterated solvents obtained from Aldrich. Size-exclusion chromatography (SEC) was conducted on Varian 390-LC system using chloroform with 2% triethylamine eluent at a flow rate of 1.0 mL/min as the mobile phase at 50 ˚C, equipped with refractive index, UV and viscometry

detectors, 2 × PLgel 5 mm mixed-D columns (300 × 7.5 mm), 1 × PLgel 5 mm guard column (50 × 7.5 mm) and autosampler. And another SEC measurements were conducted using an Agilent 1260 GPC-MDS fitted with differential refractive index (DRI), light scattering (LS) and viscometry (VS) detectors equipped with 2 × PLgel 5 mm mixed-D columns (300 × 7.5 mm), 1 × PLgel 5 mm guard column (50 × 7.5 mm) and autosampler. Commercial narrow linear poly(methyl methacrylate) standards in range of 200 to 1.0×10^6 g · mol^{-1} were used to calibrate the systems. All samples were passed through 0.45 μm PTFE filter before analysis. Matrix-assisted laser desorption/ionization-time of flight-mass spectrometry (MALDI-ToF-MS) was conducted using a Bruker Daltonics Ultraflex II MALDI-ToF-MS, equipped with a nitrogen laser delivering 2 ns laser pulses at 337 nm with positive ion ToF detection performed using an accelerating voltage of 25 kV. Solutions in tetrahydrofuran (50 μL) of trans-2-[3-(4-tert-butylphenyl)-2-methyl-2-propylidene] malonitrile (DCTB) as a matrix (saturated solution), sodium iodide as cationization agent (1.0 mg/mL) and sample (1.0 mg/mL) were mixed, and 0.7 μL of the mixture was applied to the target plate. Spectra were recorded in reflectron mode calibrating PEG-Me 1100 kDa. UV/Vis spectra were recorded on Agilent Technologies Cary 60 UV-Vis in the range of 200-1100 nm using a cuvette with 10 mm optical length.

All reactions were carried out under an inert atmosphere of oxygen-free nitrogen, using standard Schlenk techniques.

4.4.3 General procedures

General procedure for the extent of disproportionation of [Cu(Me_6TREN)]Br in DMSO and other organic solvents at 22˚C

To a Schlenk tube fitted with a magnetic stir bar and a rubber septum, solvent (2 mL) and Me_6TREN (26 μL, 0.1 mmol) were charged and the mixture was bubbled with nitrogen for 15 min. CuBr (0.1 mmol) was then carefully added under slight positive pressure of nitrogen to protect the *in-situ* generated copper (0) powder from possible side oxidation reaction. The mixture immediately became blue [Cu(Me_6TREN)]Br_2 and a purple/red precipitate Cu(0) was observed. After 15 min the solution was carefully transferred through a gas tight syringe and 0.45 μm PTFE syringe filter to another Schlenk, previously filled with nitrogen. The filtered solution was diluted in order to get an accurate UV-Vis spectrum. 0.5 mL of the solution was transferred to a vial filled with 4mL degassed DMSO. Then 3 mL of the diluted solution was transferred to a UV-Vis cuvette (optical length, 10 mm), which was fitted with a rubber septum and previously filled with nitrogen. The cuvette was directly taken for UV-Vis spectroscopy.

Subsequently, a series of $CuBr_2$ solutions, with same amount of Me_6TREN (26 μL, 0.1 mmol) and different amounts of $CuBr_2$ (0.053, 0.046, 0.044, 0.039, 0.035, 0.030, 0.026, 0.021and 0.017mmol) in a certain amount of the used solvent (2 mL), were made for UV-Vis measurements according to the same procedure as the disproportionation of [Cu(Me_6TREN)]Br in Section 4.5, Scheme 4.1. These calibration measurements made in order to calculate the concentration of [Cu(Me_6TREN)]Br_2 in disproportionation solution.

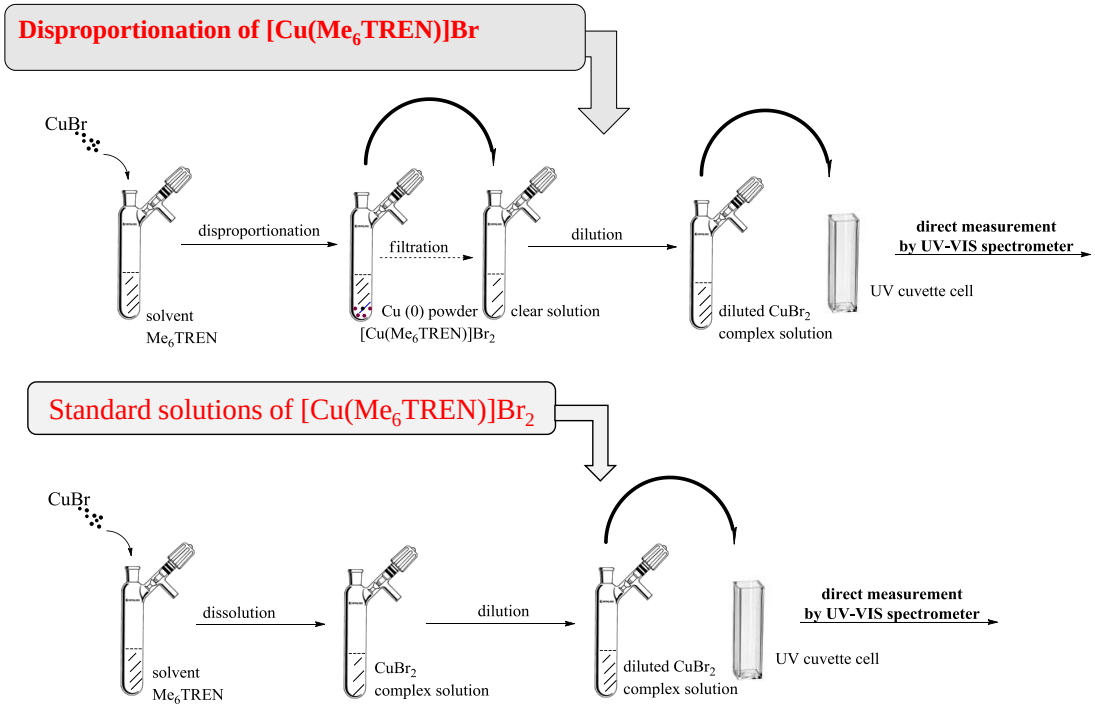

Scheme 5. Schematic of a typical disproportionation of [Cu(Me_6TREN)]Br in different solvents at 22 ˚C.

General procedure for the effect of ligand concentration on the disproportionation in DMSO at 22˚C

To a Schlenk tube fitted with a magnetic stir bar and a rubber septum, DMSO (2 mL) and different amounts of Me_6TREN (0.025, 0.05, 0.1, 0.2, 0.3 and 0.6 mmol) were charge, the mixture of each reaction was bubbled with nitrogen for 15 min. CuBr (0.1 mmol) was then carefully added under slight positive pressure of nitrogen to protect the in-situ generated copper (0) powders from possible side oxidation reaction. The mixture (CuBr : Me_6TREN, 1: 0.25, 0.5, 1, 2) immediately became green [Cu(Me_6TREN)]Br_2 and a fine colloidal Cu(0) was observed and the mixture (CuBr : Me_6TREN, 1: 3 and 6) immediately became dark green and less Cu(0). After

two different reaction times (15 min and 10 h) the solution was carefully transferred through a gas tight syringe and 0.45 μm PTFE syringe filter to another Schlenk, previously filled with nitrogen. The filtered solution was diluted in order to get an accurate UV-Vis spectrum. Then 3 mL of the diluted solution was transferred to a UV-Vis cuvette (optical length, 10 mm), which was fitted with a rubber septum and previously filled with nitrogen. The cuvette was directly taken for UV-Vis spectroscopy.

General procedure for d D. Jenkins Aubrey, G. Jones Richard and G. Moad, in *Pure Appl. Chem.*, 2009, vol. 82, p. 483. **isproportionation of [Cu(Me$_6$TREN)]Br in DMSO in the presence of monomer at 22˚C**

To a Schlenk tube fitted with a magnetic stir bar and a rubber septum, DMSO (2 mL) and Me$_6$TREN (0.1 mmol) were charged and the mixture was bubbled with nitrogen for 15 min. CuBr (0.1 mmol) was then carefully added under nitrogen atmosphere and the reaction was left for 15 min then 2 mL monomer (MA or HEA) was added for another 15 min. The solution was carefully transferred through a gas tight syringe and 0.45 μm PTFE syringe filter to another Schlenk, previously filled with nitrogen. The filtered solution was diluted in order to get an accurate UV-Vis spectrum. Then 3 mL of the degassed and diluted solution was transferred to a UV-Vis cuvette (optical length, 10 mm), which was fitted with a rubber septum and previously filled with nitrogen. The cuvette was directly taken for UV-Vis spectroscopy.

General procedure for the extent of comproportionation (comp.) of Cu(0) and $CuBr_2$ in DMSO at 22˚C

To a Schlenk tube fitted with a magnetic stir bar and a rubber septum, DMSO (2 mL), Me_6TREN (26 μL, 0.1 mmol) and $CuBr_2$ (0.05 mmol) were charged. The mixture was bubbled with nitrogen for 15 min then activated Cu(0)wire was added. After 2 h the solution was carefully transferred through a gas tight syringe and 0.45 μm PTFE syringe filter to another Schlenk, previously filled with nitrogen. The filtered solution was diluted in order to get a more accurate UV-Vis spectrum. Then 3 mL of the degassed and diluted solution was transferred to a UV-Vis cuvette (optical length, 10 mm), which was fitted with a rubber septum and previously filled with nitrogen. The cuvette was directly taken for UV-Vis spectroscopy.

Calibration curve. In order to calculate the concentration of $CuBr_2$ in disproportionation solution, a series of $CuBr_2$/Me_6TREN solutions were measured by UV-Vis, utilising the same amount of Me_6TREN (26 μl, 0.1 mmol) with different amounts of $CuBr_2$ (0.053, 0.046, 0.044, 0.039 and 0.035), in 2 ml of solvent.

General procedure for the extent of comproportionation of Cu(0) and $CuBr_2$ in DMSO in the presence of monomers at 22˚C

To a Schlenk tube fitted with a magnetic stir bar and a rubber septum, 4 mL monomer solution (2 mL MA or HEA in 2 mL DMSO), Me_6TREN (26 μL, 0.1 mmol) and $CuBr_2$ (0.05 mmol) were charged. The mixture was bubbled with nitrogen for 15 min then activated Cu(0) wire was added. After 2 h the solution was carefully transferred through a gas tight syringe and 0.45 μm PTFE syringe filter to

another Schlenk, previously filled with nitrogen. The filtered solution was diluted in order to get an accurate UV-Vis spectrum. Then 3 mL of the degassed and diluted solution was transferred to a UV-Vis cuvette (optical length, 10 mm), which was fitted with a rubber septum and previously filled with nitrogen. The cuvette was directly taken for UV-Vis spectroscopy.

Quantitative analysis of the disproportionation of CuBr using UV-vis Spectroscopy

To determine the degree of CuBr disproportionation, five known concentrations of $[Cu(Me_6TREN)]Br_2$ solution were recorded in order to create a calibration curve. However, quantification of the degree of disproportionation of CuBr in DMSO and its mixtures is problematic due to the formation of colloidal Cu(0) stabilized by DMSO. The very small colloidal Cu(0) particles have a scattering effect and also exhibit an absorption with a maximum at ~600 nm. To estimate the conversion *via* disproportionation the equation (1) has been applied[59].

$$\text{Conversion (\%) of CuBr} = \frac{\text{Abs @ the height of ~ 967nm peak - Abs @ the baseline at ~ 550 nm}}{\text{Abs}_{[Cu(Me_6TREN)]Br_2} \text{ @ ~967nm}} * 100 \quad (1)$$

Similarly, the degree of comproportionation was calculated by using equation (2).

$$\text{Conversion (\%) of CuBr}_2 = 100 - \left(\frac{\text{Abs @ the height of ~ 967nm peak - Abs @ the baseline at ~ 550 nm}}{\text{Abs}_{[Cu(Me_6TREN)]Br_2} \text{ @ ~967nm}} * 100 \right) \quad (2)$$

General procedures for exploiting the pre-disproportionation protocol for DMSO MA (DP_n = 60) at ambient temperature.

To a Schlenk tube fitted with a magnetic stir bar and a rubber septum, DMSO (2 mL) and different concentrations of Me_6TREN (0.05, 0.1, 0.3 or 0.6 mmol) for polymerisation condition [I]:[CuBr] / [1]:[0. 26] and (0.02, 0.04, 0.12 or 0.24 mmol) for polymerisation condition [1]:[0. 1] were charged and the mixture was bubbled with nitrogen for 15 min. CuBr (0.1mmol) or (0.04 mmol) was then carefully added under slight positive pressure of nitrogen. In a separate vial fitted with a magnetic stir bar and a rubber septum, monomer (MA, 2 mL) was mixed with initiator EBiB (0.37 mmol) and the resulting mixture was purged with nitrogen for 15 min. The degassed monomer/initiator solution was then transferred *via* cannula to the Schlenk tube containing disproportionation solution. The Schlenk tube was sealed and the aforementioned solution was allowed to polymerise at 22˚C. Samples of the reaction mixture were taken periodically for NMR and SEC analysis (2 and 10 h).

ATRP procedure

To a Schlenk tube fitted with a magnetic stir bar and a rubber septum, DMSO (2 mL), Me_6TREN (0.02, 0.04, 0.12 or 0.24 mmol), monomer (2 mL) and initiator EBiB (0.37 mmol) were charged and the mixture was purged with nitrogen for 15 min. CuBr (0.04 mmol) was then carefully added under slight positive pressure of nitrogen. The Schlenk tube was sealed and the solution was allowed to polymerise at 22 ˚C. Samples of the reaction mixture were taken periodically for NMR and SEC analysis (2 and 10 h).

Cu (0) wire/$CuBr_2$ procedure

To a Schlenk tube fitted with a magnetic stir bar and a rubber septum, DMSO (2 mL), Me_6TREN (0.044 mmol), $CuBr_2$ (0.018 mmol), monomer (2 mL) and initiator (EBiB, 0.367 mmol) were charged and the mixture was bubbled with nitrogen for 15 min. 5 cm of activated Cu wire by HCl was wrapped to a small magnetic stir bar then carefully added under slight positive pressure of nitrogen. The Schlenk tube was sealed and the solution was allowed to polymerise at 22 ˚C. Samples of the reaction mixture were taken periodically for NMR and SEC analysis (2 and 10 h).

4.4.4 Additional characterisation

The extent of disproportionation of [Cu(Me_6TREN)]Br in DMSO and other organic solvents

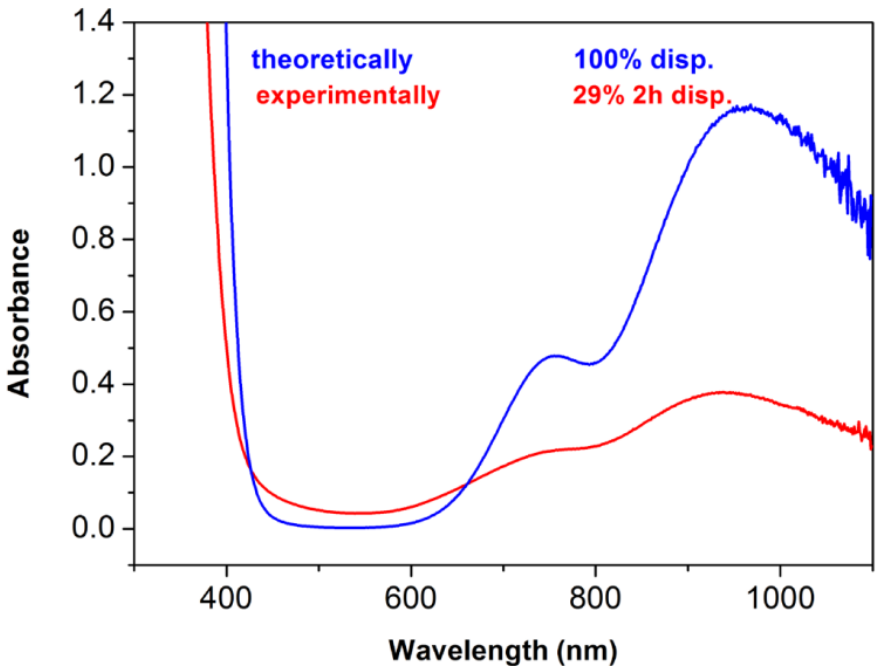

Figure 12. UV-Vis spectrum of the disproportionation of CuBr (2 h) under typical polymerisation conditions, [CuBr]:[Me_6TREN] = 1:1 in 2 mL DMSO.

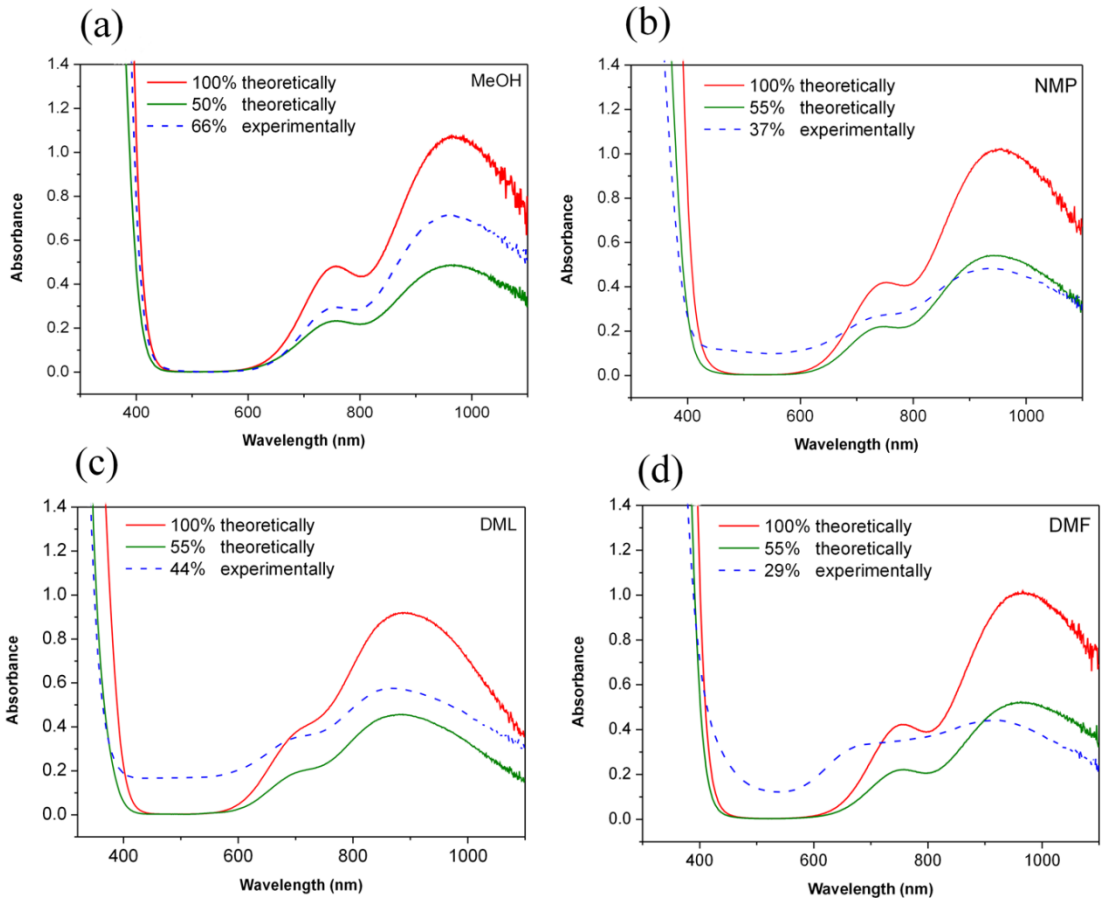

Figure 13. UV-Vis spectra of the solution of two different amounts of $CuBr_2$ in the presence of Me_6TREN (26 µL, 0.1 mmol) in MeOH, NMP, DML, and DMF 2 mL. The dashed line represents the UV-Vis spectrum of the disproportionation of CuBr (14 mg, 0.1 mmol) / Me_6TREN (26 µL, 0.1 mmol) in MeOH, NMP, DML, and DMF 2 mL. All the samples were diluted before analysis into degassed MeOH.

The effect of ligand concentration on the disproportionation of Cu(I) in DMSO

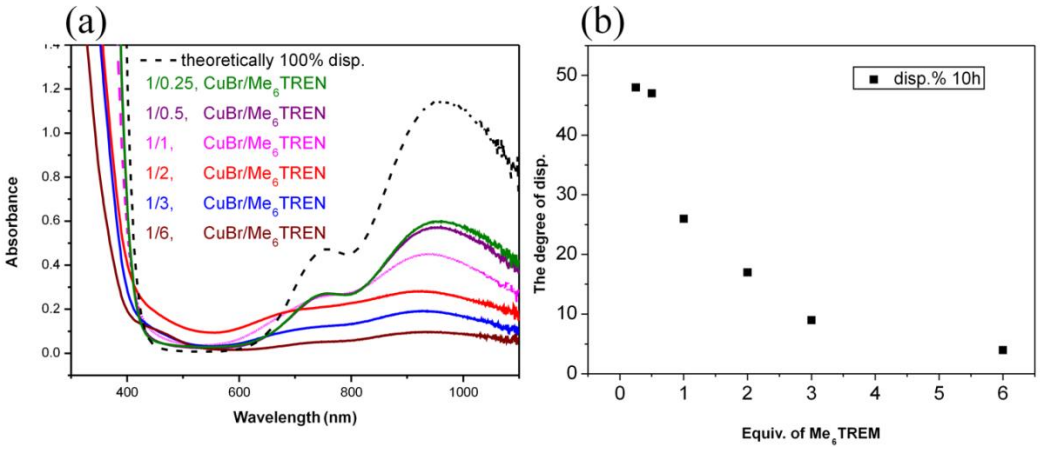

Figure 14. UV-Vis spectra of solutions of [Cu(Me_6TREN)]Br utilising different equivalents of Me_6TREN with respect to [CuBr] in 2 mL DMSO at 22 ˚C (a), the degree of disproportionation in 10 h (b).

Disproportionation of [Cu(Me_6TREN)]Br in DMSO in the presence of monomer

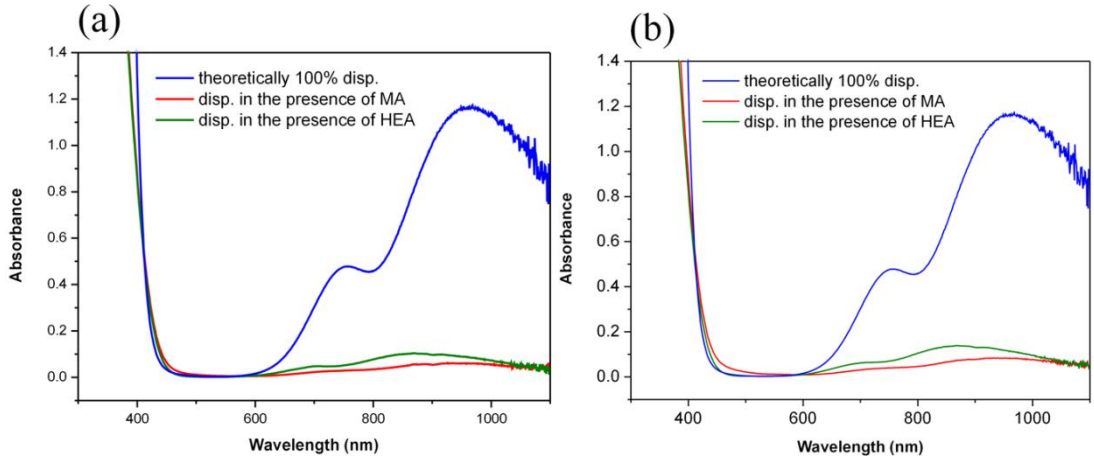

Figure 15. UV-vis spectra of [Cu(Me_6TREN)]Br_2 in the presence of MA and HEA, (a) protocol 1 and (b) protocol 2. Conditions: [CuBr]:[Me_6TREN] = 1:2.2, 50% *v*/*v* monomer in DMSO at 22 ˚C.

The extent of comproportionation of Cu(0) and $CuBr_2$ in DMSO in the presence/absence of monomers

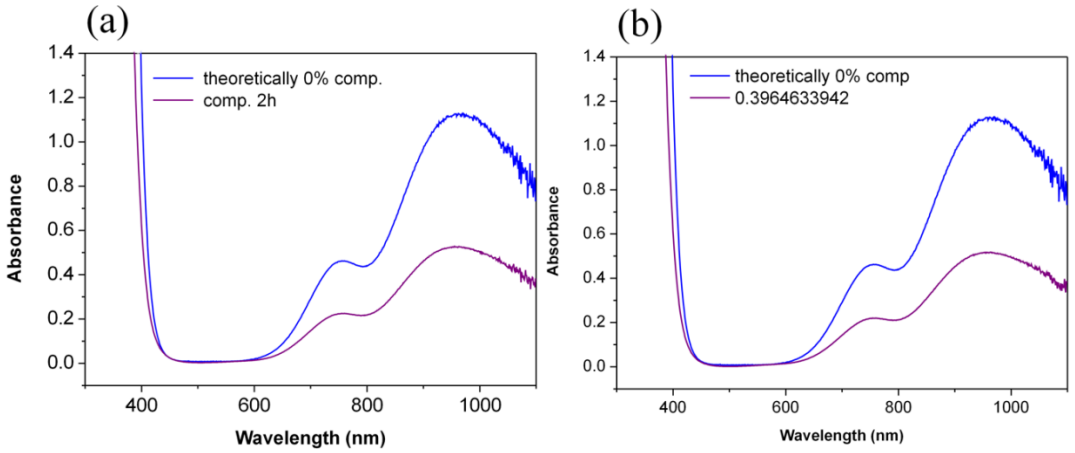

Figure 16. UV-Vis spectra of Cu (0) wire and $[Cu(Me_6TREN)]Br_2$ comp. under typical conditions, $[CuBr_2]$:$[Me_6TREN]$ = 1:2.2 in 2 mL DMSO at 22 ˚C, Cu wire (activated by HCl (a) and hydrazine (b) 5 cm, Ø 0.25 mm).

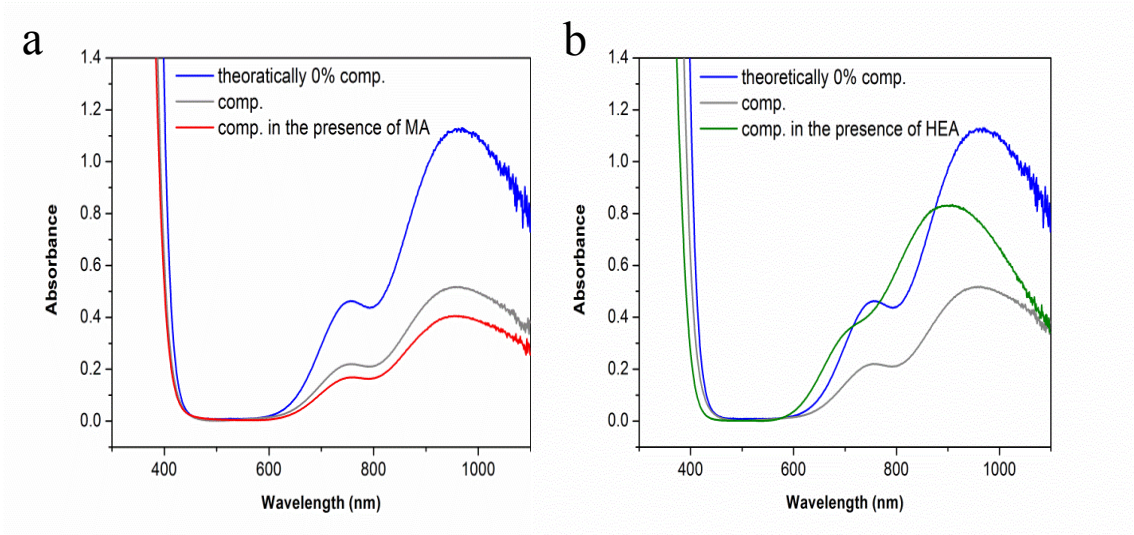

Figure 17. UV-Vis spectra of Cu(0) wire and $[Cu(Me_6TREN)]Br_2$ comproportionation in the presence of a) MA and b) HEA in DMSO. Conditions: Cu (0) wire (activated by hydrazine 5 cm, Ø 0.25 mm), $[CuBr_2]$:$[Me_6TREN]$ = 1:2.2, 50% *v/v* monomer in DMSO at 22˚C.

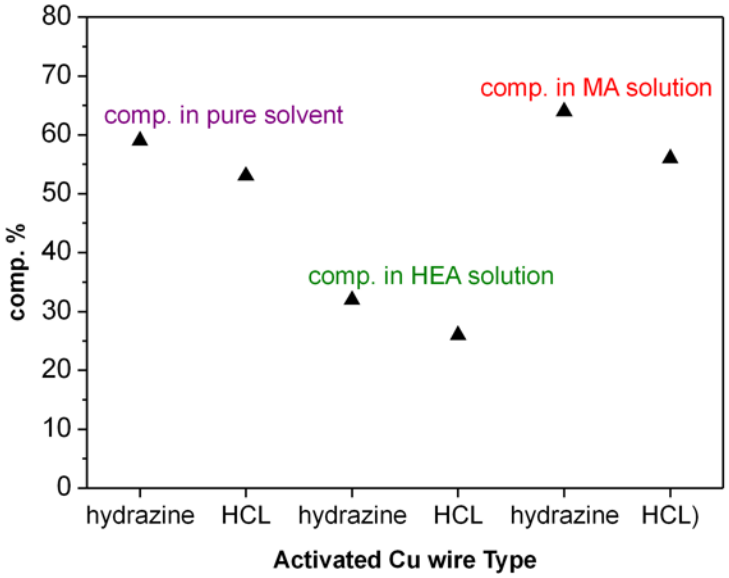

Figure 18. Percentage of comproportionation of Cu(0) wire and [Cu(Me_6TREN)]Br_2 in the presence/absence of monomers in 2 mL DMSO at 22 ˚C, under the conditions: Cu(0) wire (activated by HCl or hydrazine 5 cm, Ø 0.25 mm), [$CuBr_2$]:[Me_6TREN] = 1:2.2, 50% *v/v* monomer in DMSO at 22 ˚C.

Exploiting the pre-disproportionation protocol for DMSO

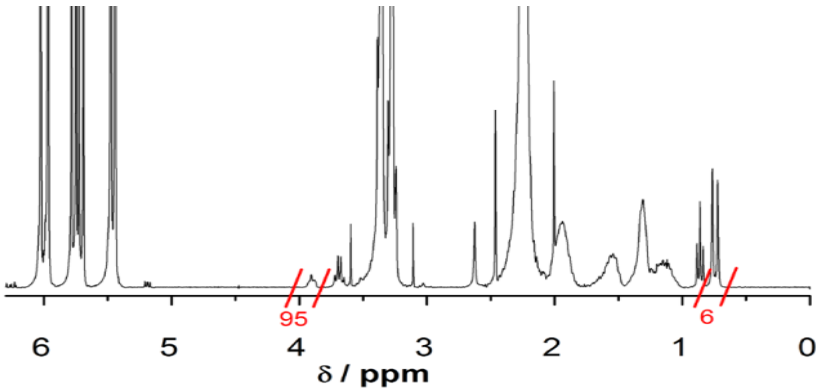

Figure 19. 1H NMR spectrum in Chloroform-*d* for SET-LRP of MA employing [CuBr]:[Me_6TREN] = [0.1]:[0.05], relative to initiator (Ethyl 2-bromoisobutyrate, Ebib), polymerisation time = overnight, 50% *v/v* MA in DMSO at 22 ˚C.

Table 5. Summary of polymerisations of MA in 50% *v/v* DMSO at 22 ˚C.

Entry	[I]:[CuBr]:[Me_6TREN]	T (h)	Conv. %	M_n g.mol^{-1}	Đ	T (h)	Conv. %	M_n g.mol^{-1}	Đ
1	[1]:[0.26]:[0.05]	2	27	2000	1.11	10	31	1900	1.09
2	[1]:[0.26]:[0.1]		24	1100	1.11		24	1400	1.09
3	[1]:[0.26]:[0.3]		37	2800	1.06		77	5900	1.05
4	[1]:[0.26]:[0.6]		41	2800	1.09		92	6600	1.10

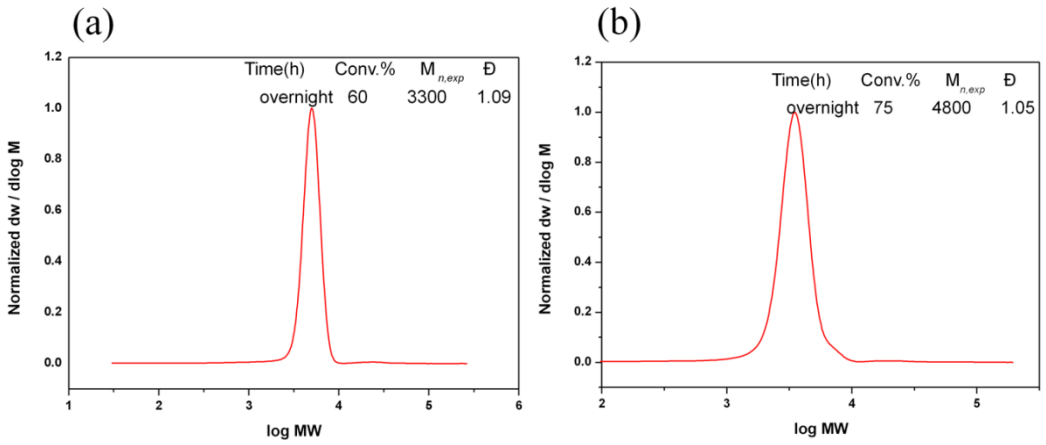

Figure 20. Molecular weight distributions of PMA by ATRP, conditions: [CuBr] : [Me_6TREN] = [1] : [0.5], MA in 50% *v/v* DMSO at 22 ˚C.*via* $CHCl_3$ SEC. After the cessation of the polymerisation (10h, 26% conversion) a second aliquot of active species (either CuBr/Me_6TREN (a) or 5 cm of copper wire/Me_6TREN (b)) were added in the reaction mixture.

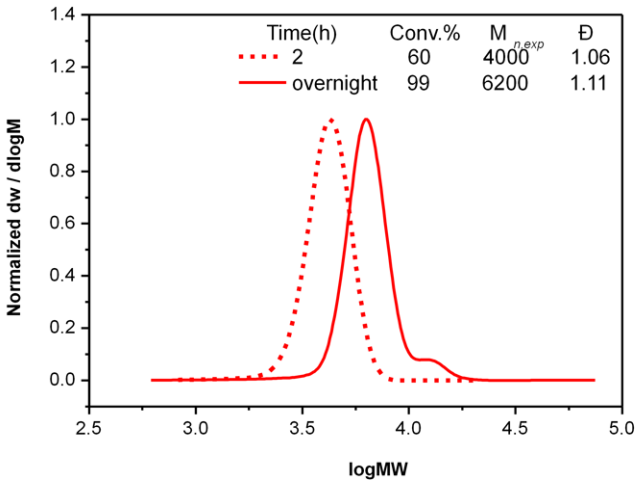

Figure 21. Molecular weight distributions of PMA by ATRP, conditions: [CuBr] : [Me_6TREN] = [1] : [6], MA in 50% *v/v* DMSO at 22 ˚C.*via* $CHCl_3$ SEC.

The role of copper wire as an activator and/or reducing agent

Cu^0 wire / $CuBr_2$ / Me_6TREN 5cm / 0.05(4mg) * / 0.12* *With respect to imitator	Comp. in DMSO and MA 2h	After calculation, 54% $CuBr_2$ comproportionated to CuBr

Scheme 6: Schematic of a typical comproportionation of [Cu(Me_6TREN)]Br_2 and Cu(0) in 2 mL DMSO and 2 mL MA at 22 ˚C.

4.5 References

1. Wang, J.-S., Matyjaszewski, K. *J. Am. Chem. Soc.* **1995,** 117, (20), 5614-5615.
2. Matyjaszewski, K. *Macromolecules* **2012,** 45, (10), 4015-4039.
3. Kato, M., Kamigaito, M., Sawamoto, M., Higashimura, T. *Macromolecules* **1995,** 28, (5), 1721-1723.
4. Percec, V., Guliashvili, T., Ladislaw, J. S., Wistrand, A., Stjerndahl, A., Sienkowska, M. J., Monteiro, M. J., Sahoo, S. *J. Am. Chem. Soc.* **2006,** 128, (43), 14156-14165.
5. Zhang, Q., Wilson, P., Li, Z., McHale, R., Godfrey, J., Anastasaki, A., Waldron, C., Haddleton, D. M. *J. Am. Chem. Soc.* **2013,** 135, (19), 7355-7363.
6. Wang, W., Zhao, J., Zhou, N., Zhu, J., Zhang, W., Pan, X., Zhang, Z., Zhu, X.*Polym. Chem.***2014,** 5, (11), 3533-3546.
7. Konkolewicz, D., Wang, Y., Krys, P., Zhong, M., Isse, A. A., Gennaro, A., Matyjaszewski, K.*Polym. Chem.***2014,** 5, (15), 4396-4417.
8. Gao, Y., Zhao, T., Wang, W. *RSC Advances* **2014,** 4, (106), 61687-61690.
9. Konkolewicz, D., Wang, Y., Zhong, M., Krys, P., Isse, A. A., Gennaro, A., Matyjaszewski, K. *Macromolecules* **2013,** 46, (22), 8749-8772.
10. Lligadas, G., Rosen, B. M., Bell, C. A., Monteiro, M. J., Percec, V. *Macromolecules* **2008,** 41, (22), 8365-8371.
11. Levere, M. E., Nguyen, N. H., Sun, H.-J., Percec, V.*Polym. Chem.***2013,** 4, (3), 686-694.
12. Nguyen, N. H., Levere, M. E., Percec, V. *J. Polym. Sci., Part A: Polym. Chem.***2012,** 50, (1), 35-46.
13. Kwak, Y., Magenau, A. J. D., Matyjaszewski, K. *Macromolecules* **2011,** 44, (4), 811-819.
14. Nguyen, N. H., Rosen, B. M., Lligadas, G., Percec, V. *Macromolecules* **2009,** 42, (7), 2379-2386.
15. Nguyen, N. H., Sun, H.-J., Levere, M. E., Fleischmann, S., Percec, V.*Polym. Chem.***2013,** 4, (5), 1328-1332.
16. Guliashvili, T., Percec, V. *J. Polym. Sci., Part A: Polym. Chem.***2007,** 45, (9), 1607-1618.
17. Levere, M. E., Nguyen, N. H., Percec, V. *Macromolecules* **2012,** 45, (20), 8267-8274.
18. Nguyen, N. H., Levere, M. E., Percec, V. *J. Polym. Sci., Part A: Polym. Chem.***2012,** 50, (5), 860-873.
19. Fischer, H. *Macromolecules* **1997,** 30, (19), 5666-5672.
20. Levere, M. E., Nguyen, N. H., Leng, X., Percec, V.*Polym. Chem.***2013,** 4, (5), 1635-1647.
21. Levere, M. E., Willoughby, I., O'Donohue, S., Wright, P. M., Grice, A. J., Fidge, C., Remzi Becer, C., Haddleton, D. M. *J. Polym. Sci., Part A: Polym. Chem.***2011,** 49, (8), 1753-1763.
22. Nguyen, N. H., Rosen, B. M., Jiang, X., Fleischmann, S., Percec, V. *J. Polym. Sci., Part A: Polym. Chem.***2009,** 47, (21), 5577-5590.
23. Rosen, B. M., Jiang, X., Wilson, C. J., Nguyen, N. H., Monteiro, M. J., Percec, V. *J. Polym. Sci., Part A: Polym. Chem.***2009,** 47, (21), 5606-5628.
24. Nguyen, N. H., Levere, M. E., Kulis, J., Monteiro, M. J., Percec, V. *Macromolecules* **2012,** 45, (11), 4606-4622.

25. Lligadas, G., Rosen, B. M., Monteiro, M. J., Percec, V. *Macromolecules* **2008,** 41, (22), 8360-8364.
26. Lligadas, G., Percec, V. *J. Polym. Sci., Part A: Polym. Chem.***2008,** 46, (20), 6880-6895.
27. Nguyen, N. H., Percec, V. *J. Polym. Sci., Part A: Polym. Chem.***2011,** 49, (19), 4227-4240.
28. Nguyen, N. H., Percec, V. *J. Polym. Sci., Part A: Polym. Chem.***2010,** 48, (22), 5109-5119.
29. Kajiwara, A., Matyjaszewski, K., Kamachi, M. *Macromolecules* **1998,** 31, (17), 5695-5701.
30. Matyjaszewski, K., Tsarevsky, N. V., Braunecker, W. A., Dong, H., Huang, J., Jakubowski, W., Kwak, Y., Nicolay, R., Tang, W., Yoon, J. A. *Macromolecules* **2007,** 40, (22), 7795-7806.
31. Magenau, A. J. D., Kwak, Y., Matyjaszewski, K. *Macromolecules* **2010,** 43, (23), 9682-9689.
32. Peng, C.-H., Zhong, M., Wang, Y., Kwak, Y., Zhang, Y., Zhu, W., Tonge, M., Buback, J., Park, S., Krys, P., Konkolewicz, D., Gennaro, A., Matyjaszewski, K. *Macromolecules* **2013,** 46, (10), 3803-3815.
33. Zhong, M., Wang, Y., Krys, P., Konkolewicz, D., Matyjaszewski, K. *Macromolecules* **2013,** 46, (10), 3816-3827.
34. Wang, Y., Zhong, M., Zhu, W., Peng, C.-H., Zhang, Y., Konkolewicz, D., Bortolamei, N., Isse, A. A., Gennaro, A., Matyjaszewski, K. *Macromolecules* **2013,** 46, (10), 3793-3802.
35. Harrisson, S., Couvreur, P., Nicolas, J. *Macromolecules* **2012,** 45, (18), 7388-7396.
36. Harrisson, S., Nicolas, J. *ACS Macro Letters* **2014,** 3, (7), 643-647.
37. Horn, M., Matyjaszewski, K. *Macromolecules* **2013,** 46, (9), 3350-3357.
38. Wang, Y., Kwak, Y., Buback, J., Buback, M., Matyjaszewski, K. *ACS Macro Letters* **2012,** 1, (12), 1367-1370.
39. Zhang, Y., Wang, Y., Peng, C.-h., Zhong, M., Zhu, W., Konkolewicz, D., Matyjaszewski, K. *Macromolecules* **2011,** 45, (1), 78-86.
40. Wang, Y., Zhong, M., Zhang, Y., Magenau, A. J. D., Matyjaszewski, K. *Macromolecules* **2012,** 45, (21), 8929-8932.
41. Lin, C. Y., Coote, M. L., Gennaro, A., Matyjaszewski, K. *J. Am. Chem. Soc.* **2008,** 130, (38), 12762-12774.
42. Ottino, J. M. *Nature* **2004,** 427, (6973), 399-399.
43. Sun, H.-J., Zhang, S., Percec, V. *Chem. Soc. Rev.* **2015**.
44. Nguyen, N. H., Percec, V. *J. Polym. Sci., Part A: Polym. Chem.***2011,** 49, (22), 4756-4765.
45. Jiang, X., Rosen, B. M., Percec, V. *J. Polym. Sci., Part A: Polym. Chem.***2010,** 48, (2), 403-409.
46. Waldron, C., Zhang, Q., Li, Z., Nikolaou, V., Nurumbetov, G., Godfrey, J., McHale, R., Yilmaz, G., Randev, R. K., Girault, M., McEwan, K., Haddleton, D. M., Droesbeke, M., Haddleton, A. J., Wilson, P., Simula, A., Collins, J., Lloyd, D. J., Burns, J. A., Summers, C., Houben, C., Anastasaki, A., Li, M., Becer, C. R., Kiviaho, J. K., Risangud, N. *Polym. Chem.***2014,** 5, (1), 57-61.
47. Anastasaki, A., Haddleton, A. J., Zhang, Q., Simula, A., Droesbeke, M., Wilson, P., Haddleton, D. M. *Macromol. Rapid Commun.* **2014,** 35, (10), 965-970.
48. Zhang, Q., Li, Z., Wilson, P., Haddleton, D. M. *Chem. Commun.***2013,** 49, (59), 6608-6610.

49. Alsubaie, F., Anastasaki, A., Wilson, P., Haddleton, D. M.*Polym. Chem.***2015**.
50. Anastasaki, A., Waldron, C., Wilson, P., McHale, R., Haddleton, D. M.Polym. Chem.**2013,** 4, (9), 2672-2675.
51. Samanta, S. R., Sun, H.-J., Anastasaki, A., Haddleton, D. M., Percec, V.*Polym. Chem.***2014,** 5, (1), 89-95.
52. Simula, A., Nurumbetov, G., Anastasaki, A., Wilson, P., Haddleton, D. M. *Eur. Polym. J.* **2015,** 62, (0), 294-303.
53. M. Haddleton, D., M. Heming, A., Kukulj, D. *Chem. Commun.***1998**, (16), 1719-1720.
54. Nyström, F., Soeriyadi, A., Boyer, C., Zetterlund, P,, and Whittaker, M. *J. Polym. Sci., Part A: Polym. Chem*. 2011 **49** (24), 5313-5321.
55. Boyer, C., Soeriyadi, A., Zetterlund, P,, and Whittaker, M. *Macromolecules* **2011,** 44 (20), 8028-8033.
56. Ciampolini, M., Nardi, N. *Inorg. Chem*.1966, **5**, 41-44.
57. Queffelec, J., Gaynor, S. G., Matyjaszewski, K. *Macromolecules* 2000, **33**,8629.
58. Keller, R.N., Wycoff, H.D. *Inorg. Synth*., 1946, **2**, 1-4.
59. Rosen, B., Jiang, X., Wilson, C.J., Nguyen, N.H., Monteiro, M.J., Percec, V. *J. Polym. Sci., Part A: Polym. Chem*.2009, **47**, 5606–5628.

Chapter 5: Investigating the mechanism of copper(0)-mediated living radical polymerisation in aqueous media

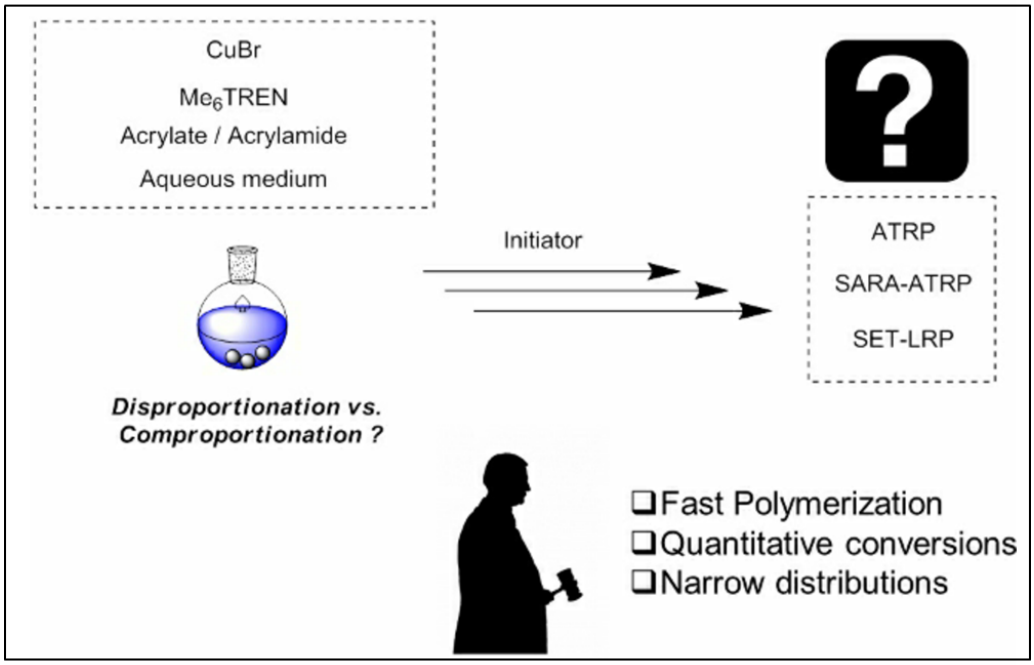

This work is the second part of a mechanistic study regarding the role of Cu(0) and CuBr during the Cu(0)-mediated polymerisation in organic and aqueous media with the aim of offering a better understanding of the mechanism. In this chapter, disproportionation and comproportionation studies in aqueous and organic/aqueous media in the presence of both Cu(0) generated in situ and Cu(0) wire were conducted. The solvent composition, the nature of the monomer and the ligand concentration dramatically affect the thermodynamic and kinetic equilibria while changing the sequence of the reagent addition caused significant variations not only on the disproportionation equilibrium but also on the dispersities of the products obtained. This was attributed to different complexation reactions between the monomer, the solvent, the ligand and the copper species. Reagent feeding experiments with low concentrations of CuBr were also conducted in an attempt to mimic the role of Cu(0) as a potential supplemental activator, further assessing the contributions of Cu(0) and CuBr on the polymerisation rate and control over the molecular weight distributions in the presence of both disproportionating Me_6TREN and non-disproportionating (TPMA) ligands. Crucially, the exploitation of stoichiometric amounts of Cu(0) and CuBr relative to $CuBr_2$ allowed for a direct comparison between the SET-LRP and ATRP protocols, revealing very different contributions of the two catalysts depending on the conditions employed.

5.1 Introduction

RDRP methods have been used widely for the synthesis of polymers with narrow molecular weight distributions MWDs, high end-group functionality and complex architectures. Among the various polymerisation techniques employed, ATRP[1-3] and SET-LRP[4-6] have attracted considerable interest due to their ability to effectively manipulate the activation/deactivation equilibrium between active and dormant species maximizing control over the MWDs.

Towards this, the use of zerovalent metals has been exploited by both Matyjaszewski[7] and Percec[4] with aim to maximize the catalyst efficiency and improve the end-group fidelity during the polymerisation of a plethora of monomers, including acrylates, methacrylates and acrylamides. Currently, there are two models available in the literature which attempt to explain the mechanism of copper-mediated polymerisations in the presence of Cu(0), SET-LRP proposed by Percec and co-workers and supplemental activator and reducing agent (SARA-ATRP) proposed by Matyjaszewski's group. Both models involve the same reagents but suggest different minor and major catalytic species (Cu(0) or CuBr) and contribution of every reaction (*e.g.* disproportionation, comproportionation).[8-11]

SET-LRP cites that the major activator of alkyl halides is Cu(0)[4] or extremely reactive "nascent" Cu(0) nanoparticles[12, 13] while CuBr is inactive due to rapid disproportionation into Cu(0) and $CuBr_2$ in the presence of suitable *N*-containing ligands[14, 15] and polar solvents (e.g. DMSO, H_2O). The disproportionation has been visualized in a variety of solvents and monomers including protic, dipolar aprotic and non-polar.[16-19] However, when non-disproportionating solvents have been utilised (*e.g.* acetonitrile (MeCN) or toluene), loss of both end group functionality

and of the control over the MWDs have been reported.[20-24] The inactivity of CuBr has been further demonstrated by a number of reports[13, 25] which highlight the role of Cu(0) as major activator and as an essential component to achieve close to 100% end-group fidelity.[26] An outer sphere electron transfer (OSET)[4, 27] has been proposed to mediate the activation process[12, 28, 29] *via* a radical anion intermediate, showing lower dissociation energies.

Conversely, the SARA-ATRP mechanism states that CuBr is the major activator of alkyl halides and the role of Cu(0) is limited to that of a supplemental activator and reducing agent while disproportionation is negligible.[30-34] Comproportionation is reported to dominate over disproportionation[35-37] and kinetic simulations are presented to argue that the control over the polymerisation is attributed mainly to CuBr as the main activator and $CuBr_2$ as the main deactivator, thus proceeding *via* an ATRP dynamic equilibrium.[33] In addition, the "ultrafast" polymerisation rate during the polymerisations attributed to rapid disproportionation by Percec is explained as a result of the effect of the increased solvent polarity on the rate constant of propagation by Matyjaszewski.[38, 39] Further experiments presented are explained as DMSO (a disproportionating solvent) and MeCN (a non-disproportionating solvent) and Me_6TREN (disproportionating ligand) and TPMA (a non-disproportionating ligand) can equally control the efficient polymerisation of acrylates. Moreover SET-LRP is been reported to violate "the principle of halogen conservation (PHC)"[40] and the "principle of microscopic reversibility (PMR)".[31] Finally, high-level *ab initio* molecular orbital calculations are given to support that for monomers bearing electron-withdrawing groups, such as acrylates, catalysts favouring inner sphere electron transfer (ISET) over OSET are required in order to avoid chain-breaking side reactions.[41]

Interestingly, the literature regarding the role of Cu(0)/CuBr in aqueous polymerisations (as opposed to DMSO polymerisations) is very limited and only preliminary results have been reported, concluding that although disproportionation is thermodynamically favoured in H_2O, CuBr can activate the alkyl halides faster than disproportionation and/or activation events mediated by Cu(0). Thus, in polymerisations in aqueous media the mechanism is still proposed to proceed *via* a SARA-ATRP pathway.[42] Nevertheless, both Percec and Matyjaszewski have supported their argumentation and views *via* many papers, that appear to be conflicting for the general audience and it is noted that in many times the conditions utilised are not directly comparable, leading to further confusion. Thus, in this chapter a further study is conducted aiming to understand some of these ambiguities and offer further mechanistic insight to copper-mediated polymerisations.

In brief, the aim of this chapter is to investigate the mechanism of copper mediated living radical polymerisation of acrylates and acrylamides in the presence of Cu(0) wire and/or Cu(0) particles in aqueous and aqueous/organic media. Variation of the solvent composition, the monomer structure and the ligand concentration will be shown to influence the disproportionation and comproportionation equilibrium while the sequence of the reagent addition is of upmost importance for the effective polymerisation of acrylates and acrylamides further affecting the disproportionation and comproportionation values. In addition, feeding experiments with low [CuBr] will be performed in order to evaluate the contribution of Cu(0) particles to the polymerisation kinetics and control. Finally, a direct comparison between the SET-LRP and the ATRP protocol will be conducted in a large variety of aqueous and binary mixtures utilizing stoichiometric amounts of $CuBr_2$ relative to Cu(0) and CuBr and the role of each species was determined and is discussed.

5.2 Results and discussion

In an attempt to gain a better understanding for the polymerisation of acrylates and acrylamides in the presence of Cu(0), the system has been analysed both as individual components and also as a whole. Hence, disproportionation and comproportionation processes were initially studied followed by the investigation of the polymerisation when all components were simultaneously included, thus directly assessing the contribution of all species in a real time polymerisation.

5.2.1 The extent of disproportionation of [Cu(Me_6TREN)]Br in H_2O and aqueous/organic mixtures

In pure H_2O, the disproportionation of [Cu(Me_6TREN)]Br was visualized within one second by the observation of insoluble Cu(0) particles and the evolution of a blue colour, corresponding to the *in situ* generated [Cu(Me_6TREN)]Br_2 complex. Disproportionation was subsequently monitored by UV-Vis absorbance (λ_{max} ~ 950 nm) corresponding to the *in situ* generated [Cu(Me_6TREN)]Br_2 complex and was found to be at least 99% (Table 1, entry 1, Figure 1). A time period of 15 min was chosen for all the measurements, as the majority of the aqueous and aqueous/organic polymerisations using this process reach full conversion within this time.[6, 43-48]

Table 1. Degree of [Cu(Me_6TREN)]Br disproportionation in H_2O and DMSO % *v*/*v* and their mixtures, [CuBr]:[Me_6TREN] = [1]:[1], 2 mL solvent at 22˚C.

entry	solvent composition		degree of disp. %
	H_2O %	DMSO%	
1	100	0	99
2	75	25	98
3	50	50	97
4	45	55	84
5	35	65	68

6	25	75	60
7	15	85	46
8	5	95	35
9	0	100	31

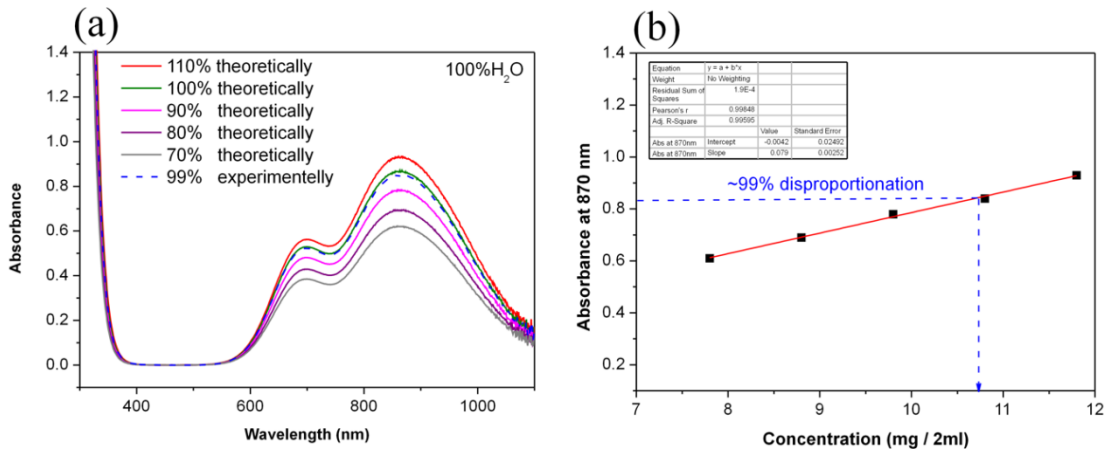

Figure 1. UV-Vis spectra of the solution of varying amounts of $CuBr_2$ in the presence of Me_6TREN (26 µL, 0.1 mmol) in H_2O (2 mL). The dashed line represents the UV-Vis spectrum of the disproportionation of CuBr (14 mg, 0.1 mmol) / Me_6TREN (26 µL, 0.1 mmol) in H_2O (2 mL). All samples were diluted before analysis into degassed H_2O (a). Calibration curve based on UV-Vis absorbance at 870 nm. The intercept for the linear fit was set as 0 (b).

It is well known there is a large thermodynamic driving force for the disproportionation of CuBr in water in the presence of suitable *N*-containing ligands, such as Me_6TREN with the equilibrium constant reported to be as high as ~ 10^6.[6, 11, 49, 50] It has been previously reported that disproportionation in DMSO under similar conditions resulted in 31% disproportionation (chapter 4)[51], suggesting that there is a significant solvent effect on the rate and extent of disproportionation between these solvents. When mixtures of H_2O/DMSO were used high values of disproportionation were retained (> 97%) for up to 50% mixtures (H_2O : DMSO = [1]:[1]) (Figure 2,

Table 1, entries 2 and 3), while this decreased considerably at <50% H_2O (Figure 3, Table 1, entries 4-8).

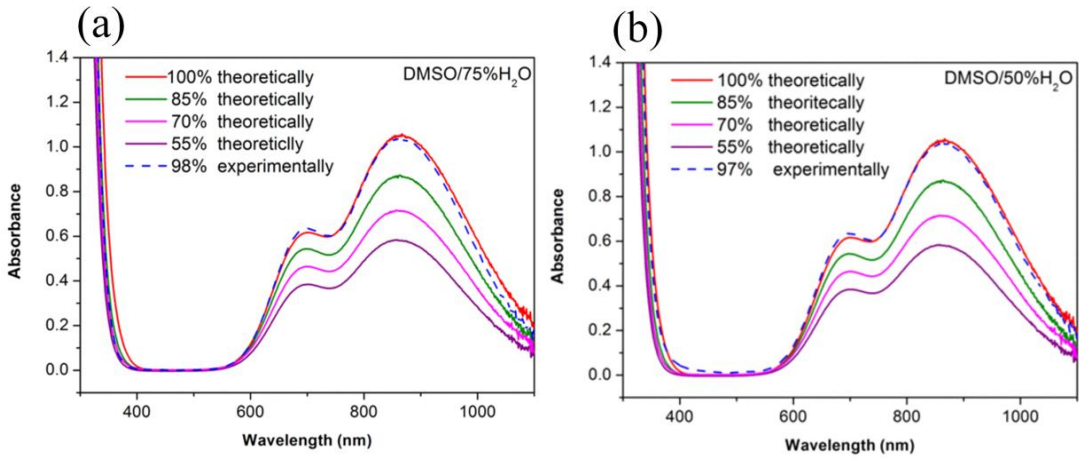

Figure 2. UV-Vis spectra of the solution of varying amounts of $CuBr_2$ in the presence of Me_6TREN (26 μL, 0.1 mmol) in the mixture (a) DMSO/ 75% H_2O and (b) DMSO/ 50% H_2O. The dashed line represents the UV-Vis spectrum of the disproportionation of CuBr (14 mg, 0.1 mmol) / Me_6TREN (26 μL, 0.1 mmol) in the mixtures. All the samples were diluted before analysis into degassed H_2O/DMSO mixture.

The high degree of disproportionation in the former mixtures is highly advantageous for solubilising more hydrophobic compounds (*e.g.* initiators, monomers) and thus the aqueous disproportionation protocol can be further expanded to include a larger diversity of monomers and functional groups.

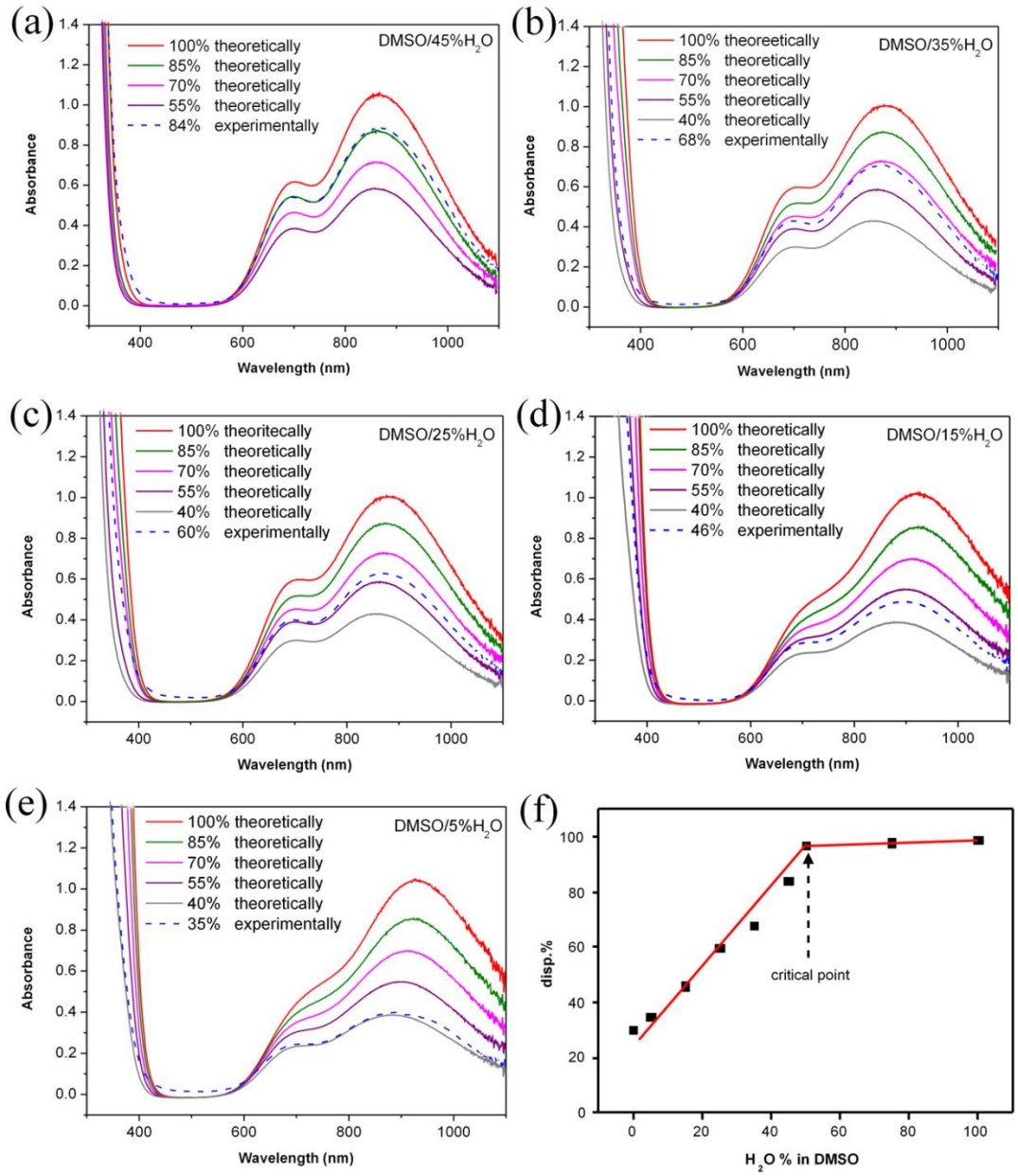

Figure 3. UV-Vis spectrum of the disproportionation of CuBr (14 mg, 0.1 mmol) / Me_6TREN (26 µL, 0.1 mmol) in the mixtures DMSO/ (a) 45% (b) 35% (c) 25% (d) 15% (e) 5% H_2O after 15 minutes under the conditions: [CuBr]:[Me_6TREN] = [1]:[1], 2 mL solvent at 22˚C. (f) Extent of [Cu(Me_6TREN)]Br disproportionation in H_2O and DMSO and their binary mixtures.

Similarly, when four different organic solvents (MeOH, NMP, DML and DMF) replaced DMSO (50% mixtures) very high degree of disproportionation (> 95%) were observed (Figure 4, Table 2).

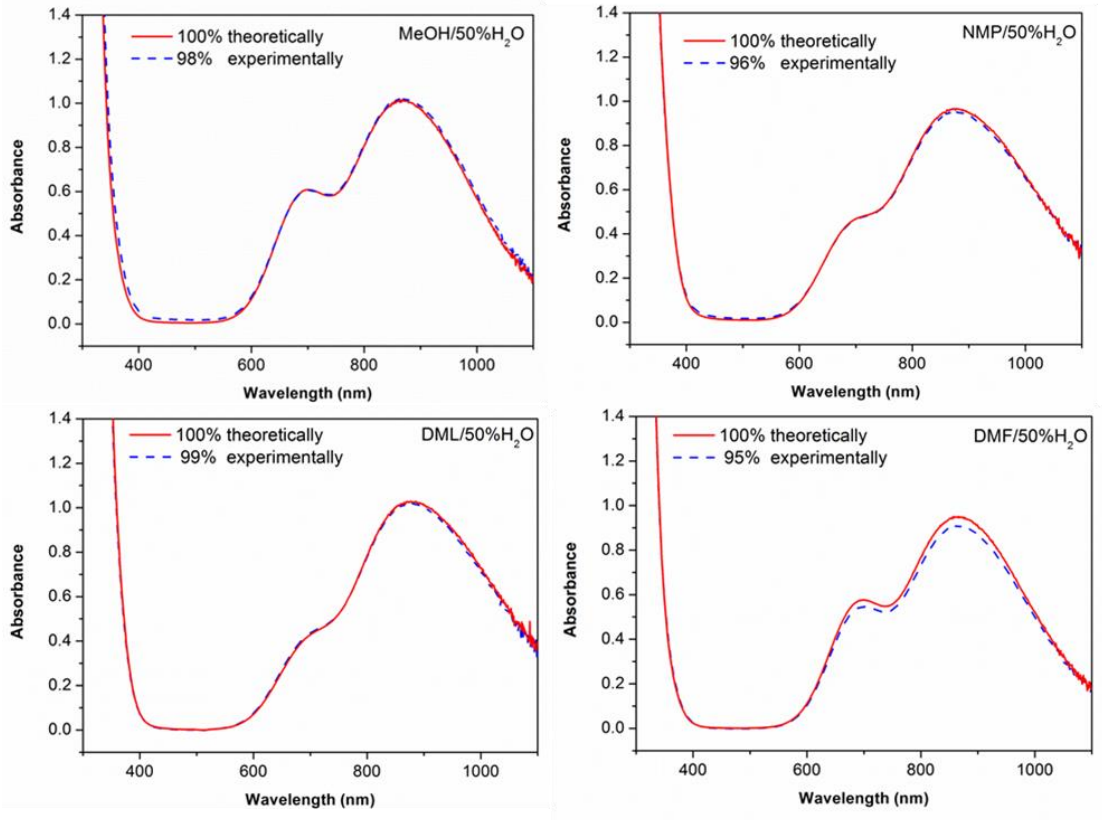

Figure 4. UV-Vis spectra of the solution of two different amounts of $CuBr_2$ in the presence of Me_6TREN (26 µL ,0.1 mmol) in the mixture (H_2O, 1 mL+ MeOH, NMP, DML and DMF 1 mL). The dashed line represents the UV-Vis spectrum of the disproportionation of CuBr (14 mg, 0.1 mmol) / Me_6TREN (26 µL, 0.1 mmol) in the mixture (H_2O, 1 mL+ MeOH, NMP, DML and DMF, 1 mL). All the samples were diluted before analysis into degassed H_2O/MeOH mixture.

Table 2. Degree of [Cu(Me_6TREN)]Br disproportionation in MeOH, NMP, DMF and DML and their binary mixtures with up to 50% *v*/*v* water: [CuBr]:[Me_6TREN] = [1]:[1], 2 mL solvent at 22 ˚C.

entry	solvent composition		degree of disp. %
	organic%	H_2O%	
1	MeOH 50	50	98
2	NMP 50	50	96
3	DML50	50	98
4	DMF 50	50	95

5.2.2 The effect of ligand concentration on the disproportionation of copper(I) in H_2O

An investigation of the ability of Me_6TREN to enhance or prohibit the disproportionation of CuBr *via* preferential stabilization of $CuBr_2$ in water was initially conducted. In a previous report[51] UV-Vis studies utilizing various amounts of Me_6TREN relative to CuBr showed that an increase in [ligand] in DMSO solution stabilizes CuBr which results in less Cu(0) produced and a lower [$CuBr_2$] obtained *via* disproportionation. However, in the case of water a completely different behaviour was observed. When 0.5 eq. of Me_6TREN relative to CuBr is employed the UV-Vis spectrum indicates 99% disproportionation occurs (Scheme 1).

$$2[Cu(Me_6TREN)]Br \underset{15min\ or\ 10h}{\overset{2ml,\ H_2O}{\rightleftharpoons}} Cu(0) + [Cu(Me_6TREN)]Br_2 + Me_6TREN$$

Scheme 1. Disproportionation of [Cu(Me_6TREN)]Br utilising different concentrations of Me_6TREN (0.25, 0.5, 1, 2, 3 and 6 with respect to CuBr) in H_2O at 22˚C.

Identical results were obtained when 1, 2, 3 and 6 eq. of Me_6TREN were utilised with 99% of disproportionation detected in all cases (Figure 5).

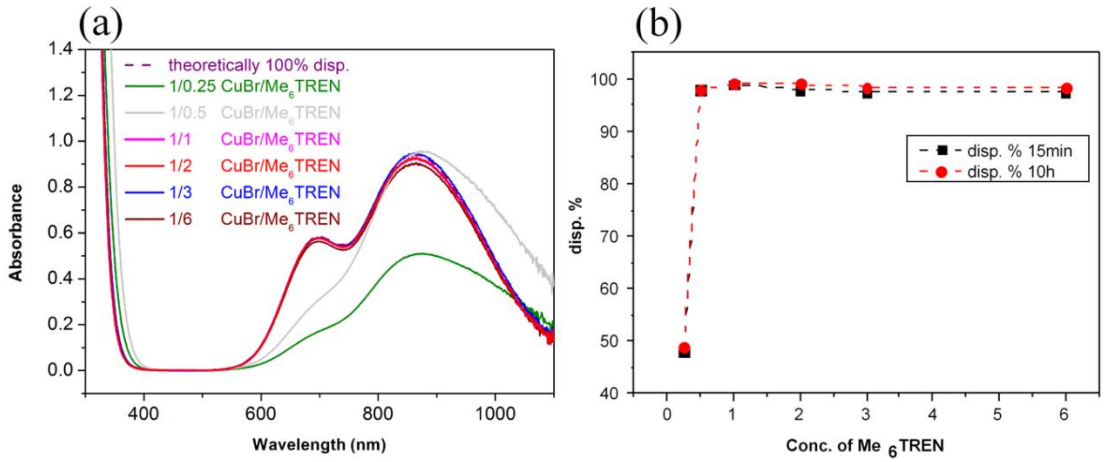

Figure 5. UV-Vis spectra of a) solution of [Cu(Me_6TREN)]Br in the presence of different equivalents of Me_6TREN with respect to [CuBr] in DMSO, b) comparison between the degree of disproportionation in DMSO, c) in water, d) in water in two different times of disproportionation 15 min and 10 h. Conditions: [CuBr]:[Me_6TREN] = [1]:[1], 2 mL solvent at 22 ˚C.

This is surprising given that if a ligand binds sufficiently to $CuBr_2$ and CuBr and stabilises $CuBr_2$ more than CuBr, then the maximum of disproportionation should occur when the ligand is half of the amount of CuBr in the solution, as any excess of Me_6TREN will shift the equilibrium towards CuBr. Moreover, when higher amounts

of Me_6TREN were used, the *in situ* generated Cu(0) particles appeared dispersed in the solution, rather than as a coarse precipitate (Figure 6).

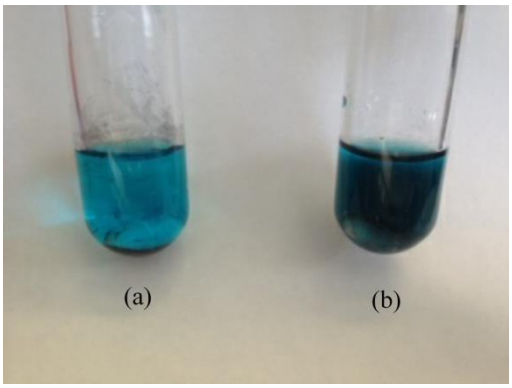

Figure 6. Visualization of the disproportionation of CuBr / Me_6TREN in H_2O. Conditions: (a) H_2O = 2 mL, CuBr = 0.1 mmol, Me_6TREN = 0.1 mmol, (b) H_2O = 2 mL, CuBr = 0.1 mmol, Me_6TREN = 0.6 mmol and nitrogen protection.

Thus, an excess of ligand can act as a dispersant/surfactant for Cu(0). Finally, ~ 50% of disproportionation was measured when lower amounts of ligand (0.25 eq.) were employed, as there was insufficient ligand present to complex the $CuBr_2$. This result is in disagreement with the DMSO system, where 0.5 and 0.25 eq. of ligand gave rise to identical levels of disproportionation. This is attributed to the significantly higher tendency of CuBr towards disproportionation in water rather than in DMSO (in DMSO a maximum degree of disproportionation of only 46% is achieved, thus even in the case of the 0.25 eq. there is still sufficient ligand to complex the generated $CuBr_2$.Therefore, in the case of H_2O varying the [ligand] does not affect the equilibrium as long as there is sufficient ligand present to solubilize the copper species.

5.2.3 Disproportionation of [Cu(Me$_6$TREN)]Br in H_2O in the presence of monomer

The effect of the presence of the monomer in the disproportionation equilibrium is of importance as this more closely resembles the polymerisation conditions. The presence of initiator was excluded from these studies as an increase in [$CuBr_2$] by UV-Vis analysis could be generated simultaneously by a number of events including disproportionation, activation by CuBr and/or bimolecular termination.

Thus, the degree of disproportionation in H_2O, in the presence of various monomers was assessed utilising two different polymerisation protocols. Following the 1st protocol (Scheme 2), 85% disproportionation was observed within 15 min with NIPAM monomer (Table 2, entry 1 and Figure 7a).

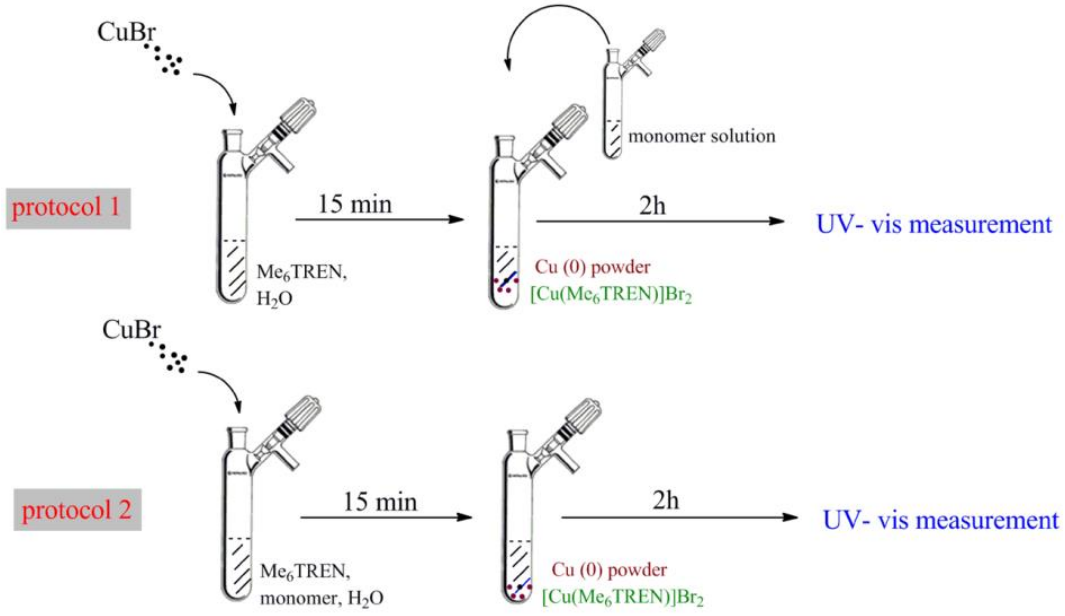

Scheme 2. Schematic representation of a typical disproportionation of [Cu(Me$_6$TREN)]Br *via* protocol 1 (top), and protocol 2 (bottom) under typical polymerisation conditions ([CuBr]:[Me$_6$TREN] = [1]:[1], 12% *v*/*v* monomer in H_2O at 22 ˚C.

Table 2. Summary of the degree of [Cu(Me_6TREN)]Br disproportionation in water under typical polymerisation conditions [CuBr]:[Me_6TREN] = [1]:[1], 12% *v*/*v* monomer in H_2O at 22˚C.

Entry	monomer	Protocol	degree of disp. %
1	NIPAM	1	85
		2	72
		3	46
2	$PEGA_{480}$	1	96
		2	88
		3	83
3	HEAA	1	88
		2	75
		3	52
4	HEA	1	95
		2	83
		3	70

Thus, a reduction in the extent of disproportionation when an acrylamide monomer is present in H_2O was observed. Conversely, with an acrylate, poly(ethylene glycol) methyl ether acrylate (average M_n 480) ($PEGA_{480}$) disproportionation remains very high with a small reduction from 99% to 96% observed, (Table 2, entry 2 and Figure 7b). It should be noted that lower degree of disproportionation has been reported in the literature for this monomer.[42] However, in that study higher ratio of monomer to solvent (18% as opposed to 12% in this current study) and significantly higher ligand concentration were employed ([20]:[1] relative to copper species), thus deviating from these current conditions. In the same report, although simulation studies confirmed the SARA-ATRP mechanism, again, high monomer content and ligand concentration have been utilised. It is therefore important to notice that even slight deviations can have a detrimental effect on the polymerisation under these conditions. In a similar trend to NIPAM and $PEGA_{480}$, acrylate monomer, HEA

resulted in 95% disproportionation after 15 min whereas acrylamide HEAA presented a higher reduction on the extent of disproportionation (88%) (Table 2, entries 3 - 4 and Figure 7c, d).

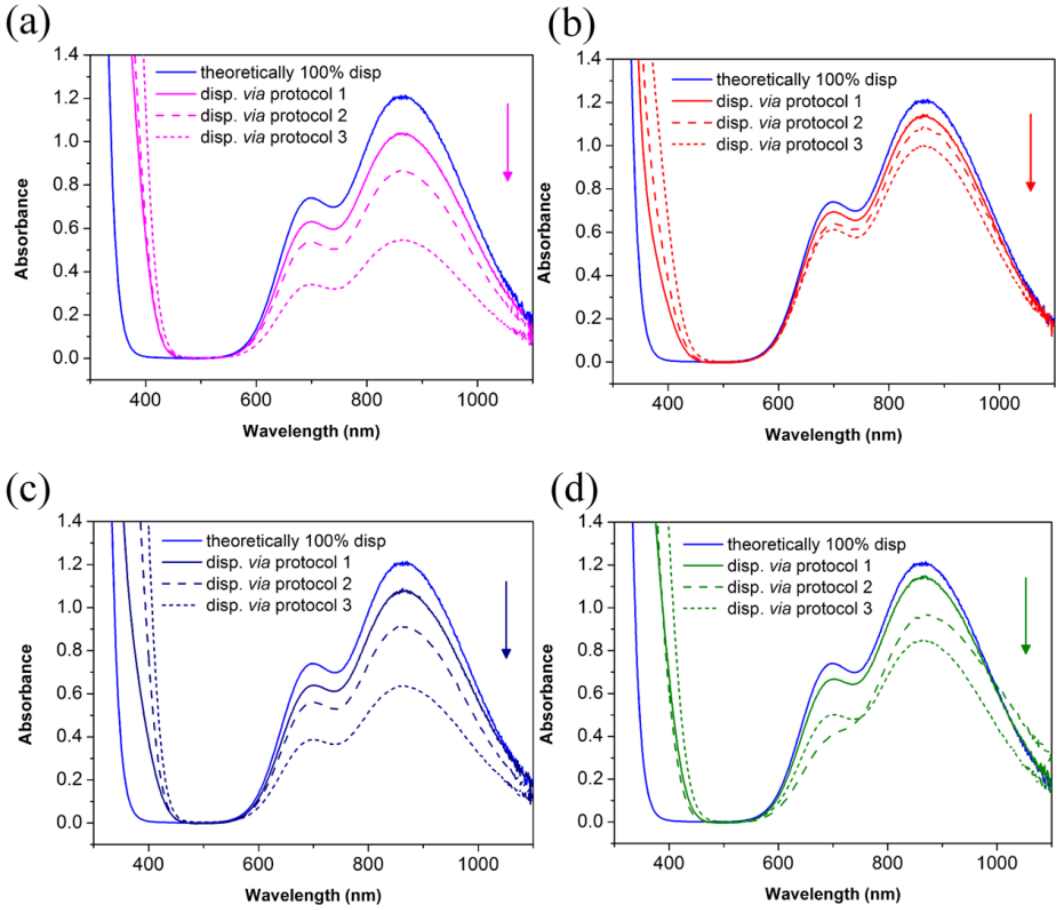

Figure 7. UV-Vis spectra of [Cu(Me_6TREN)]Br in the presence of a) NIPAM, b) $PEGA_{480}$, c) HEAA, and d) HEA. Conditions: [CuBr]:[Me_6TREN] = [1]:[1], 12% *v*/*v* monomer in H_2O at 22 ˚C.

Protocol 2 (mixing monomer, ligand and CuBr in H_2O) was additionally employed to evaluate the extent of disproportionation (Scheme 2). In the presence of all the components, the degree of disproportionation was reduced, presenting 72% for NIPAM (and 75% for HEAA) and 88% for $PEGA_{480}$ (and 83% for HEA), (Table 2,

entries 1-4 and Figure 7a, b, c, d) supporting that acrylamides impact the extent of disproportionation more than acrylates.

In order to verify this observation, a third protocol was employed (Protocol 3, Scheme 3), where the monomer (NIPAM) was pre-mixed with CuBr in H_2O for 15 mins, after which time 46% of disproportionation was seen by UV-Vis (Table 2, entry 1 and Figure 7a).

Scheme 3. Schematic of a typical disproportionation of [Cu(Me_6TREN)]Br *via* protocol 3 in H_2O under polymerisation conditions: [CuBr]:[Me_6TREN] = [1]:[1], 12% *v*/*v* monomer in H_2O at 22 ˚C.

Upon addition of Me_6TREN to the reaction mixture, the degree of disproportionation increased gradually, reaching equilibrium after approximately 16 h (Figure 8). Similar results were obtained for HEAA, $PEGA_{480}$ and HEA (Table 2, entries 2-4 and Figure 7b, c, d). In all cases, the presence of acrylamides was found to disturb the disproportionation equilibrium, by shifting the equilibrium towards comproportionation. To investigate the tendency of acrylamides and acrylates to complex the copper, additional UV experiments were conducted, where the characteristic absorbance for both CuBr and $CuBr_2$ in the presence of both $PEGA_{480}$ and NIPAM can be seen (Figure 9).

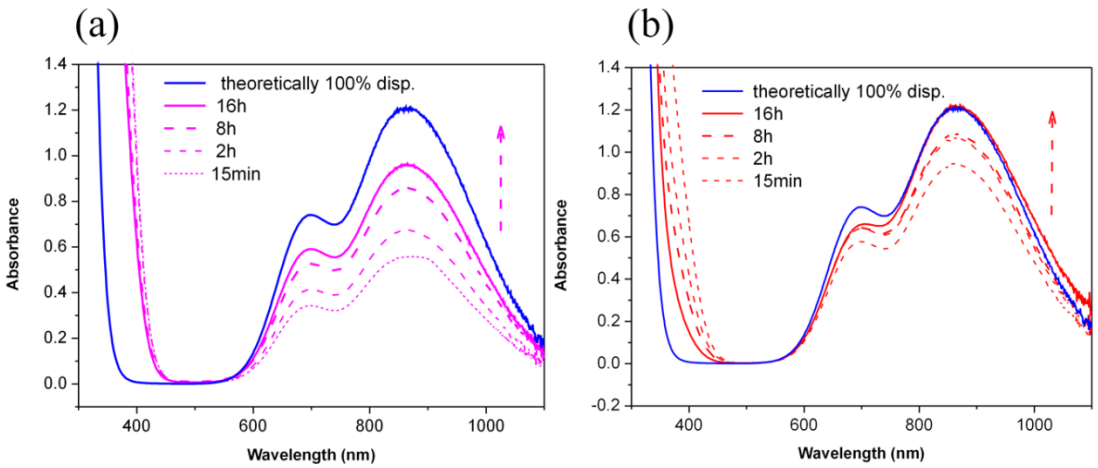

Figure 8. Evolution of UV-vis spectra of [Cu(Me$_6$TREN)]Br$_2$ in the presence of NIPAM with time (left) and PEGA$_{480}$ (right), in H_2O. Conditions: [CuBr]:[Me$_6$TREN] = [1]:[1], 12% *v/v* monomer in H_2O at 22 ˚C.

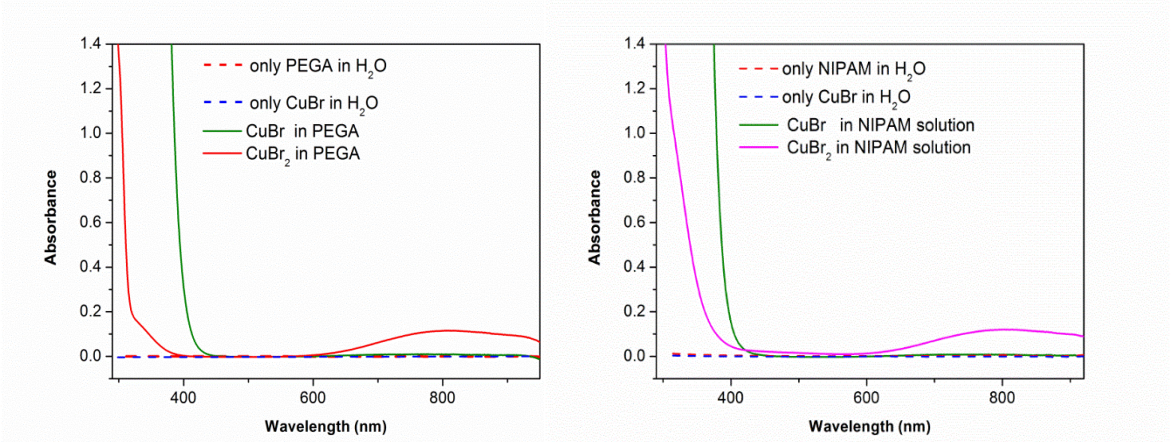

Figure 9. UV-vis spectra of complexation of CuBr and CuBr$_2$ with PEGA$_{480}$ and NIPAM in H_2O. Conditions: [CuBr]:[Me$_6$TREN] = [1]:[1], at 22˚C.

It should be noted, that with protocol 1, where the pre-disproportionation of [Cu(Me$_6$TREN)]Br in H_2O (~ 99%) was exploited and followed by the addition of monomer and initiator, is the protocol that results in the most efficient synthesis of functional water-soluble polymers with controlled chain length and narrow molecular weight distributions. Protocols 2 and 3, where less degree of

disproportionation was observed, give rise to uncontrolled polymerisation prior to initiator addition for NIPAM, HEAA and HEA (Section 5.4.4, Table 6). In the case of $PEGA_{480}$, no polymer was detected by ^{1}H NMR or SEC analysis during disproportionation, allowing the addition of initiator after mixing all of the components. However, high dispersities were observed in both cases (> 1.5) (Figure 10), suggesting that only when quantitative or near quantitative disproportionation[6, 46] (~ 99%) is allowed (protocol 1), optimum results can be achieved (full conversion within 15 min and $Đ$ ~ 1.1). Thus, this is the protocol of choice for aqueous copper-mediated polymerisations.

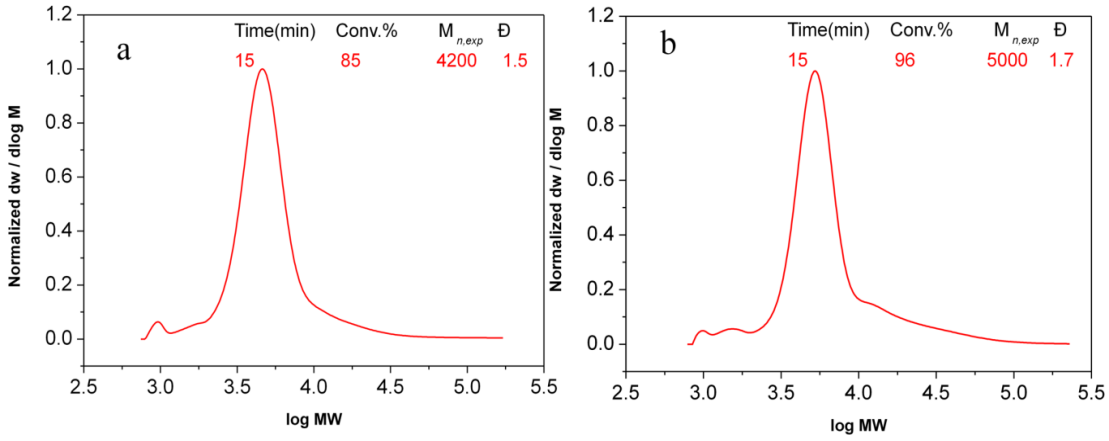

Figure 10. Molecular weight distributions of PEGA by a) protocol 2, b) protocol 3 at 0 ˚C *via* DMF SEC.

5.2.4 The extent of comproportionation of Cu(0) and $CuBr_2$ in H_2O in the presence/absence of monomer

In order to investigate the degree of comproportionation, Cu(0) wire (activated by both HCl and hydrazine)[23, 24, 51, 52] and $CuBr_2$ were employed (Scheme 4).

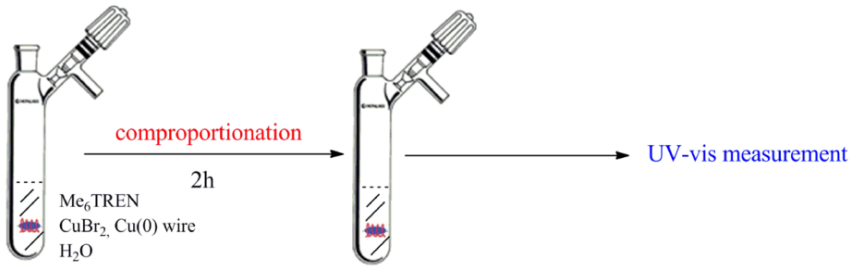

Scheme 4. Schematic representation of a typical comproportionation of $[Cu(Me_6TREN)]Br_2$ in H_2O under typical polymerisation conditions: $[CuBr_2]$:$[Me_6TREN]$ = [1]:[2] at 22˚C.

Both methods showed that in pure H_2O, no comproportionation was observed (Figure 11a), even when the reaction mixture was left overnight, suggesting that disproportionation in H_2O is quantitative, or near-quantitative in agreement with previously reported data.[42] The effect of both acrylates and acrylamides on the disproportionation equilibrium was also considered. Despite the presence of either NIPAM or $PEGA_{480}$ (Figure 11b) and (Section 5.4.4, Figure 34), 0% comproportionation was obtained after 15 min and negligible (< 2%) after 8 hrs was detected by UV-Vis (Figure 12).

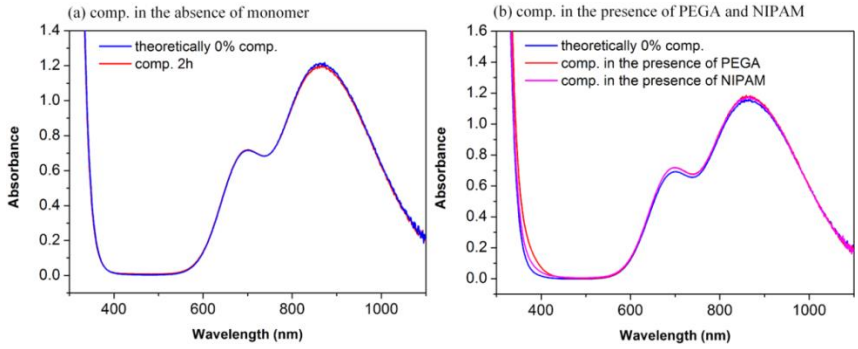

Figure 11. UV-Vis spectra of potential $[Cu(Me_6TREN)]Br_2$ comproportionation a) in the absence of monomers, (b) in the presence of NIPAM and $PEGA_{480}$. Conditions: $[CuBr_2]$:$[Me_6TREN]$ = [1]:[2], 12% *v*/*v* monomer, Cu(0) wire (diameter 0.25mm) activated by HCl in H_2O at 22 ˚C.

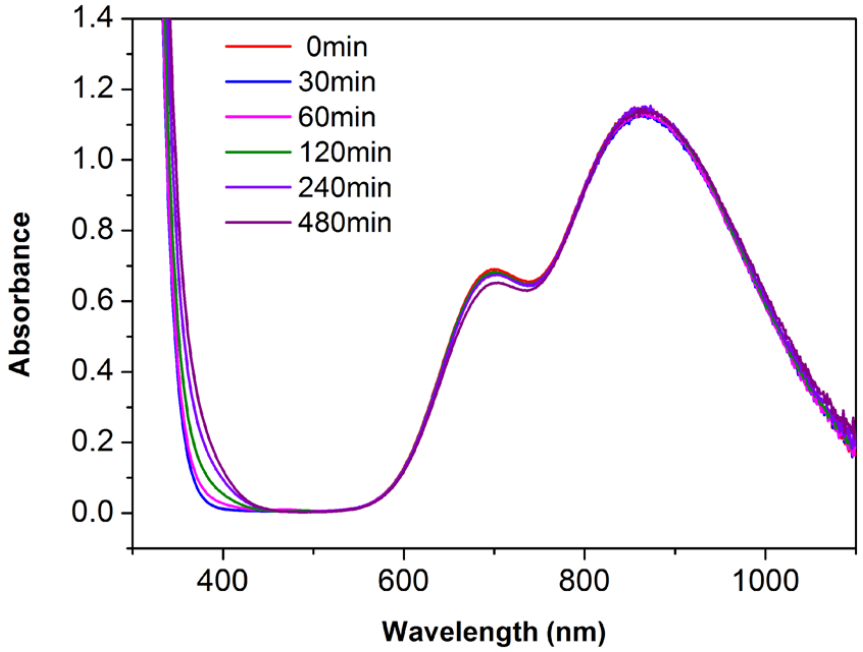

Figure 12. UV-Vis spectra of potential [Cu(Me_6TREN)]Br_2 comproportionation for a long period in the presence of $PEGA_{480}$. Conditions: [$CuBr_2$]:[Me_6TREN] = [1]:[2], 12% *v*/*v* monomer, Cu(0) wire (diameter 0.25mm) activated by HCl in H_2O at 22 ˚C.

This is in disagreement with previously reported data which reported 15% comproportionation (5 h) in the presence of $PEGA_{480}$.[42] On close inspection, a very large excess of Me_6TREN was utilised for these reported experiments which do not represent the conditions employed in the typical polymerisation (see chapter 2 and 3). Polymerisation using this system ([CuBr]:[Me_6TREN] = 1:1 in which much less Me_6TREN is used than in reference (42) reached full conversion in < 15 min thus the comproportionation equilibrium at these prolonged timescales is not relevant for the polymerisation that has been used in the first chapter.

5.2.5 The role of Cu(0) in aqueous polymerisations

In order to clarify the mechanism further a series of 5 different protocols were conducted under different reaction conditions. We have recently introduced a new polymerisation protocol, exploiting the rapid disproportionation of $[Cu(Me_6TREN)]Br_2$ in water.[43-48] In these aqueous systems no comproportionation takes place within the polymerisation time scale (approximately 15 min). Thus, it can be concluded that Cu(0) does not act as a reducing agent or that the role of Cu(0) as a reducing agent is negligible. Percec and co-workers claim that Cu(0) is the main activator and Matyjaszewski's group reports that CuBr is the main activator and that Cu(0) is a supplemental activator. If the latter statement is correct, then the role of Cu(0) is to act as a "storage of CuBr" to continuously generate CuBr when the concentration is depleting *via* termination reactions. Thus, it can be rationalised that if CuBr could be slowly introduced into the polymerisation mixture in low concentrations (Scheme 5), the role of Cu(0) should be reproduced and obtain well-controlled polymers, maintaining fast polymerisation rates. Therefore, the first protocol ("feeding protocol") involves feeding the reaction mixture (consisting of $CuBr_2$, monomer, initiator and solvent) with CuBr/solvent/ligand. For comparison reasons, a second protocol was also conducted, where the total amount of CuBr was directly injected (without feeding) into the reaction mixture in one pot ("control feeding protocol"). The third protocol involves performing a "typical ATRP" (only CuBr is used as the copper source) while the fourth one is utilizing the same amount of CuBr to allow full disproportionation to occur prior the addition of the other reagents ("SET-LRP protocol"). However, protocols 3 and 4 cannot be compared as full disproportionation reduces the amount of the catalyst (Cu(0)) at half (CuBr disproportionates into Cu(0) and $CuBr_2$ under appropriate conditions) and hence a

direct comparison between the latter two protocols cannot be made. In order to address this, a fifth protocol is also followed ("ATRP with $CuBr_2$ protocol"), where equivalent amounts of CuBr and $CuBr_2$ are employed to facilitate a direct comparison between ATRP ([CuBr]:[$CuBr_2$]=[1]:[1]) and SET-LRP ([Cu(0)]:[$CuBr_2$] =[1]:[1]).

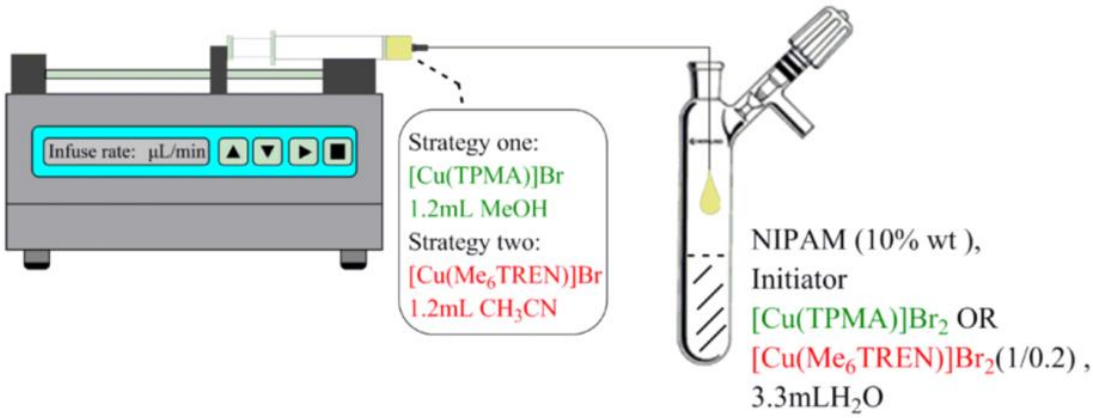

Scheme 5. Schematic of the slow feeding system with CuBr following two strategies in order to avoid the disproportionation event, conditions in the syringe: [CuBr]:[TPMA] = [0.1]:[0.1] with respect to initiator, in MeOH, or in CH_3CN at 22˚C. Conditions in Schlenk tube, conditions: [I]:[NIPAM]:[$CuBr_2$]:[ligand] = [1]:[20]:[0.05]:[0.05] at 0˚C.

Polymerisation of acrylamides with TPMA

Due to the high disproportionation constant of [Cu(Me_6TREN)]Br in H_2O, feeding the complex as an aqueous solution is not feasible as [Cu(Me_6TREN)]Br instantly disproportionates in the syringe prior to addition to the reaction (Figure 13).

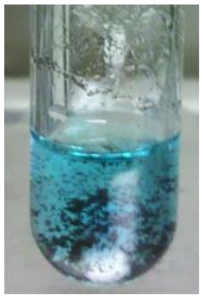

Figure 13. Visualization of the disproportionation of [Cu(Me_6TREN)]Br in H_2O. Conditions: H_2O = 2 mL, [CuBr]:[Me_6TREN] = [1]:[1] (CuBr = 0.1 mmol, Me_6TREN = 0.1 mmol) under nitrogen protection.

In order to circumvent this, two different strategies were employed. Firstly, Me_6TREN (that preferentially stabilizes $CuBr_2$) was replaced with TPMA (preferentially stabilizes CuBr) which is reported to be one of the most highly active ligands for ATRP.[53] TPMA has been previously reported in aqueous polymerisations as a non-disproportionating ligand.[54] Thus, minimal, if any, Cu(0) should be generated in the syringe during the feed. The same amount of $CuBr_2$ was placed as it would have been produced if the disproportionation was quantitative or near quantitative in the Schlenk tube, thus mimicking the established aqueous reaction conditions,[6] however, in the absence of Cu(0). An equivalent amount of ligand was also added to ensure efficient complexation with $CuBr_2$. Monomer (NIPAM), initiator and H_2O were also added. Subsequently, a solution of CuBr/ligand was fed, *via* a syringe pump, with different flow rates and the progress of the reaction was monitored by ^{1}H NMR and SEC.

Although TPMA is freely soluble in water, the addition of CuBr caused the precipitation of a TPMA/CuBr complex within 1 min and thus feeding [Cu(TPMA)]Br in water proved not possible (Figure 14).

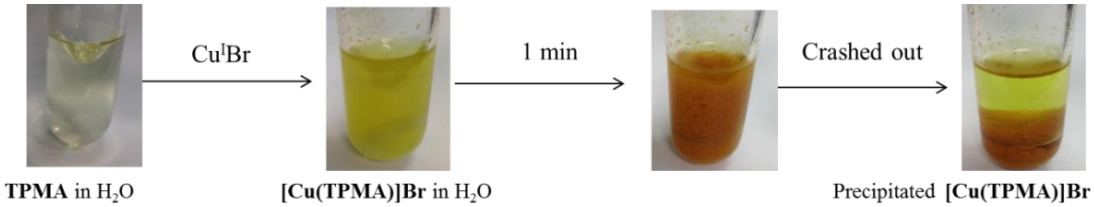

Figure 14. Visualization of the mixture of CuBr / TPMA in H_2O. Conditions: H_2O = 2 mL, [CuBr]:[TPMA] = [1]:[1] (CuBr = 0.1 mmol, TPMA = 0.1 mmol under nitrogen protection.

Thus, H_2O was replaced with MeOH as the feed solvent as it has been found to be the second best solvent for disproportionation. That said, the presence of TPMA should suppress, if not completely eliminate disproportionation. Although many different flow rates were utilised, uncontrolled polyacrylamides were obtained and a high molecular weight peak was always visible in the SEC (Figure 15), potentially arising from the large extent of termination events even at extremely low [CuBr]. Moreover, slow polymerisation rates were observed, suggesting that for acrylamides, under these conditions, the presence of Cu(0) is essential to establish equilibria required for a controlled polymerisation. However, in this study two variables were modified simultaneously, thus deviating from the initial polymerisation system, the solvent (from H_2O to H_2O/MeOH) and the ligand (from Me_6TREN to TPMA). For a more direct comparison strategy 2 was subsequently employed.

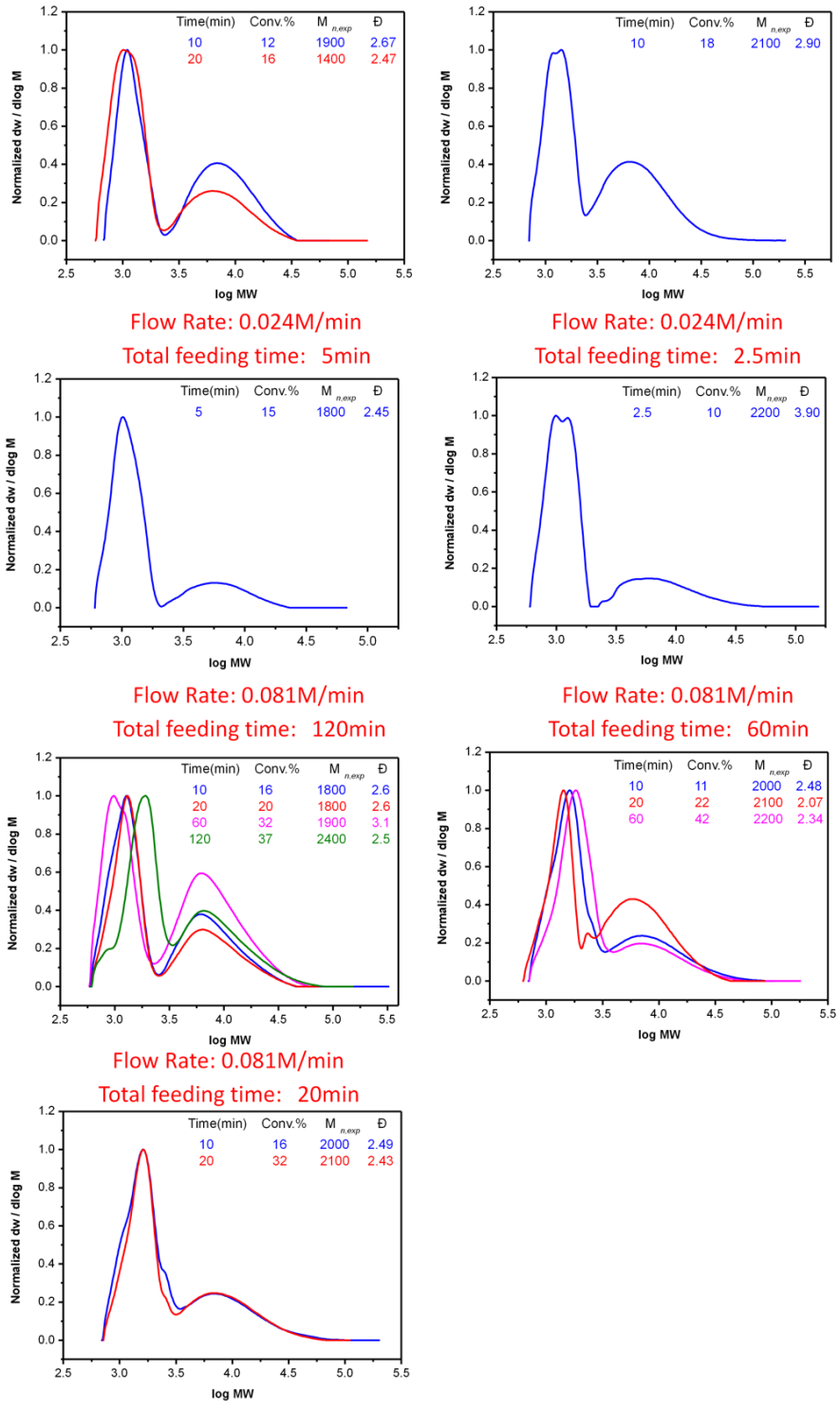

Figure 15. DMF SEC of PNIPAM *via* slow feeding with [Cu(TPMA)]Br protocol under different flow rate conditions at 0˚C. In the syringe, conditions: [CuBr]:[TPMA] = [1]:[1] with respect to initiator, in MeOH, at 22˚C. In Schlenk tube, conditions: [I]:[NIPAM]:[$CuBr_2$]:[ligand] = [1]:[20]:[0.05]:[0.05] at 0˚C.

Polymerisation of acrylamides with Me_6TREN in [MeCN]:[H_2O]=[26]:[74]

In the second strategy Me_6TREN was maintained as the ligand. However, [Cu(Me_6TREN)]Br had to be stabilised as both H_2O and MeOH result in rapid disproportionation. In order to circumvent this, MeCN was used as the feed solvent (Scheme 5, Figure 16).[21]

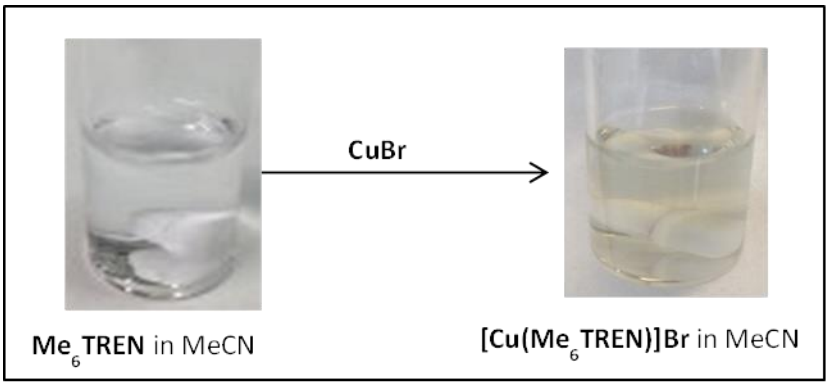

Figure 16. CuBr / Me_6TREN in MeCN. Conditions: MeCN = 2 mL, [CuBr]:[Me_6TREN] = [0.1]:[0.1] (CuBr = 0.1 mmol, Me_6TREN = 0.1 mmol and nitrogen protection.

Feeding a solution of [Cu(Me_6TREN)]Br ([MeCN]$_{final}$ = 26% *v/v*) allowed for the controlled polymerisation of NIPAM, reaching full conversion within 2 h while maintaining narrow molecular weight distributions (*Đ* ~ 1.09) (Table 3, Figure 17).

Table 3. Summary of different polymerisation protocols when NIPAM is employed as a model monomer and Me_6TREN as the ligand. Conditions for typical ATRP and SET-LRP: [I]:[NIPAM]:[CuBr]:[Me_6TREN] = [1]:[20]:[0.1]:[0.15]. Conditions for ATRP with $CuBr_2$: [I]:[NIPAM]:[CuBr]:[Me_6TREN]:[$CuBr_2$] = [1]:[20]:[0.05]:[0.15]:[0.05] at 0˚C. ($M_{n,th}$ = 2500g.mol^{-1}).

MeCN/H_2O (%*v/v*)	**Protocol**	**t (min)**	**Conv. (%)**	***M*$_{n,SEC}$ (g.mol^{-1})**	***Đ***

26/74	**Feeding**	60	80	4500	1.10
		120	100	5900	1.09
	Control feeding	60	60	3700	1.05
		120	81	4700	1.07
	Typical ATRP	60	81	4900	1.06
		120	100	6100	1.08
	SET-LRP	60	68	4400	1.06
		120	93	5800	1.09
	ATRP with $CuBr_2$	120	9	-	-
6/94	**Feeding**	60	93	5600	1.10
	Typical ATRP	15	99	7300	1.70
	SET-LRP	15	100	6300	1.08
	ATRP with $CuBr_2$	15	66	4400	1.08
0/100	**Typical ATRP**	15	99	5300	2.0
	SET-LRP	15	99	4700	1.08
	ATRP with $CuBr_2$	15	17	-	-

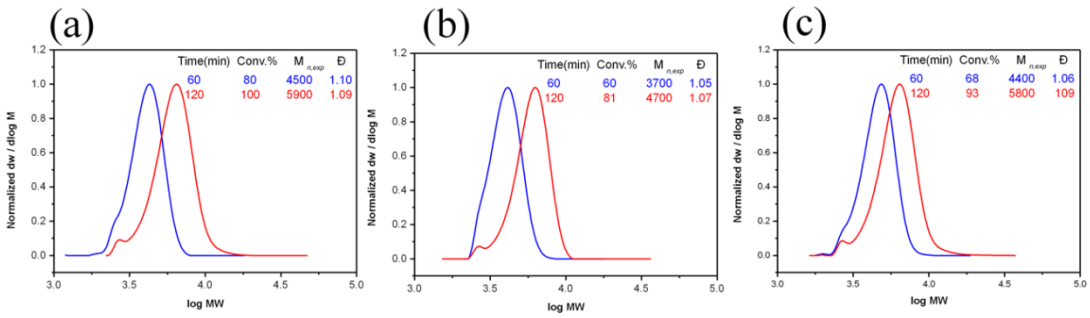

Figure 17. DMF SEC of PNIPAM (a) *via* slow feeding with [Cu(Me_6TREN)]Br in 3.3 mL H_2O + 1.2 mL MeCN system. In the syringe, conditions: [CuBr]:[Me_6TREN] = [0.1]:[0.1] with respect to initiator, in 1.2 mL MeCN, at 22˚C. In Schlenk tube, conditions: [I]:[NIPAM]:[$CuBr_2$]:[Me_6TREN] = [1]:[20]:[0.05]:[0.05], in 3.3 mL H_2O, (b) *via* control slow feeding with (c) *via* SET-LRP protocol, conditions: [I]:[NIPAM]:[CuBr]:[Me_6TREN] = [1]:[20]:[0.1]:[0.15] , in 3.3 mL H_2O + 1.2 mL MeCN system at 0 ˚C.

When the total amount of CuBr/Me_6TREN/MeCN was added directly into the reaction mixture without feeding (control feeding protocol), slower polymerisation rates were obtained (~ 80% in 2 h, *Đ* ~ 1.07) (Table 3, Figure 17). This could be attributed to one of two possible reasons. In the control experiment ([CuBr]:[$CuBr_2$] = [1]:[0.5]) all of the catalyst is injected as a mixture in a single addition, causing premature termination events at the beginning of the reaction and thus an accumulation of $CuBr_2$ which would slow the polymerisation rate. Alternatively, in the feed experiment, MeCN was slowly injected into the reaction mixture which would impose a detrimental effect on the polymerisation. A typical ATRP (1 eq. of CuBr relative to initiator) experiment in the absence of initial $CuBr_2$ was also performed. Due to the lack of deactivating species in the early stages of the polymerisation, an acceleration in the rate was observed reaching quantitative conversion in 2 h with a final dispersity of 1.08 (Table 3, Figure 18).

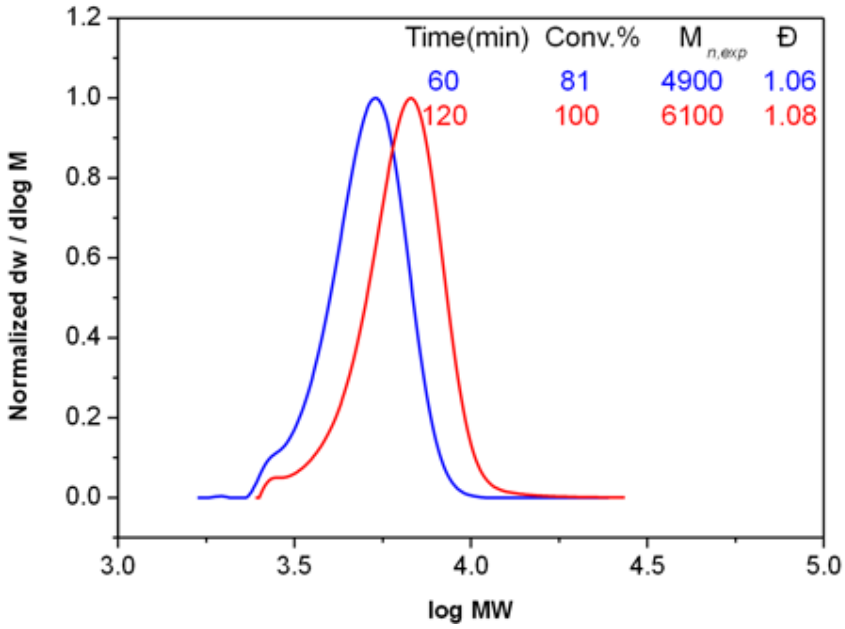

Figure 18. DMF SEC of PNIPAM *via* typical ATRP protocol, conditions: [I]:[NIPAM]:[CuBr]:[Me_6TREN] = [1]:[20]:[0.1]:[0.15] , in 3.3 mL H_2O + 1.2 mL MeCN system at 0 ˚C.

Thus, the polymerisation of acrylamides in organic mixtures (26% *v/v* MeCN in H_2O) can be successfully conducted under typical ATRP conditions. Interestingly, when an equal amount of CuBr was allowed to disproportionate in pure water prior to addition of monomer, initiator and MeCN ("SET-LRP protocol", Section 5.4.4, Scheme 10), a slighter slower polymerisation rate was detected, achieving 93% conversion in 2 h (Table 3, Figure 17c, Figure 19).

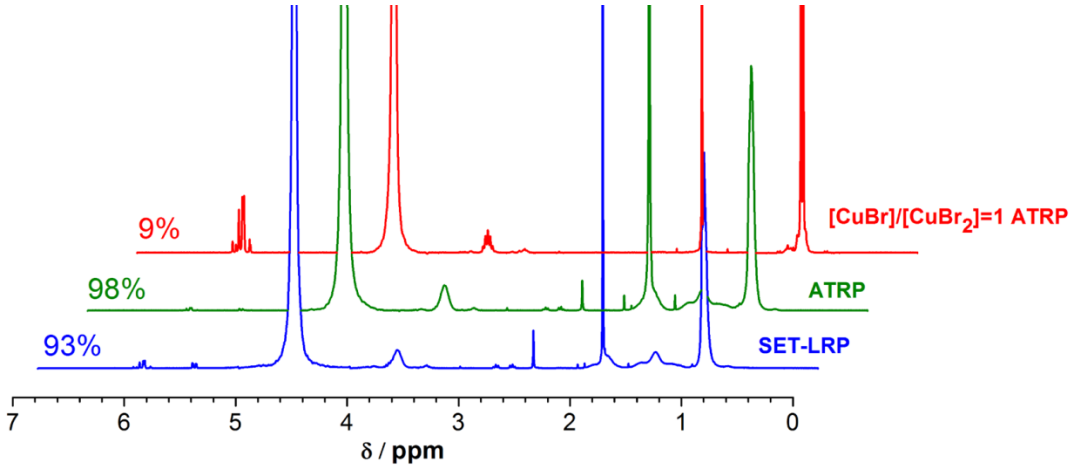

Figure 19. ^{1}H NMR spectra for PNIPAM catalyzed by three different protocols, Conditions for typical ATRP and SET-LRP: [I]:[NIPAM]:[CuBr]:[Me_6TREN] = [1]:[20]:[0.1]:[0.15]. Conditions for ATRP with $CuBr_2$: [I]:[NIPAM]:[CuBr]:[Me_6TREN]:[$CuBr_2$] = [1]:[20]:[0.05]:[0.15]:[0.05] in 3.3 mL H_2O +1.2 mL MeCN system at 0 ˚C.

However, it is noted that this is not an accurate comparison between the ATRP and the aqueous SET-LRP protocol, as the near quantitative disproportionation of CuBr (1 eq.) generates 0.5 eq. of activator Cu(0) and 0.5 eq. of $CuBr_2$, while in the typical ATRP protocol more activator is employed (1 eq. CuBr), in the absence of any deactivating species, which would compromise the polymerisation rate. For a more

reliable comparison, 0.5 eq. of CuBr and 0.5 eq. of $CuBr_2$ were employed (ATRP with $CuBr_2$ protocol) in an attempt to mimic the ratio between activator/deactivator in the SET-LRP protocol. Under the aforementioned conditions only 9% conversion was detected within 2 h (Table 3, Figure 19).

Interestingly, a higher amount of CuBr relative to $CuBr_2$ is required to successfully catalyse the polymerisation *via* a typical ATRP (CuBr) approach when an efficient amount of MeCN is present (see control protocol, where a higher ratio of CuBr/$CuBr_2$ was employed). Nevertheless, the *in situ* generated Cu(0) particles *via* the disproportionation of CuBr in H_2O proved to be a faster activator than CuBr, when comparable conditions (equal amount of activator/$CuBr_2$) were applied.

Polymerisation of acrylamides with Me_6TREN in [MeCN]:[H_2O]=[6]:[94]

Subsequently, the amount of MeCN was further minimized (6% *v/v* MeCN in H_2O), thus more closely resembling aqueous conditions. This small amount of MeCN is still required for the feeding experiment in order to avoid disproportionation of CuBr in the syringe. When 0.5 eq. of CuBr ($[MeCN]_{final}$ = 6% *v/v*) were slowly fed, 93% conversion was achieved within 60 min maintaining a narrow molecular weight distribution ($Đ \sim 1.1$) ("feeding protocol", Table 3, Figure 20).

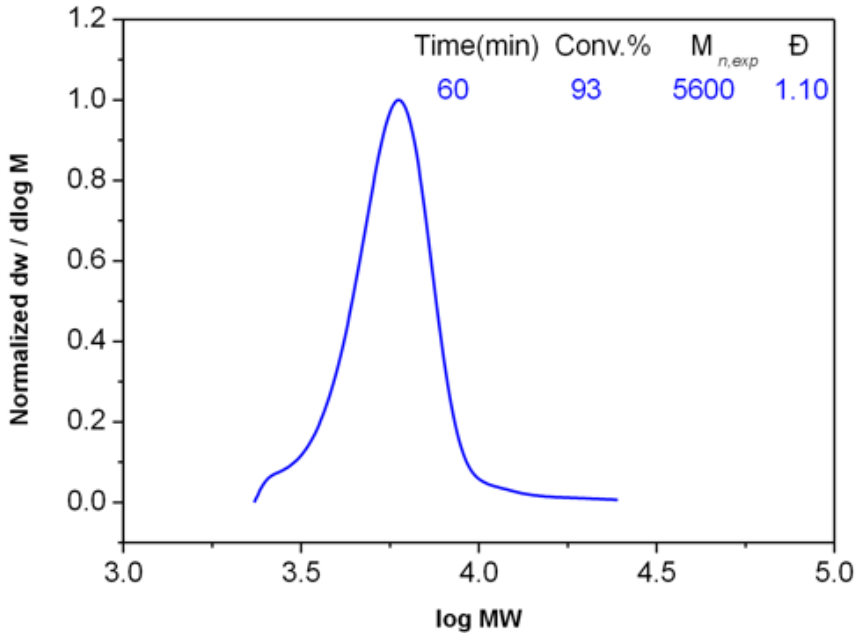

Figure 20. DMF SEC of PNIPAM *via* slow feeding with [Cu(Me_6TREN)]Br in 3.3 mL H_2O + 0.2 mL MeCN system at 0 ˚C. In the syringe, conditions: [CuBr]:[Me_6TREN] = [0.05]:[0.1] with respect to initiator, in 0.2 mL MeCN, at 22˚C. In Schlenk tube, conditions: [I]:[NIPAM]:[$CuBr_2$]:[Me_6TREN] = [1]:[20]:[0.05]:[0.05], in 3.3 mL H_2O at 0˚C.

Typical ATRP (0.5 eq. of CuBr) in the same reaction mixture (6% *v/v* MeCN in H_2O) resulted in quantitative conversion within 15 min, however, a broad molecular weight distribution was obtained (*Đ* ~ 1.7) (Table 3, Figure 21 a, 22). This is not unexpected given the higher aqueous content which would compromise deactivation. Conversely, the "SET-LRP protocol", exploiting the rapid disproportionation prior to addition of monomer, initiator and MeCN, gave 100% conversion (Table 3, Figure 21b, 22) within 15 min with dispersity = 1.08. Since Cu(0) gave optimum results in the presence of 0.5 eq. of deactivator, ATRP should also be conducted in the presence of the same amount of $CuBr_2$.

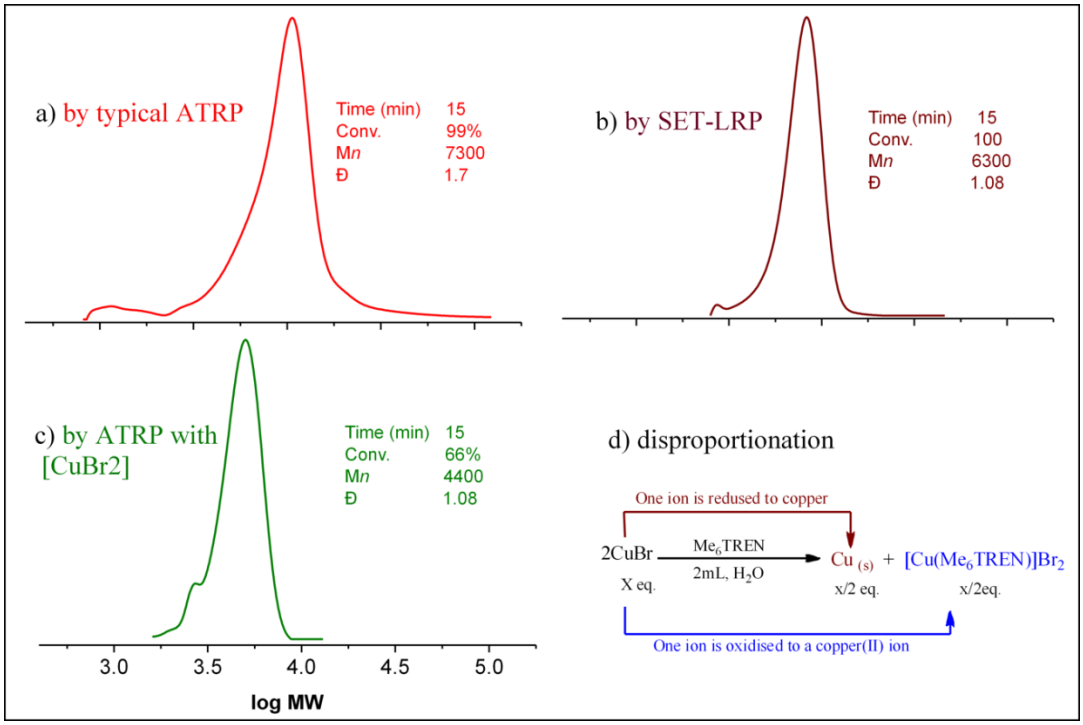

Figure 21. A comparison of different protocols for NIPAM Polymerisation (DP = 20) in the system 6% *v/v* MeCN in H_2O at 0 ˚C. a) Disproportionation of CuBr. Conditions for, b) SET-LRP and c) typical ATRP: [I]:[NIPAM]:[CuBr]:[Me_6TREN] = [1]:[20]:[0.1]:[0.15] at 0˚C and d) ATRP with $CuBr_2$: [I]:[NIPAM]:[CuBr]:[Me_6TREN]:[$CuBr_2$] = [1]:[20]:[0.05]:[0.15]:[0.05] at 0˚C. ($M_{n,th}$ = 2500 g.mol^{-1}).

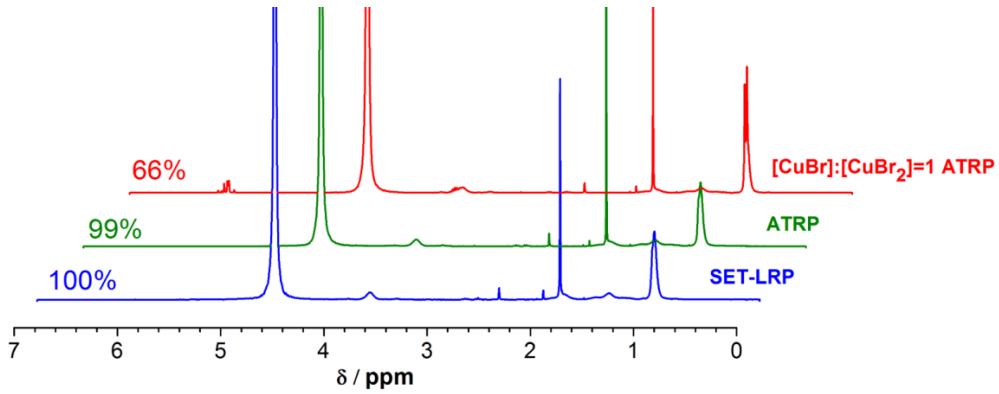

Figure 22. ^{1}H NMR spectra for PNIPAM catalyzed by three different protocols, Conditions for typical ATRP and SET-LRP: [I]:[NIPAM]:[CuBr]:[Me_6TREN] = [1]:[20]:[0.1]:[0.15] at 0˚C. Conditions for ATRP with $CuBr_2$:

[I]:[NIPAM]:[CuBr]:[Me_6TREN]:[$CuBr_2$] = [1]:[20]:[0.05]:[0.15]:[0.05] at 0˚C, in 3.3 mL H_2O + 0.2 mL MeCN system at 0˚C.

When a ratio of [CuBr]:[$CuBr_2$] = [0.5]:[0.5], ("ATRP with $CuBr_2$ protocol") was employed, only 66% conversion (Table 3, Figure 21c, 22) was detected by ^{1}H NMR. However, the control over the molecular weight distributions was significantly improved (*Đ* ~ 1.08, Table 3). Nevertheless, the "SET-LRP protocol" ([Cu(0)]:[$CuBr_2$] = [0.5]:[0.5]) appeared again faster than the ATRP protocol [CuBr]:[$CuBr_2$] = [0.5]:[0.5], when identical conditions were compared. Thus, the role of Cu(0) under almost aqueous conditions (6% *v/v* MeCN in H_2O) is significant and cannot be attributed to only supplemental activation.

Polymerisation of acrylamides with Me_6TREN in pure H_2O

Finally, a comparison of the three protocols in pure H_2O was carried out. As mentioned earlier, feeding in H_2O could not be feasible due to the high disproportionation constant under the studied conditions. Typical ATRP (1 eq. of CuBr) in H_2O gave rise to quantitative conversion within 15 min and a dispersity = 2 (Table 3, Figure 23a).

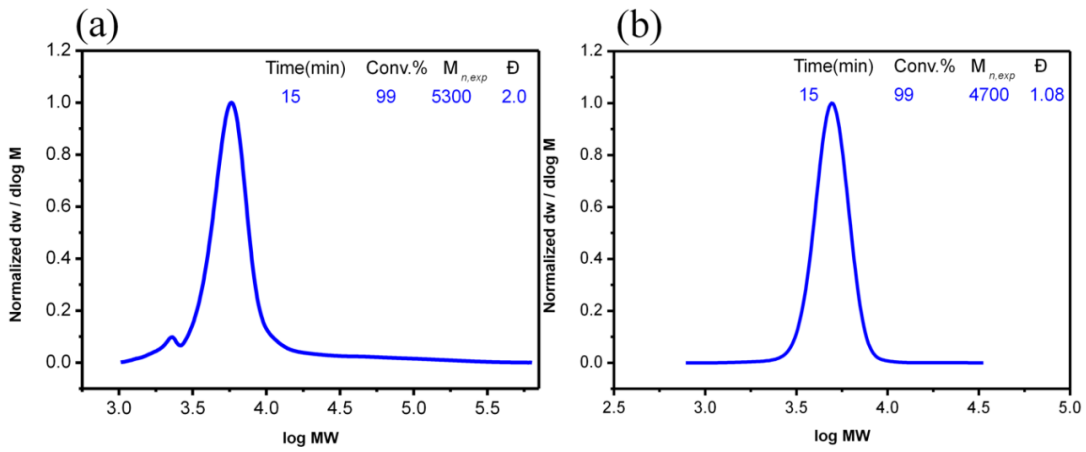

Figure 23. DMF SEC of PNIPAM *via* typical ATRP protocol (a), (b) SET-LRP protocol. Conditions: [I]:[NIPAM]:[CuBr]:[Me_6TREN] = [1]:[20]:[0.1]:[0.15], in 4.5 mLH_2O at 0˚C.

This is not surprising given the lack of deactivating species. Similarly, when only Cu(0) (1 eq.), obtained *via* the pre-disproportionation of CuBr, was utilised in the absence of deactivating species broad molecular weight distributions were also reported,[6] suggesting that the presence of $CuBr_2$ is required for a controlled polymerisation. On the contrary, when 1 eq. of CuBr was allowed to pre-disproportionate in H_2O ("SET-LRP protocol", 0.5 eq. of Cu(0) and 0.5 eq. of $CuBr_2$), 99% of conversion was attained within 15 min with dispersity = 1.08 (Table 3, Figure 23b).

Replacing 0.5 eq. of Cu(0) with 0.5 eq. of CuBr in the aforementioned protocol ("ATRP with $CuBr_2$ protocol", [CuBr]:[$CuBr_2$] = [0.5]:[0.5]) gave rise to inconsistent results (Table 3, Figure 24). These inconsistencies were attributed to competing reactions that occur under the polymerisation of acrylamides in aqueous solutions. Thus, pre-disproportionation of CuBr (SET-LRP) should be the protocol

of choice for the aqueous controlled polymerisation of acrylamides as this technique is versatile regardless of the solvent mixtures used.[43]

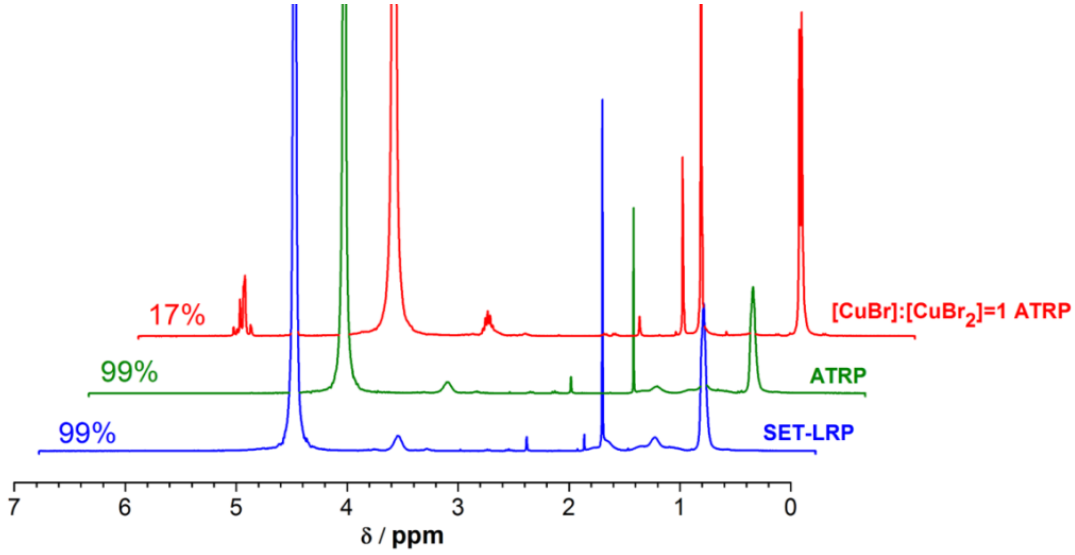

Figure 24. ^{1}H NMR spectra for PNIPAM catalyzed by three different protocols. Conditions for typical ATRP and SET-LRP: [I]:[NIPAM]:[CuBr]:[Me_6TREN] = [1]:[20]:[0.1]:[0.15] at 0˚C. Conditions for ATRP with $CuBr_2$: [I]:[NIPAM]:[CuBr]:[Me_6TREN]:[$CuBr_2$] = [1]:[20]:[0.05]:[0.15]:[0.05] at 0˚C, in 4.5 mL H_2O system at 0 ˚C. (For the ATRP with [$CuBr_2$] protocol ([CuBr]:[$CuBr_2$]=1 ATRP) most of the times conversion was low, as this was the result that we got most of the times).

Polymerisation of acrylates with TPMA

Since acrylates have both different k_p values and complex binding constants to copper, slow feeding of CuBr/TPMA/MeOH in a $CuBr_2$/$PEGA_{480}$/H_2O/initiator solution was carried out (Table 4), (Section 5.4.3, Scheme 6 “feeding protocol”,) which resulted in well-controlled polyacrylates with 60% conversion within 2 h ($Đ$ ~ 1.09) (Figure 25a). Interestingly, no major difference was detected between the

typical ATRP and the SET-LRP protocol and ~ 45% conversion (Table 4, Figure 25c,d) was attained in both cases within 2 h. This is not surprising given that TPMA does not facilitate disproportionation by stabilising CuBr and thus it is reasonable that the disproportionation protocol will resemble the classical ATRP polymerisation. When more deactivator was added ("ATRP with $CuBr_2$ protocol", [CuBr]:[$CuBr_2$] = [0.5]:[0.5]) slightly lower conversions were attained (Table 4, Figure 25b), as expected, due to the presence of $CuBr_2$. Thus, when a non-disproportionating ligand is utilised minimal differences are observed between the protocols.

Table 4. Summary of different polymerisation protocols when $PEGA_{480}$ is employed as a model monomer and TPMA as the ligand Conditions for typical ATRP and SET-LRP: [I]:[$PEGA_{480}$]:[CuBr]:[TPMA] = [1]:[10]:[0.1]:[0.15] at 0˚C. Conditions for ATRP with $CuBr_2$: [I]:[$PEGA_{480}$]:[CuBr]:[TPMA]:[$CuBr_2$] = [1]:[10]:[0.05]:[0.15]:[0.05] at 0˚C. ($M_{n,th}$ = 5068g.mol^{-1}).

Protocol	**t (min)**	**Conv. (%)**	$M_{n,SEC}$ **(g.mol^{-1})**	$Đ$
Feeding	120	60	6800	1.09
Control feeding	120	34	4300	1.10
Typical ATRP	120	44	5900	1.08
SET-LRP	120	46	6000	1.09
ATRP with $CuBr_2$	120	37	4400	1.13

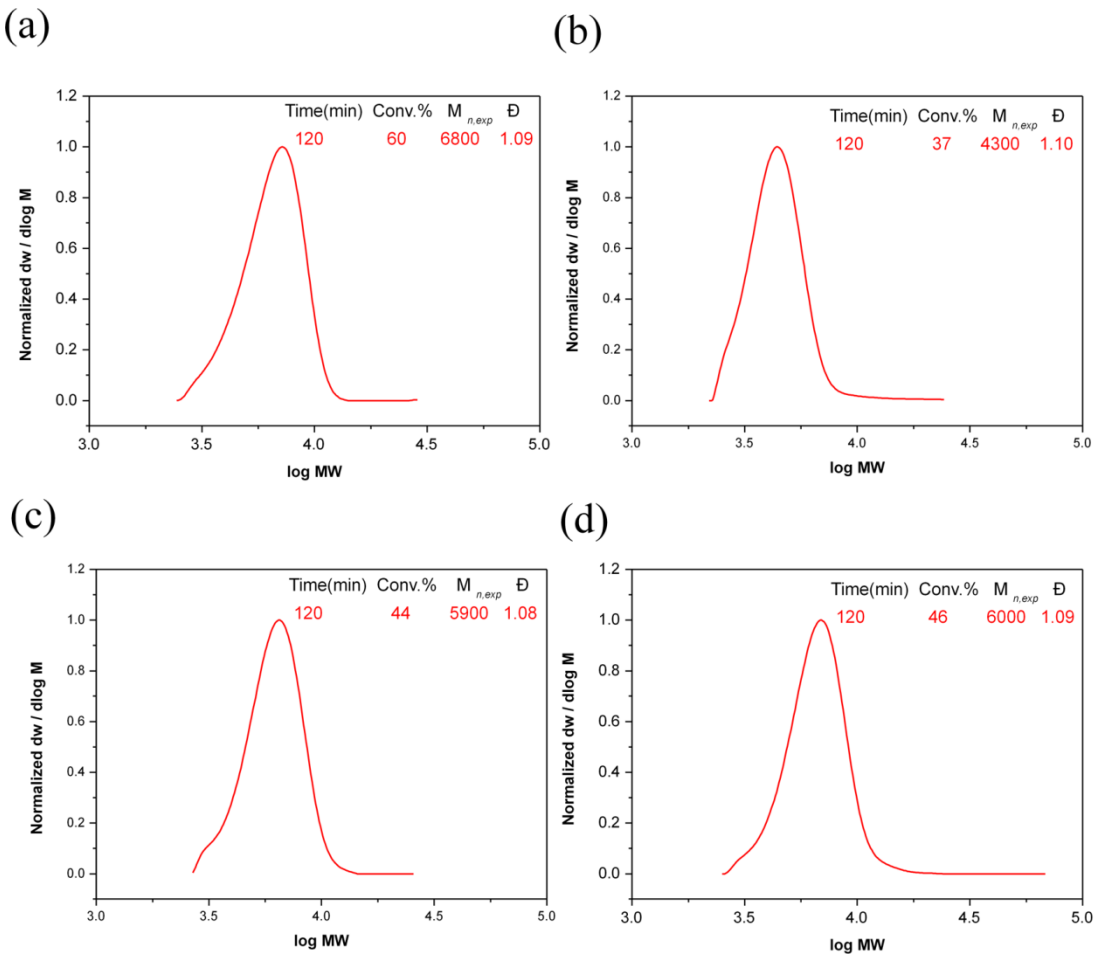

Figure 25. DMF SEC of $PEGA_{480}$ (a) *via* slow feeding with [Cu(TPMA)]Br protocol. In the syringe, conditions: [CuBr]:[TPMA] = [0.1]:[0.1] with respect to initiator, in 1.2 mL MeOH. In Schlenk tube, conditions: [I]:[$PEGA_{480}$]:[$CuBr_2$]:[TPMA] = [1]:[10]:[0.05]:[0.05], in 3.3 mL H_2O. (b) *via* ATRP with [$CuBr_2$] protocol, (c) *via* typical ATRP protocol (d) via SET-LRP protocol. Conditions: [I] : [$PEGA_{480}$] : [CuBr] : [TPMA] : [$CuBr_2$] = [1]:[10]:[0.05]:[0.15]:[0.05] at 0 ˚C.

Polymerisation of acrylates with Me_6TREN in 26% MeCN/74% H_2O

Subsequently, the 2nd strategy was applied for the polymerisation of $PEGA_{480}$ (Section 5.5, Scheme 5.5), where a mixture of CuBr/Me_6TREN/MeCN ($[MeCN]_{final}$ = 26% *v/v*) was gradually injected in the reaction mixture ("feeding protocol",

$CuBr_2$, Me_6TREN, $PEGA_{480}$, initiator, H_2O (74% *v/v*)) 92% conversion was attained within 2 h while maintaining narrow molecular weight distributions (*Đ* ~ 1.11), while the "control feeding protocol" gave rise to 59% conversion in the same timescale (Table 5, Figure 26).

Table 5. Summary of different polymerisation protocols when $PEGA_{480}$ is employed as a model monomer. Conditions for typical ATRP and SET-LRP: [I]:[$PEGA_{480}$]:[CuBr]:[Me_6TREN] = [1]:[10]:[0.1]:[0.15] at 0˚C. Conditions for ATRP with $CuBr_2$: [I] : [$PEGA_{480}$] : [CuBr] : [Me_6TREN] : [$CuBr_2$] = [1]:[10]:[0.05]:[0.15]:[0.05] at 0˚C. ($M_{n,th}$ = 5068 g.mol^{-1}).

Organic/$H_2$0 (%*v/v*)	**Protocol**	**t (min)**	**Conv. (%)**	$M_{n,SEC}$ **(g.mol^{-1})**	***Đ***
[MeCN]:[H_2O] 26/74	**Feeding**	60	56	6100	1.10
		120	92	7700	1.11
	Control feeding	60	54	5700	1.16
		120	59	5900	1.16
	Typical ATRP	60	90	8800	1.12
		120	92	8900	1.17
	SET-LRP	60	68	6300	1.10
		120	75	6600	1.10
	ATRP with $CuBr_2$	120	5	-	-
[MeCN]:[H_2O] 6/94	**Feeding**	60	7	-	-
	Typical ATRP	15	99	8500	1.90
	SET-LRP	15	99	8900	1.08
	ATRP with $CuBr_2$	15	77	5400	1.09
0/100	**Typical ATRP**	15	99	10000	4.0
	SET-LRP	15	100	7900	1.12
	ATRP with $CuBr_2$	15	99	6800	1.20
[MeOH]:[H_2O] 26/74	**Typical ATRP**	15	98	7800	1.15
	SET-LRP	15	99	8000	1.04
	ATRP with $CuBr_2$	15	92	6900	1.09
		30	98	7200	1.08

The typical ATRP protocol (only CuBr) was also conducted yielding 92% conversion within 2 h and low dispersity (*Đ* ~ 1.12) (Table 5, Figure 26). Thus, in the presence of relatively high amounts of MeCN (26% *v/v* MeCN in H_2O), no $CuBr_2$ (either external or *in situ* generated) is required to invoke control over the MWDs.

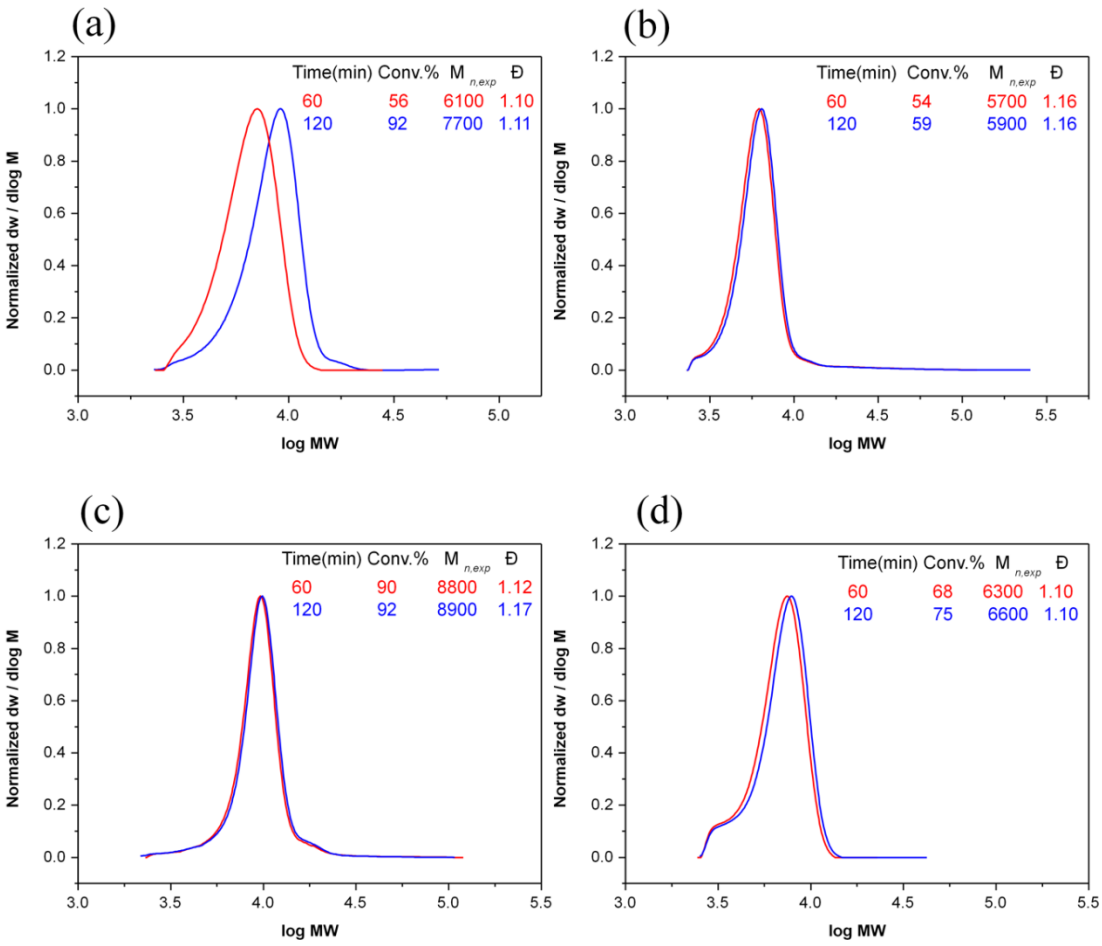

Figure 26. DMF SEC of $PEGA_{480}$ (a) *via* slow feeding with [Cu(Me_6TREN)]Br protocol. In the syringe, conditions: [CuBr]:[Me_6TREN] = [0.1]:[0.1] with respect to initiator, in 1.2 mL MeCN, at 22˚C. In Schlenk tube, conditions: [I]:[$PEGA_{480}$]:[$CuBr_2$]:[TPMA] = [1]:[10]:[0.05]:[0.05], in 3.3 mL H_2O, (b) *via* control slow feeding. (c) *via* typical ATRP protocol. (d) *via* SET-LRP protocol, conditions: [I]:[$PEGA_{480}$]:[CuBr]:[Me_6TREN] = [1]:[10]:[0.1]:[0.15] , in 3.3 mL H_2O + 1.2 mL MeCN system at 0˚C.

Interestingly, following the "SET-LRP protocol", where the disproportionation was performed in pure H_2O prior to addition of MeCN, initiator and monomer, 68% and 75% conversion was attained in 1 and 2 h respectively (Table 5, Figure 26d, 27), suggesting slower polymerisation rates under the selected conditions as opposed to typical ATRP. In the former case, complete visual consumption of the *in situ* generated Cu(0) particles was observed within 1 h (Section 5.4.4, Figure 35), suggesting that [Cu(Me_6TREN)]Br is stabilized under these conditions and/or large extent of termination events. However, when an equal amount of activator/deactivator was employed ("ATRP with $CuBr_2$ protocol, [CuBr]:[$CuBr_2$] = [0.5]:[0.5])), only 5% conversion within 2 h was observed (Table 5, Figure 27), suggesting that in this solvent composition (26% *v/v* MeCN in H_2O) and when stoichiometric amounts of CuBr and $CuBr_2$ are utilised, the polymerisation rate is dramatically reduced. Thus, this comparison (SET-LRP with [Cu(0)]:[$CuBr_2$] = [0.5]:[0.5] *vs* ATRP with [CuBr]:[$CuBr_2$] = [0.5]:[0.5]) revealed faster polymerisation rates when the disproportionation of CuBr/Me_6TREN and subsequently the *in situ* generation of Cu(0) particles was exploited.

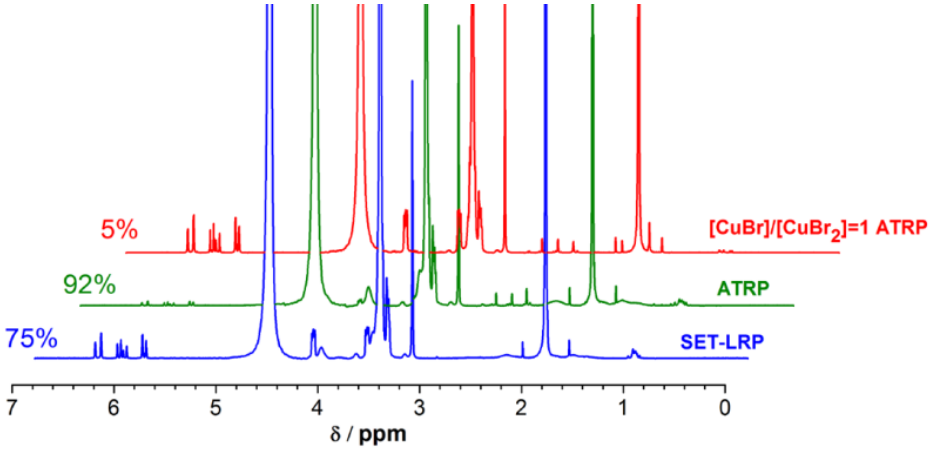

Figure 27. ^{1}H NMR spectra for $PEGA_{480}$ catalyzed by three different protocols. Conditions for typical ATRP and SET-LRP: [I]:[$PEGA_{480}$]:[CuBr]:[Me_6TREN] = [1]:[10]:[0.1]:[0.15] at 0˚C. Conditions for ATRP with $CuBr_2$: [I]:[$PEGA_{480}$]:[CuBr]:[Me_6TREN]:[$CuBr_2$] = [1]:[10]:[0.05]:[0.15]:[0.05], in 3.3 mL H_2O + 1.2 mL MeCN system at 0 ˚C.

Polymerisation of acrylates with Me_6TREN in 6% MeCN/94% H_2O

The lowest content of MeCN was subsequently selected (6% *v/v* MeCN in H_2O) for the feeding of [Cu(Me_6TREN)]Br into the reaction mixture, as this solvent composition gives similar reaction characteristics to the aqueous system. Surprisingly, only 7% of conversion was obtained within 1 h ("feeding protocol", Table 5), indicating that the slow introduction of CuBr under these conditions was not beneficial for the polymerisation and/or that CuBr is unable to catalyse the polymerisation in the presence of a high concentration of deactivating species ($CuBr_2$). A strict comparison of the SET-LRP and ATRP protocol was also conducted, resulting in 99% ("SET-LRP protocol", Table 5, [Cu(0)]:[$CuBr_2$] = [0.5]:[0.5]) and 77% conversion ("ATRP with $CuBr_2$ protocol", [CuBr]:[$CuBr_2$] = [0.5]:[0.5]) (Table 5, Figure 28, 29) respectively and narrow MWDs within 15 min. Thus, when Cu(0) was generated *in situ via* the disproportionation of

[Cu(Me_6TREN)]Br in H_2O, faster polymerisation rates were achieved, suggesting that the role of Cu(0) is a major or a co-activator under these conditions. The typical ATRP protocol (only CuBr), resulted in broad molecular weight distributions (*Đ* ~ 1.9) (Table 5, Figure 28b, 29) which was attributed to the low content of organic solvent.

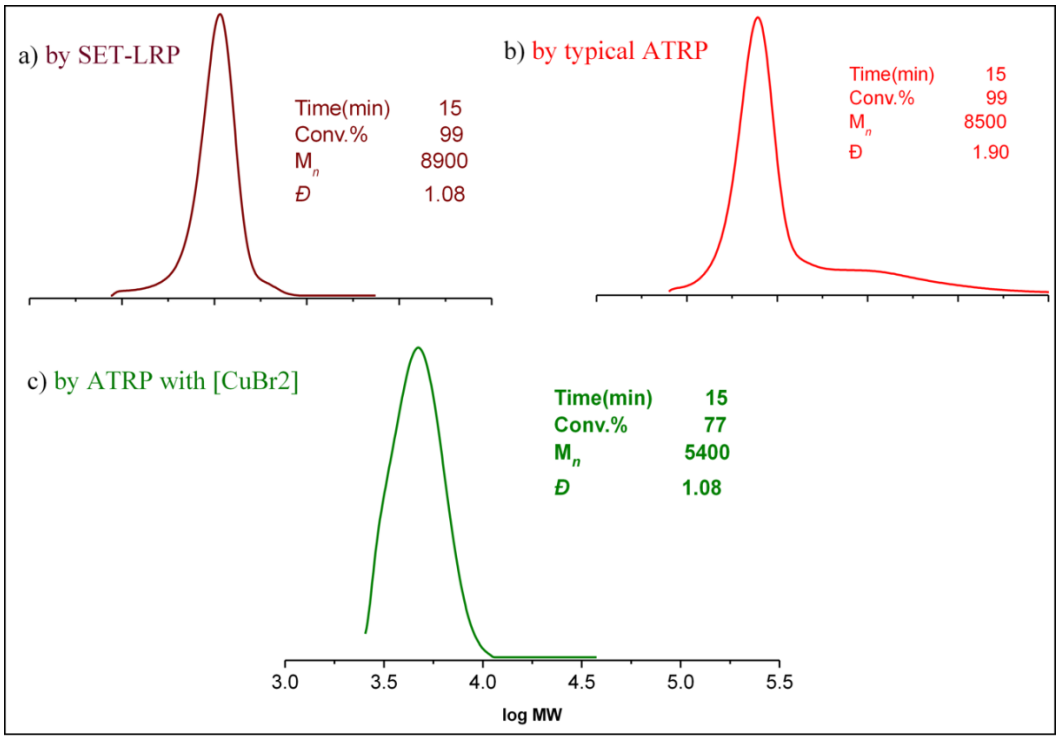

Figure 28. A comparison of different protocols of $PEGA_{480}$ Polymerisation (DP = 10) in the system 6% *v/v* MeCN in H_2O at 0˚C. Conditions for typical ATRP and SET-LRP: [I]:[$PEGA_{480}$]:[CuBr]:[Me_6TREN] = [1]:[10]:[0.1]:[0.15] at 0˚C. Conditions for ATRP with $CuBr_2$: [I]:[$PEGA_{480}$]:[CuBr]:[Me_6TREN]:[$CuBr_2$] = [1]:[10]:[0.05]:[0.15]:[0.05] at 0˚C. ($M_{n,th}$ = 5068 g.mol^{-1}).

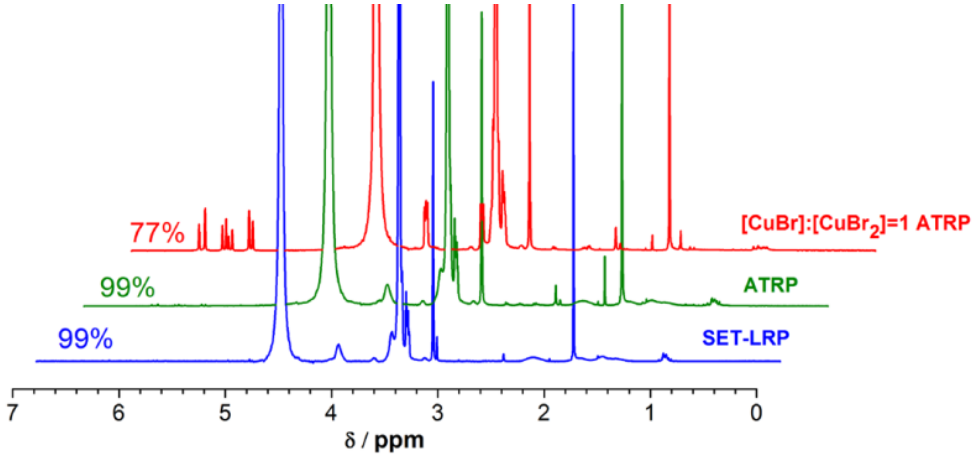

Figure 29. ^{1}H NMR spectra for $PEGA_{480}$ catalyzed by three different protocols. Conditions for typical ATRP and SET-LRP: [I]:[$PEGA_{480}$]:[CuBr]:[Me_6TREN] = [1]:[10]:[0.1]:[0.15] at 0˚C. Conditions for ATRP with $CuBr_2$: [I]:[$PEGA_{480}$]:[CuBr]:[Me_6TREN]:[$CuBr_2$] = [1]:[10]:[0.05]:[0.15]:[0.05], in 3.3 mL H_2O + 0.2 mL MeCN system at 0˚C.

Effect of MeCN on SET-LRP

The previous experiments suggest that the use of MeCH has a detrimental effect on the polymerisation rate when the SET-LRP protocol was applied. In order to verify this, SET-LRP with different ratios of MeCN/H_2O was conducted. Regardless of the amount of MeCN, the disproportionation of [Cu(Me_6TREN)]Br was allowed to occur in pure H_2O in all cases. As demonstrated earlier, polymerisations in (26% *v/v* MeCN in H_2O) resulted in 34% conversion within 1 h while when lower concentrations of MeCN were selected (11% *v/v* MeCN in H_2O), an acceleration of the rate of the polymerisation was observed with 77% attained within 1 h (Figure 30a).

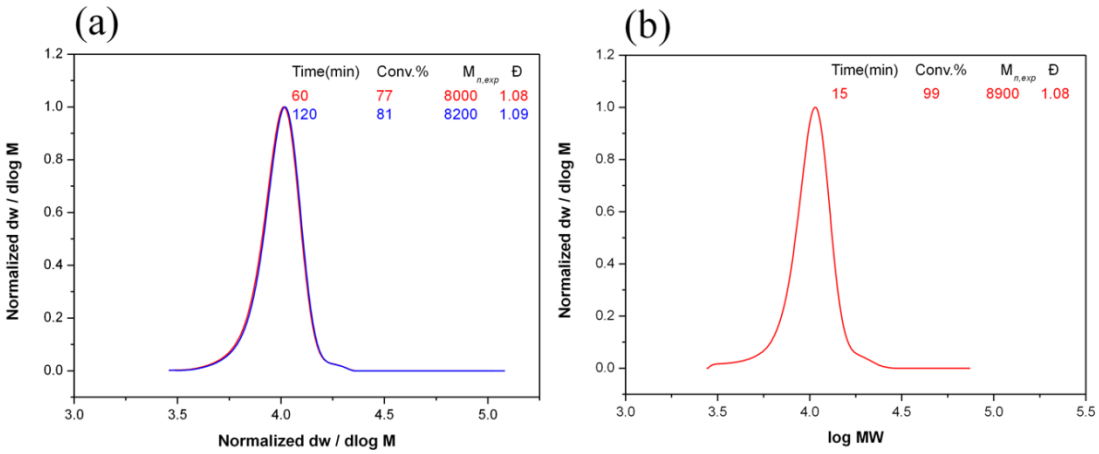

Figure 30. DMF SEC of $PEGA_{480}$ *via* SET-LRP protocol, conditions: [I]:[$PEGA_{480}$]:[CuBr]:[Me_6TREN] = [1]:[10]:[0.1]:[0.15], in (3.3 mL H_2O + (a) 0.4 mL or (b) 0.2 mL MeCN) system at 0˚C.

Interestingly, when the amount of MeCN was lowered, (6% *v/v* MeCN in H_2O) quantitative conversion was achieved within 15 min (Figure 30b), and thus resembling the rate of the aqueous polymerisations. It should be noted that narrow MWDs were obtained in all cases. Thus, MeCN acts as a polymerisation retarder but not as an inhibitor.

Polymerisation of acrylates with Me_6TREN in pure H_2O

In the absence of MeCN (pure H_2O) an interesting phenomenon occurred with the "SET-LRP protocol" giving 99% conversion in 15 min, as expected, and narrow MWDs (Đ ~ 1.12) (Table 5, Figure 31a). Interestingly, when stoichiometric amounts of CuBr and $CuBr_2$ ("ATRP with $CuBr_2$ protocol [CuBr]:[$CuBr_2$] = [0.5]:[0.5]) were employed, 99% conversion was also attained within 15 min (*Đ* ~ 1.2) (Table 5, Figure 31b), suggesting that under purely aqueous conditions, both Cu(0) and CuBr

can efficiently mediate the controlled polymerisation of poly(acrylates) in the presence of a stoichiometric amount of $CuBr_2$.

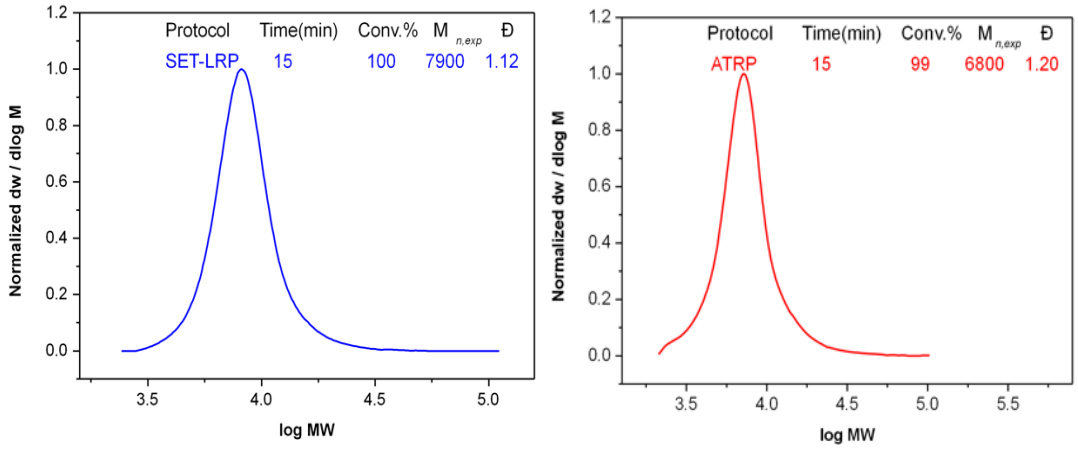

Figure 31. DMF SEC of $PEGA_{480}$ a) *via* SET-LRP protocol, b) ATRP with [$CuBr_2$] protocol conditions: [I]:[$PEGA_{480}$]:[CuBr]:[Me_6TREN] = [1]:[10]:[0.1]:[0.15], in 4.5 mL H_2O at 0˚C.

Thus, it is shown that aqueous ATRP ("ATRP with $CuBr_2$ protocol") for acrylates can occur with rapid polymerisation rates, achieving full monomer conversion and narrow molecular weight distributions within minutes. It is noted, that even a small amount of MeCN can dramatically affect the polymerisations kinetics, potentially due to the dual role of MeCN as a solvent and as a coordinating ligand that stabilizes the copper(I) species. In the absence of any deactivator (typical ATRP protocol, only CuBr) ATRP resulted in broad molecular weight distributions ($Đ$ ~ 4) (Table 5, Figure 32).

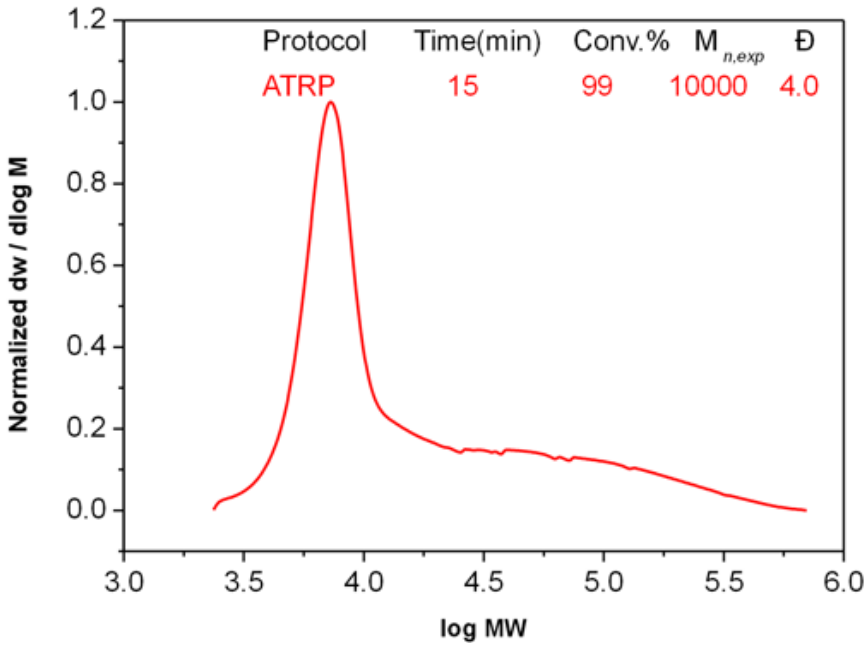

Figure 32. DMF SEC of $PEGA_{480}$ *via* typical ATRP protocol conditions: [I]:[$PEGA_{480}$]:[CuBr]:[Me_6TREN] = [1]:[10]:[0.1]:[0.15], in 4.5 mL H_2O at 0˚C.

Polymerisation of acrylates with Me_6TREN in [MeOH]:[H_2O]=[26]:[74]

Finally, to demonstrate the unique nature of MeCN as a coordinating ligand, MeCN were replaced with MeOH (26% *v/v* in H_2O). Under these conditions, both SET-LRP ([Cu(0)]:[$CuBr_2$] = [0.5]:[0.5]) and ATRP with $CuBr_2$ protocol ([CuBr]:[$CuBr_2$] = [0.5]:[0.5]) resulted in near identical results (near quantitative conversion within 30 min) with Cu(0) demonstrating slightly faster polymerisation rates (Table 5, Figure 33a). Moreover, the high content of alcohol allows for typical ATRP (only CuBr) to be conducted in the absence of deactivating species ($CuBr_2$) (Table 5, Figure 33b).

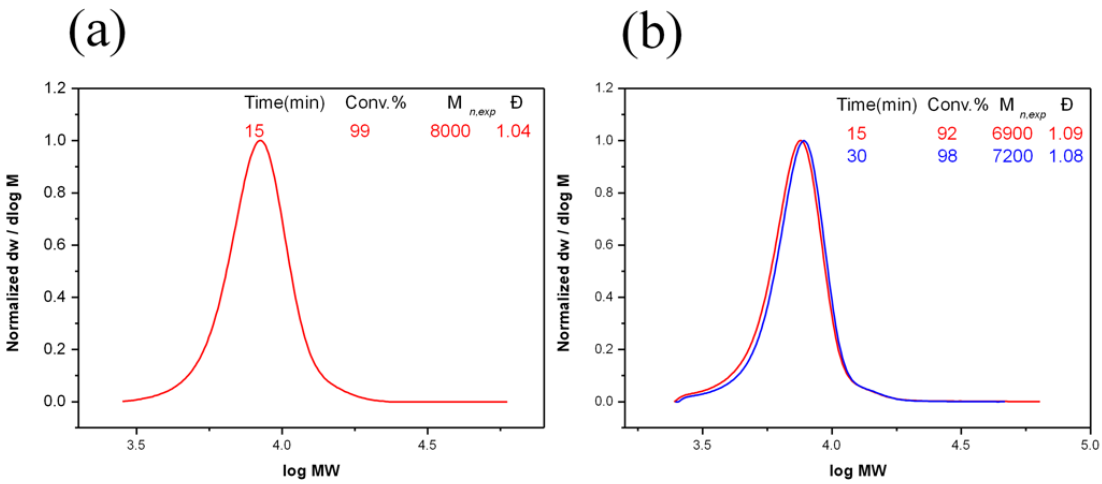

Figure 33. DMF SEC of $PEGA_{480}$ (a) *via* SET-LRP protocol conditions: [I]:[$PEGA_{480}$]:[CuBr]:[Me_6TREN] = [1]:[10]:[0.1]:[0.15] , in (3.3 mL H_2O + 1.2 mL MeOH). (b) *via* ATRP with [$CuBr_2$] protocol, conditions: [I]:[$PEGA_{480}$]:[CuBr]:[Me_6TREN]:[$CuBr_2$] = [1]:[10]:[0.05]:[0.15]:[0.05], in (3.3 mL H_2O +1.2 mL MeOH) at 0˚C.

5.3 Conclusions

In this chapter, the mechanism of copper mediated RPRD of acrylates and acrylamides in the presence of Cu(0) wire and/or Cu(0) particles has been studied in aqueous and aqueous/organic media. Disproportionation and comproportionation equilibria were determined and found to be strongly affected by the nature of the solvent and the monomer, and the type (disproportionating or non-disproportionating) and concentration of the ligand employed. In pure water, there is a large thermodynamic driving force for the disproportionation of CuBr in the presence of *N*-containing ligands, which is near-quantitative (~99%). Variation of the [ligand] did not affect the thermodynamic equilibrium as long as there is sufficient ligand present to solubilise the copper species while even in the presence of PEGA the disproportionation remained as high as 96%. No comproportionation, even in the presence of monomer, was detected within 15 min, which is the

timescale of the polymerisations. Aqueous mixtures (up to 50% organic content) were also effective (> 95% disproportionation), but the rate and extent of disproportionation in non-aqueous solvents is dramatically reduced. The sequence of the reagent addition was also studied and proved to be crucial for the control over the MWDs, potentially due to competitive complexation of the reagents (monomer, solvent, ligand, copper species). It was found that optimum polymerisation rates and control are obtained when disproportionation occurs in the absence of monomer. In addition, slowly feeding of the reaction mixture with low concentrations of CuBr was also conducted, utilizing both TPMA and Me_6TREN, in an effort to resemble the role of Cu(0), highlighting that the presence of Cu(0) is essential to establish equilibria required for a well-controlled polymerisation. Importantly, a direct comparison between the SET-LRP and the ATRP protocols was also performed, where the ratio between activator Cu(0) or CuBr and deactivator ($CuBr_2$) was matched, revealing the contribution of each catalyst to the overall mechanism and kinetics. For acrylates, it was shown that both Cu(0) and CuBr can equally contribute to an effective polymerisation, while for the case of acrylamides, the role of Cu(0) is significant and should not be neglected when evaluating the reaction mechanism.

5.4 Experimental

5.4.1 Materials and methods

All chemicals were purchased from Sigma-Aldrich or Fischer Scientific unless otherwise stated. *N*-Isopropylacrylamide (NIPAM, 97%) was purified by recrystallization from hexane to remove the inhibitor. All monomers were passed through a basic alumina column prior to use. The water soluble initiator (WSI) 2, 3-dihydroxypropyl 2-bromo-2-methylpropanoate was prepared as reported in the literature[55]. *Tris*(2-(dimethylamino)ethyl)amine (Me_6TREN) was synthesized according to literature procedures and stored under nitrogen prior to use[56]. Copper(I) bromide (CuBr), was sequentially washed with acetic acid and ethanol and dried under vacuum. Copper wire (diameter = 0.25 mm) was pre-treated by washing in hydrochloric acid or hydrazine for 30 min and rinsed thoroughly with MiliQ water, dried under nitrogen and used immediately.

5.4.2 Instrumentation

Proton Nuclear Magnetic Resonance (^{1}H NMR) spectra were recorded on Bruker DPX-300 and DPX-400 spectrometers using deuterated solvents obtained from Aldrich. Size-exclusion chromatography (SEC) was conducted on Varian 390-LC system using DMF as the mobile phase (5 mM NH_4BF_4) at 50 ˚C, equipped with refractive index, UV and viscometry detectors, 2 × PLgel 5 mm mixed-D columns (300 × 7.5 mm), 1 × PLgel 5 mm guard column (50 × 7.5 mm) and autosampler. And another SEC measurements were conducted using an Agilent 1260 GPC-MDS fitted with differential refractive index (DRI), light scattering (LS) and viscometry (VS) detectors equipped with 2 × PLgel 5 mm mixed-D columns (300 × 7.5 mm), 1

× PLgel 5 mm guard column (50 × 7.5 mm) and autosampler. Commercial narrow linear poly(methyl methacrylate) standards in range of 200 to 1.0 × 10^6 g · mol^{-1} were used to calibrate the systems. All samples were passed through 0.45 μm PTFE filter before analysis. UV/Vis spectra were recorded on Agilent Technologies Cary 60 UV-Vis in the range of 200-1100 nm using a cuvette with 10 mm optical length.

All reactions were carried out under an inert atmosphere of oxygen-free nitrogen, using standard Schlenk techniques.

5.4.3 General procedures

General procedure for the extent of disproportionation (disp.) of [Cu(Me_6TREN)]Br in H_2O, and aqueous/organic mixtures at 22°C

To a Schlenk tube fitted with a magnetic stir bar and a rubber septum, solvent (2 mL) and Me_6TREN (26 μL, 0.1 mmol) were charged and the mixture was bubbled with nitrogen for 15 min. CuBr (0.1 mmol) was then carefully added under slight positive pressure of nitrogen to protect the *in-situ* generated copper (0) powder from possible side oxidation reaction. The mixture immediately became blue [Cu(Me_6TREN)]Br_2 and a purple/red precipitate Cu(0) was observed. After 15 min the solution was carefully transferred through a gas tight syringe and 0.45 μm PTFE syringe filter to another Schlenk, previously filled with nitrogen. The filtered solution was diluted in order to get an accurate UV-Vis spectrum. Then 3 mLof the diluted solution was transferred to a UV-Vis cuvette (optical length, 10 mm), which was fitted with a rubber septum and previously filled with nitrogen. The cuvette was directly taken for UV-Vis spectroscopy.

Subsequently, a series of $CuBr_2$ solutions, with same amount of Me_6TREN (26 μL, 0.1 mmol) and different amounts of $CuBr_2$ in a certain amount of the used solvent, were made for UV-Vis measurements according to the same procedure as the disproportionation of [Cu(Me_6TREN)]Br in chapter 4. These calibration measurements made in order to calculate the concentration of [Cu(Me_6TREN)]Br_2 in disproportionation solution.

General procedure for the effect of ligand concentration on the disproportionation in H_2O at 22˚C

To a Schlenk tube fitted with a magnetic stir bar and a rubber septum, H_2O (2 mL) and different amounts of Me_6TREN (0.025, 0.05, 0.1, 0.2, 0.3 and 0.6 mmol) were charge, the mixture of each reaction was bubbled with nitrogen for 15 min. CuBr (0.1 mmol) was then carefully added under slight positive pressure of nitrogen to protect the in-situ generated copper (0) powders from possible side oxidation reaction. The mixture (CuBr : Me_6TREN, 1: 0.2 ,0.5 ,1 , and 2 in water as the solvent) immediately became blue [Cu(Me_6TREN)]Br_2 and a purple/red precipitate Cu(0) was observed and the mixture (CuBr : Me_6TREN, 1: 3 and 6) immediately became dark blue and a fine colloidal Cu(0) was observed. After two different reaction times (15 min and 10 h) the solution was carefully transferred through a gas tight syringe and 0.45 μm PTFE syringe filter to another Schlenk, previously filled with nitrogen. The filtered solution was diluted in order to get an accurate UV-Vis spectrum. Then 3 mLof the diluted solution was transferred to a UV-Vis cuvette (optical length, 10 mm), which was fitted with a rubber septum and previously filled with nitrogen. The cuvette was directly taken for UV-Vis spectroscopy.

General procedure for the disproportionation of [Cu(Me_6TREN)]Br in H_2O in the presence of monomer at 22˚C

To a Schlenk tube fitted with a magnetic stir bar and a rubber septum, H_2O (2 mL) and Me_6TREN (0.1 mmol) were charged and the mixture was bubbled with nitrogen for 15 min. CuBr (0.1 mmol) was then carefully added under nitrogen atmosphere and the reaction was left for 15 min then 2.5mLmonomer solution (0.5 mL$PEGA_{480}$, HEA, HEAA or NIPAM in 2 mL water) in the case of disp. in water was added for another 15 min. The solution was carefully transferred through a gas tight syringe and 0.45 μm PTFE syringe filter to another Schlenk, previously filled with nitrogen. The filtered solution was diluted in order to get an accurate UV-Vis spectrum. Then 3 mL of the degassed and diluted solution was transferred to a UV-Vis cuvette (optical length, 10 mm), which was fitted with a rubber septum and previously filled with nitrogen. The cuvette was directly taken for UV-Vis spectroscopy.

General procedure for the extent of comproportionation (comp.) of Cu(0) and $CuBr_2$ in H_2O at 22˚C

To a Schlenk tube fitted with a magnetic stir bar and a rubber septum, H_2O (2 mL), Me_6TREN (26 μL, 0.1 mmol) and $CuBr_2$ (0.05 mmol) were charged. The mixture was bubbled with nitrogen for 15 min then activated Cu(0) wire was added. After 2 h the solution was carefully transferred through a gas tight syringe and 0.45 μm PTFE syringe filter to another Schlenk, previously filled with nitrogen. The filtered solution was diluted in order to get an accurate UV-Vis spectrum. Then 3 mL of the degassed and diluted solution was transferred to a UV-Vis cuvette (optical length, 10

mm), which was fitted with a rubber septum and previously filled with nitrogen. The cuvette was directly taken for UV-Vis spectroscopy.

Calibration curve

To calculate the concentration of $CuBr_2$ in disproportionation solution, a series of $CuBr_2$/Me_6TREN solutions were measured by UV-Vis, utilizing the same amount of Me_6TREN (26 μl, 0.1 mmol) with different amounts of $CuBr_2$ (7.8, 8.8, 9.8, 10.8, 11.8 mg), in 2 mL of solvent.

General procedure for the extent of comproportionation of Cu(0) and $CuBr_2$ in H_2O in the presence of monomers at 22˚C

To a Schlenk tube fitted with a magnetic stir bar and a rubber septum, 5 mL monomer solution (0.5 mL$PEGA_{480}$, HEA, HEAA or NIPAM in 4.5 mL water) or 4 mL monomer solution, Me_6TREN (26 μL, 0.1 mmol) and $CuBr_2$ (0.05 mmol) were charged. The mixture was bubbled with nitrogen for 15 min then activated Cu(0) wire was added. After 2 h the solution was carefully transferred through a gas tight syringe and 0.45 μm PTFE syringe filter to another Schlenk, previously filled with nitrogen. The filtered solution was diluted in order to get an accurate UV-Vis spectrum. Then 3 mL of the degassed and diluted solution was transferred to a UV-Vis cuvette (optical length, 10 mm), which was fitted with a rubber septum and previously filled with nitrogen. The cuvette was directly taken for UV-Vis spectroscopy.

Quantitative analysis of the disproportionation of CuBr using UV-vis Spectroscopy

To determine the degree of CuBr disproportionation, five known concentrations of $[Cu(Me_6TREN)]Br_2$ solution were recorded in order to create a calibration curve. However, quantification of the degree of disproportionation of CuBr in DMSO and its mixtures is problematic due to the formation of colloidal Cu(0) stabilized by DMSO. The very small colloidal Cu(0) particles have a scattering effect and also exhibit an absorption with a maximum at ~ 600 nm. To estimate the conversion *via* disproportionation the equation (1) has been applied[19].

$$\text{Conversion (\%) of CuBr} = \frac{\text{Abs @ the height of}\sim 967\text{nm peak - Abs @ the baseline at} \sim 550\text{ nm}}{\text{Abs}_{\,[Cu(Me_6TREN)]Br_2}\ @\ \sim 967\text{nm}} * 100 \quad (1)$$

Similarly, the degree of comproportionation was calculated by using equation (2).

$$\text{Conversion (\%) of}CuBr_2 = \left(\frac{\text{Abs @ the height of}\sim 967\text{nm peak - Abs @ the baseline at} \sim 550\text{ nm}}{\text{Abs}_{\,[Cu(Me_6TREN)]Br_2}\ @\ \sim 967\text{nm}} * 100\right) - 1 \quad (2)$$

The role of Cu(0) particles in aqueous polymerisations

Polymerisation of NIPAM (DP=20): slow feeding with [Cu(TPMA)]Br

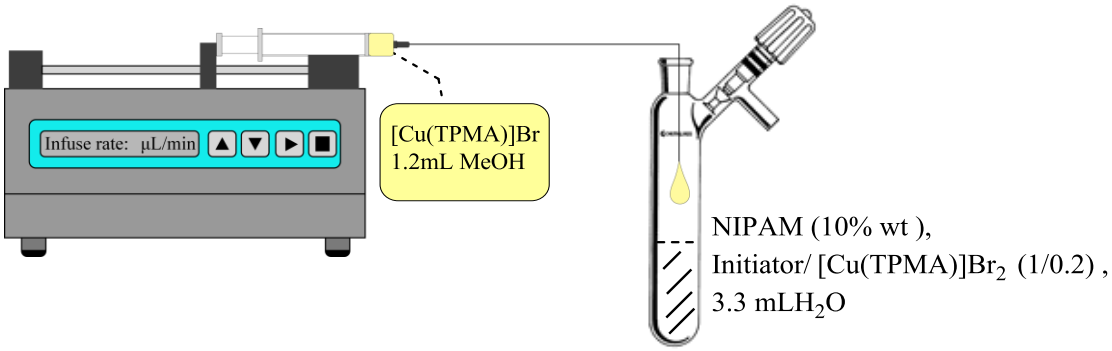

Scheme 6. Schematic of a typical slow feeding polymerisation system with [Cu(TPMA)]Br protocol at 0˚C.

To a Schlenk tube fitted with a magnetic stir bar and a rubber septum, H_2O (3.3 mL), TPMA (0.05 mmol), $CuBr_2$ (0.05 mmol), monomer (5 mmol) and initiator (WSI, 0.25 mmol) were charged and the mixture was bubbled with nitrogen for 15 min at 0 $^{\circ}$C. Subsequently a solution of TPMA (0.1 mmol in 1.2 mL H_2O or MeOH) and CuBr (0.1 mmol) was then carefully added *via* a pump syringe (Harvard, PHD/ULTRA) under slight positive pressure of nitrogen. However, after 1min the complex was precipitated.

The polymerisation system was supplied with Cu(I) complex under different flow rate conditions. Samples of the reaction mixture were then removed for analysis at different times. The sample for ^{1}H NMR was directly diluted with D_2O. Catalyst residues were removed by filtering through a column of basic alumina prior to DMF SEC analysis.

Polymerisation of NIPAM (DP=20): slow feeding with [Cu(Me$_6$TREN)]Br

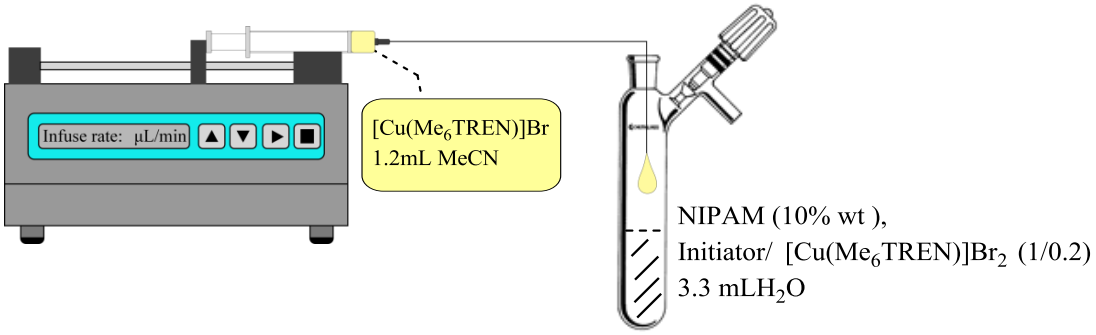

Scheme 7. Schematic of a typical slow feeding polymerisation system with [Cu(Me$_6$TREN)]Br protocol at 0˚C.

Identical procedure was followed when replacing TPMA, MeOH solution with solution of (0.1 mmol Me$_6$TREN in 1.2 or 0.2 mL MeCN).

The polymerisation system was supplied with Cu(I) complex under certain flow rates (0.081 M/min. feeding time 120 min).

Polymerisation of PEGA$_{480}$ (DP=10): slow feeding with [Cu(TPMA)]Br

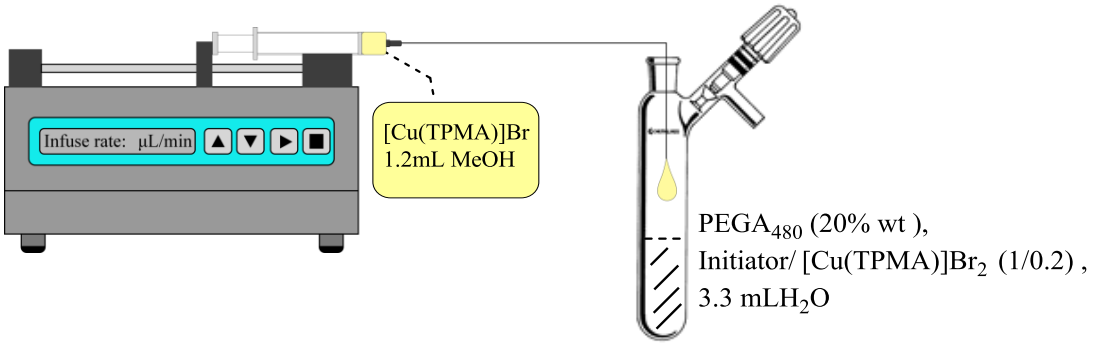

Scheme 8. Schematic of a typical slow feeding polymerisation system with [Cu(TPMA)]Br protocol at 0˚C.

Conditions: H_2O (3.3 mL), TPMA (0.05 mmol), $CuBr_2$ (0.05 mmol), monomer (5 mmol) and initiator (WSI, 0.25mmol). The catalytic system (TMPA, 0.1mmol in 1.2 mL MeOH) and CuBr (0.1 mmol) was gradually fed in the reaction mixture.

Polymerisation of $PEGA_{480}$ (DP=10): slow feeding with [Cu(Me_6TREN)]Br protocol

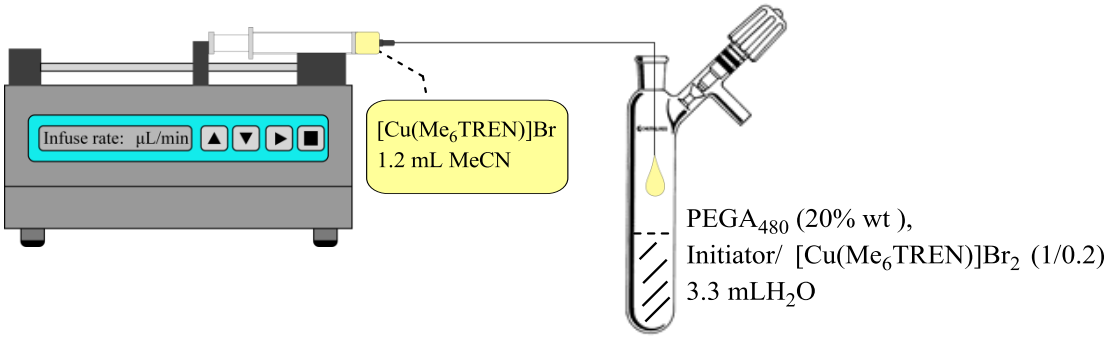

Scheme 9. Schematic of a typical slow feeding polymerisation system with [Cu(Me_6TREN)]Br protocol at 0 ˚C. Conditions: H_2O (3.3 mL), Me_6TREN (0.05 mmol), $CuBr_2$ (0.05 mmol), monomer (5 mmol) and initiator (WSI, 0.25 mmol). The catalytic system (Me_6TREN, 0.1 mmol in 1.2 or 0.2 mL MeCN) and CuBr (0.1 mmol) was gradually fed in the reaction mixture.

General procedure for the control experiment resembling conditions utilised during feeding experiment at one pot (without feeding) at 0˚C.

To a Schlenk tube fitted with a magnetic stir bar and a rubber septum, a mixture of H_2O (3.3 mL) and co-solvent (MeOH or MeCN (1.2 mL), resembling the feeding mixture), monomer, Me_6TREN, $CuBr_2$ and initiator were charged and the mixture was purged with nitrogen for 15 min. Also, the same amount of CuBr that used in

slow feeding was then added under slight positive pressure of nitrogen. The Schlenk tube was sealed and the solution was allowed to polymerise at 0 ˚C. Samples of the reaction mixture were then removed for analysis at certain times. The sample for ^{1}H NMR was directly diluted with D_2O, which confirmed the percentage of the conversion by monitoring the disappearance of vinyl groups. Catalyst residues were removed by filtering through a column of basic alumina prior to DMF SEC analysis.

General procedure for SET-LRP protocol at 0˚C

To a Schlenk tube fitted with a magnetic stir bar and a rubber septum, H_2O (2 mL) and Me_6TREN (0.15 mmol) were charged and the mixture was bubbled with nitrogen for 15 min. CuBr (0.1 mmol) was then carefully added under slight positive pressure of nitrogen. The mixture immediately became blue Cu(II) and a purple/red precipitate Cu(0) was observed (Section 5.5, Scheme 5.5). In a separate vial fitted with a magnetic stir bar and a rubber septum monomer (2.5 mmol) was dissolved in three different systems, 1) H_2O 1.3 mL+ MeCN or MeOH 1.2, 2) H_2O 1.3 mL+ MeCN 0.2, and 3) H_2O 2.5mLprior to addition of initiator (WSI, 0.25 mmol) and the resulting mixture was purged with nitrogen for 15 min. The degassed monomer / initiator aqueous solution was then transferred *via* a degassed syringe to the Schlenk tube containing Cu(0) / $CuBr_2$ / Me_6TREN catalyst. The Schlenk tube was sealed and the solution was allowed to polymerise at 0 ˚C. Samples of the reaction mixture were then removed for analysis. The sample for ^{1}H NMR was directly diluted with D_2O. Catalyst residues were removed by filtering through a column of basic alumina prior to DMF SEC analysis.

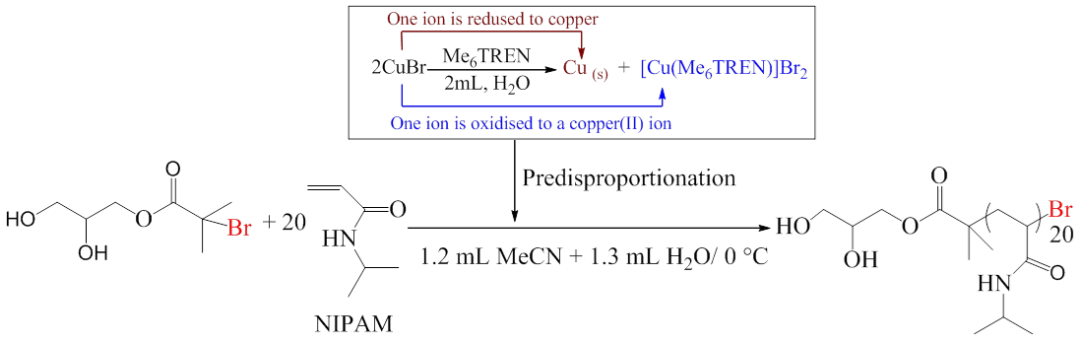

Scheme 10. Schematic representation for synthesis of PNIPAM by SET-LRP in H_2O.

General procedure for typical ATRP protocol at 0˚C

A mixture of H_2O/MeOH or MeCN, monomer, Me_6TREN or TPMA (0.15 mmol) and initiator was charged in a Schlenk tube and purged with nitrogen for 15 min. Then CuBr (0.1 mmol) was then carefully added under slight positive pressure of nitrogen. The solution was allowed to polymerise at 0 ˚C. Samples of the reaction mixture were then removed for analysis at certain times. The samples for ^{1}H NMR was directly diluted with D_2O, which confirmed the percentage the conversion by monitoring the disappearance of vinyl groups.Catalyst residues were removed by filtering through a column of neutral alumina prior to DMF SEC analysis.

General procedure for ATRP with [$CuBr_2$] protocol at 0˚C

The procedure followed is identical with the ATRP protocol, however, a stoichiometric amount of CuBr (0.5 equiv. with respect to the ATRP protocol where 1 equiv. was used) and $CuBr_2$ (0.5 equiv.) were utilised. $CuBr_2$ was placed in the Schlenk tube prior to addition of the CuBr.

5.4.4 Additional characterisation

Disproportionation of [Cu(Me_6TREN)]Br in H_2O and DMSO in the presence of monomer

Table 6. Summary of polymerisations in the absence of initiator at in 15 min at 22˚C.

Entry	Monomer	Protocol	Conv.%	M_n	Đ
1	**NIPAM**	**2**	**51**	**18000**	**2.7**
		3	**60**	**18700**	**2.6**
2	**$PEGA_{480}$**	**2**	**0**	**0**	**-**
		3	**0**	**0**	**-**
3	**HEAA**	**2**	**50**	**11800**	**1.7**
		3	**20**	**15800**	**1.9**
4	**HEA**	**2**	**20**	**33000**	**1.7**
		3	**15**	**38700**	**1.6**

The extent of comproportionation of Cu(0) and $CuBr_2$ in H_2O in the presence/absence of monomers

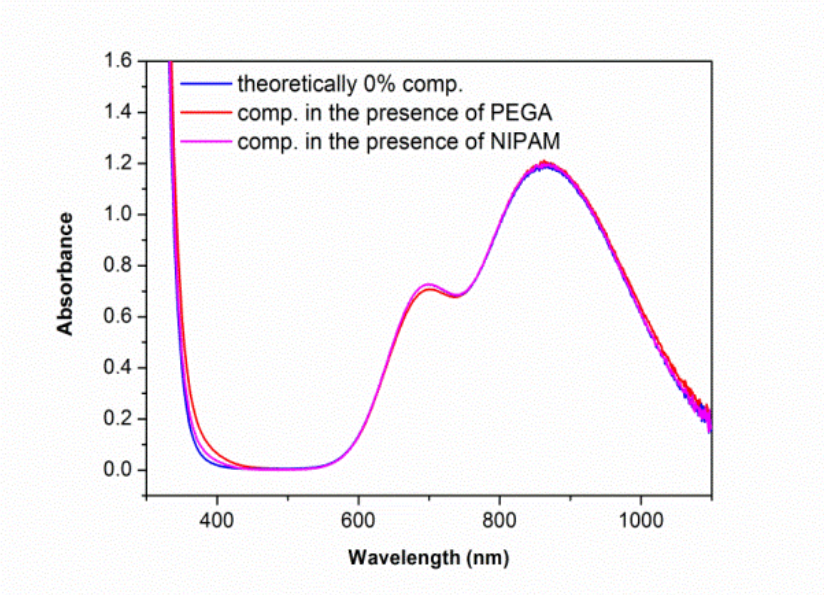

Figure 34. UV-Vis spectra of comproportionation in the presence of NIPAM and $PEGA_{480}$, Conditions: Cu(0) wire (activated by hydrazine 5 cm, Ø 0.25 mm), $[CuBr_2]$:$[Me_6TREN]$ = [1]:[2], 12% *v/v* monomer in H_2O at 22 ˚C.

The role of Cu(0) particles in aqueous polymerisations

Figure 35. Visualization of the *in situ* generated Cu(0) during $PEGA_{480}$ polymerisation (DP=10) in 26% *v/v* MeCN in H_2O systems at 0˚C. Conditions: [I]:$[PEGA_{480}]$:[CuBr]:$[Me_6TREN]$ = [1]:[10]:[0.1]:[0.15] , in 3.3 mL H_2O + 1.2 mL MeCN system at 0˚C.

5.5 References

1. J.-S. Wang and K. Matyjaszewski, *J. Am. Chem. Soc.*, 1995, **117**, 5614-5615.
2. M. Kato, M. Kamigaito, M. Sawamoto and T. Higashimura, *Macromolecules*, 1995, **28**, 1721-1723.
3. K. Matyjaszewski, *Macromolecules*, 2012, **45**, 4015-4039.
4. V. Percec, T. Guliashvili, J. S. Ladislaw, A. Wistrand, A. Stjerndahl, M. J. Sienkowska, M. J. Monteiro and S. Sahoo, *J. Am. Chem. Soc.*, 2006, **128**, 14156-14165.
5. V. Percec, A. V. Popov, E. Ramirez-Castillo, M. Monteiro, B. Barboiu, O. Weichold, A. D. Asandei and C. M. Mitchell, *J. Am. Chem. Soc.*, 2002, **124**, 4940-4941.
6. Q. Zhang, P. Wilson, Z. Li, R. McHale, J. Godfrey, A. Anastasaki, C. Waldron and D. M. Haddleton, *J. Am. Chem. Soc.*, 2013, **135**, 7355-7363.
7. K. Matyjaszewski, S. Coca, S. G. Gaynor, M. Wei and B. E. Woodworth, *Macromolecules*, 1997, **30**, 7348-7350.
8. D. Konkolewicz, Y. Wang, P. Krys, M. Zhong, A. A. Isse, A. Gennaro and K. Matyjaszewski, *Polym. Chem.*, 2014, **5**, 4396-4417.
9. D. Konkolewicz, Y. Wang, M. Zhong, P. Krys, A. A. Isse, A. Gennaro and K. Matyjaszewski, *Macromolecules*, 2013, **46**, 8749-8772.
10. Y. Gao, T. Zhao and W. Wang, *RSC Adv.*, 2014, **4**, 61687-61690.
11. W. Wang, J. Zhao, N. Zhou, J. Zhu, W. Zhang, X. Pan, Z. Zhang and X. Zhu, *Polym. Chem.*, 2014, **5**, 3533-3546.
12. G. Lligadas, B. M. Rosen, C. A. Bell, M. J. Monteiro and V. Percec, *Macromolecules*, 2008, **41**, 8365-8371.
13. M. E. Levere, N. H. Nguyen, H.-J. Sun and V. Percec, *Polym. Chem.*, 2013, **4**, 686-694.
14. N. H. Nguyen, M. E. Levere and V. Percec, *J. Polym. Sci., Part A: Polym. Chem.*, 2012, **50**, 35-46.
15. Y. Kwak, A. J. D. Magenau and K. Matyjaszewski, *Macromolecules*, 2011, **44**, 811-819.
16. M. E. Levere, N. H. Nguyen, X. Leng and V. Percec, *Polym. Chem.*, 2013, **4**, 1635-1647.
17. M. E. Levere, I. Willoughby, S. O'Donohue, P. M. Wright, A. J. Grice, C. Fidge, C. Remzi Becer and D. M. Haddleton, *J. Polym. Sci., Part A: Polym. Chem.*, 2011, **49**, 1753-1763.
18. N. H. Nguyen, B. M. Rosen, X. Jiang, S. Fleischmann and V. Percec, *J. Polym. Sci., Part A: Polym. Chem.*, 2009, **47**, 5577-5590.
19. B. M. Rosen, X. Jiang, C. J. Wilson, N. H. Nguyen, M. J. Monteiro and V. Percec, *J. Polym. Sci., Part A: Polym. Chem.*, 2009, **47**, 5606-5628.
20. N. H. Nguyen, M. E. Levere, J. Kulis, M. J. Monteiro and V. Percec, *Macromolecules*, 2012, **45**, 4606-4622.
21. G. Lligadas, B. M. Rosen, M. J. Monteiro and V. Percec, *Macromolecules*, 2008, **41**, 8360-8364.
22. G. Lligadas and V. Percec, *J. Polym. Sci., Part A: Polym. Chem.*, 2008, **46**, 6880-6895.
23. N. H. Nguyen and V. Percec, *J. Polym. Sci., Part A: Polym. Chem.*, 2011, **49**, 4227-4240.
24. N. H. Nguyen and V. Percec, *J. Polym. Sci., Part A: Polym. Chem.*, 2010, **48**, 5109-5119.

25. M. E. Levere, N. H. Nguyen and V. Percec, *Macromolecules*, 2012, **45**, 8267-8274.
26. N. H. Nguyen, M. E. Levere and V. Percec, *J. Polym. Sci., Part A: Polym. Chem.*, 2012, **50**, 860-873.
27. T. Guliashvili and V. Percec, *J. Polym. Sci., Part A: Polym. Chem.*, 2007, **45**, 1607-1618.
28. N. H. Nguyen, B. M. Rosen, G. Lligadas and V. Percec, *Macromolecules*, 2009, **42**, 2379-2386.
29. N. H. Nguyen, H.-J. Sun, M. E. Levere, S. Fleischmann and V. Percec, *Polym. Chem.*, 2013, **4**, 1328-1332.
30. A. Kajiwara, K. Matyjaszewski and M. Kamachi, *Macromolecules*, 1998, **31**, 5695-5701.
31. K. Matyjaszewski, N. V. Tsarevsky, W. A. Braunecker, H. Dong, J. Huang, W. Jakubowski, Y. Kwak, R. Nicolay, W. Tang and J. A. Yoon, *Macromolecules*, 2007, **40**, 7795-7806.
32. A. J. D. Magenau, Y. Kwak and K. Matyjaszewski, *Macromolecules*, 2010, **43**, 9682-9689.
33. M. Zhong, Y. Wang, P. Krys, D. Konkolewicz and K. Matyjaszewski, *Macromolecules*, 2013, **46**, 3816-3827.
34. C.-H. Peng, M. Zhong, Y. Wang, Y. Kwak, Y. Zhang, W. Zhu, M. Tonge, J. Buback, S. Park, P. Krys, D. Konkolewicz, A. Gennaro and K. Matyjaszewski, *Macromolecules*, 2013, **46**, 3803-3815.
35. Y. Wang, M. Zhong, W. Zhu, C.-H. Peng, Y. Zhang, D. Konkolewicz, N. Bortolamei, A. A. Isse, A. Gennaro and K. Matyjaszewski, *Macromolecules*, 2013, **46**, 3793-3802.
36. S. Harrisson, P. Couvreur and J. Nicolas, *Macromolecules*, 2012, **45**, 7388-7396.
37. S. Harrisson and J. Nicolas, *ACS Macro Lett.*, 2014, **3**, 643-647.
38. M. Horn and K. Matyjaszewski, *Macromolecules*, 2013, **46**, 3350-3357.
39. Y. Wang, Y. Kwak, J. Buback, M. Buback and K. Matyjaszewski, *ACS Macro Letters*, 2012, **1**, 1367-1370.
40. Y. Wang, M. Zhong, Y. Zhang, A. J. D. Magenau and K. Matyjaszewski, *Macromolecules*, 2012, **45**, 8929-8932.
41. C. Y. Lin, M. L. Coote, A. Gennaro and K. Matyjaszewski, *J. Am. Chem. Soc.*, 2008, **130**, 12762-12774.
42. D. Konkolewicz, P. Krys, J. R. Góis, P. V. Mendonça, M. Zhong, Y. Wang, A. Gennaro, A. A. Isse, M. Fantin and K. Matyjaszewski, *Macromolecules*, 2014, **47**, 560-570.
43. C. Waldron, Q. Zhang, Z. Li, V. Nikolaou, G. Nurumbetov, J. Godfrey, R. McHale, G. Yilmaz, R. K. Randev, M. Girault, K. McEwan, D. M. Haddleton, M. Droesbeke, A. J. Haddleton, P. Wilson, A. Simula, J. Collins, D. J. Lloyd, J. A. Burns, C. Summers, C. Houben, A. Anastasaki, M. Li, C. R. Becer, J. K. Kiviaho and N. Risangud, *Polym. Chem.*, 2014, **5**, 57-61.
44. A. Anastasaki, A. J. Haddleton, Q. Zhang, A. Simula, M. Droesbeke, P. Wilson and D. M. Haddleton, *Macromol. Rapid Commun.*, 2014, **35**, 965-970.
45. Q. Zhang, Z. Li, P. Wilson and D. M. Haddleton, *Chem. Commun.*, 2013, **49**, 6608-6610.
46. F. Alsubaie, A. Anastasaki, P. Wilson and D. M. Haddleton, *Polym. Chem.*, 2015.

47. A. Simula, V. Nikolaou, A. Anastasaki, F. Alsubaie, G. Nurumbetov, P. Wilson, K. Kempe and D. M. Haddleton, *Polym. Chem.*, 2015.
48. Q. Zhang, P. Wilson, A. Anastasaki, R. McHale and D. M. Haddleton, *ACS Macro Letters*, 2014, **3**, 491-495.
49. S. Ahrland and J. Rawsthorne, *Journal*, 1970, **24**, 157-172.
50. F. Fenwick, *J. Am. Chem. Soc.*, 1926, **48**, 860-870.
51. Alsubaie, F.; Anastasaki, A.; Nikolaou, V.; Simula, A.;Nurumbetov, G Wilson, P.; Kempe, K.; Haddleton, D. M. Macromolecules 2015, 48, 5517−5525.
52. A. Simula, G. Nurumbetov, A. Anastasaki, P. Wilson and D. M. Haddleton, *Eur. Polym. J.*, 2015, **62**, 294-303.
53. W. Tang and K. Matyjaszewski, *Macromolecules*, 2006, **39**, 4953-4959.
54. A. Simakova, S. E. Averick, D. Konkolewicz and K. Matyjaszewski, *Macromolecules*, 2012, **45**, 6371-6379.
55. S. Perrier, S. P. Armes, X. S. Wang, F. Malet and D. M. Haddleton, *J. Polym. Sci., Part A: Polym. Chem.*, 2001, **39**, 1696-1707.
56. M. Ciampolini and N. Nardi, *Inorg.Chem.*, 1966, **5**, 41-44.

Chapter 6: Conclusions and Future Outlook

The main goal of this thesis was to identify the potential and the limitations of aqueous Cu(0)-mediated RDRP and to thoroughly investigate the mechanism of this complex reaction system.

The first goal of the thesis was completed *via* the efficient one pot synthesis of multiblock copolymers using Cu(0)-mediated RDRP in aqueous media. A particular emphasis was placed on carefully evaluating the polymerisation rate in order to minimise the amount of bromine loss. Careful experimental design enabled the synthesis of a well-defined 'nonablock' PNIPAM and hexablock copolymers comprised of three hydrophilic acrylamides (NIPAM, HEAA and DMA) in alternated sequence at, or below, ambient temperature without the need for intermediate purification steps. Disproportionation of CuBr in water *prior* to addition of initiator and monomer was successfully exploited resulting in unprecedented rates of polymerisation whilst maintaining good control over the molecular weight distributions ($Đ < 1.10$).

Comprehensive chain extension studies were also conducted in order to investigate the role of monomer structure in the rates of chain end loss for a range of acrylamides. It was revealed that tertiary acrylamides (DMA, DEA, NAM) showed an enhanced rate of ω-Br chain end loss relative to secondary acrylamides (NIPAM, HEAA). These results highlighted another consideration that needs to be taken prior incorporating a new monomer into multiblock copolymers.

The versatility of aqueous Cu(0)-mediated RDRP technique has been also examined assessing the synthesis of high molecular weights materials. Based on the

aforementioned considerations, the successful preparation block homopolymers and block copolymers of high molecular weight were accomplished. The synthesis of well-defined homopolymers including PNIPAM, PHEAA and PDMA has been obtained utilising aqueous Cu(0)-mediated RDRP at 0ºC. Moreover, under carefully optimised conditions, the successive *in situ* chain extension and block copolymerisation of PNIPAM and PHEAA can be achieved. Thus, the polymer chain length per block can be extended from DP_n = 10 to DP_n = 100, providing polymeric material with precise structures and compositions.

In the second part of this thesis, the mechanistic study of Cu(0)-mediated RDRP of acrylate monomers in the presence of copper (*i.e.* Cu(0) wire or Cu(0) particles) was investigated in organic media. It was found that disproportionation and comproportionation equilibria can be strongly affected by different factors including the concentration of the ligand, the nature of the solvent and the monomer structure. UV-Vis disproportionation experiments revealed that in DMSO comproportionation generally dominates over disproportionation. Moreover, the degree of disproportionation of CuBr/Me_6TREN was reduced in the presence of hydrophobic monomer such as MA. It was also demonstrated that the sequence of the reagent addition is crucial for the controlled polymerisation. This was attributed to the possible competitive complexation of the reagents (*e.g.* monomer, solvent, ligand and copper species) in reaction mixture.

In addition, it was demonstrated that Cu(0) particles obtained by the *in situ* disproportionation of CuBr in DMSO are less active species than Cu(I). When [CuBr] is maximised (at high ligand concentrations), the rate of the polymerisation is accelerated without compromising the control over the molecular weight distribution. These findings are in disagreement with the initially proposed SET-

LRP mechanism, where instantaneous disproportionation and extremely reactive "nascent" Cu(0) particles is reported to be a major activator. However, copper wire showed very different behaviour when only 5 cm of Cu(0) wire was utilised as a catalyst in the presence of the same ligand (Me_6TREN), faster polymerisation rate was detected. By comparing this with 9.4 mM of CuBr (previously reported to match the activity of CuBr with Cu(0), 19 km of copper wire would be required), the rates of polymerisation by Cu(0) wire is faster. Thus, it was concluded that although the mechanism of the activation of R-X by copper wire has been ambiguous in DMSO, it defiantly pushes the polymerisation to faster rates whilst the termination reaction at very minimal amount.

In the final chapter, the mechanism of copper mediated living radical polymerisation of acrylates and acrylamides in aqueous media was also investigated in aqueous media. Unlike DMSO, it was shown that disproportionation dominates over comproportionation. As recognised in the case of DMSO, the nature of the solvent, monomer and ligand (disproportionating or non-disproportionating) strongly affected on the disproportionation equilibria. In pure water, variation of the [ligand] did not influence the thermodynamic equilibrium as long as there is sufficient ligand present to solubilise the copper species. In contrast with previous report, no comproportionation, even in the presence of monomer, was detected by UV-Vis spectroscopy within the timescale of the polymerisations. Interestingly, aqueous mixtures (up to 50% organic content) has been shown to facilitate the disproportionation of CuBr/Me_6TREN, which would be beneficial for solubilising more hydrophobic initiators and monomers. The sequence of the reagent addition was also found to be important for the control over the polymer chains. Attempts to mimic the role of ''nascent'' Cu(0) *in situ* by slowly feeding experiments ppm

concentrations of CuBr were also conducted. All results indicated that the presence of Cu(0) is essential to perform a controlled polymerisation.

Finally, a direct comparison between the SET-LRP and the ATRP protocols was performed. In this study, the ratio between Cu(0) or CuBr (activator species) and $CuBr_2$ (deactivator species) was matched, revealing the contribution of each catalyst to the overall mechanism and kinetics. Importantly, in the case of acrylates, both Cu(0) and CuBr can equally contribute to an effective polymerisation, whilst for the case of acrylamides, Cu(0) outperforms Cu(I) and cannot be considered as a supplemental activator.

Currently, aqueous Cu(0)-mediated RDRP offers a simple synthetic route to design well-defined water soluble polymers of acrylamide and acrylate monomers. In future, the monomer pool can be expanded to include a range of hydrophilic monomers especially methacrylamides and methacrylates in order to synthesise hydrophilic macromolecules. These polymers can be self-assembled into nano-objects offering wide applications for nanomedicine and industry. There are many ways in which this phenomenon would be investigated in the future. Varying the molecular weights and/or changing the sequence of monomers in copolymers should confer new mechanical and thermal properties.